COUPLED DYNAMICS OF THE SPREAD OF COVID-19, INTERVENTIONS AND HUMAN BEHAVIOUR

Dissertation
for the award of the degree
"Doctor rerum naturalium" (Dr.rer.nat.)
of the Georg-August-Universität Göttingen

within the doctoral program International Max Planck Research School
Physics of Biological and Complex Systems
of the Georg-August University School of Science (GAUSS)

submitted by
Emil Nafis Iftekhar

from Nürnberg, Germany

Göttingen, 2024

ACKNOWLEDGMENTS

And I want to acknowledge every other researcher from across Europe and around the globe that I had the honor to work together with to take action against the pandemic as well as all those I have not met but have all played their part in the vast COVID-19 literature of these past few years.

Next I want to acknowledge the care work that was behind the completion of this thesis: Thanks to Mona, Mareike, and all my friends for persevering through these years with me and for making sure that I am coming out of this PhD without any mental issues. Also thanks to Hannah for proofreading. Finally, I want to thank my parents and family for being a foundational support.

Writing the acknowledgements, I was wondering what the purpose of it is and who it is even for because most people mentioned here will not ever read this. My conclusion is that I want to nudge the reader to actively appreciate and thank whoever they are supported by not only at the end but also throughout their journey. And here I do not only mean their closest circles but also everyone in society who contributes to making the general infrastructure run on an every day basis. The pandemic has shown us how essential these essential workers are and also how little they get back from society. Beyond merely clapping hands a few times, I want to continue contributing to work, such as this research, that acknowledges and supports their work.

CONTENTS

LIST OF PUBLICATIONS

This dissertation is the result of research at the Max Planck Institute for Dynamics and Self-Organization, partly carried out in close collaboration with scientists worldwide. Publications [2], [3], [7], [8], and [9] constitute chapters of this thesis.

[1] Viola Priesemann, Melanie M. Brinkmann, Sandra Ciesek, Sarah Cuschieri, Thomas Czypionka, Giulia Giordano, Deepti Gurdasani, Claudia Hanson, Niel Hens, Emil N. Iftekhar, et al. "Calling for pan-European commitment for rapid and sustained reduction in SARS-CoV-2 infections." In: *The Lancet* 397.10269 (2021), pp. 92–93. DOI: https://doi.org/10.1016/S0140-6736(20)32625-8.

[2] Emil N. Iftekhar*, Viola Priesemann, Rudi Balling, Simon Bauer, Philippe Beutels, André Calero Valdez, Sarah Cuschieri, Thomas Czypionka, Uga Dumpis, Enrico Glaab, et al. "A look into the future of the COVID-19 pandemic in Europe: an expert consultation." In: *The Lancet Regional Health–Europe* 8 (2021). DOI: https://doi.org/10.1016/j.lanepe.2021.100185.

[3] Simon Bauer, Sebastian Contreras, Jonas Dehning, Matthias Linden, Emil N. Iftekhar, Sebastian B. Mohr, Alvaro Olivera-Nappa, and Viola Priesemann. "Relaxing restrictions at the pace of vaccination increases freedom and guards against further COVID-19 waves." In: *PLoS computational biology* 17.9 (2021), e1009288. DOI: https://doi.org/10.1371/journal.pcbi.1009288.

[4] Karen Y. Oróstica, Sebastian Contreras, Sebastian B. Mohr, Jonas Dehning, Simon Bauer, David Medina-Ortiz, Emil N. Iftekhar, Karen Mujica, Paulo C. Covarrubias, Soledad Ulloa, et al. "Mutational signatures and transmissibility of SARS-CoV-2 Gamma and Lambda variants." In: *arXiv preprint arXiv:2108.10018* (2021). DOI: https://doi.org/10.48550/arXiv.2108.10018.

[5] Viola Priesemann, Rudi Balling, Simon Bauer, Philippe Beutels, André Calero Valdez, Sarah Cuschieri, Thomas Czypionka, Uga Dumpis, Enrico Glaab, Eva Grill, et al. "Towards a European strategy to address the COVID-19 pandemic." In: *The Lancet*

398.10303 (2021), pp. 838–839. DOI: https://doi.org/10.1016/S0140-6736(21)01808-0.

[6] André Calero Valdez, Emil N. Iftekhar, Miquel Oliu-Barton, Robert Böhm, Sarah Cuschieri, Thomas Czypionka, Uga Dumpis, Giulia Giordano, Claudia Hanson, Zdenek Hel, et al. "Europe must come together to confront omicron." In: *BMJ* (2022). DOI: https://doi.org/10.1136/bmj.o90.

[7] Thomas Czypionka*, Emil N. Iftekhar*, Barbara Prainsack*, Viola Priesemann*, Simon Bauer, Andre Calero Valdez, Sarah Cuschieri, Enrico Glaab, Eva Grill, Jenny Krutzinna, et al. "The benefits, costs and feasibility of a low incidence COVID-19 strategy." In: *The Lancet Regional Health–Europe* 13 (2022). DOI: https://doi.org/10.1016/j.lanepe.2021.100294.

[8] Philipp Dönges*, Joel Wagner*, Sebastian Contreras*, Emil N. Iftekhar*, Simon Bauer, Sebastian B. Mohr, Jonas Dehning, André Calero Valdez, Mirjam Kretzschmar, Michael Mäs, et al. "Interplay Between Risk Perception, Behavior, and COVID-19 Spread." In: *Frontiers in Physics* 10 (2022). ISSN: 2296-424X. DOI: 10.3389/fphy.2022.842180.

[9] Jonas Dehning, Sebastian B. Mohr, Sebastian Contreras, Philipp Dönges, Emil N. Iftekhar, Oliver Schulz, Philip Bechtle, and Viola Priesemann. "Impact of the Euro 2020 championship on the spread of COVID-19." In: *Nature Communications* 14.1 (2023), p. 122. ISSN: 2041-1723. DOI: 10.1038/s41467-022-35512-x.

[10] Seba Contreras, Emil N. Iftekhar, and Viola Priesemann. "From emergency response to long-term management: the many faces of the endemic state of COVID-19." In: *The Lancet Regional Health–Europe* (2023). DOI: https://doi.org/10.1016/j.lanepe.2023.100664.

* Asterisks mark publications as first author or with equal contribution.

Part I

INTRODUCTION

OUTLINE

Physical science is that department of knowledge which relates to the order of nature, or, in other words, to the regular succession of events.

— James Clerk Maxwell [1]

Although this definition or other similar definitions of physics are often understood as only being concerned about abstract phenomena and non-living matter, Maxwell also had "more complex phenomena" of "living" systems in mind [1]. Indeed, the field of complex systems draws from this broader notion of physics that tries to find and understand "regular[ity]" in a "succession of events"; it uses the analytical methods of conventional physics to try to make sense of any kind of complex system: be it the brain, an ecosystem, or even society [2]. In this thesis, we use the mindset and tools of physics and complex systems to approach a real-life problem that has affected and still affects the global population: the COVID-19 pandemic.

The COVID-19 pandemic, caused by the SARS-CoV-2 virus, presented a global crisis affecting every facet of human life (e.g [3]). Mitigating the spread of COVID-19 has required a multi-faceted approach, encompassing not only pharmaceutical and medical aspects but also non-pharmaceutical interventions (NPIs) (e.g. [4]). Various NPIs have been implemented worldwide, such as wearing masks, physical distancing, and even stay-at-home orders (e.g. [5, 6]).

However, the interplay between the disease spread, mitigation measures, and changes in human behavior caused non-linear dynamics that made it difficult to determine the sufficient scale of mitigation measures beforehand. An example concerns the NPI of testing, contact tracing, and isolating (TTI). TTI contributes to mitigation of the spread. However, at higher incidence, tracing capacities at public health offices may be reached, making TTI less effective. If incidence is already rising, the rise will become steeper, making TTI even less effective. Thereby, regaining control of the spread then requires even more measures than it does when TTI works at peak effectiveness. Hence, looking at TTI from a complex systems point-of-view and understanding the TTI capacity limit as a tipping point facilitates determining a sufficient set of NPIs [7].

In this thesis, we elaborate on further such examples where (i) the complex systems approach can be helpful in understanding the complex dynamics of disease spread, measures, and behaviour in a pandemic as well as (ii) the implications for mitigating the spread of the disease.

In chapter 2, we first explain some important complex systems concepts and tools that we use in our examples, ranging from stability and feedback loops in dynamical systems theory and compartmental models based on ordinary differential equations.

In chapter 3, we get an understanding of which dynamics and variables play crucial roles in the COVID-19 pandemic in Europe. As physicists, contributing to such a trans-disciplinary endeavour requires getting input from experts of other fields to identify the variables of the complex system in question first and then prioritise which ones to include in the analyses. Hence, we systematically consult with such experts to identify important problems and mechanisms that motivate the following chapters.

In chapter 4, we consider the situation in Europe in early 2021, when NPIs were implemented and vaccines had just become available. However, the roll-out of vaccination programs takes time, leaving a time window where health systems would still be fully vulnerable to the spread of the disease. To prevent a full overwhelming of hospitals, how much longer would it be necessary to keep NPIs implemented? And to what extent? What would be the direct damages to public health depending on the choice? We attempt to answer these questions using a set of delay differential equations and a proportional-derivative control approach.

In chapter 5, we turn to the winter of 2021/2021. Especially due to the emergence of the Omicron variant of concern, it was again important to understand the extent of necessary NPIs. To approach this problem, we now do not only consider changes in the population's health protective behaviour due to mandatory measures but also voluntary behaviour changes. Depending on the current severity of the disease spread and, e.g., the corresponding risk perception, the population might go beyond what is required of them in terms of, e.g., physical distancing, or decide to get vaccinated even if they were hesitant before. This feedback would eventually cause the spread to decrease again and in turn cause a decrease in risk perception. Thus, we receive a feedback loop, whose impact we investigate in multiple NPI scenarios to find that a moderate level of NPIs can protect health systems due to the population's self-regulation of behaviour.

In chapter 6, we investigate the impact of a large-scale public event on the COVID-19 pandemic in Europe: the football Euro 2020 championship. Using Bayesian inference, we quantify the number of additional COVID-19 cases due to social gatherings around the matches in the different countries and determine which starting conditions lead to fewer additional cases.

In chapter 7, we use some of the resulting insights of the previous chapters about the benefits of low incidence to formulate recommendations for policy.

In chapter 8, we provide an overarching discussion of our and other work to draw lessons for pandemic response and an outlook for further research.

In chapter 9, we conclude by clarifying the role of research such as this for understanding and taking action against pandemics.

BACKGROUND

2.1 STABILITY IN DYNAMICAL SYSTEMS

The dynamics of systems can be studied by formulating mathematical models, often in the form of coupled differential equations. Analyzing these models reveals important dynamic phenomena. For a dynamical system described by, e.g., autonomous ordinary differential equations of the form

$$\frac{d\mathbf{x}}{dt} = f(\mathbf{x}), \tag{2.1}$$

fix(ed) points or equilibria are values $\mathbf{x}_*$ where the system's state does not change, i.e.

$$\frac{d\mathbf{x}}{dt} = f(\mathbf{x}_*) = \mathbf{0}. \tag{2.2}$$

To characterise such equilibria, the concept of stability is important [8]. Here, we are especially concerned about local stability, which refers to how a dynamical system responds to small perturbations of its current state. A locally stable system, i.e. a system in a locally stable equilibrium, will return to the equilibrium after a small perturbation, while an unstable system will diverge away from it. More formally, a fixed point or equilibrium is locally stable if for any $\epsilon > 0$, there exists a $\delta > 0$ such that if

$$||\mathbf{x}(0) - \mathbf{x}_*|| < \delta, \tag{2.3}$$

then

$$||\mathbf{x}(t) - \mathbf{x}_*|| < \epsilon \quad \forall t \geq 0. \tag{2.4}$$

Basically, staying near $\mathbf{x}_*$ initially means staying near it at all future times. If the equilibrium is locally stable, and it also holds that

$$||\mathbf{x}(t) - \mathbf{x}_*|| \to 0 \tag{2.5}$$

as $t \to \infty$, it is called locally asymptotically stable. This means that not only will the system stay at the fixed point, but it will also converge to it from any of point of a certain vicinity, called the basin of attraction. The fixed point is then also called an attractor [8].

From the perspective of linear stability analysis, the local stability of fixed points is determined by the eigenvalues λ_i of the Jacobian matrix $J = \frac{\partial f}{\partial \mathbf{x}}|_{\mathbf{x}=\mathbf{x}_*}$. A fixed point is

- locally stable if $\text{real}(\lambda_i) \leq 0 \ \forall i$,

- locally asymptotically stable if $\text{real}(\lambda_i) < 0 \ \forall i$,

- and unstable if $\text{real}(\lambda_i) > 0$ for any i.

In the case of locally asymptotic stability, complex eigenvalues allow oscillatory convergence towards the attractor [8].

2.2 COMPARTMENTAL MODELS OF DISEASE SPREAD

2.2.1 *The SIR model*

The basis for the mathematical models in chapter 4, chapter 5, and chapter 6 that describe the spread of COVID-19 in the population is the class of so-called compartmental models. It refers to a special case of a more general mathematical theory of infectious disease spread established in 1927 [9].

Compartmental models divide the population of size N into compartments, with each compartment representing people being in a specific stage of the disease. The most basic compartmental model is the SIR model, which consists of three compartments: susceptible to being infected with the pathogen causing the disease (S), infected (I), and recovered from the disease (R) (Figure 2.1). Between these compartments, people can transition with specific rates and mechanisms, governed by a set of ordinary differential equations with respect to time t [10]:

$$\frac{dS}{dt} = -\beta SI/N, \tag{2.6}$$

$$\frac{dI}{dt} = \beta SI/N - \gamma I, \tag{2.7}$$

$$\frac{dR}{dt} = \gamma I, \tag{2.8}$$

where β is the effective contact rate (i.e., the number of contacts per person per time multiplied by the probability of disease transmission in a contact between a susceptible and an infectious subject), and γ is the recovery rate (i.e., the proportion of infected individuals who recover from the disease per unit of time).

The first equation signifies the rate of change of susceptible individuals in the population. It shows that the number of susceptible individuals
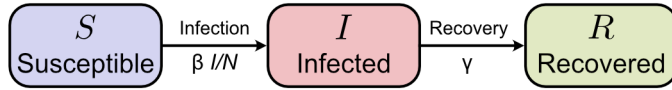
Figure 2.1: **SIR model.** In a compartmental model such as this one, individuals of a population transition between the compartments with certain transition rates and mechanisms.

decreases over time at a rate proportional to the number of susceptible individuals, the number of infected individuals, and the effective contact rate. This decrease in susceptible people is reflected in an equivalent increase in infected people in the second equation. However, the number of infected also decreases at a constant recovery rate, increasing the number of recovered in the third equation.

As $N = S + I + R$ is constant, the first two differential equations are sufficient to describe the system. It is easy to see that the system has a trivial fixed point $(S_*, I_*) = (N, 0)$. In epidemiological terms, this represents a disease-free equilibrium. As explained in Section 2.1, the corresponding Jacobian matrix

$$J = \begin{pmatrix} 0 & -\beta \\ 0 & \beta - \gamma \end{pmatrix} \tag{2.9}$$

can tell us about the local stability of the equilibrium. For a two-dimensional matrix, the eigenvalues are negative iff the trace is negative and the determinant is positive, and non-positive iff the trace is non-positive and the determinant non-negative. As the trace $\operatorname{tr}(J) = \beta - \gamma$ and the determinant $\det(J) = 0$, we can deduce that the disease-free equilibrium is locally stable if $\beta \leq \gamma$ and unstable otherwise. This means that if $\beta \leq \gamma$, an introduction of a few infected individuals into the population will not cause an outbreak and vice versa.

2.2.2 *Reproduction numbers*

To further determine the dynamics of a compartmental model, we want to analyse an outbreak in a completely susceptible population from a different perspective. At the beginning of an outbreak, it holds that $S \approx N$. This leads to the further simplified equation

$$\frac{dI}{dt} = (\beta - \gamma)I \tag{2.10}$$

with the solution

$$I(t) = I_0 \exp\left((\beta - \gamma)t\right), \tag{2.11}$$
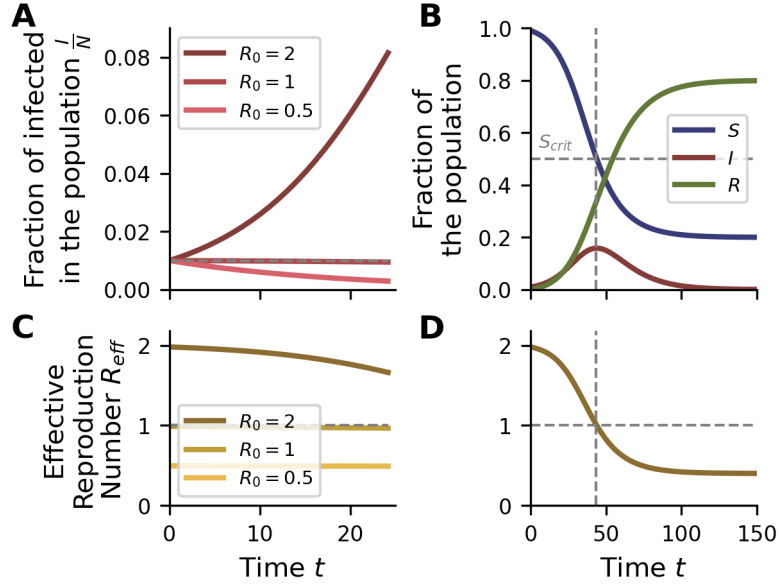
Figure 2.2: **SIR-Dynamics.** The recovery rate is set to $\gamma = 0.1$ for every simulation. The effective contact rate β is varied to receive different basic reproduction numbers $R_0 = \beta/\gamma$. **A:** At the beginning of an outbreak, R_0 is able to describe the evolution of the infected compartment I. For $R_0 > 1$ there is exponential growth. At the phase transition $R_0 = 1$, the number of infected stays constant. For $R_0 < 1$ there is exponential decay. **B:** For $R_0 > 1$, the number of infected individuals peaks when the number of susceptible individuals S reaches S_{crit}. **C:** In general, the dynamics are governed by the effective reproduction number R_{eff} that is close to R_0 when most of the population is susceptible, but decreases as the susceptible compartment becomes smaller. **D:** When R_{eff} is larger than one, the number of infected increases. When it falls under one, the number of infected decreases.

with the initial number of infected people I_0.

The initial growth rate can be rewritten as

$$\beta - \gamma = \gamma(R_0 - 1), \tag{2.12}$$

introducing the basic reproduction number $R_0 = \frac{\beta}{\gamma}$. This number essentially describes the average number of individuals an infected individual infects until immunity and determines where the phase transitions of the system occur. Equivalent to the linear stability analysis above, if $R_0 > 1$, there is an exponential increase in infected individuals (Figure 2.2**A, B**, dark red line). If $R_0 < 1$, the number of infected will decrease exponentially (Figure 2.2**A**, medium red line). Lastly, if $R_0 = 1$, the number of infected will be constant because every infected individual infect exactly one other individual [10] (Figure 2.2**A**, light red line).

However, once the approximation $S \approx N$ does not hold anymore, it becomes necessary to consider that not every potential interaction of an infected individual is with a susceptible person. Only $\frac{S}{N}$ of all contacts will be potentially contagious. Hence, one defines the effective reproduction number

$$R_{\text{eff}} = R_0 \frac{S}{N}, \tag{2.13}$$

whose values govern the dynamics analogously to R_0 (Figure 2.2**C, D**). I.e. when the critical value of $R_{\text{eff}} = 1$ is reached, the number of infected will peak [10] (Figure 2.2**B, D**). It is easy to determine the number of susceptible at this point:

$$R_{\text{eff}} = R_0 \frac{S}{N} \overset{!}{=} 1 \quad \Rightarrow \quad S_{\text{crit}} = \frac{N}{R_0}. \tag{2.14}$$

Although this simple model can perform quite well in describing the beginning of an outbreak (e.g. [11]), it is often not able to represent the further course of an outbreak (e.g. [12]). To correctly interpret insights from analysing and using this model it is therefore important to be aware of the underlying (simplifying) assumptions, e.g., [9, 10]:

- The term $\beta S I$ suggests that the population 'mixes perfectly', i.e. it is assumed that any member of the population has an equal chance to meet any other member of the population.

- The population is homogeneous, i.e. every individual has the same effective contact rate β and the same recovery rate γ.

- The transition rates β and γ are constant factors. This implies that, e.g., the behaviour of the population stays the same throughout the outbreak.

- Recovered individuals become immune to reinfections and there is no waning of this immunity.

- Vital dynamics, i.e. births and deaths due to other reasons, happen on a longer time-scale than the infectious disease dynamics and are therefore negligible.

However, the SIR model can be further extended and modified to represent scenarios where the model assumptions do not hold or more complex mechanisms, such as recovery or vital dynamics, need to be considered. This can be achieved by including more or different compartments and modelling more (non-linear) transitions, which we did in chapter 4, chapter 5 and chapter 6. It is important to note here,
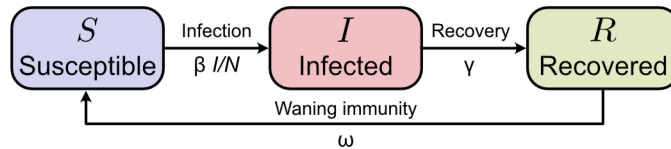
Figure 2.3: **SIRS model.** Compared to the SIR model, the immunity of recovered individuals wanes over time.

however, that more details to a model do not necessarily make it better: the more degrees of freedom the more difficult it becomes to understand the dynamics of the system. More mechanisms will also need more data to validate them. In the end, one should use a model that is only as complex as necessary for the research question at hand.

2.3   FEEDBACK LOOPS IN DYNAMICAL SYSTEMS

2.3.1   *Positive and negative feedback loops*

An example of the type of modifications to compartmental models is the introduction of feedback loops. They are fundamental mechanisms that govern the behavior of many dynamical systems, from biological systems (e.g. [13]), climate systems (e.g. [14]), to social (e.g. [15]) and economic systems (e.g. [16]). A feedback loop occurs when the output of a system is used as its own input. There are two main types of feedback loops: positive feedback loops and negative feedback loops [13].

In a positive feedback loop, the output of a system is amplified, leading to further increase in the output. This can result in exponential growth (e.g. [17]) or other forms of system instability (e.g. [18]). We have already encountered positive feedback loops in the SIR model (Equation 2.6): The exponential growth of infected I for $R_0 > 1$ at the beginning of an outbreak stems from infected people causing more infections through $\frac{dI}{dt} \propto I$, which cause even more infections (Figure 2.2**A**, dark red line).

Negative feedback loops, on the other hand, serve to stabilize the system. In these loops, an increase in output leads to mechanisms that reduce that output [19]. In the context of the SIR model, we get a negative feedback loop if $R_0 < 1$: The infected people recover more quickly than they are able to infect others, resulting in fewer infected, and so on (Figure 2.2**A**, light red line).

2.3.2 *Waning immunity and the SIRS model*

The SIR model also entails another negative feedback: Rising infection numbers reduce the susceptible compartment and thereby result in fewer further infections. Ultimately, this negative feedback counteracts the discussed positive feedback loop and stabilises the system in the form of ending the spread of the disease (Figure 2.2**B**). However, if recovered do not stay immune indefinitely but their immunity wanes with rate ω, the negative feedback is cancelled out and the dynamics change. We can derive this using an SIR model with waning immunity, also called *SIRS* model [10] (Figure 2.3):

$$\frac{dS}{dt} = -\beta SI/N + \omega R, \tag{2.15}$$

$$\frac{dI}{dt} = \beta SI/N - \gamma I, \tag{2.16}$$

$$\frac{dR}{dt} = \gamma I - \omega R. \tag{2.17}$$

As the population size $N = S + I + R$ is assumed constant, the system of ordinary differential questions reduces to

$$\frac{dS}{dt} = -\beta SI/N + \omega(N - S - I), \tag{2.18}$$

$$\frac{dI}{dt} = \beta SI/N - \gamma I. \tag{2.19}$$

This system has a non-trivial fixed point if $R_0 > 1$ (Figure 2.4):

$$\frac{dS}{dt} = -\beta SI/N + \omega(N - S - I) \overset{!}{=} 0, \tag{2.20}$$

$$\frac{dI}{dt} = \beta SI/N - \gamma I \overset{!}{=} 0 \tag{2.21}$$

$$\Rightarrow (\bar{S}, \bar{I}) = \left(\frac{\gamma}{\beta}, \frac{\omega(N - \frac{\gamma}{\beta})}{\omega + \frac{\gamma}{N}} \right). \tag{2.22}$$

This fixed point is locally asymptotically stable because the corresponding Jacobi matrix

$$\begin{pmatrix} -\beta \bar{I}/N - \omega & -\beta \bar{S}/N - \omega \\ \beta \bar{I}/N & 0 \end{pmatrix} \tag{2.23}$$

has a negative trace and a positive determinant. In epidemiological terms, we get an endemic state [10].

Waning immunity also plays a crucial role in chapter 5. However, due to other feedbacks and phenomena in that model, there is no endemic equilibrium but multiple waves of infections.
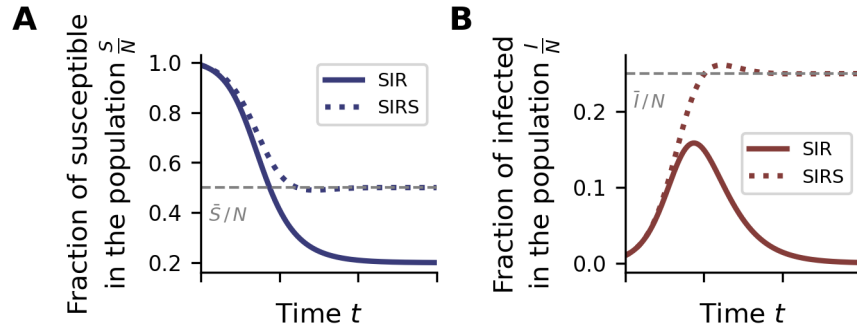
Figure 2.4: **Endemic state in the SIRS model.** Including waning immunity in the SIR model, introduces a positive feedback causes the initial outbreak to stabilise into a state with non-zero fraction of infections. The fix point $(\bar{S}, \bar{I})$ is locally asymptotically stable.

In general, feedbacks and feedback loops, particularly when they interact, can give rise to complex dynamics: ranging from multi-stability (e.g. [19]), to oscillations (e.g. [20]), to chaos (e.g. [21]). Hence, understanding these feedback mechanisms is crucial in understanding the behavior of the system as a whole. In chapter 5, the feedback loop between disease spread and human behaviour is analysed in detail.

2.4 PID CONTROL

Feedback loops can also be actively introduced into systems to control or stabilise the output and outcome. Proportional-integral-derivative (PID) control is one of the most widely used feedback control algorithms in the field of control systems. In essence, PID control adjusts the inputs to a system based on the difference between the desired and actual output u, known as the error signal e [22] (Figure 2.5**A**).

The proportional term u_p in PID control responds to the present error. The controller output is proportional to the current error, with the proportionality constant being the gain k_p [22]:

$$u_p(t) = k_p\, e(t). \tag{2.24}$$

The higher the gain, the stronger the response to error. However, high gains can cause the system to become unstable. If the gain is too low, the system may stabilise with a residual steady-state error (Figure 2.5**B**, light purple line).
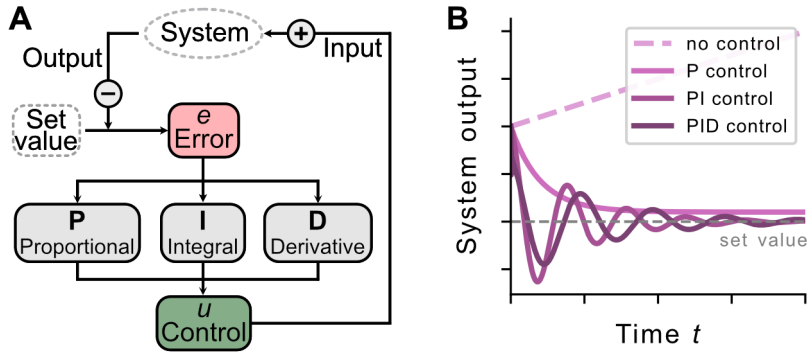
Figure 2.5: **PID control. A:** Schematic overview of the PID control feedback loop. **B:** Effects of the PID components. Without PID control, the example system produces constantly increasing output. The proportional feedback P brings the system close to the set value, but stabilises with an off-set (light purple line). Adding the integral feedback I removes this off-set, but causes oscillations (medium purple line). Adding the derivative term D dampens these oscillations (dark purple line).

The integral term u_i can eliminate this error by responding to past errors. It integrates the error over time, which means it is sensitive to how long the error has persisted. Its gain is denoted by k_i [22]:

$$u_i(t) = k_i \int^t e(t') \, dt'. \tag{2.25}$$

However, a strong integral gain causes the control to lag behind, leading to oscillations (Figure 2.5**B**, medium purple line).

The derivative term u_d can dampen these oscillations by predicting future errors based on the current rate of change of the error and being proactive in response (Figure 2.5**B**, dark purple line). It is characterized by the derivative gain k_d [22]:

$$u_d(t) = k_d \frac{d}{dt} e(t). \tag{2.26}$$

Together they make up the total control input

$$u(t) = u_p(t) + u_i(t) + u_d(t). \tag{2.27}$$

How does a PID control feedback loop affect the dynamics of an SIR model? For illustration, we imagine a scenario where the fraction of infected should stabilise around some set point I_{set} through the implementation and lifting of non-pharmaceutical interventions. To model these interventions with PID control, we understand the difference of the current number of infections to the set point as the error $e(t)$ and add the control term $u(t)$ to the differential equation for $I(t)$ (Equation 2.6). For certain parameter choices, we observe dampened
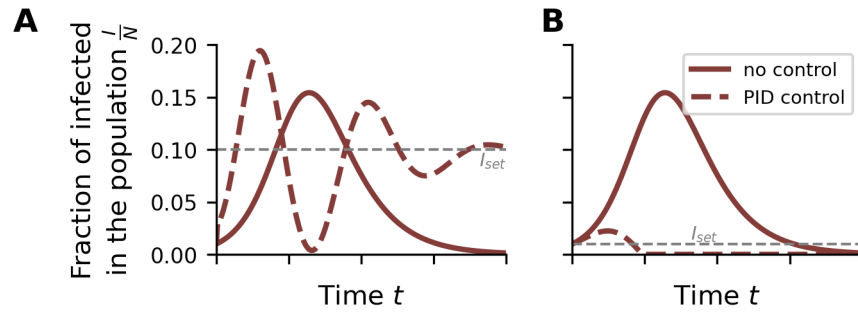
Figure 2.6: **PID control in an SIR model. A:** Incorporating PID control in a compartmental model can lead to dampened oscillations towards some chosen set point I_{set}. **B:** However, if I_{set} is chosen low enough, the PID control will end the outbreak. Here, $\frac{I_{\text{set}}}{N} = 0.01$ is chosen, which is also the initial fraction of infected.

oscillations around the set point (Figure 2.6**A**). If I_{set} is chosen small enough, there are no oscillations, but a forced end of the outbreak (Figure 2.6**B**). Different parameter choices can also lead to reoccurring outbreaks or reaching of the set value without oscillations [23]. In chapter 4, we use PD control in a more complex setting to model the implementation of non-pharmaceutical interventions to limit the number of patients in intensive care units.

Part II

DISEASE SPREAD, INTERVENTIONS, AND HUMAN BEHAVIOUR: THE EXAMPLE OF THE COVID-19 PANDEMIC

A LOOK INTO THE FUTURE OF THE COVID-19 PANDEMIC IN EUROPE: AN EXPERT CONSULTATION

This chapter is identical to the article [3]. The Methods can be found in Appendix A. The article is published in

Iftekhar, E.N., Priesemann, V., Balling, R., Bauer, S., Beutels, P., Calero Valdez, A., Cuschieri, S., Czypionka, T., Dumpis, U., Glaab, E. et al., A look into the future of the COVID-19 pandemic in Europe: an expert consultation, The Lancet Regional Health–Europe, 8 (2021),

under the terms of a Creative Common License (http://creativecommons.org/licenses/by/4.0/).

I am the first author of this publication. Roles: Conceptualisation, Methodology, Project Administration, Writing – original draft, Writing – review & editing.

Viewpoint

A look into the future of the COVID-19 pandemic in Europe: an expert consultation

Emil Nafis Iftekhar[a], Viola Priesemann[a,*], Rudi Balling[b], Simon Bauer[a], Philippe Beutels[c], André Calero Valdez[d], Sarah Cuschieri[e], Thomas Czypionka[f], Uga Dumpis[g], Enrico Glaab[b], Eva Grill[h], Claudia Hanson[i], Pirta Hotulainen[j], Peter Klimek[k], Mirjam Kretzschmar[l], Tyll Krüger[m], Jenny Krutzinna[n], Nicola Low[o], Helena Machado[p], Carlos Martins[q], Martin McKee[r], Sebastian Bernd Mohr[a], Armin Nassehi[h], Matjaž Perc[s], Elena Petelos[t], Martyn Pickersgill[u], Barbara Prainsack[v], Joacim Rocklöv[w], Eva Schernhammer[x], Anthony Staines[y], Ewa Szczurek[z], Sotirios Tsiodras[aa], Steven Van Gucht[ab], Peter Willeit[ac]

[a] *Max Planck Institute for Dynamics and Self-Organization, Göttingen, Germany*
[b] *University of Luxembourg, Luxembourg, Luxembourg*
[c] *University of Antwerp, Antwerp, Belgium*
[d] *RWTH Aachen University, Aachen, Germany*
[e] *University of Malta, Msida, Malta*
[f] *Institute for Advanced Studies, Vienna, Austria, and London School of Economics, London, UK*
[g] *Pauls Stradins Clinical University Hospital, University of Latvia, Riga, Latvia*
[h] *Ludwig-Maximilians-University München, München, Germany*
[i] *Karolinska Institute, Stockholm, Sweden, and London School of Hygiene & Tropical Medicine, London, UK*
[j] *Minerva Foundation Institute for Medical Research, Helsinki, Finland*
[k] *Medical University of Vienna, Vienna, Austria, and Complexity Science Hub Vienna, Vienna, Austria*
[l] *University Medical Center Utrecht, Utrecht, The Netherlands*
[m] *Wroclaw University of Science and Technology, Wroclaw, Poland*
[n] *University of Bergen, Bergen, Norway*
[o] *University of Bern, Bern, Switzerland*
[p] *Institute for Social Sciences, University of Minho, Braga, Portugal*
[q] *Department of Community Medicine, Health Information and Decision Sciences of the Faculty of Medicine, University of Porto, Porto, Portugal*
[r] *London School of Hygiene & Tropical Medicine, London, UK*
[s] *University of Maribor, Maribor, Slovenia, and Department of Medical Research, China Medical University Hospital, China Medical University, Taichung, Taiwan*
[t] *University of Crete, Crete, Greece, and Maastricht University, Maastricht, The Netherlands*
[u] *University of Edinburgh, Edinburgh, UK*
[v] *Department of Political Science, University of Vienna, Vienna, Austria*
[w] *Department of Public Health and Clinical Medicine, Section of Sustainable Health, Umeå University, Umeå, Sweden*
[x] *Medical University of Vienna, Vienna, Austria*
[y] *Dublin City University, Dublin, Ireland*
[z] *University of Warsaw, Warsaw, Poland*
[aa] *National and Kapodistrian University of Athens, Athens, Greece*
[ab] *Sciensano, Brussels, Belgium*
[ac] *Medical University of Innsbruck, Innsbruck, Austria, and University of Cambridge, Cambridge, UK*

ARTICLE INFO

ABSTRACT

How will the coronavirus disease 2019 (COVID-19) pandemic develop in the coming months and years? Based on an expert survey, we examine key aspects that are likely to influence the COVID-19 pandemic in Europe. The challenges and developments will strongly depend on the progress of national and global vaccination programs, the emergence and spread of variants of concern (VOCs), and public responses to non-pharmaceutical interventions (NPIs). In the short term, many people remain unvaccinated, VOCs continue to emerge and spread, and mobility and population mixing are expected to increase. Therefore, lifting restrictions too much and too early risk another damaging wave. This challenge remains despite the reduced opportunities for transmission given vaccination progress and reduced indoor mixing in summer 2021. In autumn

* Corresponding author.
E-mail address: viola.priesemann@ds.mpg.de (V. Priesemann).

2021, increased indoor activity might accelerate the spread again, whilst a necessary reintroduction of NPIs might be too slow. The incidence may strongly rise again, possibly filling intensive care units, if vaccination levels are not high enough. A moderate, adaptive level of NPIs will thus remain necessary. These epidemiological aspects combined with economic, social, and health-related consequences provide a more holistic perspective on the future of the COVID-19 pandemic.

1. Introduction

More than a year after the World Health Organization declared the coronavirus disease 2019 (COVID-19) a Public Health Emergency of International Concern, Europe continues to struggle with it. Although future developments are highly uncertain, we aim to provide (a) a systematic assessment of the factors that will affect the course of the COVID-19 pandemic in Europe, and (b) a tentative forecast of how the pandemic may evolve prior to coming to an end in Europe. We chose a method inspired by the Delphi method of forecasting [1] as the most suitable way to elicit expert opinions about key developments and themes regarding the COVID-19 pandemic. The facilitators developed questionnaires with open-ended questions and asked scientists from various European countries, disciplines, and research fields, to provide their input and predictions. As the guiding questionnaires were focussed on epidemiology, virology, public health, and social science, some other important perspectives, such as those of clinical medicine, economics, and the humanities, are not covered in great detail (see SI). Here we set out the results of the expert consultation—outlining salient commonalities and divergent responses. Of necessity, this paper represents a partial synthesis of the rich and diverse contributions, and not all authors necessarily agree in detail with every single statement.

We first summarize insights on three critical factors that shape the development of the epidemic: population immunity and vaccination, variants of concern (VOCs), and public responses to pandemic policy. Second, we present scenarios based on the available knowledge as of April 2021 for three distinct time periods: for (a) summer 2021, (b) autumn and winter 2021, and (c) for a period of 3−5 years from spring 2021. For the latter period, we give a high-level overview of the consequences of the COVID-19 pandemic for health, society, and the economy. In the last section, we elaborate in more detail on central topics mentioned in the main text: long-term strategy, vaccination coverage, organization of mass vaccinations, waning immunity, evolution of the virus, improving adherence, airborne transmission, and One Health. We hope that the insights of our synthesis will serve as a scientific basis for policy debates by generating a comprehensive overview of key considerations in moving beyond the pandemic, while informing other foresight studies.

2. Key factors determining the course of the pandemic

Our starting point is the situation as of spring 2021. During the COVID-19 waves in winter 2020−2021, many European countries experienced high numbers of infections that, in some places, overwhelmed hospitals. This was partly due to insufficient ICU capacity in some countries [2]. Delayed responses and lower effectiveness of non-pharmaceutical interventions (NPIs) compared to the first wave also played a part [3]. Even countries that have had relatively few cases and a low death toll until then were hit severely in the winter. As of early 2021, Europe is experiencing another surge in cases, which appears to have peaked in April 2021. The emergence and severity of these waves has varied greatly across Europe (see Figs. 1 and 2). The future development of the pandemic will also likely be heterogeneous. In the following sections we focus on three key factors that contribute to this heterogeneity.

2.1. Population immunity and vaccination

Population immunity (also referred to as herd immunity) describes a situation in which enough people in the population are immune to a pathogen, such that it is not able to spread widely (WHO, 2020a). The proportion of immune people in the population needed to reach population immunity in a given country is mainly driven by the infectivity of severe acute respiratory syndrome coronavirus 2 (SARS-CoV-2) and the ability of either past natural infection or vaccines to reduce transmission [4]. Models that assume basic reproduction numbers of 2.5−3.5 have previously estimated that transmission-blocking immunity of 60−72% of the population is required in the case of SARS-CoV-2 [5,6]. This figure is higher for more transmissible variants. Therefore a *minimum* immunization level of 80% of the entire population is likely to be required [7,8]. This figure would be difficult to achieve with vaccination alone if vaccines are not fully protective against infection or prevent onward transmission. Furthermore, immunization needs to be homogeneous across all population groups, otherwise pockets of transmission can prevail. To achieve this goal, one might consider mandatory vaccinations - the effectiveness of which remains contested, as vaccination uptake depends on a complex interplay of different factors [9,10]. A 2016 systematic review found that mandatory childhood vaccination policies were associated with improved uptake [11], a finding supported by later experience in Italy [12,13]. However, there are many legal, ethical, cultural, and technical issues involved and it has been argued that it should only be considered when all other reasons for low uptake, such as accessibility, have been addressed and the decision should take account of the particular context and the risk of unintended consequences [9,14-17]. In any case, for the short term it is more important to distribute available vaccines to locations where they are most needed [18].

One contribution to population immunity comes from so-called natural immunity, as a result of prior infection with SARS-CoV-2 and potentially by cross-immunity due to prior exposure to other coronaviruses [19,20]. The fraction of those who are naturally immune in the population varies widely between European countries. However, in all countries the majority of the population remained susceptible to infection [21].

In individuals who have had a SARS-CoV-2 infection, antibodies have been shown to persist for up to nine months after infection [22]. About 95% of people retain immune memory at six months after infection [23-25]. This indicates that the likelihood of reinfection and severe disease progression is low in this time frame, but reinfection is still possible [26-28].

The second, major, contributor to population immunity is vaccination. The first vaccines are, as of April 2021, licensed for use in adults and the vaccines appear to reduce infections by varying amounts, typically in the 80−90% range for mRNA vaccines (after two doses) [29-31] and potentially lower for others [32,33]. Vaccines are, however, still likely to reduce transmissibility even if breakthrough infection occurs [34]. Importantly, they seem especially likely to prevent severe symptoms and hospitalization, reaching relative risk reductions of about 70−95% [30,32,35-37]. The progress of vaccination programs is continuing in Europe (see Fig. 3) [38].

The chances of achieving high vaccination coverage depend on a multitude of factors including political leadership, trust in public
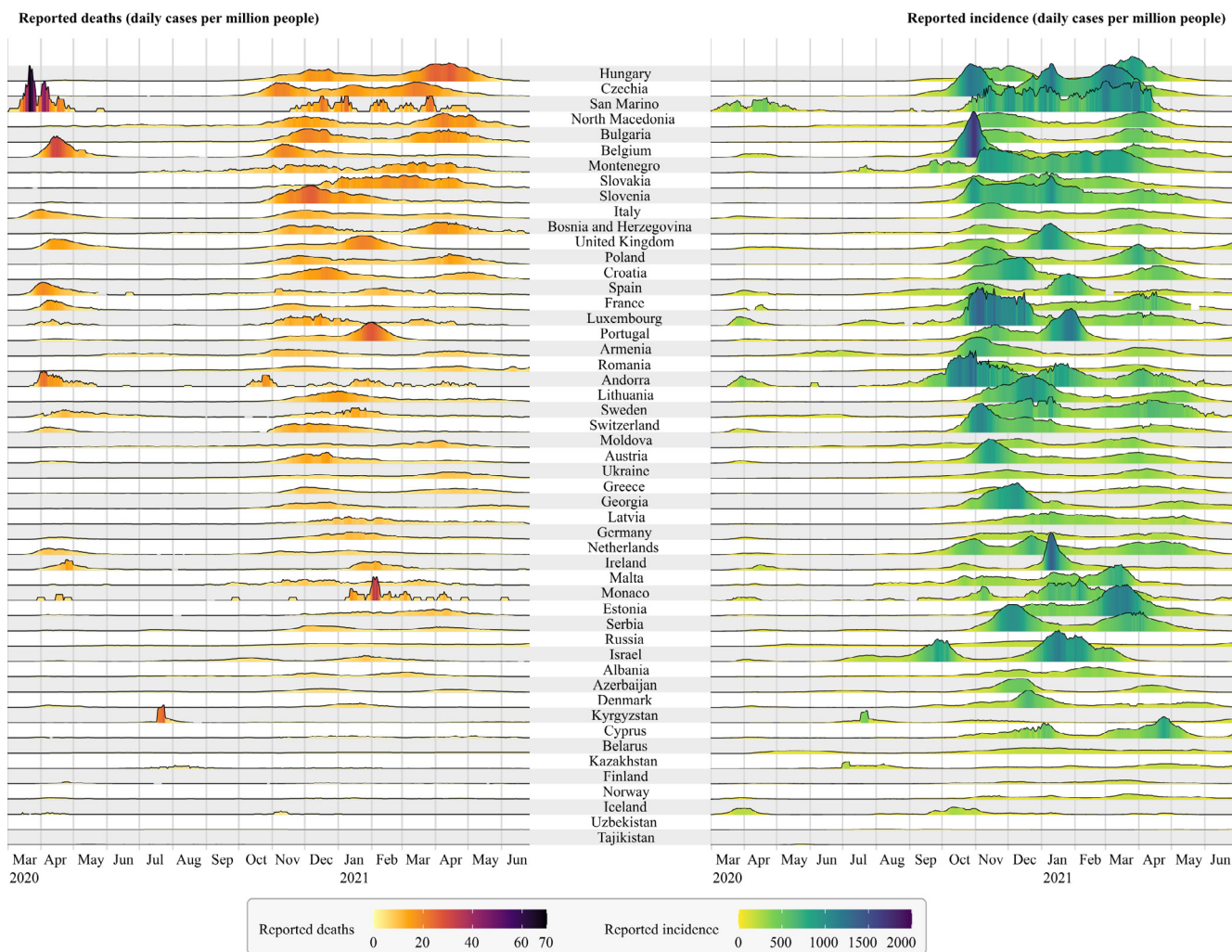
Fig. 1. Comparison of the COVID-19 pandemic in all countries of the WHO European Region (except for Turkey and Turkmenistan, as there was no appropriate data available in the data set). Countries are ordered from top to bottom with a decreasing cumulative number of COVID-19 related deaths per million people. The y-axis scale of the ridgeline plots is the same for all countries for reported deaths and incidence, respectively. Even though reported numbers are associated with wide uncertainty, the differences between countries and waves are evident. Data source: https://corona-api.com (Accessed: June 28, 2021).

health and other public authorities, access to and eligibility for vaccines, and vaccine acceptance. The last is especially crucial. As of April 2021, acceptance is lower for the non-mRNA-vaccines with lower reported efficacies. Repeatedly changing policy recommendations and constant media coverage further unsettled people, especially after evidence of possible links to rare adverse, sometimes fatal, side-effects emerged mid-rollout for the AZD1222 (AstraZeneca) and Ad26.COV2.S (Johnson & Johnson) vaccines [39,40]. Among older people and the most vulnerable, who have been receiving the vaccine in the initial phase, vaccine uptake has been generally high [41,42]. In younger age groups, willingness to get vaccinated appears lower [43,44]—in France, only about 40% of the working age population currently plan to accept a vaccine [45]. Moreover, vaccine uptake in the groups of healthcare workers is rather disconcerting in some countries—e.g., Belgium and France—has been low [46–48]. However, perception of increasing vaccine uptake might motivate those who are hesitant [49]. To conclude, the issue of vaccine uptake presents an ever-changing situation [50].

2.2. Variants of concern

VOCs are so called because they harbour certain mutations that have consequences for SARS-CoV-2 pathogenicity. Existing and newly emerging SARS-CoV-2 VOCs are challenging because,

compared to the original variant, they may increase transmissibility or severity, prolong the duration of the infectious period, shorten the duration of post-infection immunity, or escape host immune responses to natural infection or to vaccines. They could also affect diagnostic testing accuracy, the spectrum of detectable symptoms, and therapeutic management. The frequency and the spectrum of variants of SARS-CoV-2 will depend on functional constraints and evolutionary pressure.

The Alpha (B.1.1.7) variant, which was first detected in the United Kingdom, demonstrated enhanced transmissibility [51,52], a longer duration of acute infection [53], a higher hospitalization rate [54], and probably a higher infection fatality rate than previously circulating variants [51,55-57]. The Beta (B.1.351) variant, which was first detected in South Africa, exhibits higher transmissibility [58], while the impact on disease severity of this variant remains uncertain as of April 2021 [59]. The Beta and Gamma (P.1) variants, the latter originated in Brazil, seem to partially evade the immune response of previously infected individuals [26,60]. In Europe, the Alpha variant became the dominant variant in December/January 2020 in, e.g., the UK, Ireland and Portugal, and in February/March 2021 in, e.g., France and Germany [61]. In contrast, the Beta and Gamma variants have not become widely distributed in Europe so far. The Delta (B.1.617.2) variant appears to be more transmissible than previous strains [62].

Fig. 2. Comparison of the COVID-19 pandemic in a selection of European countries grouped by geographical proximity. Many differences in reported incidence, reported deaths and excess mortality can be observed. Even though reported numbers are associated with wide uncertainty, the differen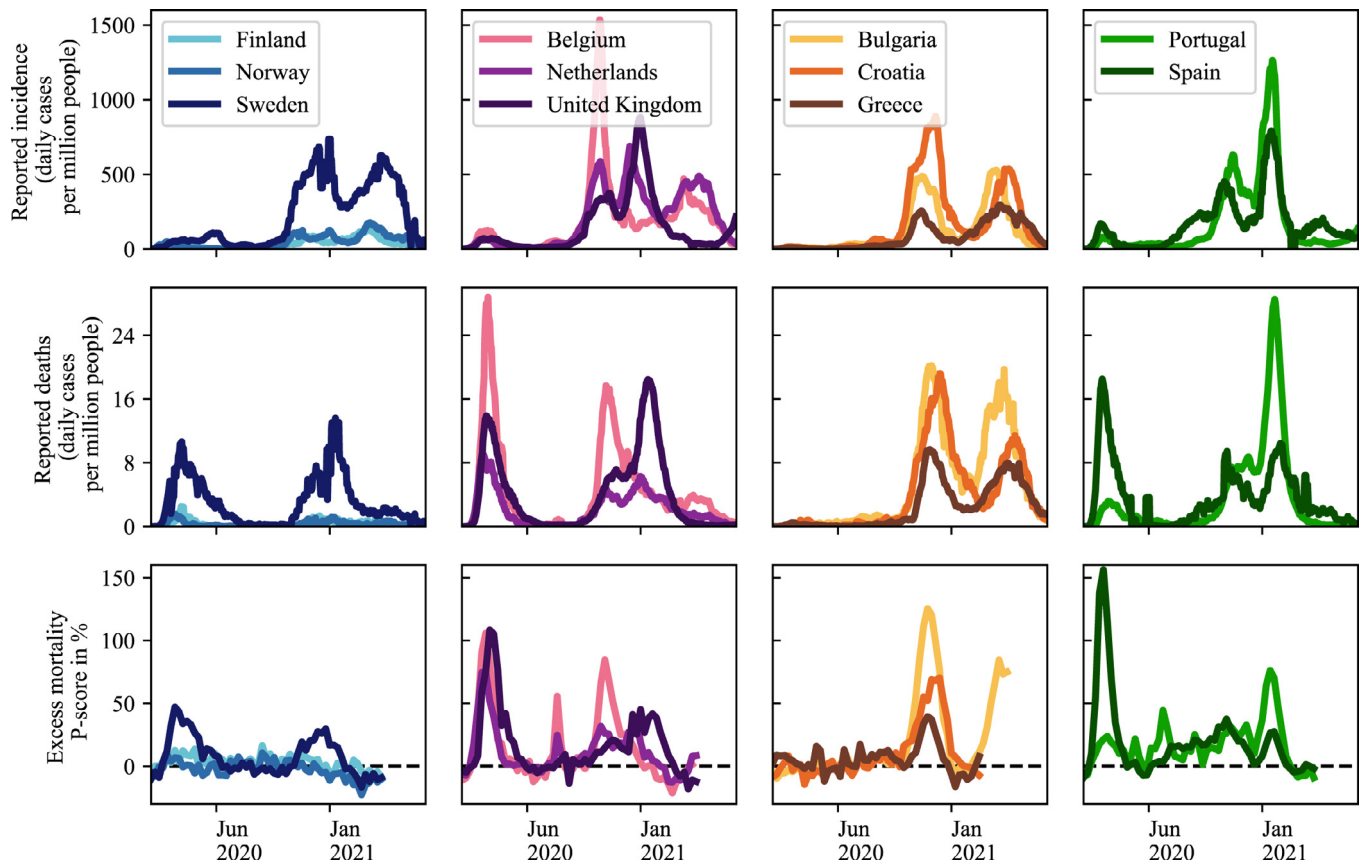ces between countries and waves are evident. Data sources: https://ourworldindata.org/covid-cases and https://ourworldindata.org/excess-mortality-covid (Accessed: June 29, 2021).

There is uncertainty about the efficacy of available vaccines in relation to VOCs. Current vaccines appear to be effective against Alpha [29,31]. However, there is some evidence that the efficacy of some vaccines might be reduced for Beta, Gamma, and Delta [32,62-64]. It remains unclear to which degree this is the case, and how much the protection against severe courses of disease might be affected.

The more infections are present in the human population, the higher the rate of mutation. This can lead to selection for VOCs with transmission advantage or, in places with high rates of natural or vaccinal immunity, VOCs with escape mutations. In countries without well established genetic surveillance, this may permit uncontrolled spread. In this case, vaccines will need to be updated to protect against these new VOCs, with the consequent requirements to gain approval, be manufactured, and distributed anew. However, the more widespread infections are, the more mutations will occur that could end up with an evolutionary advantage. Consequently, the best safeguard is to reduce transmission. Only after sufficient global vaccination coverage will the mutation rate decrease due to lower viral spread in the post-pandemic phase [8].

2.3. Public responses to pandemic policy

As long as population immunity has not been reached, maintaining appropriate and widely accepted levels of NPIs to mitigate the spread remains crucial [65,66]. When there is a rise in infections, NPIs must be reimplemented or strengthened; the earlier this is done, the more effective it is [67]. However, the resoluteness and timeliness with which NPIs are being implemented and remain in place depends on leadership and public opinion [68]. Moreover, the

higher the efficacy of NPIs the more the public accept and support them [69].

As of spring 2021, pandemic policies are not being received well in many parts of Europe [70]. A range of factors likely contribute to this, including continued high economic [71-73] and psychological burdens [74-79], inadequate risk communication [80-83], the lack of transparent long-term strategies from governments [68], increasing vaccination coverage (see Fig. 3) and a general erosion of trust [84-88]. All this results in lower adherence to rules and recommendations for mitigating the spread of SARS-CoV-2 compared to the first wave [70,89].

The effectiveness of rules and recommendations depends on the ability and willingness of the population to adhere to them [81]. Adherence in the past year has varied from country to country. In some countries, adherence was initially quite high in general [89-93]. In others, there have been strong protests against measures, sometimes resulting in their relaxation [94-96]. In general, voluntary adherence will be more likely if the necessity for and strategy behind instituted measures is communicated clearly and systematically, and if interpersonal trust and public trust in government is higher [70,97-100]. However, if COVID-19-induced morbidity and mortality reaches levels that societies deem intolerable, acceptance of NPIs rises again [70]

Given these key factors underlying the future evolution of the pandemic, we can consider what to expect in the future, beginning with the summer of 2021.

3. The perspective for the summer of 2021

Summer 2021 is likely to bring some relief in Europe as people spend more time outside [101], vaccination proceeds, and control
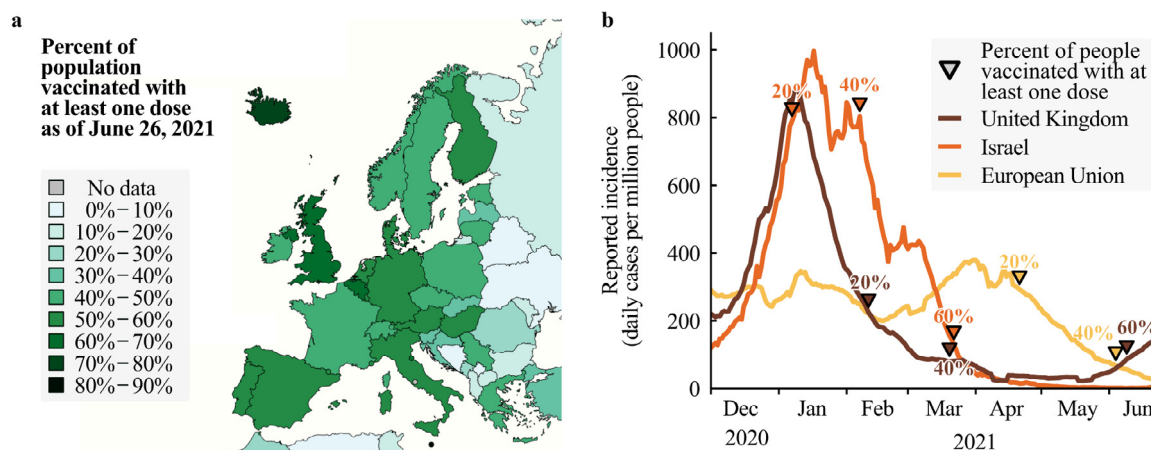
Fig. 3. Vaccination progress in Europe. **a.** Fraction of the population having received at least one dose of COVID-19 vaccines in Europe as of June 26, 2021. There are large differences in vaccination coverage. **b.** Reported incidence (lines) and reached vaccination milestones (triangles) since the start of vaccination programs. Data source: https://ourworldindata.org/covid-vaccinations (Accessed: June 29, 2021).

strategies improve, e.g., via improved availability and variety of testing technology [102]. The expected relief might be compromised if the combination of natural immunity and vaccination coverage is low and relaxation of NPIs is not managed carefully. Furthermore, increased international travel will increase the risk of importing any VOCs that emerge from outside of Europe, and the risk of circulating any VOCs that emerge from within the continent across European nations. If VOCs with an ability to evade immune responses emerge, NPIs may need to be reinstated or strengthened even in populations where relatively high levels of immunity have been achieved. A common European goal to keep infection levels low and to internationally coordinate close surveillance of incidence and viral genomes, especially of infected international travelers, would help to reduce the risk of emergence of VOCs [103].

Once vaccination coverage is deemed sufficiently high by decision makers, countries might come under further pressure to ease measures again. With (most) risk groups vaccinated first, there will be a lower fraction of severe illnesses and deaths related to COVID-19 in the population. Consequently, a lower burden on healthcare systems is also expected. However, some individuals at risk might not (yet) have been vaccinated, protection by vaccination is not perfect and may wane over time, and unvaccinated and possibly some vaccinated people will continue to transmit. This makes it unlikely that restrictions can be lifted *completely* without risking another larger wave. Another wave would result in increased morbidity and mortality of unvaccinated people, or in general those to whom the vaccines did not confer protection [104]. With vaccine strategies first targeting older people, a wave in summer would predominantly hit relatively younger age groups. It would also further strain exhausted healthcare personnel and healthcare systems now functioning beyond capacity for protracted periods of time. Hence, certain mitigation strategies will need to remain in place in an adaptive manner [105]. When considering retaining NPIs, countries might also take the opportunity to achieve low case numbers as, with increasing immunization, the containment of COVID-19 is facilitated. In a situation of low case numbers, an effective test-trace-and-isolate (TTI) system, supported by digital contact tracing apps, further facilitates epidemic control [106]. In such a regime, only a few NPIs, such as wearing (FFP2) masks or basic hygiene measures, might have to stay in place.

To summarise, in the summer of 2021, countries could still be faced with overwhelmed intensive care units and ongoing strict imposition of NPIs. This is a consequence of the limits of the vaccines available, inadequate vaccination coverage, increased mobility across borders and regions, and the possibility of escape variants. However, if a country succeeds in maintaining low case numbers and slows down the influx and spread of any new VOC with sound epidemiological surveillance and reactive measures, then moderately strict NPIs similar to those in summer 2020, or potentially even fewer restrictions, may be possible. The exact extent of NPIs that are necessary to prevent an overburdening of health systems regionally depends on various factors, such as the characteristics of prevalent VOCs and vaccination coverage. A full lifting of all restrictions (e.g., for large indoor gatherings), however, is unlikely to be possible in summer 2021 without risking further outbreaks.

4. The perspective for the autumn and winter of 2021

What can be expected in the autumn and winter of 2021 depends substantially on what happens in the summer; specifically, the success of vaccination programs both in Europe and worldwide, and the emergence and spread of (new) VOCs. Compared to the summer, autumn and winter bring the additional complication of unfavorable seasonal effects.

The seasonality of coronaviruses is expected to increase infections in the autumn and winter months [101,107,108], with increased indoor contacts [109]. Additionally, other seasonal viruses, such as influenza and respiratory syncytial virus, could cause more pressure on health services than in 2020. Since there might be fewer restrictions, and possibly lower-than-usual levels of population immunity because one season of transmission was "skipped", these other seasonal viruses are likely to circulate in greater numbers than in 2020 [110,111]. Overall, the transition to autumn and winter could be problematic because restrictions might have to be tightened again to prevent a rapid rise in case numbers. Based on experiences in several European states in autumn and winter 2020-2021, there is a risk that reintroduction of the necessary public health measures may come too late to succeed in preventing another wave in autumn. It will be the task of governments not to repeat these mistakes.

In the *best-case* scenario, vaccination efforts will have been sufficient to drive down case and fatality numbers substantially, allowing for an almost complete lifting of restrictions. Although vaccination of children aged 12 years and over might have started by this point [112], other groups which have yet to be vaccinated might still suffer from relatively high incidence rates. As the oldest and most vulnerable population groups at highest risk of death from COVID-19 have been prioritised for vaccination, the overall fatality rate in the population and the health burden imposed by SARS-CoV-2 will decline. Hence, the perception of the remaining danger might be low: more than 10% of infected individuals are expected to suffer long-term

sequelae of COVID-19 ("long-COVID") - symptoms of which can include shortness of breath, fatigue, and muscle weakness [113-117].

Assuming increased international mobility due to, in particular, high vaccination coverage, a potential outbreak of a new VOC in one country may spread quickly to others. Without rapid intervention, increased mobility may result in simultaneous outbreaks across countries and regions - potentially putting healthcare systems under high pressure. In light of this danger, a joint effort of all European countries to prevent the emergence and circulation of VOCs seems crucial [118,119].

In short, countries with good access to vaccines and high vaccine uptake can, at worst, expect only modest waves of COVID-19 over the winter when maintaining moderate NPIs (e.g. no large indoor gatherings, face masks, physical distancing, good ventilation, and hygiene). In contrast, countries that have a lower level of vaccination coverage will experience more severe waves unless appropriate NPIs are implemented. Any new VOCs might challenge a successful mitigation or containment strategy, and in case of increased mobility, they are likely to spread quickly.

5. The perspective for the coming 3−5 years

For the coming three to five years, the central questions are: Will we leave the pandemic behind? And if we do—when and how? To what degree will COVID-19 continue to play a role? Regarding the direct health impact of COVID-19, it is possible that it could become a disease that a child will encounter at a young age [120], acquiring a mild infection similar to contracting other coronaviruses. The time scale for this shift is uncertain. Early childhood exposure and recovery may help the immune system to protect the individual, should they encounter the virus again later in life, and should prevent them from experiencing severe symptoms. On the other hand, SARS-CoV-2 (and more so new VOCs) is more infectious and lethal than the known endemic human coronaviruses, and there is the continued risk of long-COVID. Similarities to Chikungunya suggest that long-COVID may become a great burden [121]. However, relief might come from new and improved post-exposure therapeutic options, such as antiviral medication and monoclonal antibodies [122]. Hence, there is mixed evidence whether SARS-CoV-2 will remain a serious threat to health in the long-term.

It is unclear whether eradication of SARS-CoV-2, i.e., a global reduction to zero incidence of infection [123], can be achieved. Global mass vaccination programs might only provide imperfect immunity to some individuals and will usually not reach certain subpopulations, leaving pockets of susceptibility. Transmissions within these subpopulations, the high proportion of asymptomatic COVID-19 infections, and waning of post-infection and vaccine-induced immunity could maintain the circulation of the virus in the global population. Even if eliminated in humans, the multitude of documented non-human hosts [124-127] suggest the virus could remain circulating with ongoing risks of infection of and potential further spread between susceptible human hosts. Furthermore, the virus could mutate within human or non-human hosts to escape immune response, potentially requiring repeated booster vaccinations. In any case, eradicating SARS-CoV-2 would require global political commitment and unified and uniform public assent that eradication is the overarching target. With the smallpox virus, the only virus able to infect humans to have been eradicated, a targeted and globally concerted approach over decades was necessary [128,129], with a particular focus also on reaching deprived populations [130].

Elimination, meaning here a temporary reduction to zero incidence of infection in one region or country through deliberate and continued measures, has been achieved in a small number of countries; e.g., Australia, China, New Zealand, Singapore, and Vietnam. With widespread vaccination, others may try to follow as elimination strategies can offer advantages over mitigation or suppression strategies with continued virus circulation [131]. Assuming that children will also be vaccinated, some of these countries might achieve high enough vaccine uptake to sustainably prevent local transmission. In other countries where immunity in the population is insufficient or too heterogeneous for elimination, SARS-CoV-2 is expected to remain prevalent at a comparatively low level, with recurring local and seasonal outbreaks [120,132]. In the absence of eradication, epidemiological surveillance (and TTI) will need to remain in place and be further improved [53]. The level of immunity in the population will prevent widespread morbidity and mortality, but a significant danger might remain for unvaccinated vulnerable people [4]. A key societal question will be which level of such risk is deemed acceptable when balancing other societal goals.

Finally, Europe faces numerous indirect long-term impacts of the pandemic. Without intending to present a complete list, the consequences include:

Health: During the past year there has been a direct impact on healthcare services in regular care, particularly for patients with chronic conditions [133-135]. This includes reduced access to primary care [136], cancellation of elective medical and surgical procedures [137], and disruptions to screening programs [138,139]. Potential suboptimal healthcare provision for non-communicable diseases might cause a progression of chronic diseases and complications of acute diseases. At-risk populations not sufficiently covered by screening programs might now develop serious disease within a 3- to 5-year period. Hence, further health- and economic burdens (increased sick days, decreased workforce, lost productivity, and increased healthcare costs) might be experienced by some countries due to the rise in the prevalence of non-communicable diseases [140]. With potentially increasing investment into pandemic preparedness, there is a risk of cuts in other public health sectors, aggravating the effects on prevention and chronic disease control. Additionally, the enormous consequences for mental health during this pandemic, especially in young people [75,79], healthcare workers [141], and individuals already suffering from social disadvantage and discrimination [142-145], will have a protracted effect. Whilst the consequences do not appear to extend to higher suicide rates [146], there is the need to redirect services and ensure sound mental health and social care support to the population.

Economy: Although many facets of the economy in some wealthy countries may soon recover [71], others will struggle to overcome the economic crisis. The tourism industry has suffered gravely, endangering livelihoods and economies in countries that depend on it; and driving a widening divide between Northern and Southern Europe [147]. The cultural sector has also been hit economically by the pandemic [148-151]. Public debt has been growing, and this poses a risk to financial stability - especially in countries more strongly hit by the pandemic. Increasing digitalization, and remote and flexible work plans, will potentially change employment [152]. Meanwhile, the legislative and regulatory frameworks for these new forms of work, along with supporting mechanisms (e.g., for sound occupational health), are lagging behind.

Society: Inequalities have been exacerbated because of this pandemic [144,153,154]. This extends well beyond health inequalities [155] to gender [156,157] and educational [158] inequalities. Many children have missed out on extended periods of face-to-face education, as well as general social interaction. At the same time, there has been further erosion of trust between citizens and states through a widening of the socioeconomic gap [145,159-161]. These two factors present a threat to social cohesion and might cause social unrest in the years to come. Furthermore, the narrative of "outside threats" and "secure borders" in discussions about the virus might contribute to the intensification of pre-existing nationalistic and sometimes overtly xenophobic, social and political discourses [162]. The weakened cultural sector might further be challenged by long-lasting

gathering restrictions, eliminating many platforms where communities could approach and engage with these issues. Moreover, a lot of progress on the Sustainable Development Goals, in particular on poverty reduction, will be reversed [163].

Even if the rate of new infections eventually significantly decreases, the health-related, economic and social damages of the pandemic will be felt for a long time.

6. The way forward

We can conclude that COVID-19 will continue to pose many challenges over the coming years. The economic, cultural, and health consequences of the pandemic are already immense and societies may need a long time to recover. The increasing availability of vaccines will bring significant relief over the next months, but if not accompanied with comprehensive strategies and public support they alone will not protect from further damaging outbreaks in the coming years. Limited uptake of vaccines and declining public adherence to NPIs impede the way out of the pandemic and in the worst case new VOCs can render current vaccines less effective.

The eradication, i.e. the complete global elimination, of SARS-CoV-2 seems unlikely. However, even if eradication cannot be achieved, strategies that aim to locally eliminate SARS-CoV-2 might be effective in some settings. If achieved, local elimination offers clear advantages over mitigation or suppression with continued virus circulation, at least until sufficient protection against severe symptoms is granted in the population. A successful strategy for elimination or suppression of SARS-CoV-2 would require a political commitment, unified and uniform public assent that elimination or the goal of low case numbers is the overarching target. To achieve said target, a clear, evidence-informed, and context-relevant strategy, as well as concerted efforts and actioning are crucial. Countries committing to that strategy would need to have (a) rapid vaccination programs across age groups, (b) sufficient NPIs that may only be lifted if the susceptible population at risk is small, (c) close communication between policymakers and a wide range of experts to weigh the societal costs and benefits of measures against each other, (d) mitigation of virus influx from regions with higher incidence, and (e) sufficient public health infrastructure. This infrastructure entails basic public health resources, well-trained personnel of sufficient number, well-functioning TTI systems, widespread sequencing of the virus variants, and well-established molecular surveillance mechanisms. International coordination and cooperation on all these points and on continued development of new drugs and vaccines (also for potential new VOCs) is essential.

In line with the Sustainable Development Goals, healthy lives should be a global common good and initiatives like COVID-19 Vaccines Global Access (COVAX) should receive more support. Support of low- and middle-income countries by high-income countries is not only crucial to mitigate VOCs, but is mandated by the principle of solidarity [103,164,165]. In the long-term, a global One Health approach to pandemic preparedness and control is crucial - respecting the interdependence of humans, animals, and the environment [166].

7. Discussion of parameters, strategies and their context

The following presents more detailed elaborations of some of the aspects discussed in the preceeding sections and a summary of important additional topics. For a more comprehensive narrative in each of these sections there is, inevitably, some overlap with previous text.

7.1. Long-term strategy

To minimize the damage caused by the COVID-19 pandemic, a long-term strategy set on a common, global and overarching goal is required. By communicating a common goal that societies are working towards and by clearly formulating the reasoning behind the implementation of measures, they will be perceived as less arbitrary [77]. Such a strategy must be comprehensible and based on scientific evidence not only from epidemiology, but from a wide range of disciplines. Communication between politicians and experts for transparent, evidence-informed policymaking and comprehensive systematically updated context-relevant risk communication strategies is crucial. However, to be comprehensible a strategy also needs consistent concepts that are perceived as both understandable and fair. Hence, and vitally, any strategy needs to be underpinned by considerations of justice and (global) inequalities. The more comprehensible and fairer such models of pandemic management are, the more people will be willing to support more extensive interventions in their everyday life [83]. This also includes showing that not all population groups are affected by the pandemic in the same way.

Specifics of the strategy will necessarily vary locally and also change over time in the face of more data about (a) the virus, particularly current and newly-emerging VOCs, (b) the development of vaccines and treatments, and (c) the harms accrued to individuals, communities, and societies through restrictions. Any strategy needs to balance the damage of being harmed by the virus against the damage by the measures to contain it. This will shift in response to the vaccination progress. Thus, it would be problematic if governments became fixed upon a specific strategy and remained committed to it regardless of new evidence and circumstances.

Any strategy should not simply be developed by politicians and imposed on the public: such impactful strategies should, as far as possible, be based on societal consensus, although recognising that some politicians may base their views purely on ideological premises. Moreover, measures are much more likely to be successful if they are developed through a process of co-production with those who must implement them and who are most affected [167].

7.2. Vaccination coverage

7.2.1. When will sufficient vaccination coverage be reached?

Vaccination programs are progressing in Europe (see Fig. 3) [38]. The chances of achieving high vaccination coverage depend on political leadership, access to vaccines and concerns and anxieties in relation to vaccination [168]. The latter especially differs from country to country [169]. At present, with mostly the eldest and most vulnerable receiving the vaccine, vaccine uptake has been generally high [41,42]. In the younger groups, willingness to be vaccinated is lower [43,44], limiting the final average uptake. In some countries, only about 40% of the adult population currently plan to accept the offer of vaccination [45]. Moreover, it is concerning that, in some countries, there is significant vaccine hesitancy among healthcare workers [46,47]. However, perception of increasing vaccine uptake might motivate those who are hesitant [49].

If the aim is to reach population immunity, children will have to be vaccinated as well, because the required level of immunization for population immunity likely cannot be reached otherwise. If not immunized, infections in children might become central for an annual autumn or winter epidemic. High incidence in children also poses the risk that the virus may spread to vulnerable individuals in the general population with waning immunity. Children are likely to become eligible for vaccination in 2021 [112]. However, parental perspectives on and ethical considerations around childhood vaccination may pose significant challenges [170].

As of April 2021, vaccination programs in many countries have slowed down. Repeatedly changing policy recommendations and constant media coverage seem to have unsettled many people, after evidence of rare adverse, sometimes fatal, side-effects emerged mid-rollout for the AZD1222 (AstraZeneca) and Ad26.COV2.S (Johnson & Johnson) vaccines [39,40]. Likely because of this, some people rather

prefer to wait for a vaccine of their choice. At a later stage, increasing vaccination coverage and successful control of the pandemic may decrease the willingness to get vaccinated at all because the perceived risk of unwanted severe side-effects of vaccination might exceed the risk of contracting the disease [171]. This can be seen with other potentially-lethal infectious diseases. Once those who can and want to be vaccinated have been done, significant efforts may be required to encourage further people to become vaccinated. This would ideally be achieved through a coherent risk-communication strategy to effectively address the 'infodemic' and limit and address the circulation of inaccurate or misleading information about vaccines.

Despite these challenges, it is to be expected that most high-income countries will finish their first round of vaccination this year, whereas sufficient vaccination coverage in many low- and middle-income countries will take considerably longer. Widespread vaccine nationalism [172], underfunding [173] and patent laws [172] make the COVAX initiative function sub-optimally. With the current vaccines and manufacturing capacities, sufficient coverage for achieving population immunity in the poorest countries is not expected to happen before 2023. Thus, the production and global distribution of the vaccines must be increased massively and rapidly. Potential escape variants, arising from poorly controlled viral spread in countries without adequate vaccine access, or waning immunity might necessitate repeated vaccinations, further slowing down the process of global vaccination.

7.2.2. Measures during vaccination rollout

Without careful containment and test-trace-isolate measures, the population remains vulnerable to COVID-19 during the rollout of vaccination programmes. A lack of appropriate caution in the relaxation of restrictions will lead to high morbidity, with risk of long-COVID, and mortality. High incidence also favors the emergence of new variants, which can threaten the success of the vaccinations. However, there is an increasing pressure to ease measures as a larger fraction of the population has been vaccinated. As can be observed in the example of Chile, this can have grave consequences [174]. All public health policy responses to these demands should thus be well considered.

Immunity certificates or passports to enable the return to normal life for vaccinated, tested, or recovered people have been considered or introduced in some regions [175,176]. These have significant ethical and social issues associated with them. The rules for any use of such immunity certificates (or similar) will have to be openly and thoroughly discussed regarding their immunological and ethical consequences, specifically in the light of escape variants and restricted availability of vaccinations [177]. The distinction between vaccinated and not (yet) being vaccinated could become another engine of inequality.

Furthermore, there is a need to reconsider the core metric for measuring the state of the epidemic: namely, incidence. Incidence denotes the number of positively-tested COVID-19 cases during a certain time interval normalized to the population. Many discussions or rules for implementing or lifting NPIs are guided by incidence thresholds. However, if more and more people become vaccinated, the infections will concentrate only in those groups of the population that are still susceptible, i.e., younger people. In this case, a low incidence would still mean a large number of cases in younger age groups.

For example, an incidence of 50 per million people per day could initially mean that 0•005% of under 30-year-olds were infected each day. If we then assume that a third of the population were under 30 years of age and the rest of the population was completely immunized, the same incidence would mean that 0•015%, thus three times more, of under 30-year-olds were infected each day. This incidence

in the total population would then correspond to a three-fold higher incidence in those under 30 years old.

Keeping incidence thresholds for tightening and loosening measures as they are now will therefore put younger people more at risk, further burdening a group that has been severely affected by the pandemic, psychologically [75,79,178], economically [178], and educationally [178,179]. On the other hand, younger people tend to be less risk-averse [180] and may be willing to take the risk in exchange for more individual freedom. Moreover, with increased vaccination among the elderly, the same incidence means a lower burden on hospitals and lower deaths. This means that current incidence thresholds would at a later stage correspond to lower risks to healthcare systems than they do now. A last aspect to consider on the matter of incidence is that the total incidence remains a rough measure of how well contact tracing can work, even after vaccination. As the feasibility of contact tracing should be a main factor for deciding incidence thresholds [106], this would be an argument against changing the thresholds. Nevertheless, this issue will need to be openly discussed with involvement of all stakeholders.

7.3. Digital health systems and operations research to organize mass vaccinations

The delivery of vaccines and medical accessories involves complex supply chains, and the fragility of mRNA vaccines, which require a very good low-temperature cold chain, and may have to be stored at -20° to -80°Celsius, further complicates planning and logistics [181]. Countries with successful early vaccination programs during the COVID-19 pandemic, such as Israel and the United Kingdom, have benefited from an early start of mass vaccination and a steady vaccine supply:

Israel stands out for its national digital health network and electronic medical record system, which covers all citizens and can be accessed by all health management organizations (HMOs) in the country. The HMOs are independent and compete for members with a mix of public and private health care services, but a tight regulation and hierarchical structure in combination with the interconnected digital network allows the HMOs to implement a national health operation efficiently. Furthermore, organizational and logistic frameworks to facilitate the cooperation between government, hospitals and emergency care providers are well-established, and operations and health policy research, as well as digital health concepts are used to improve healthcare procedures [181,182]. A detailed review of these and other factors which contributed to Israel's successful vaccination program has been provided by Balicer and Afek [183].

Digital health systems also played a key role in the British vaccination program. As part of the prior operations research planning, optimal locations of vaccination centers were computationally estimated in a manner that ensured that every citizen could reach the nearest center within 10 miles from home [184]. For the supply chain management, a data analytics company was contracted to create a comprehensive supply database for vaccines, accessories and equipment [185]. The system also integrates information on trained staff for the vaccinations, non-identifiable patient data, and required materials in order to help prevent delays. Additionally, it provides up-to-date progress reports on vaccinations to the NHS to facilitate close monitoring. Further elements of the vaccination program that may have contributed to the early success in the UK have been discussed more comprehensively in a recent article by Baraniuk [186].

Overall, many of the tools and strategies used in Israel and the UK in the areas of digital health management and analytics, as well as operations research, are transferable to other countries. Their deployment could help to increase the efficiency of vaccine delivery in settings with interdependent supply constraints.

7.4. Engineering controls to reduce airborne transmission

There is unequivocal evidence that airborne spread is the dominant route of spread for SARS-CoV-2. Studies on human behaviors, practices and interactions in choir meetings, slaughterhouses, gyms and care homes have presented evidence consistent with airborne spread of SARS-CoV-2 [187]. Long-range transmission between people in adjacent rooms but never in each other's presence has been documented in quarantine hotels [188]. Healthy building controls, such as better ventilation and enhanced filtration, are a fundamental—but often overlooked—part of risk reduction strategies that could have benefits beyond the current pandemic [189].

Steps should be taken to ensure good ventilation in populated buildings to mitigate aerosol transmission. Priority should be given to spaces where ventilation is absent or inadequate, where there are several people in close proximity or for extended periods of time and those where infectious persons are more likely to be present. Optimizing natural ventilation by opening windows, increased air exchange in small rooms with low ceiling heights, scaling up the ventilation in high-occupant-density situations or in locations where masks are not worn all of the time are suggested [109]. Improving on this can become a global challenge since significant additional resources, not directly linked to healthcare budgets, will be needed. In addition, there has been limited guidance on specific ventilation and filtration targets. Notwithstanding, improved air quality in confined spaces may not only help to prevent infectious diseases well, but also to improve well-being and performance, e.g. learning in school children.

7.5. Waning immunity

The duration of post-infection and vaccine-induced immunity to COVID-19 might show pronounced individual heterogeneity with some people not forming efficient immunity at all and others developing an immune response that might protect from reinfection for decades. Antibodies against SARS-CoV-2 have been shown at nine months post-infection [22]. About 95% of subjects retain immune memory at six months after infection [23-25]. However, reinfections have also been observed [26-28]. In some individuals reinfections are possible even just a few months apart [190]. Mechanisms for that as well as the expected average frequency of reinfection are not well known. In the case of SARS-CoV-1, humoral immunity was described to last for up to two to three years whereas antigen-specific T-cells were detected up to 17 years after infection [191]. It is important to keep in mind that circulating antibody levels are not necessarily predictive of T-cell memory or the level of protection. To conclude, waning immunity is a realistic risk and may necessitate booster shots in the years to come.

When they occur, reinfections are likely to be less severe because leftover baseline immunity may shorten the course of infection and dampen inflammatory responses. Antibody disease enhancement, analogous to what has been observed in Dengue fever [192], could in principle occur. However, no evidence so far exists that a reinfection will lead to more severe symptoms.

7.6. Evolution of SARS-CoV-2

A key unknown in relation to the future of the pandemic is the ability of the virus to evolve in ways that increase its transmissibility, its disease severity, or its potential to escape from vaccine induced immunity. It was thought that the SARS-CoV-2 virus would evolve more slowly than other RNA viruses as it contains a proofreading mechanism. However, there has been a clear step change in emergence of constellations of mutations over time, termed "variants of concern". These often include specific mutations, for example, D614G, in the spike protein which enhanced binding to the ACE2

receptors on human cells [193]. This mutation is present in the currently important VOCs, including Alpha, Beta, Gamma and Delta. Another mutation, N501Y, involving a substitution of asparagine for tyrosine as the amino acid at position 501, allows the spike protein to bind more tightly to the ACE2 receptor, thereby further increasing the transmissibility of disease [194]. This mutation is also present in the VOCs Alpha, Beta and Gamma. A third mutation, E484K, reduces the ability of antibodies generated following vaccination or previous infection to bind to the spike protein [58,195]. This mutation is present in Beta, Gamma and other variants under investigation.

The rollout of vaccination will inevitably change the environment within which the virus is circulating, creating an evolutionary pressure for further mutations against which existing vaccines may be less effective. However, many mutations do not increase the fitness of the virus and may even weaken it, for example by reducing the ability of the spike protein to bind to the receptor. Thus, much will depend on whether there is one or a small number of genotypes of the virus that are optimally configured for transmission. Research showing convergence of evolution of the spike protein in different SARS-CoV-2 lineages supports this possibility [196].

This question has been addressed in an analysis of three variants of concern that have emerged in the pandemic, Alpha, Beta, and Gamma [197]. Martin and colleagues note that the same mutations have arisen independently in geographically dispersed populations, suggesting that, at least in some ways, the evolution of the virus may be converging on an optimally fit genotype [197]. However, they note that changes in the environment in which the viruses are being transmitted may create new opportunities. Variants bearing the N501Y mutation only began to emerge in the autumn of 2020. Having reviewed the evolution of the virus so far and of coronaviruses in other hosts, Martin and colleagues suggest that the most likely scenario is that the virus will evolve in ways that converge on one or more related "supervariants" with increased transmissibility and potential for vaccine evasion and they list a set of codons that such variants might be expected to possess [197]. However, it is not possible to exclude the situation in which other evolutionary pressures arise, particularly given the very short time during which this virus has been circulating in humans, and based on experience with other viruses.

7.7. How to improve adherence to rules and recommendations

7.7.1. Clearer communication

As the assumed effectiveness of measures is a key predictor of their protective effects [84], it will remain critically important to improve scientific communication about them [77]. This is crucial because specific policies, such as the goal of very low incidence, require the understanding of complex underlying systems. Politicians and scientists must speak clearly and truthfully to the public, neither underplaying nor overplaying the risks associated with the pandemic or the effectiveness of interventions. Scientists with a public profile must be extremely mindful of demarcating personal opinion and interpretation from widely accepted scientific fact. Failure to do so risks undermining the very public health measures and campaigns (e.g., vaccination) that scientists are propagating.

The media also has a role to play. It is apparent that coverage has regularly been influenced by the ideological stance of the media outlet. In the United States, for example, conservative media outlets have been highly critical of those warning about the risks of COVID-19, such as Anthony Fauci, and have promoted conspiracy theories. Studies at an individual and area level have demonstrated associations between use of conservative media outlets, such as Fox News, and belief in conspiracy theories, reduced mask wearing, and lower reductions in mobility. Another study, using survey data from the United States and United Kingdom, found that intention to be vaccinated was associated with use of broadcast and print media (as well

as support for Hilary Clinton in 2016 or the Labour Party in the United Kingdom) but not with social media, except in one study that asked about reliance on it for information, which found an association with reduced intention [198].

7.7.2. Empowering measures

Adherence to public health measures can only be achieved if people have the capacity to do so [199]. This insight is supported by the fact that especially low adherence has been observed for people in precarious working conditions [200,201]. We thus need to focus on making measures socially acceptable, and focus on mental health and ways to prevent, or at least relieve, social, economic, and psychological burdens associated with the pandemic. Helping people to cope with the situation and strengthening society will ultimately benefit adherence and ensure the effectiveness of measures [202]. Therefore, governments need to provide more support of multiple kinds (economic aid, more mental healthcare, social help etc.). It is of critical importance to support people from lower socio-economic backgrounds. Where possible, stress in parents and thereby in children should be reduced. This is especially since children have been hit particularly hard from a mental health perspective [75,79]. It is also vital to make help accessible to those unfamiliar with the local language, those unable to apply for help (for instance, due to digital exclusion), and those unaware of support offers. Support must be directed at those residing in a country, not merely official citizens of it, to prevent the aggravation of existing inequalities.

7.7.3. Physical, not social, distancing

It should be stressed that restricting the virus does not necessarily mean restricting social interactions per se. Politicians and scientific advisors should pursue policies that actively animate community at a time of loneliness, depression, and anxiety; but in ways that remain in agreement with the important mission of driving down cases and fatalities of COVID-19. For instance, investment in urban public health is very important, from green spaces to small and safe community gatherings. For the latter, people should be encouraged to meet outside in small groups to have social interactions in a physically-distanced way [203].

7.8. One Health

A One Health approach to disease control considers the interdependence of humans, animals and the environment with interdisciplinary thinking and measures [204,205]. Such a holistic multi- and transdisciplinary approach is required because it is insufficient to only consider a human health perspective in our interconnected world. Animal reservoirs most likely play an important role in SARS-CoV-2 and other viral infections. This is certainly the case with respect to the origin of viral human pathogens, e.g. in bats, pigs or chicks [206]. One particularly relevant animal in this regard might be the bat as a source animal from which viruses can emerge that are resistant to high temperatures or fever in humans [207]. As SARS-CoV-2 is now a mainly human-to-human transmitted virus, it is not entirely clear how much other animals, such as household animals or farmed animals, play an important role. Several animals that have been in contact with infected humans have been tested positive for SARS-CoV-2: minks, dogs, domestic cats, lions and tigers [124,125,127]. We should monitor the appearance of SARS-CoV-2 in these and other species closely.

Due to animal reservoirs and because COVID-19 is most likely a zoonosis [208], human intrusion into the habitat of animals needs to be considered in the context of pandemics. Overexploitation and habitat destruction significantly increases the risk of newly emerging and rapidly spreading vectors and diseases [209]. Environmental factors that are relevant in this context include light pollution and deforestation, mainly driven by expansion of land for agriculture [210]. From a One Health perspective, it seems essential to reduce global land use for agriculture.

The connections between animal, human, and environmental health are complex and require systems thinking. More focus on this interconnectivity should be placed in education, to foster awareness of the importance of human actions on such large scales. As we move further into climate change, a range of serious health issues will become more common [211-214]. A One Health framework as part of a planetary and global health perspective to study and manage these will be helpful [166,215].

8. Contributors

ENI, VP, SB, SBM were involved in conceptualisation, methodology, project administration, and writing. PK, MEK, CM, BP, ES were involved in conceptualisation. RB, PB, ACV, SC, TC, UD, EGl, EGr, CH, PH, PK, MEK, TK, JK, NL, HM, CM, MM, AN, MPe, EP, MPi, JR, ESc, AS, ESz, ST, SVG, PW were involved in providing content and writing - review & editing.

Declaration of interests

Acknowledgements

Data availability

Not applicable.

Supplementary materials

Supplementary material associated with this article can be found, in the online version, at doi:10.1016/j.lanepe.2021.100185.

The authors' translations of this Viewpoint are available online at https://www.containcovid-pan.eu/.

References

[1] Linstone HA, Turoff M. The delphi method. Reading, MA: Addison-Wesley; 1975.
[2] Bauer J, Brüggmann D, Klingelhöfer D, Maier W, Schwettmann L, Weiss DJ, et al. Access to intensive care in 14 European countries: a spatial analysis of intensive care need and capacity in the light of COVID-19. Intensive Care Med 2020;46 (11):2026–34.
[3] Sharma M, Mindermann S, Rogers-Smith C, Leech G, Snodin B, Ahuja J, et al. Understanding the effectiveness of government interventions in Europe's second wave of COVID-19. medRxiv 2021 2021.03.25.21254330.
[4] Veldhoen M, Simas JP. Endemic SARS-CoV-2 will maintain post-pandemic immunity. Nat Rev Immunol 2021;21(3):131–2.
[5] Anderson RM, Vegvari C, Truscott J, Collyer BS. Challenges in creating herd immunity to SARS-CoV-2 infection by mass vaccination. Lancet 2020;396 (10263):1614–6.
[6] Ab Hogan P, Winskill OJ, Watson O, Walker P, Whittaker C, Baguelin M, et al. Report 33: modelling the allocation and impact of a COVID-19 vaccine. Imperial College London; 2020 2020 September 25. Available from:. doi: 10.25561/82822.
[7] Spellberg B, Nielsen TB, Casadevall A. Antibodies, Immunity, and COVID-19. JAMA Intern Med 2021;181(4):460–2.
[8] Fontanet A, Autran B, Lina B, Kieny MP, Karim SSA, Sridhar D. SARS-CoV-2 variants and ending the COVID-19 pandemic. Lancet 2021;397(10278):952–4.
[9] Siciliani L, Wild C, McKee M, Kringos D, Barry MM, Barros PP, et al. Strengthening vaccination programmes and health systems in the European Union: a framework for action. Health Policy 2020;124(5):511–8.
[10] Paul KT, Loer K. Contemporary vaccination policy in the European Union: tensions and dilemmas. J Public Health Policy 2019;40(2):166–79.
[11] Lee C, Robinson JL. Systematic review of the effect of immunization mandates on uptake of routine childhood immunizations. J Infect 2016;72(6):659–66.
[12] D'Ancona F, D'Amario C, Maraglino F, Rezza G, Ricciardi W, Iannazzo S. Introduction of new and reinforcement of existing compulsory vaccinations in Italy: first evaluation of the impact on vaccination coverage in 2017. Euro Surveill 2018;23(22).
[13] MacDonald NE, Harmon S, Dube E, Steenbeek A, Crowcroft N, Opel DJ, et al. Mandatory infant & childhood immunization: rationales, issues and knowledge gaps. Vaccine 2018;36(39):5811–8.
[14] Mckee M, Siziliani L, Wild C, Kringos D, Barry M, Barros P, et al. Vaccination programmes and health systems in the European Union. Report of the Expert Panel

[15] on effective ways of investing in Health. European Journal of Public Health 2019;29(Supplement_4) ckz185. 373.
[15] Luyten J, Vandevelde A, Van Damme P, Beutels P. Vaccination policy and ethical challenges posed by herd immunity, suboptimal uptake and subgroup targeting. Public Health Ethics 2011;4(3):280–91.
[16] Luyten J, Dorgali V, Hens N, Beutels P. Public preferences over efficiency, equity and autonomy in vaccination policy: an empirical study. Social Science & Medicine 2013;77:84–9.
[17] Giubilini A, Douglas T, Savulescu J. The moral obligation to be vaccinated: utilitarianism, contractualism, and collective easy rescue. Medicine, Health Care and Philosophy 2018;21(4):547–60.
[18] The Lancet Infectious Diseases. Should we vaccinate children against SARS-CoV-2? Elsevier; 2021.
[19] Kashir J, AlKattan K, Yaqinuddin A. COVID-19: cross-immunity of viral epitopes may influence severity of infection and immune response. Signal Transduct Target Ther 2021;6(1):102.
[20] Yaqinuddin A. Cross-immunity between respiratory coronaviruses may limit COVID-19 fatalities. Med Hypotheses 2020;144:110049.
[21] Rostami A, Sepidarkish M, Leeflang MMG, Riahi SM, Nourollahpour Shiadeh M, Esfandyari S, et al. SARS-CoV-2 seroprevalence worldwide: a systematic review and meta-analysis. Clin Microbiol Infect 2021;27 (3):331–40.
[22] Rockstroh A, Wolf J, Fertey J, Kalbitz S, Schroth S, Lübbert C, et al. Correlation of humoral immune responses to different SARS-CoV-2 antigens with virus neutralizing antibodies and symptomatic severity in a German COVID-19 cohort. Emerg Microbes Infect 2021;10(1):774–81.
[23] Dan JM, Mateus J, Kato Y, Hastie KM, Yu ED, Faliti CE, et al. Immunological memory to SARS-CoV-2 assessed for up to 8 months after infection. Science 2021;371 (6529).
[24] Wajnberg A, Amanat F, Firpo A, Altman DR, Bailey MJ, Mansour M, et al. Robust neutralizing antibodies to SARS-CoV-2 infection persist for months. Science 2020;370(6521):1227–30.
[25] Lumley SF, O'Donnell D, Stoesser NE, Matthews PC, Howarth A, Hatch SB, et al. Antibody Status and Incidence of SARS-CoV-2 Infection in Health Care Workers. N Engl J Med 2021;384(6):533–40.
[26] European Centre for Disease Prevention and Control. Reinfection with SARS-CoV-2: implementation of a surveillance case definition within the EU/EEA. Stockholm: ECDC; 2021 8 April 20212021 April 8.
[27] Lumley SF, Wei J, O'Donnell D, Stoesser NE, Matthews PC, Howarth A, et al. The duration, dynamics and determinants of SARS-CoV-2 antibody responses in individual healthcare workers. Clin Infect Dis 2021.
[28] Pilz S, Chakeri A, Ioannidis JP, Richter L, Theiler-Schwetz V, Trummer C, et al. SARS-CoV-2 re-infection risk in Austria. Eur J Clin Invest 2021;51(4): e13520.
[29] Hall VJ, Foulkes S, Saei A, Andrews N, Oguti B, Charlett A, et al. Effectiveness of BNT162b2 mRNA vaccine against infection and COVID-19 vaccine coverage in healthcare workers in England, multicentre prospective cohort study (the SIREN Study). SSRN; 2021.
[30] Pawlowski C, Lenehan P, Puranik A, Agarwal V, Venkatakrishnan AJ, Niesen MJM, et al. FDA-authorized COVID-19 vaccines are effective per real-world evidence synthesized across a multi-state health system. medRxiv 2021 2021.02.15.21251623.
[31] Thompson MG, Burgess JL, Naleway AL, Tyner HL, Yoon SK, Meece J, et al. Interim Estimates of Vaccine Effectiveness of BNT162b2 and mRNA-1273 COVID-19 Vaccines in Preventing SARS-CoV-2 Infection Among Health Care Personnel, First Responders, and Other Essential and Frontline Workers - Eight U.S. Locations, December 2020-March 2021. MMWR Morb Mortal Wkly Rep 2021;70(13):495–500.
[32] Voysey M, Clemens SAC, Madhi SA, Weckx LY, Folegatti PM, Aley PK, et al. Safety and efficacy of the ChAdOx1 nCoV-19 vaccine (AZD1222) against SARS-CoV-2: an interim analysis of four randomised controlled trials in Brazil, South Africa, and the UK. Lancet 2021;397(10269):99–111.
[33] Pritchard E, Matthews PC, Stoesser N, Eyre DW, Gethings O, Vihta K-D, et al. Impact of vaccination on SARS-CoV-2 cases in the community: a population-based study using the UK's COVID-19 Infection Survey. medRxiv 2021 2021.04.22.21255913.
[34] Harris RJ, Hall JA, Zaidi A, Andrews NJ, Dunbar JK, Dabrera G. Impact of vaccination on household transmission of SARS-COV-2 in England. Public Health England; 2021.
[35] Polack FP, Thomas SJ, Kitchin N, Absalon J, Gurtman A, Lockhart S, et al. Safety and Efficacy of the BNT162b2 mRNA Covid-19 Vaccine. N Engl J Med 2020;383 (27):2603–15.
[36] Baden LR, El Sahly HM, Essink B, Kotloff K, Frey S, Novak R, et al. Efficacy and Safety of the mRNA-1273 SARS-CoV-2 Vaccine. N Engl J Med 2021;384(5):403–16.
[37] Dagan N, Barda N, Kepten E, Miron O, Perchik S, Katz MA, et al. BNT162b2 mRNA Covid-19 Vaccine in a Nationwide Mass Vaccination Setting. N Engl J Med 2021;384(15):1412–23.
[38] Harris C. COVID-19 vaccine rollout: which country in Europe is leading the race? Euronews 2021 [updated 2021 March 17; accessed 2021 June 12; cited. Available from: https://www.euronews.com/2021/03/17/covid-19-vaccinations-in-europe-which-countries-are-leading-the-way.
[39] European Medicines Agency. AstraZeneca's COVID-19 vaccine: EMA finds possible link to very rare cases of unusual blood clots with low blood platelets. EMA; 2021. [updated 2021 April 7; accessed 2021 June 12. Available from: https://

www.ema.europa.eu/en/news/astrazenecas-covid-19-vaccine-ema-finds-possi-
ble-link-very-rare-cases-unusual-blood-clots-low-blood.

[40] European Medicines Agency. COVID-19 Vaccine Janssen: EMA finds possible link to very rare cases of unusual blood clots with low blood platelets. EMA; 2021. [updated 2021 April 20; accessed 2021 June 12]. Available from: https://www.ema.europa.eu/en/news/covid-19-vaccine-janssen-ema-finds-possible-link-very-rare-cases-unusual-blood-clots-low-blood.

[41] European Centre for Disease Prevention and Control. Covid-19 Vaccine Tracker, European Centre for Disease Prevention and Control. Stockholm: European Centre for Disease Prevention and Control; 2021. [accessed 2021 June 12]. Available from: https://qap.ecdc.europa.eu/public/extensions/COVID-19/vaccine-tracker.html#target-group-tab.

[42] Office for National Statistics. Coronavirus and vaccination rates in people aged 70 years and over by sociodemographic characteristic, England: 8 December 2020 to 11 March 2021. Statistical bulletin March 29, 2021 2021. Available from: https://www.ons.gov.uk/peoplepopulationandcommunity/healthandsocialcare/healthinequalities/bulletins/coronavirusandvaccinationratesinpeopleaged70yearsandoverbysociodemographiccharacteristicengland/8december2020to11march2021.

[43] Kelly BJ, Southwell BG, McCormack LA, Bann CM, MacDonald PDM, Frasier AM, et al. Predictors of willingness to get a COVID-19 vaccine in the U.S. BMC Infect Dis 2021;21(1):338.

[44] Robertson E, Reeve KS, Niedzwiedz CL, Moore J, Blake M, Green M, et al. Predictors of COVID-19 vaccine hesitancy in the UK Household Longitudinal Study. medRxiv 2021 2020.12.27.20248899.

[45] Schwarzinger M, Watson V, Arwidson P, Alla F, Luchini S. COVID-19 vaccine hesitancy in a representative working-age population in France: a survey experiment based on vaccine characteristics. Lancet Public Health 2021;6(4):e210–e21.

[46] Gagneux-Brunon A, Detoc M, Bruel S, Tardy B, Rozaire O, Frappe P, et al. Intention to get vaccinations against COVID-19 in French healthcare workers during the first pandemic wave: a cross-sectional survey. J Hosp Infect 2021;108:168–73.

[47] Verger P, Scronias D, Dauby N, Adedzi KA, Gobert C, Bergeat M, et al. Attitudes of healthcare workers towards COVID-19 vaccination: a survey in France and French-speaking parts of Belgium and Canada, 2020. Euro Surveill 2021;26(3).

[48] European Centre for Disease Prevention and Control. Key figures on the vaccine rollout in the EU/EEA as of week 16, 2021. COVID-19 Vaccine rollout review. Stockholm: ECDC; 2021 2021 April 25. Available from: https://covid19-vaccine-report.ecdc.europa.eu/#Key_figures_on_the_vaccine_rollout_in_the_EUEEA_as_of_week_16,_2021_(25_April_2021).

[49] Xiao X, Borah P. Do Norms Matter? Examining Norm-Based Messages in HPV Vaccination Promotion. Health Commun 2020:1–9.

[50] Kluge H, McKee M. COVID-19 vaccines for the European region: an unprecedented challenge. Lancet 2021;397(10286):1689–91.

[51] Davies NG, Jarvis CI, Edmunds WJ, Jewell NP, Diaz-Ordaz K, Keogh RH. Increased mortality in community-tested cases of SARS-CoV-2 lineage B.1.1.7. Nature 2021;593(7858):270–4.

[52] Volz E, Mishra S, Chand M, Barrett JC, Johnson R, Geidelberg L, et al. Transmission of SARS-CoV-2 Lineage B.1.1.7 in England: insights from linking epidemiological and genetic data. medRxiv 2021 2020.12.30.20249034.

[53] Kissler SM, Tedijanto C, Goldstein E, Grad YH, Lipsitch M. Projecting the transmission dynamics of SARS-CoV-2 through the postpandemic period. Science 2020;368(6493):860–8.

[54] Bager P, Wohlfahrt J, Fonager J, Albertsen M, Yssing Michaelsen T, Holten Møller C, et al. Increased risk of hospitalisation associated with infection with SARS-CoV-2 lineage B. 1.1. 7 in Denmark. 2021.

[55] Challen R, Brooks-Pollock E, Read JM, Dyson L, Tsaneva-Atanasova K, Danon L. Risk of mortality in patients infected with SARS-CoV-2 variant of concern 202012/1: matched cohort study. Bmj 2021;372:n579.

[56] Frampton D, Rampling T, Cross A, Bailey H, Heaney J, Byott M, et al. Genomic characteristics and clinical effect of the emergent SARS-CoV-2 B.1.1.7 lineage in London, UK: a whole-genome sequencing and hospital-based cohort study. Lancet Infect Dis 2021.

[57] Grint DJ, Wing K, Williamson E, McDonald HI, Bhaskaran K, Evans D, et al. Case fatality risk of the SARS-CoV-2 variant of concern B.1.1.7 in England, 16 November to 5 February. Euro Surveill 2021;26(11).

[58] Tegally H, Wilkinson E, Giovanetti M, Iranzadeh A, Fonseca V, Giandhari J, et al. Emergence and rapid spread of a new severe acute respiratory syndrome-related coronavirus 2 (SARS-CoV-2) lineage with multiple spike mutations in South Africa. medRxiv 2020 2020.12.21.20248640.

[59] Funk T, Pharris A, Spiteri G, Bundle N, Melidou A, Carr M, et al. Characteristics of SARS-CoV-2 variants of concern B.1.1.7, B.1.351 or P.1: data from seven EU/EEA countries, weeks 38/2020 to 10/2021. Euro Surveill 2021;26(16).

[60] Wibmer CK, Ayres F, Hermanus T, Madzivhandila M, Kgagudi P, Oosthuysen B, et al. SARS-CoV-2 501Y.V2 escapes neutralization by South African COVID-19 donor plasma. bioRxiv 2021 2021.01.18.427166.

[61] Hodcroft E, Aksmentov I, Neher R, Bedford T, Hadfield J, Zuber M, et al. Overview of Variants in Countries.: CoVariants; 2021 [accessed 2021 June 12]. Available from: https://covariants.org/per-country.

[62] Public Health England. SARS-CoV-2 variants of concern and variants under investigation in England - Technical briefing 17. 25 June 2021.

[63] Altmann DM, Boyton RJ, Beale R. Immunity to SARS-CoV-2 variants of concern. Science 2021;371(6534):1103–4.

[64] Wang Z, Schmidt F, Weisblum Y, Muecksch F, Barnes CO, Finkin S, et al. mRNA vaccine-elicited antibodies to SARS-CoV-2 and circulating variants. bioRxiv 2021.

[65] Haug N, Geyrhofer L, Londei A, Dervic E, Desvars-Larrive A, Loreto V, et al. Ranking the effectiveness of worldwide COVID-19 government interventions. Nat Hum Behav 2020;4(12):1303–12.

[66] Lytras T, Tsiodras S. Lockdowns and the COVID-19 pandemic: What is the endgame? Scand J Public Health 2021;49(1):37–40.

[67] Dehning J, Zierenberg J, Spitzner FP, Wibral M, Neto JP, Wilczek M, et al. Inferring change points in the spread of COVID-19 reveals the effectiveness of interventions. Science 2020;369(6500).

[68] Greer SL, King E, Massard da Fonseca E, Peralta-Santos A. Coronavirus politics: the comparative politics and policy of COVID-19. Ann Arbor: University of Michigan Press; 2021.

[69] Tkachenko AV, Maslov S, Elbanna A, Wong GN, Weiner ZJ, Goldenfeld N. Time-dependent heterogeneity leads to transient suppression of the COVID-19 epidemic, not herd immunity. Proc Natl Acad Sci U S A. 2021;118(17).

[70] Petherick A, Goldszmidt RG, Andrade EB, Furst R, Pott A, Wood A. A worldwide assessment of COVID-19 pandemic-policy fatigue. SSRN; 2021.

[71] OECD. OECD Economic Outlook, Interim Report March 2021. Paris: OECD Publishing; 2021 Available from:. doi: 10.1787/34bfd999-en.

[72] Jin H, Wang H, Li X, Zheng W, Ye S, Zhang S, et al. Economic burden of COVID-19, China, January-March, 2020: a cost-of-illness study. Bull World Health Organ 2021;99(2):112–24.

[73] Atkeson A. What will be the economic impact of COVID-19 in the US? Rough estimates of disease scenarios. National Bureau of Economic Research; 2020 Working Paper SeriesNo. 26867.

[74] Vindegaard N, Benros ME. COVID-19 pandemic and mental health consequences: systematic review of the current evidence. Brain Behav Immun 2020;89:531–42.

[75] Ravens-Sieberer U, Kaman A, Erhart M, Devine J, Schlack R, Otto C. Impact of the COVID-19 pandemic on quality of life and mental health in children and adolescents in Germany. Eur Child Adolesc Psychiatry 2021:1–11.

[76] Röhr S, Reininghaus U, Riedel-Heller SG. Mental wellbeing in the German old age population largely unaltered during COVID-19 lockdown: results of a representative survey. BMC Geriatr 2020;20(1):489.

[77] Bavel JJV, Baicker K, Boggio PS, Capraro V, Cichocka A, Cikara M, et al. Using social and behavioural science to support COVID-19 pandemic response. Nat Hum Behav 2020;4(5):460–71.

[78] Dubey S, Biswas P, Ghosh R, Chatterjee S, Dubey MJ, Chatterjee S, et al. Psychosocial impact of COVID-19. Diabetes Metab Syndr 2020;14(5):779–88.

[79] Marques de Miranda D, da Silva Athanasio B, Sena Oliveira AC, Simoes ESAC. How is COVID-19 pandemic impacting mental health of children and adolescents? Int J Disaster Risk Reduct 2020;51:101845.

[80] Dietscher C, Nowak P, Pelikan J. Health literacy in austria: interventions and research. Stud Health Technol Inform 2020;269:192–201.

[81] World Health Organization. Risk communication and community engagement readiness and response to coronavirus disease (COVID-19): interim guidance 2020 [accessed 2021 June 12]. Available from: https://apps.who.int/iris/handle/10665/331513.

[82] Tsiodras S. COVID-19 research and science in the service of public health: the example of Greece. Nat Immunol 2021;22(5):531–2.

[83] Heydari ST, Zarei L, Sadati AK, Moradi N, Akbari M, Mehralian G, et al. The effect of risk communication on preventive and protective Behaviours during the COVID-19 outbreak: mediating role of risk perception. BMC Public Health 2021;21(1):54.

[84] Kojan L, Burbach L, Ziefle M, Calero Valdez A. Perceptions of behaviour efficacy, not perceptions of threat, are drivers of COVID-19 protective behaviour in Germany. 2021.

[85] Devine D, Gaskell J, Jennings W, Stoker G. Trust and the Coronavirus Pandemic: What are the Consequences of and for Trust? An Early Review of the Literature. Political Studies Review 2021;19:274–85.

[86] Schernhammer E, Weitzer J, Laubichler MD, Birmann BM, Bertau M, Zenk L, et al. Correlates of COVID-19 vaccine hesitancy in Austria: trust and the government. J Public Health (Oxf) 2021.

[87] Harring N, Jagers SC, Löfgren Å. COVID-19: Large-scale collective action, government intervention, and the importance of trust. World Dev 2021;138:105236.

[88] YouGov. COVID-19: government handling and confidence in health authorities 2021 [accessed 2021 June 12]. Available from: https://yougov.co.uk/topics/international/articles-reports/2020/03/17/perception-government-handling-covid-19.

[89] COVID-19 Snapshot Monitoring. Zusammenfassung Und Empfehlungen Welle 37. 2021 March 12. Available from: https://projekte.uni-erfurt.de/cosmo2020/web/summary/37/.

[90] Reicher S, Drury J. Pandemic fatigue? How adherence to covid-19 regulations has been misrepresented and why it matters. Bmj 2021;372:n137.

[91] Wieler L, Rexroth U, Gottschalk R. Emerging Covid-19 Success Story: Germany's Strong Enabling Environment - Our World in Data. Our World in Data; 2020. Available from: https://ourworldindata.org/covid-exemplar-germany-2020?country=.

[92] Cuschieri S. COVID-19 panic, solidarity and equity-the Malta exemplary experience. Z Gesundh Wiss 2020:1–6.

[93] Folmer CR, Kuiper M, Olthuis E, Kooistra EB, de Bruijn AL, Brownlee M, et al. Compliance in the 1.5 Meter Society: Longitudinal Analysis of Citizens' Adherence to COVID-19 Mitigation Measures in a Representative Sample in the Netherlands. PsyArXiv 2020. doi: 10.31234/osf.io/dr9q3.

[94] Grande E, Hutter S, Hunger S, Kanol E. Alles Covidioten? Politische Potenziale des Corona-Protests in Deutschland. WZB; 2021.

[95] Reicher S, Stott C. On order and disorder during the COVID-19 pandemic. Br J Soc Psychol 2020;59(3):694–702.

[96] Pleyers G. The Pandemic is a battlefield. Social movements in the COVID-19 lockdown. Journal of Civil Society 2020:1–18.

[97] Bargain O, Aminjonov U. Trust and compliance to public health policies in times of COVID-19. Journal of Public Economics 2020;192:104316.

[98] Oksanen A, Kaakinen M, Latikka R, Savolainen I, Savela N, Koivula A. Regulation and Trust: 3-Month Follow-up Study on COVID-19 Mortality in 25 European Countries. JMIR Public Health Surveill 2020;6(2):e19218.

[99] Nivette A, Ribeaud D, Murray A, Steinhoff A, Bechtiger L, Hepp U, et al. Non-compliance with COVID-19-related public health measures among young adults in Switzerland: Insights from a longitudinal cohort study. Soc Sci Med 2021;268:113370.

[100] Pak A, McBryde E, Adegboye OA. Does High Public Trust Amplify Compliance with Stringent COVID-19 Government Health Guidelines? A Multi-country Analysis Using Data from 102,627 Individuals. Risk Manag Healthc Policy 2021;14:293–302.

[101] Merow C, Urban MC. Seasonality and uncertainty in global COVID-19 growth rates. Proc Natl Acad Sci U S A 2020;117(44):27456–64.

[102] Wilmes P, Zimmer J, Schulz J, Glod F, Veiber L, Mombaerts L, et al. SARS-CoV-2 transmission risk from asymptomatic carriers: Results from a mass screening programme in Luxembourg. Lancet Reg Health Eur 2021;4:100056.

[103] Priesemann V, Balling R, Brinkmann MM, Ciesek S, Czypionka T, Eckerle I, et al. An action plan for pan-European defence against new SARS-CoV-2 variants. Lancet 2021;397(10273):469–70.

[104] Moore S, Hill EM, Tildesley MJ, Dyson L, Keeling MJ. Vaccination and non-pharmaceutical interventions for COVID-19: a mathematical modelling study. Lancet Infect Dis 2021;21(6):793–802.

[105] Bauer S, Contreras S, Dehning J, Linden M, Iftekhar E, Mohr SB, et al. Relaxing restrictions at the pace of vaccination increases freedom and guards against further COVID-19 waves in Europe. arXiv preprint arXiv:210306228. 2021.

[106] Contreras S, Dehning J, Loidolt M, Zierenberg J, Spitzner FP, Urrea-Quintero JH, et al. The challenges of containing SARS-CoV-2 via test-trace-and-isolate. Nat Commun 2021;12(1):378.

[107] Anastassiou OE, Hüsing A, Korth J, Theodoropoulos F, Taube C, Jöckel KH, et al. Seasonality of Non-SARS, Non-MERS Coronaviruses and the Impact of Meteorological Factors. Pathogens 2021;10(2).

[108] Byun WS, Heo SW, Jo G, Kim JW, Kim S, Lee S, et al. Is coronavirus disease (COVID-19) seasonal? A critical analysis of empirical and epidemiological studies at global and local scales. Environmental Research 2021:110972.

[109] Allen JG, Ibrahim AM. Indoor Air Changes and Potential Implications for SARS-CoV-2 Transmission. Jama 2021;325(20):2112–3.

[110] Servick K. How will COVID-19 affect the coming flu season? Scientists struggle for clues. Science 2020 [updated 2020 August 14; accessed 2021 June 12]. Available from: https://www.sciencemag.org/news/2020/08/how-will-covid-19-affect-coming-flu-season-scientists-struggle-clues.

[111] Gomez GB, Mahé C, Chaves SS. Uncertain effects of the pandemic on respiratory viruses. Science 2021;372(6546):1043–4.

[112] Mahase E. Covid vaccine could be rolled out to children by autumn. Bmj 2021;372:n723.

[113] Huang C, Huang L, Wang Y, Li X, Ren L, Gu X, et al. 6-month consequences of COVID-19 in patients discharged from hospital: a cohort study. Lancet 2021;397 (10223):220–32.

[114] Augustin M, Schommers P, Stecher M, Dewald F, Gieselmann L, Gruell H, et al. Recovered not restored: Long-term health consequences after mild COVID-19 in non-hospitalized patients. medRxiv 2021 2021.03.11.21253207.

[115] Han X, Fan Y, Alwalid O, Li N, Jia X, Yuan M, et al. Six-month Follow-up Chest CT Findings after Severe COVID-19 Pneumonia. Radiology 2021;299(1):E177–e86.

[116] Himmels JPW, Qureshi SA, Brurberg KG, Gravningen KM. LongTerm Effects of COVID-19 [Langvarige effekter av covid-19. Hurtigoversikt 2021]. Oslo: Norwegian Institute of Public Health; 2021. Available from: https://www.fhi.no/globalassets/dokumenterfiler/rapporter/2021/covid-19-long-term-effects-of-covid-19-report-2021.pdf.

[117] National Office for Statistics. The prevalence of long COVID symptoms and COVID-19 complications. Available from: https://www.ons.gov.uk/news/statementsandletters/theprevalenceoflongcovidsymptomsandcovid19complications.

[118] World Federation of Public Health Associations. Together We Can Overcome the COVID-19 Pandemic: Letters to G7 & G20. Available from: https://www.wfpha.org/together-we-can-overcome-the-covid-19-pandemic-letters-to-g7-g20/.

[119] Bainimarama Prime Minister of Thailand JV, da Costa Prime Minister of Portugal António Luís Santos, Draghi Prime Minister of Italy Mario, Iohannis President of Romania Klaus, Johnson Prime Minister of the United Kingdom Boris, Kagame President of Rwanda Paul, Kenyatta President of Kenya Uhuru, Macron President of France Emmanuel, Merkel Chancellor of Germany Angela, Michel President of the European Council Charles, Mitsotakis Prime Minister of Greece Kyriakos, Jae-in President of the Republic of Korea Moon, Piñera President of Chile Sebastián, Plenković Prime Minister of Croatia Andrej, Quesada President of Costa Rica Carlos Alvarado, Rama Prime Minister of Albania Edi, Ramaphosa President of South Africa Cyril, Rowley Prime Minister of Trinidad and Tobago Keith, Rutte Prime Minister of the Netherlands Mark, Saied President of Tunisia Kais, Sall President of Senegal Macky, Sánchez Prime Minister of Spain Pedro, Solberg Prime Miniser of Norway Erna, Vučić President of Serbia Aleksandar, Widodo President of Indonesia Joko, Zelensky President of Ukraine Volodymyr, Ghebreyesus Dr Tedros Adhanom, Director-General of the World Health Organization. COVID-19 shows why united action is needed for more robust international health architecture. WHO; 2021.

[120] Phillips N. The coronavirus is here to stay - here's what that means. Nature 2021;590(7846):382–4.

[121] Simon F, Watson H, Meynard J-B, de Santi VP, Tournier J-N. What chikungunya teaches us about COVID-19. The Lancet Infectious Diseases 2021.

[122] Taylor PC, Adams AC, Hufford MM, de la Torre I, Winthrop K, Gottlieb RL. Neutralizing monoclonal antibodies for treatment of COVID-19. Nature Reviews Immunology 2021:1–12.

[123] Dowdle WR. The principles of disease elimination and eradication. Bull World Health Organ 1998;76(Suppl 2(Suppl 2)):22–5.

[124] Abdel-Moneim AS, Abdelwhab EM. Evidence for SARS-CoV-2 Infection of Animal Hosts. Pathogens 2020;9(7).

[125] Mahdy MAA, Younis W, Ewaida Z. An Overview of SARS-CoV-2 and Animal Infection. Front Vet Sci 2020;7:596391.

[126] Oude Munnink BB, Sikkema RS, Nieuwenhuijse DF, Molenaar RJ, Munger E, Molenkamp R, et al. Transmission of SARS-CoV-2 on mink farms between humans and mink and back to humans. Science 2021;371(6525):172–7.

[127] de Morais HA, Dos Santos AP, do Nascimento NC, Kmetiuk LB, Barbosa DS, Brandão PE, et al. Natural Infection by SARS-CoV-2 in Companion Animals: A Review of Case Reports and Current Evidence of Their Role in the Epidemiology of COVID-19. Front Vet Sci 2020;7:591216.

[128] Horton R. Offline: The lessons of smallpox eradication for COVID-19. Lancet 2021;396(10267):1951.

[129] Klepac P, Metcalf CJ, McLean AR, Hampson K. Towards the endgame and beyond: complexities and challenges for the elimination of infectious diseases. Philos Trans R Soc Lond B Biol Sci 2013;368(1623):20120137.

[130] Schmidt H, Weintraub R, Williams MA, Miller K, Buttenheim A, Sadecki E, et al. Equitable allocation of COVID-19 vaccines in the United States. Nature Medicine 2021:1–10.

[131] Baker MG, Wilson N, Blakely T. Elimination could be the optimal strategy for covid-19 and other emerging pandemic diseases. Bmj 2020;371:m4907.

[132] Murray CJL, Piot P. The Potential Future of the COVID-19 Pandemic: Will SARS-CoV-2 Become a Recurrent Seasonal Infection? Jama 2021;325(13):1249–50.

[133] Arora T, Grey I. Health behaviour changes during COVID-19 and the potential consequences: A mini-review. J Health Psychol 2020;25(9):1155–63.

[134] Richards M, Anderson M, Carter P, Ebert BL, Mossialos E. The impact of the COVID-19 pandemic on cancer care. Nat Cancer 2020:1–3.

[135] Topriceanu CC, Wong A, Moon JC, Hughes AD, Bann D, Chaturvedi N, et al. Evaluating access to health and care services during lockdown by the COVID-19 survey in five UK national longitudinal studies. BMJ Open 2021;11(3):e045813.

[136] Mansfield KE, Mathur R, Tazare J, Henderson AD, Mulick AR, Carreira H, et al. Indirect acute effects of the COVID-19 pandemic on physical and mental health in the UK: a population-based study. Lancet Digit Health 2021;3(4):e217–e30.

[137] Mishra B, Shenouda M, Owen J, Collaborators B, Roy B. BODS/BOA Survey of impact of COVID-19 on UK orthopaedic practice and implications on restoration of elective services. British Orthopaedic Association; 2020. Available from: https://www.boa.ac.uk/resources/knowledge-hub/bods-boa-survey-of-impact-of-covid-19-on-uk-orthopaedic-practice-and-implications-on-restoration-of-elective-services.html.

[138] Maringe C, Spicer J, Morris M, Purushotham A, Nolte E, Sullivan R, et al. The impact of the COVID-19 pandemic on cancer deaths due to delays in diagnosis in England, UK: a national, population-based, modelling study. Lancet Oncol 2020;21(8):1023–34.

[139] Sprague BL, Lowry KP, Miglioretti DL, Alsheik N, Bowles EJA, Tosteson ANA, et al. Changes in Mammography Utilization by Women's Characteristics during the First 5 Months of the COVID-19 Pandemic. J Natl Cancer Inst 2021.

[140] Kluge HHP, Wickramasinghe K, Rippin HL, Mendes R, Peters DH, Kontsevaya A, et al. Prevention and control of non-communicable diseases in the COVID-19 response. Lancet 2020;395(10238):1678–80.

[141] Vizheh M, Qorbani M, Arzaghi SM, Muhidin S, Javanmard Z, Esmaeili M. The mental health of healthcare workers in the COVID-19 pandemic: A systematic review. J Diabetes Metab Disord 2020;19(2):1–12.

[142] Rose N, Manning N, Bentall R, Bhui K, Burgess R, Carr S, et al. The social underpinnings of mental distress in the time of COVID-19 - time for urgent action. Wellcome Open Res 2020;5:166.

[143] Office for National Statistics. Office for National Statistics. (2020). Coronavirus and the social impacts on disabled people in Great Britain. 2020 2021 April 9. Available from: https://www.ons.gov.uk/peoplepopulationandcommunity/healthandsocialcare/disability/articles/coronavirusandthesocialimpactsondisabledpeopleingreatbritain/february2021.

[144] Bambra C, Riordan R, Ford J, Matthews F. The COVID-19 pandemic and health inequalities. J Epidemiol Community Health 2020;74(11):964–8.

[145] Devakumar D, Shannon G, Bhopal SS, Abubakar I. Racism and discrimination in COVID-19 responses. Lancet 2020;395(10231):1194.

[146] Appleby L. What has been the effect of covid-19 on suicide rates? Bmj 2021;372:n834.

[147] Celi G, Guarascio D, Simonazzi A. A fragile and divided European Union meets Covid-19: further disintegration or 'Hamiltonian moment'? Journal of Industrial and Business Economics 2020;47(3):411–24.

[148] Travkina E, Sacco PL. Culture shock: COVID-19 and the cultural and creative sectors. Paris: OECD; 2020. 2020 September 7. Available from: https://www.oecd.org/coronavirus/policy-responses/culture-shock-covid-19-and-the-cultural-and-creative-sectors-08da9e0e/.

[149] Hall S. This is how COVID-19 is affecting the music industry. World Economic Forum; 2020. [updated 2020 May 27; accessed 2021 June 12]. Available from: https://www.weforum.org/agenda/2020/05/this-is-how-covid-19-is-affecting-the-music-industry/.

[150] Jeannotte MS. When the gigs are gone: Valuing arts, culture and media in the COVID-19 pandemic. Social Sciences & Humanities Open 2021;3(1):100097.

[151] Comunian R, England L. Creative and cultural work without filters: Covid-19 and exposed precarity in the creative economy. Cultural Trends 2020;29(2):112–28.

[152] Maqui E, Morris R. The long-term effects of the pandemic: insights from a survey of leading companies. Economic Bulletin Boxes 2021;8.

[153] United Nations Development Program. Coronavirus vs. inequality. Available from: https://feature.undp.org/coronavirus-vs-inequality/.

[154] Patel JA, Nielsen FBH, Badiani AA, Assi S, Unadkat VA, Patel B, et al. Poverty, inequality and COVID-19: the forgotten vulnerable. Public Health 2020;183:110–1.

[155] Krouse HJ. COVID-19 and the Widening Gap in Health Inequity. Otolaryngol Head Neck Surg 2020;163(1):65–6.

[156] European Commission. 2021 report on gender equality in the EU. Brussels: EU; 2021. 2021 March 6. Available from: https://epws.org/eu-2021-report-on-gender-equality/.

[157] World Health Organization. The rise and rise of interpersonal violence–an unintended impact of the COVID-19 response on families. 2020.

[158] Di Pietro G, Biagi F, Costa P, Karpiński Z, Mazza J. The likely impact of COVID-19 on education: reflections based on the existing literature and recent international datasets. Publications Office of the European Union; 2020.

[159] Cairney P, Wellstead A. COVID-19: effective policymaking depends on trust in experts, politicians, and the public. Policy Design and Practice; 2020. p. 1–14.

[160] Fancourt D, Steptoe A, Wright L. The Cummings effect: politics, trust, and behaviours during the COVID-19 pandemic. Lancet 2020;396(10249):464–5.

[161] Lofredo MPP. Social cohesion, trust, and government action against pandemics. Eubios Journal of Asian and International Bioethics 2020;30(182-188).

[162] Elias A, Ben J, Mansouri F, Paradies Y. Racism and nationalism during and beyond the COVID-19 pandemic. Ethnic and Racial Studies 2020:1–11.

[163] World Bank. Poverty and Shared Prosperity 2020: Reversals of Fortune. Washington, DCAvailable from: https://openknowledge.worldbank.org/handle/10986/34496.

[164] Javed S, Chattu VK. Strengthening the COVID-19 pandemic response, global leadership, and international cooperation through global health diplomacy. Health Promot Perspect 2020;10(4):300–5.

[165] Priesemann V, Brinkmann MM, Ciesek S, Cuschieri S, Czypionka T, Giordano G, et al. Calling for pan-European commitment for rapid and sustained reduction in SARS-CoV-2 infections. Lancet 2021;397(10269):92–3.

[166] Pan-European Commission on Health and Sustainable Development. Rethinking Policy Priorities in the light of Pandemics: a call to action 2021 Available from: https://www.euro.who.int/en/health-topics/health-policy/european-programme-of-work/pan-european-commission-on-health-and-sustainable-development/multimedia/rethinking-policy-priorities-in-the-light-of-pandemics-a-call-to-action.

[167] Turk E, Durrance-Bagale A, Han E, Bell S, Rajan S, Lota MMM, et al. International experiences with co-production and people centredness offer lessons for covid-19 responses. Bmj 2021;372:m4752.

[168] Paul E, Steptoe A, Fancourt D. Attitudes towards vaccines and intention to vaccinate against COVID-19: implications for public health communications. Lancet Reg Health Eur 2021;1:100012.

[169] Institute of Global Health Innovation. Covid-19: Global attitudes towards a COVID-19 vaccine. Report, February 2021. Available from: https://www.imperial.ac.uk/media/imperial-college/institute-of-global-health-innovation/EMBARGOED-0502.-Feb-21-GlobalVaccineInsights_ICL-YouGov-Covid-19-Behaviour-Tracker_20210301.pdf.

[170] Montalti M, Rallo F, Guaraldi F, Bartoli L, Po G, Stillo M, et al. Would Parents Get Their Children Vaccinated Against SARS-CoV-2? Rate and Predictors of Vaccine Hesitancy According to a Survey over 5000 Families from Bologna, Italy. Vaccines (Basel) 2021;9(4).

[171] Messinger Cayetano S, Crandall L. Paradox of success and public perspective: COVID-19 and the perennial problem of prevention. J Epidemiol Community Health 2020;74(8):679.

[172] Katz IT, Weintraub R, Bekker LG, Brandt AM. From Vaccine Nationalism to Vaccine Equity - Finding a Path Forward. N Engl J Med 2021;384(14):1281–3.

[173] Forman R, Shah S, Jeurissen P, Jit M, Mossialos E. COVID-19 vaccine challenges: What have we learned so far and what remains to be done? Health Policy 2021;125(5):553–67.

[174] Chambers J. Chile sees Covid surge despite vaccination success. BBC News 2021 [updated 2021 April 16; accessed 2021 June 12]. Available from: https://www.bbc.com/news/world-latin-america-56731801.

[175] Dye C, Mills MC. COVID-19 vaccination passports. American Association for the Advancement of Science; 2021.

[176] Council of the European Union. COVID-19: Council agrees its negotiating mandate on the Digital Green Certificate [press release]. April 14 2021.

[177] Phelan AL. COVID-19 immunity passports and vaccination certificates: scientific, equitable, and legal challenges. Lancet 2020;395(10237):1595–8.

[178] Gonzalez SP, Gardiner D, Bausch J. Youth and COVID-19: impacts on jobs, education, rights and mental well-being: survey report 2020. Geneva: ILO; 2020.

[179] Koronakomisjonen. NOU 2021: 6. The authorities handling of the COVID-19 pandemic. Chapter 2. Summary. Available from: https://www.regjeringen.no/contentassets/5d388acc92064389b2a4e1a449c5865e/no/sved/01kap02engelsk.pdf.

[180] Albert SM, Duffy J. Differences in Risk Aversion between Young and Older Adults. Neurosci Neuroecon 2012;2012(1).

[181] Kollewe J. Pfizer and BioNTech's vaccine poses global logistics challenge. The Guardian 2020 November 10 [accessed 2021 June 6]. Available from: https://www.theguardian.com/business/2020/nov/10/pfizer-and-biontechs-vaccine-poses-global-logistics-challenge.

[182] Clarfield AM, Manor O, Nun GB, Shvarts S, Azzam ZS, Afek A, et al. Health and health care in Israel: an introduction. Lancet 2017;389(10088):2503–13.

[183] Balicer RD, Afek A. Digital health nation: Israel's global big data innovation hub. Lancet 2017;389(10088):2451–3.

[184] Care UKDoHaS. In: Care UKDoHaS, editor. editor, 2021, editor. UK COVID-19 vaccines delivery plan (2021, January 11); 2021. editor.

[185] Neville S, Warrell H. UK vaccine rollout success built on NHS determination and military precision. Financial Times. Available from: https://www.ft.com/content/cd66ae57-657e-4579-be19-85efcfa5d09b.

[186] Baraniuk C. Covid-19: How the UK vaccine rollout delivered success, so far. Bmj 2021;372:n421.

[187] Lewis D. Superspreading drives the COVID pandemic - and could help to tame it. Nature 2021;590(7847):544–6.

[188] Eichler N, Thornley C, Swadi T, Devine T, McElnay C, Sherwood J, et al. Transmission of Severe Acute Respiratory Syndrome Coronavirus 2 during Border Quarantine and Air Travel, New Zealand (Aotearoa). Emerg Infect Dis 2021;27(5):1274–8.

[189] Vijayan VK, Paramesh H, Salvi SS, Dalal AA. Enhancing indoor air quality -The air filter advantage. Lung India 2015;32(5):473–9.

[190] Tuan J, Spichler-Moffarah A, Ogbuagu O. A new positive SARS-CoV-2 test months after severe COVID-19 illness: reinfection or intermittent viral shedding? BMJ Case Rep 2021;14(2).

[191] Le Bert N, Tan AT, Kunasegaran K, Tham CYL, Hafezi M, Chia A, et al. SARS-CoV-2-specific T cell immunity in cases of COVID-19 and SARS, and uninfected controls. Nature 2020;584(7821):457–62.

[192] Halstead SB. Dengue hemorrhagic fever: two infections and antibody dependent enhancement, a brief history and personal memoir. Rev Cubana Med Trop 2002;54(3):171–9.

[193] Zhang J, Cai Y, Xiao T, Lu J, Peng H, Sterling SM, et al. Structural impact on SARS-CoV-2 spike protein by D614G substitution. Science 2021;372(6541):525–30.

[194] Fiorentini S, Messali S, Zani A, Caccuri F, Giovanetti M, Ciccozzi M, et al. First detection of SARS-CoV-2 spike protein N501 mutation in Italy in August, 2020. Lancet Infect Dis 2021;21(6):e147.

[195] Faria NR, Mellan TA, Whittaker C, Claro IM, Candido DDS, Mishra S, et al. Genomics and epidemiology of a novel SARS-CoV-2 lineage in Manaus, Brazil. medRxiv 2021.

[196] Wu Y. Strong evolutionary convergence of receptor-binding protein spike between COVID-19 and SARS-related coronaviruses. bioRxiv 2020 2020.03.04.975995.

[197] Martin DP, Weaver S, Tegally H, San EJ, Shank SD, Wilkinson E, et al. The emergence and ongoing convergent evolution of the N501Y lineages coincides with a major global shift in the SARS-CoV-2 selective landscape. medRxiv 2021.

[198] Allington D, McAndrew S, Moxham-Hall VL, Duffy B. Media usage predicts intention to be vaccinated against SARS-CoV-2 in the US and the UK. Vaccine 2021;39(18):2595–603.

[199] Abstiens K, Czypionka T, Gangl K, Grosch K, Koenig T, Spitzer F, et al. Zehn Gebote der Verhaltenswissenschaften in der Pandemiebekämpfung. Institute for Advance Studies Vienna; 2021. Available from: https://irihs.ihs.ac.at/id/eprint/5702/1/ihs-policy-brief-2021-abstiens-czypionka-spitzer-et-al-verhaltenswissenschaften-corona.pdf.

[200] Lüdecke D, von dem Knesebeck O. Protective Behavior in Course of the COVID-19 Outbreak-Survey Results From Germany. Front Public Health 2020;8:572561.

[201] Kretchy IA, Asiedu-Danso M, Kretchy JP. Medication management and adherence during the COVID-19 pandemic: Perspectives and experiences from low- and middle-income countries. Res Social Adm Pharm 2021;17(1):2023–6.

[202] Prainsack B. Solidarity in Times of Pandemics. Democratic Theory 2020;7(2):124–33.

[203] Sun C, Zhai Z. The efficacy of social distance and ventilation effectiveness in preventing COVID-19 transmission. Sustainable cities and society 2020;62:102390.

[204] Zinsstag J, Schelling E, Wyss K, Mahamat MB. Potential of cooperation between human and animal health to strengthen health systems. Lancet 2005;366(9503):2142–5.

[205] Degeling CJ, Dawson A, Gilbert GL. The ethics of One Health editor. In: Walton M, editor. One Planet, One Health. Sydney, Australia: Sydney University Press; 2019.

[206] Shi Z, Hu Z. A review of studies on animal reservoirs of the SARS coronavirus. Virus Res 2008;133(1):74–87.

[207] Calisher CH, Childs JE, Field HE, Holmes KV, Schountz T. Bats: important reservoir hosts of emerging viruses. Clin Microbiol Rev 2006;19(3):531–45.

[208] Haider N, Rothman-Ostrow P, Osman AY, Arruda LB, Macfarlane-Berry L, Elton L, et al. COVID-19-Zoonosis or Emerging Infectious Disease? Front Public Health 2020;8:596944.

[209] Karlsson O, Rocklöv J, Lehoux AP, Bergquist J, Rutgersson A, Blunt MJ, et al. The human exposome and health in the Anthropocene. Int J Epidemiol 2021;50(2):378–89.

[210] Poore J, Nemecek T. Reducing food's environmental impacts through producers and consumers. Science 2018;360(6392):987–92.

[211] Allen T, Murray KA, Zambrana-Torrelio C, Morse SS, Rondinini C, Di Marco M, et al. Global hotspots and correlates of emerging zoonotic diseases. Nature communications 2017;8(1):1–10.

[212] Watts N, Amann M, Arnell N, Ayeb-Karlsson S, Beagley J, Belesova K, et al. The 2020 report of The Lancet Countdown on health and climate change: responding to converging crises. The Lancet 2020.

[213] Rocklöv J, Dubrow R. Climate change: an enduring challenge for vector-borne disease prevention and control. Nature immunology 2020;21(5):479–83.

[214] Semenza JC, Lindgren E, Balkanyi L, Espinosa L, Almqvist MS, Penttinen P, et al. Determinants and drivers of infectious disease threat events in Europe. Emerging infectious diseases 2016;22(4):581.

[215] Schmiege D, Perez Arredondo AM, Ntajal J, Minetto Gellert Paris J, Savi MK, Patel K, et al. One Health in the context of coronavirus outbreaks: a systematic literature review. One Health 2020;10:100170.

4

RELAXING RESTRICTIONS AT THE PACE OF VACCINATION INCREASES FREEDOM AND GUARDS AGAINST FURTHER COVID-19 WAVES

This chapter is identical to the article [24]. The Supplementary Information S1 can be found in Appendix B. The article is published in Bauer, S., Contreras, S., Dehning, J., Linden, M., Iftekhar, E.N., Mohr, S.B., Olivera-Nappa, A. and Priesemann, V., Relaxing restrictions at the pace of vaccination increases freedom and guards against further COVID-19 waves. PLoS computational biology, 17(9), p.e1009288 (2021),

under the terms of a Creative Common License (http://creativecommons.org/licenses/by/4.0/).

Roles: Investigation, Writing – review & editing.

RESEARCH ARTICLE

Relaxing restrictions at the pace of vaccination increases freedom and guards against further COVID-19 waves

Simon Bauer[1☯], Sebastian Contreras[1,2☯], Jonas Dehning[1], Matthias Linden[1,3], Emil Iftekhar[1], Sebastian B. Mohr[1], Alvaro Olivera-Nappa[2], Viola Priesemann[1,4]*

1 Max Planck Institute for Dynamics and Self-Organization, Göttingen, Germany, **2** Centre for Biotechnology and Bioengineering, Universidad de Chile, Santiago, Chile, **3** Institute for Theoretical Physics, Leibniz University, Hannover, Germany, **4** Institute for the Dynamics of Complex Systems, University of Göttingen, Göttingen, Germany

☯ These authors contributed equally to this work.
* viola.priesemann@ds.mpg.de
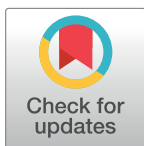
Abstract

Mass vaccination offers a promising exit strategy for the COVID-19 pandemic. However, as vaccination progresses, demands to lift restrictions increase, despite most of the population remaining susceptible. Using our age-stratified SEIRD-ICU compartmental model and curated epidemiological and vaccination data, we quantified the rate (relative to vaccination progress) at which countries can lift non-pharmaceutical interventions without overwhelming their healthcare systems. We analyzed scenarios ranging from immediately lifting restrictions (accepting high mortality and morbidity) to reducing case numbers to a level where test-trace-and-isolate (TTI) programs efficiently compensate for local spreading events. In general, the age-dependent vaccination roll-out implies a transient decrease of more than ten years in the average age of ICU patients and deceased. The pace of vaccination determines the speed of lifting restrictions; Taking the European Union (EU) as an example case, all considered scenarios allow for steadily increasing contacts starting in May 2021 and relaxing most restrictions by autumn 2021. Throughout summer 2021, only mild contact restrictions will remain necessary. However, only high vaccine uptake can prevent further severe waves. Across EU countries, seroprevalence impacts the long-term success of vaccination campaigns more strongly than age demographics. In addition, we highlight the need for preventive measures to reduce contagion in school settings throughout the year 2021, where children might be drivers of contagion because of them remaining susceptible. Strategies that maintain low case numbers, instead of high ones, reduce infections and deaths by factors of eleven and five, respectively. In general, policies with low case numbers significantly benefit from vaccination, as the overall reduction in susceptibility will further diminish viral spread. Keeping case numbers low is the safest long-term strategy because it considerably reduces mortality and morbidity and offers better preparedness against emerging escape or more contagious virus variants while still allowing for higher contact numbers (freedom) with progressing vaccinations.

Author summary

In this work, we quantify the rate at which non-pharmaceutical interventions can be lifted as COVID-19 vaccination campaigns progress. With the constraint of not exceeding ICU capacity, there exists only a relatively narrow range of plausible scenarios. We selected different scenarios ranging from the immediate release of restrictions to more conservative approaches aiming at low case numbers. In all considered scenarios, the increasing overall immunity (due to vaccination or post-infection) will allow for a steady increase in contacts. However, deaths and total cases (potentially leading to *long covid*) are only minimized when aiming for low case numbers, and restrictions are lifted at the pace of vaccination. These qualitative results are general. Taking EU countries as quantitative examples, we observe larger differences only in the long-term perspectives, mainly due to varying seroprevalence and vaccine uptake. Thus, the recommendation is to keep case numbers as low as possible to facilitate test-trace-and-isolate programs, reduce mortality and morbidity, and offer better preparedness against emerging variants, potentially escaping immune responses. Keeping moderate preventive measures in place (such as improved hygiene, use of face masks, and moderate contact reduction) is highly recommended will further facilitate control.

Introduction

The rising availability of effective vaccines against SARS-CoV-2 promises the lifting of restrictions, thereby relieving the social and economic burden caused by the COVID-19 pandemic. However, it is unclear how fast the restrictions can be lifted without risking another wave of infections; we need a promising long-term vaccination strategy [1]. Nevertheless, a successful approach has to take into account several challenges; vaccination logistics and vaccine allocation requires a couple of months [2–4], vaccine eligibility depends on age and eventually serostatus [5], vaccine acceptance may vary across populations [6], and more contagious [7] and escape variants of SARS-CoV-2 that can evade existing immunity [8, 9] may emerge, thus posing a persistent risk. Last but not least, disease mitigation is determined by how well vaccines block infection, and thus prevent the propagation of SARS-CoV-2 [3, 4], the time to develop effective antibody titers after vaccination, and their efficacy against severe symptoms. All these parameters will greatly determine the design of an optimal strategy for the transition from epidemicity to endemicity [10].

To bridge the time until a significant fraction of the population is vaccinated, a sustainable public health strategy has to combine vaccination with non-pharmaceutical interventions (NPIs). Otherwise it risks further waves and, consequently, high morbidity and excess mortality. However, the overall compliance with NPIs worldwide has on average decreased due to a "pandemic-policy fatigue" [11]. Therefore, the second wave has been more challenging to tame [12] although NPIs, in principle, can be highly effective, as seen in the first wave [13, 14]. After vaccinating the most vulnerable age groups, the urge and social pressure to lift restrictions will increase. However, given the wide distribution of fatalities over age groups and the putative incomplete protection of vaccines against severe symptoms and against transmission, NPIs cannot be lifted entirely or immediately. With our study, we want to outline at which pace restrictions can be lifted as the vaccine roll-out progresses.

Public-health policies in a pandemic have to find a delicate ethical balance between reducing the viral spread and restricting individual freedom and economic activities. However, the interest of health on the one hand and society and economy on the other hand are not always

contradictory. For the COVID-19 pandemic, all these aspects clearly profit from low case numbers [15–17], i.e., an incidence where test-trace-and-isolate (TTI) programs can efficiently compensate for local spreading events. The challenge is to reach low case numbers and maintain them [18, 19]. Especially with the progress of vaccination, restrictions should be lifted when the threat to public health is reduced. However, the apparent trade-off between public health interest and freedom is not always linear and straightforward. Taking into account that low case numbers facilitate TTI strategies (i.e., health authorities can concentrate on remaining infection chains and stop them quickly) [18–20], an optimal strategy with a low public health burden *and* large freedom may exist and be complementary to vaccination.

Here, we quantitatively study how the planned vaccine roll-out in the European Union (EU), together with the cumulative post-infection immunity (seroprevalence), progressively allows for lifting restrictions. In particular, we study how precisely the number of contacts can be increased without rendering disease spread uncontrolled over the year 2021. Our study builds on carefully curated epidemiological and contact network data from Germany, France, the UK, and other European countries. Thereby, our work can serve as a blueprint for an opening strategy.

Analytical framework

Our analytical framework builds on our deterministic, age-stratified, SEIRD-ICU compartmental model, modified to incorporate vaccination through delay differential equations. It includes compartments for a 2-dose staged vaccine roll-out, immunization delays, intensive care unit (ICU)-hospitalized, and deceased individuals. A central parameter for our model is the gross reproduction number R_t. It is essentially the time-varying effective reproduction number without considering the effects of immunity nor of TTI. That number depends (among several factors) on i) the absolute number of contacts per individual, and ii) the probability of being infected given a contact. In other words, R_t is defined as the average number of contacts an infected individual has that would lead to an offspring infection in a fully susceptible population. Therefore, an increase in R_t implies an increase in contact frequency or the probability of transmission per contact, e.g., due to less mask-wearing. The core idea is that increasing immunity levels among the population (post-infection or due to vaccination) allows for a higher average number of potentially contagious contacts and, thus, freedom (quantified by R_t), given the same level of new infections or ICU occupancy. Hence, with immunization progress reducing the susceptible fraction of the population, R_t can be dynamically increased while maintaining control over the pandemic, i.e., while keeping the effective reproduction number below one (Fig 1A).

To adapt the gross reproduction number R_t such that a specific strategy is followed (e.g. staying below TTI or ICU capacity), we include an automatic, proportional-derivative (PD) control system [21]. This control system allows for steady growth in R_t as long as it does not lead to overflowing ICUs (or surpassing the TTI capacity). However, when risking surpassing the ICU capacity, restrictions might be tightened again. In that way, we approximate the feedback-loop between political decisions, people's behavior, reported case numbers, and ICU occupancy.

The basic reproduction number is set to $R_0 = 4.5$, reflecting the dominance of the B.1.1.7 variant [3, 7]. We further assume that the reproduction number can be decreased to about 3.5 by hygiene measures, face masks, and mild social distancing. This number is informed by the estimates of Sharma et al. [22], who estimate the combined effectiveness of mask wearing, limiting gatherings to at most 10 people and closing night clubs to a reduction of about 20–40%, thus leading to a reproduction number between 2.7 and 3.6. We use a conservative estimate, as
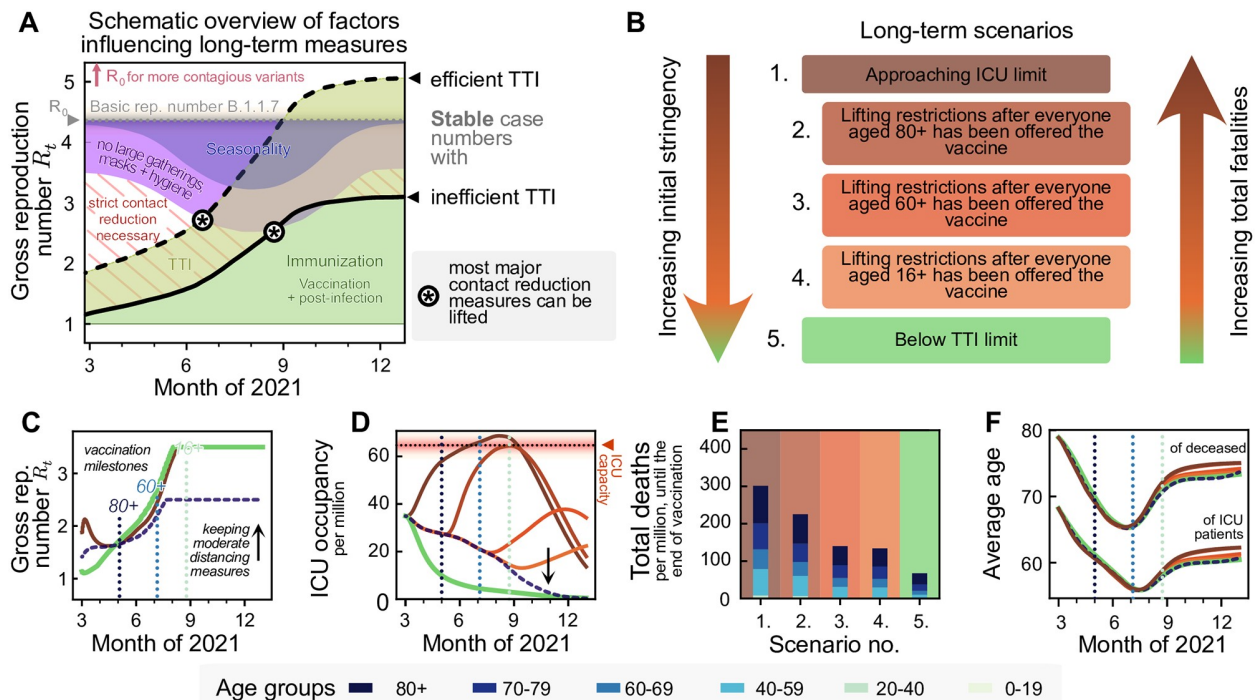
Fig 1. With progressing vaccination in the European Union, a slow but steady increase in freedom will be possible. However, premature lifting of NPIs considerably increases the total fatalities without a major reduction in restrictions in the middle term. A: A schematic outlook into the effect of vaccination on societal freedom. Freedom is quantified by the maximum time-varying gross reproduction number (R_t) allowed to sustain stable case numbers. As R_t does not consider the immunized population, gross reproduction numbers above one are possible without rendering the system unstable. A complete return to pre-pandemic behavior would be achieved when R_t reaches the value of the basic reproduction number R_0 (or possibly at a lower value due to seasonality effects during summer, purple-blue shaded area). The thick full and dashed lines indicate the gross reproduction number R_t allowed to sustain stable case numbers if test-trace-isolate (TTI) programs are inefficient and efficient, respectively, which depends on the case numbers level. Increased population immunity (green) is expected to allow for lifting the most strict contact reduction measures while only keeping mild NPIs (purple) during summer 2021 in the northern hemisphere. Note that seasonality is not explicitly modeled in this work. See S4 Fig for an extended version including the year 2020. **B**: We explore five different scenarios for lifting restrictions in the EU, in light of the EU-wide vaccination programs. We sort them according to the initial stringency that they require and the total fatalities that they may cause. One extreme (Scenario 1) offers immediate (but still comparably little) freedom by approaching ICU-capacity limits quickly. The other extreme (Scenario 5) uses a strong initial reduction in contacts to allow long-term control at low case numbers. Finally, the intermediate scenarios initially maintain moderate case numbers and lift restrictions at different points in the vaccination program. **C**: All extreme strategies allow for a steady noticeable increase in contacts in the coming months (cf. panel **A**), but vary greatly in the (**D**) ICU-occupancy profiles and (**E**) total fatalities. **F**: Independent on the strategy, we expect a transient but pronounced decrease in the average age of ICU patients and deceased over the summer.

this is only a exemplary set of restrictions. Therefore, we restrict R_t in general not to exceed 3.5 (Fig 1C).

Efficient TTI contributes to reducing the effective reproduction number. Hence, it increases the average number of contacts (i.e., R_t) that people may have under the condition that case numbers remain stable (Fig 1A) [18]. This effect is particularly strong at low case numbers, where the health authorities can concentrate on tracing every case efficiently [19]. Here, we approximate the effect of TTI on R_t semi-analytically to achieve an efficient implementation (see Methods).

For vaccination, we use as default parameters an average vaccine efficacy of 90% protection against severe illness [23] and of 75% protection against infection [24]. We further assume that vaccinated individuals with a breakthrough infection carry a lower viral load and thus are 50% less infectious [25] than unvaccinated infected individuals. We assume a total average vaccine uptake of 80% [26] that increases with age from 73% in the 0–19 to 89% in the 80+ age group, and an age-prioritized vaccine delivery as described in the Methods section. In detail, most of
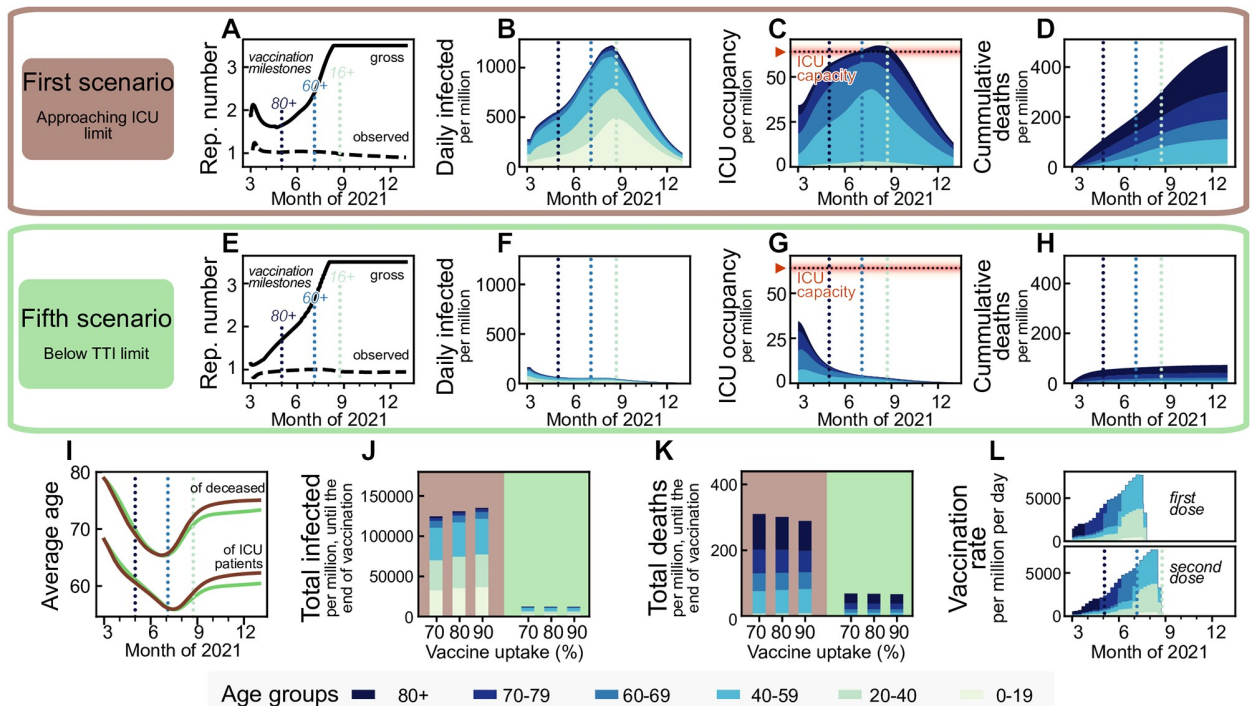
Fig 2. Maintaining low case numbers during vaccine roll-out reduces the number of ICU patients and deaths by about a factor five compared to quickly approaching the ICU limit while hardly requiring stronger restrictions. Aiming to maximize ICU occupancy (**A–D**) allows for a slight increase of the allowed gross reproduction number R_t early on, whereas lowering case numbers below the TTI capacity limit (**E–H**) requires comparatively stronger initial restrictions. Afterwards, the vaccination progress allows for a similar increase in freedom (quantified by increments in R_t) for both strategies, starting approximately in May 2021. **B–D, F–H**: These two strategies lead to a completely different evolution of case numbers, ICU occupancy, and cumulative deaths, but differ only marginally in the evolution of the average age of deceased and ICU patients (**I**), as the latter is rather an effect of the age-prioritized vaccination than of a particular strategy. **J,K**: The total number of cases until the end of the vaccination period (of the 80% uptake scenario, i.e., end of August, the rightmost dotted light blue line in sub-panels **A–H**) differ by a factor of eleven between the two strategies, and the total deaths by a factor of five. Vaccine uptake (i.e., the fraction of the eligible, 16+, population that gets vaccinated) has a minor impact on these numbers until the end of the vaccine roll-out but determines whether a wave would follow afterward (see below). **L**: Assumed vaccination rate as projected for Germany, which is expected to be similar across the European Union. For a full display of the time-evolution of the compartments for different uptakes see S6–S8 Figs.

the vaccines are distributed first to the age group 80+, then 70+, 60+, and then to anyone of age 16+. A small fraction of the weekly available vaccines is distributed randomly (e.g. because of profession). After everyone got a vaccine offer roughly by the end of August, we assume no further vaccination (see Fig 2L). The daily amount of vaccine doses per million is derived from German government projections, but is expected to be similar across the EU. For the course of the disease, the age-dependent fraction of non-vaccinated, infected individuals requiring intensive care is estimated from German hospitalization data, using the infection-fatality-ratio (IFR) reported in [27] (see Table 1 and Methods).

In our default scenario we use a contact structure between age groups as measured during pre-pandemic times [28]. However, we halve the infection probability in the 0–19 year age group to account for reduced in-person classes and better ventilation and systematic random screening in school settings using rapid COVID-19 tests. Under these assumptions, the infection probability among the 0–19 age group is similar to the one among the 20–39 and 40–69 age groups. We start our simulations at the beginning of March 2021, with an incidence of 200 daily infections per million, two daily deaths per million, an ICU occupancy of 30 patients per million, a seroprevalence of 10%, and about 4% of the population already vaccinated. This is

Table 1. Age-dependent infection-fatality-ratio (IFR), probability of requiring intensive care due to the infection (ICU probability) and ICU fatality ratio (ICU-FR). The IFR is defined as the probability of an infected individual dying, whereas the ICU-FR is defined as the probability of an infected individual dying while receiving intensive care.

Age	IFR [27]	ICU probability	ICU-FR	Avg. ICU time (days)
0–19	0.00002	0.00014	0.0278	5
20–39	0.00022	0.00203	0.0389	5
40–59	0.00194	0.01217	0.0678	11
60–69	0.00739	0.04031	0.1046	11
70–79	0.02388	0.05435	0.1778	9
>80	0.08292	0.07163	0.4946	6
Average	0.00957	0.02067	0.0969	9

https://doi.org/10.1371/journal.pcbi.1009288.t001

comparable to German data (assuming a case under-reporting factor of 2, which had been measured during the first wave in Germany [29]) and typical for EU countries at the beginning of March 2021 (further details in the Methods section). We furthermore explore the impact of important differences between EU countries, namely the seroprevalance by the start of the vaccination program, demographics, and vaccine uptake exemplary for Finland, Italy and the Czech Republic in addition to the default German parameters.

Results

Aiming for low case numbers has the best long-term outcome

We first present the two extreme scenarios: case numbers quickly rise so that the ICU capacity limit is approached (Scenario 1), or case numbers quickly decline below the TTI capacity limit (Scenario 5; Fig 2). We set the ICU capacity limit at 65 patients/million, reflecting the maximal occupancy and improved treatments during the second wave in Germany [30] and use German demographics. The incidence (daily new cases) limit up to which TTI is fully efficient is set to 20 daily infections per million [15], but depends strongly on the gross reproduction number, as described in Methods.

The first scenario ('approaching ICU limit', Fig 2A–2D) maximizes the initial freedom individuals might have (quantified as the allowed gross reproduction number R_t). However, the gained freedom is only transient as, once ICUs approach their capacity limit, restrictions need to be tightened (Fig 2J and 2K). Additionally, stabilization at high case numbers leads to many preventable fatalities, especially in light of likely temporary overflows of the ICU capacity due to the hard-to-control nature of high case numbers.

The fifth scenario ('below TTI limit', Fig 2E and 2F) requires maintaining stronger restrictions for about two months to lower case numbers below the TTI capacity. Afterward, the progress of the vaccination allows for a steady increase in R_t while keeping case numbers low, enabling TTI to contribute to the containment effectively. From May 2021 on, this fifth scenario would allow for slightly more freedom, i.e., a higher R_t, than the first scenario (Fig 1C). Furthermore, this scenario reduces morbidity and mortality: Deaths until the of the vaccination period (end of August) are reduced by a factor of five, total infections even by a factor of eleven. Due to the prioritization of the elderly in vaccination, the average age of ICU patients and fatalities drops by roughly 12 and 15 years, respectively, independently of the choice of scenarios (Fig 2I). Overall, the low-case-number scenario thus allows for a very similar increase in freedom over the whole time frame (quantified as the increase in R_t) and implies about fives times fewer deaths by the end of the vaccination program compared to the first scenario with high case numbers (Fig 2K).

The vaccine uptake has little influence on the number of deaths and total cases during the vaccination period (Fig 2J and 2K), mainly because restrictions are quickly enacted when reaching the ICU capacity. However, uptake becomes a crucial parameter; It controls the pandemic progression after completing the vaccine roll-out as it determines the residual susceptibility of the population (cf. below). With insufficient vaccination uptake, a novel wave will follow as soon as restrictions are lifted [3].

Maintaining low case numbers at least until vulnerable groups (60+) are vaccinated is necessary to prevent a severe further wave

Between the two extreme scenarios 1 and 5, which respectively allow maximal or minimal initial freedom, we explore three alternative scenarios, where the vaccination progress and the slow restriction lifting roughly balance out (Figs 3 and 1B). These scenarios assume approximately constant case numbers and then a swift lifting of most of the remaining restrictions within a month after three different vaccination milestones: when the age group 80+ has been vaccinated (Scenario 2, Fig 3A–3D), when the age groups 60+ has been vaccinated (Scenario 3, Fig 3E–3H) and when the entire adult population (16+) has been vaccinated (Scenario 4, Fig 3I–3L).

The relative freedom gained by lifting restrictions early in the vaccination timeline (Scenario 2) hardly differs from the freedom gained from the other two scenarios (Fig 3M), as since new contact restrictions need to take place once reaching the ICU capacity limit, and the initial freedom is partly lost. Significantly, lifting restrictions later reduces the number of infections and deaths by more than 50% and 35% respectively if case numbers have been kept at a moderate level (250 daily infections per million) and by more than 85% and 65%, respectively if case numbers have been kept at a low level (50 per million) beforehand (Fig 3N and 3O). Lifting restrictions entirely after either offering vaccination to everyone aged 60+ or everyone aged 16+ only changes the total fatalities by a small amount, mainly because the vaccination pace is planned to be quite fast by then, and the 60+ age brackets make up the bulk of the highest-risk groups. Hence, a potential subsequent wave only unfolds after the end of the planned vaccination campaign (Fig 3F and 3H). Thus, with the current vaccination plan, it is recommended to keep case numbers at moderate or low levels, at least until the population at risk and people of age 60+ have been vaccinated.

If maintaining low or intermediate case numbers in the initial phase, vaccination starts to decrease the ICU occupancy considerably in May 2021 (Fig 3G and 3K). However, This decrease in ICU occupancy must not be mistaken for a generally stable situation. As soon as restrictions are relaxed too quickly, ICU occupancy surges again (Fig 3C, 3G and 3H), without any relevant gain in freedom for the total population. Nonetheless, the progress in vaccination will, in any case, allow lifting restrictions gradually.

The long-term success of the vaccination campaign strongly depends on vaccine uptake and vaccine efficacy

The vaccination campaign's long-term success will depend on both people's vaccine uptake and the efficacy of the vaccine against those variants of SARS-CoV-2 prevalent at the time of writing of this paper. A vaccine's efficacy has two contributions: first, vaccinated individuals become less likely to develop severe symptoms and require intensive care [31–33] (vaccine efficacy, κ). Second, a fraction η of vaccinated individuals gains sterilizing immunity, i.e., is completely protected against infections and does not contribute to viral spread at all [24, 34]. We also assume that breakthrough infections among vaccinated individuals would bear lower viral loads, thus exhibit reduced transmissibility [25] (reduced viral load, σ). However, the
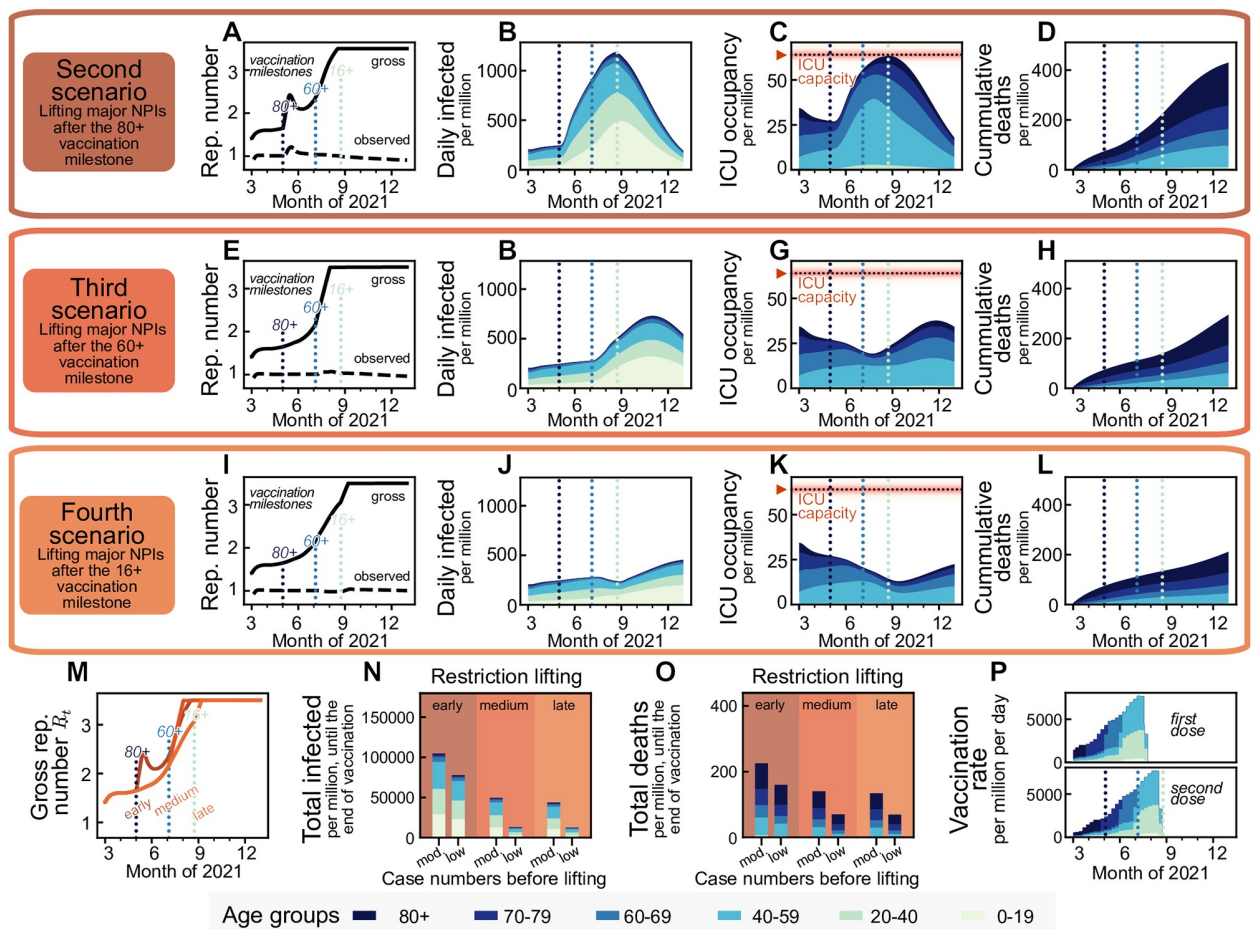
Fig 3. Vaccination offers a steady return to normality until the end of summer 2021 in the northern hemisphere, no matter whether a transient easing of restrictions is allowed earlier or later (second and fourth scenario, respectively). However, lifting restrictions later reduces fatalities by more than 35%. We assume that the vaccine immunization progress is balanced out by a slow lifting of restrictions, keeping case numbers at a moderate level (≤ 250 daily new cases per million people). We simulated lifting all restrictions within a month starting from different time points: when (**A–D**) the 80+ age group, (**E–H**) the 60+ age group or (**I–L**) everyone 16+ has been offered vaccination. Restriction lifting leads to a new surge of cases in all scenarios. New restrictions are put in place if ICUs would otherwise collapse. **M**: Lifting all restrictions too early increases the individual freedom only temporarily before new restrictions have to be put in place to avoid overwhelming ICUs. Overall, trying to lift restrictions earlier has a small influence on the additional increase in the allowed gross reproduction number R_t. **N,O**: Relaxing major restrictions only medium-late or late reduces fatalities by more than 35% and infections by more than 50%. Fatalities and infections can be cut by an additional factor of more than two when aiming for a *low* (50 per million) instead of *moderate* (250 per million) level of daily infections before major relaxations. **P**: Assumed daily vaccination rates, same as in Fig 2.

https://doi.org/10.1371/journal.pcbi.1009288.g003

possibly reduced effectiveness of vaccines against current variants of concern (VOCs), e.g., B.1.351 and P.1 [32, 35, 36], and potential future VOCs render long-term scenarios about the success of vaccination uncertain.

Therefore, we explore different parameters of vaccine uptake and effectiveness. We quantify the success, or rather the lack of success of the vaccination campaign by the duration of the period where ICUs function near capacity limit, until population immunity is reached. Two different scenarios are considered upon finishing the vaccination campaign: in the first scenario, most restrictions are lifted, like in the previous scenarios (Fig 4B). In the second, restrictions are only lifted partially, to a one third lower gross reproduction number (R_t = 2.5) (Fig 4C). This second scenario presents the long-term maintenance of moderate social distancing
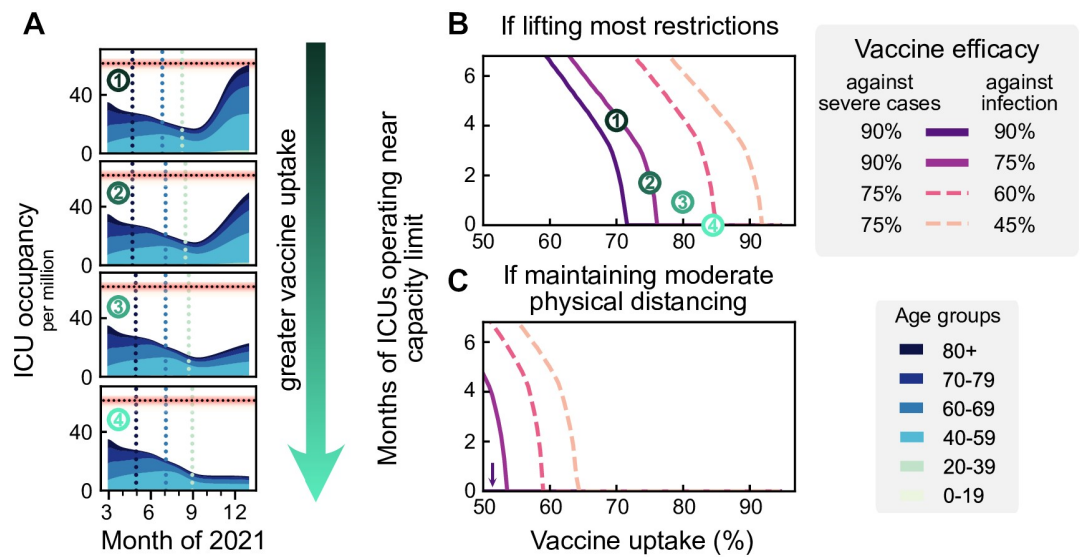
Fig 4. A high vaccine uptake (> 90% or higher among the eligible population) is crucial to prevent a wave when lifting restrictions after completing vaccination campaigns. A: We assume that infections are kept stable at 250 daily infections until all age groups have been vaccinated. Then restrictions are lifted, leading to a wave if the vaccine uptake has not been high enough (top three plots). **B**: The duration of the wave (measured by the total time that ICUs function close to their capacity limit) depends on vaccine uptake and vaccine efficacy. We explore the dependency on the efficacy both for preventing severe cases (full versus dashed lines) and preventing infection (shades of purple). The dashed lines might correspond to vaccine efficacy in the event of the emergence of escape variants of SARS-CoV-2. **C**: If some NPIs remain in place (such that the gross reproduction number stays at R_t = 2.5), ICUs will not overflow even if the protection against infection is only around 60%. See S2 Fig for all possible combinations of vaccine efficacies, also in the event of different contact structures.

measures, including the restriction of large gatherings to smaller than 100 people, encouraging home-office, enabling effective test-trace-and-isolate (TTI) programs at very low case numbers, and supporting hygiene measures and face mask usage. Fig 4B and 4C indicates how long ICUs are expected to be full in both scenarios, and for different parameters of vaccine efficacy (which may account for the emergence of vaccine escape variants).

The primary determinant for the success of vaccination programs after lifting most restrictions is the vaccine uptake among the population aged 20+; only with a high vaccine uptake (> 90%) we can avoid a novel wave of full ICUs (default parameters as in scenario 3; Fig 4B, κ = 90%, η = 75%). However, if vaccine uptake was lower or vaccines prove to be less effective against prevalent or new variants, lifting most restrictions would imply that ICUs will work at the capacity limit for months.

In contrast, maintaining moderate social distancing measures (Fig 4C) may prevent a wave after completing the vaccine roll-out. This strategy can also compensate for a low vaccine uptake, requiring only about 55% uptake to avoid surpassing ICU capacity for our default parameters. Nonetheless, any increase in vaccine uptake lowers intensive care numbers, increases freedom, and most importantly, provides better protection in case of the emergence of escape variants, as this would involve an effective reduction of vaccine efficacy (dashed lines). A full exploration of vaccine efficacy parameter combinations and different contact structures is presented in S2 Fig.

Heterogeneity among countries on an EU-wide level will affect the probability and strength of a new wave after completing vaccination campaigns. We chose some exemplary European countries to investigate how our results depend on age demographics, contact structure, and the degree of initial post-infection immunization (seroprevalence). We obtained the
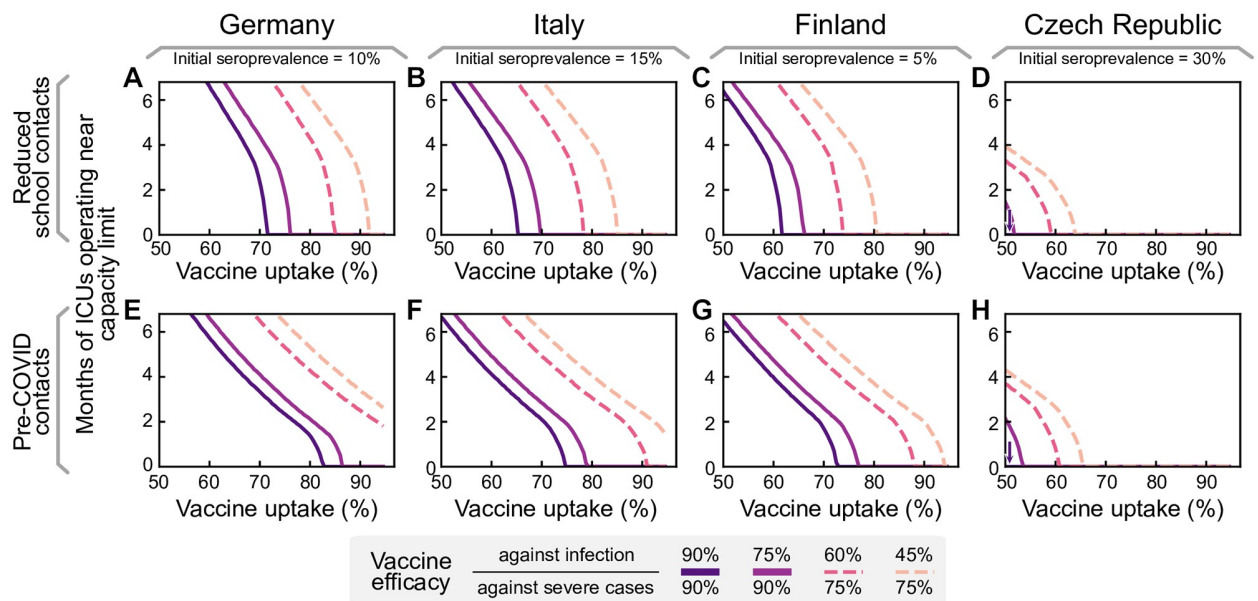
Fig 5. Seroprevalence and different demographics across EU countries determine the vaccine uptake required for population immunity. As in Fig 4B, we assume that case numbers are stable at 250 daily infections per million per day until the end of vaccination, when most restrictions are lifted (such that the gross reproduction number goes up to 3.5). We vary the initial seroprevalence and age demographics and contact structures to represent German, Italian, Finnish, and Czech data. **A–D**: Projected ICU occupancy in a subsequent wave depending on vaccine uptake, assuming reduced transmission risk in schools but otherwise default pre-pandemic contact structures. **E–H**: Projected ICU occupancy depending on vaccine uptake, assuming default pre-pandemic contact structures everywhere (including schools). See S3 Fig for a more comprehensive exploration of combinations of vaccine efficacies.

seroprevalence in the different countries by scaling the German 10% seroprevalence with the relative differences in cumulative reported case numbers between Germany and the other countries, i.e., we assume the under-reporting factor to be roughly the same across the chosen countries. All other parameters are left unchanged. Specifically, we leave the capacities of the health systems at the estimated values for Germany, as lacking TTI data and varying definitions of ICU treatment make any comparison difficult. We repeated the analysis presented above (Fig 4) for Finland, Italy and the Czech Republic (see Fig 5A–5D). Germany, Finland, and Italy would need a similarly high vaccine uptake in the population to prevent another severe wave. In the Czech Republic, a much smaller uptake is sufficient. The largest deviations in the necessary vaccine uptake are due to the initial seroprevalence, which we estimate to range from 5% in Finland to 30% in the Czech Republic. In contrast, the differences in age demographics and contact structures only have a minor effect on the dynamics (see also S1 Fig).

If no further measures remain in place to reduce the potential contagious contacts in school settings, the young age group (0–19 years) will drive infections after completing the vaccination program as they remain mostly unvaccinated. The combination of intense contacts and high susceptibility among school-aged children considerably increase the vaccine uptake required in the adult population to restrain a further wave (Fig 5E–5H). High seroprevalence, also in this age group, reduces the severity of this effect for the Czech Republic (Fig 5H).

Discussion

Our results demonstrate that the pace of vaccination first and foremost determines the expected gain in freedom (i.e., lifting of restrictions) during and after completion of the

COVID-19 vaccination programs. Any premature lifting of restrictions risks another wave with high COVID-19 incidence and full ICUs. Moreover, the increase in freedom gained by these premature strategies is only transient because once ICU capacity is reached again, restrictions would have to be reinstated. Simultaneously, these early relaxations significantly increase morbidity and mortality rates, as a fraction of the population has not yet been vaccinated and thus remains susceptible. In contrast, maintaining low case numbers avoids another wave, and *still* allows to lift restrictions steadily and at a similar pace as with high case numbers. Despite this qualitative behavior being general, the precise quantitative results depend on several parameters and assumptions, which we discuss in the following.

The specific time evolution of the lifting of restrictions is dependent on the progress of the vaccination program. Therefore, a steady lifting of restrictions may start in May 2021, when the vaccination rate in the European Union gains speed. However, if the vaccination roll-out stalls more than we assume, the lifting of restrictions has to be delayed proportionally. In such a slowdown, the total number of cases and deaths until the end of the vaccination period increases accordingly. Thus, cautious lifting of restrictions and a fast vaccination delivery is essential to reduce death tolls and promptly increase freedom.

The spreading dynamics after concluding vaccination campaigns (Fig 4B and 4C) will be mainly determined by i) final vaccine uptake, ii) the contact network structure, iii) vaccine effectiveness, and iv) initial seroprevalence. Regarding vaccine uptake, we assumed that after the vaccination of every willing person, no further people would get vaccinated. This assumption enables us to study the effects of each parameter separately. However, vaccination willingness might change over time: it will probably be higher if reported case numbers and deaths are high, and vice versa. This poses a fundamental challenge: If low case numbers are maintained during the vaccine roll-out, the overall uptake might be comparably low, thus leading to a more severe wave once everyone has received a vaccination offer and restrictions are fully lifted. In contrast, a severe wave during vaccine roll-out might either increase vaccine uptake, because of individuals looking to protect themselves, or reduce it, because of damaged credibility on vaccine efficacy among vaccine hesitant groups. Thus, to avoid any further wave, policymakers have to maintain low case numbers *and* foster high vaccine uptake.

Besides vaccine uptake, the population's contact network also determines whether population immunity will be reached. We studied different real-world and theoretical possibilities for the contact matrices in Germany and other EU countries and evaluated how our results depend on the connectivity among age groups. For the long-term success of the vaccination programs, there must be exceptionally sensible planning of measures to prevent contagion among school-aged children. Otherwise, they could become the drivers of a novel wave because they might remain mostly unvaccinated. Provided adequate vaccine uptake among the adult population, our results suggest that reducing either the intensity of contacts or the infectiousness in that age group by half would be sufficient for preventing a rebound wave. This reduction is attainable by implementing soft-distancing measures, plus systematic, preventive random screening with regular COVID-19 rapid tests in school settings or via vaccination [22]. Although at the time of writing some vaccines have been provisionally approved for use in children aged 12–15 years old, vaccine uptake among children remains highly uncertain because of their very low risk for severe illness from COVID-19. We therefore did not include their vaccination in our model.

One of the largest uncertainties regarding the dynamics after vaccine roll-out arises from the efficacies of the vaccines. First, the sterilizing immunity effect (i.e., blocking the transmission of the virus), is still not well quantified and understood [24]. Second, the emergence of new viral variants that at least partially escape immune response is continuously under

investigation [35, 37, 38]. Furthermore, there is no certainty about whether escape variants might produce a more severe course of COVID-19 or whether reinfections with novel variants of SARS-CoV-2 would be milder. Therefore, we cannot conclusively quantify the level of contact reductions necessary in the long term to avoid a further wave of infections or whether such wave would overwhelm ICUs. However, for our default parameters, moderate contact reductions and hygiene measures would be sufficient to prevent further waves.

Although most examples are presented for countries from the European Union, our results can also be generalized to other countries. Differences across countries come from i) demographics, ii) varying seroprevalence —which originated from large differences in the severity of past waves—, iii) vaccines (types, availability, delivery scheme, and uptake), as well as iv) capacities of the health systems, including hospitals and TTI capabilities. For the EU, we find that during the mass vaccination phase, all these differences have only a minor effect on the pace at which restrictions can be lifted (cf. S1 Fig). However, differences become evident in the long term when most restrictions are lifted by the end of the vaccination campaigns. Demographics and contact patterns are qualitatively very similar across EU countries and thus do not strongly change the expected outcome. On the contrary, we found the initial seroprevalence to significantly determine the minimum vaccine uptake required to guard against further waves after the vaccine roll-out (cf. Fig 5). Naturally acquired immunity, like vaccinations, contributes to reducing the overall susceptibility of the population and thus impedes viral spread. Notably, naturally acquired immunity can compensate for drops in vaccine uptake in specific age groups unwilling to vaccinate or that cannot access the vaccine, e.g. in children. Furthermore, expected vaccine uptake considerably varies across EU countries (e.g., Serbia 38%, Croatia 41%, France 44%, Italy 70%, Finland 81% [6], Czech Republic 40% [39], Germany 80% [26]). The risk of rebound waves after the mass vaccinations might thus be highly heterogeneous across the EU.

Since we neither know what kind of escape variants might still surface nor their potential impact on vaccine efficacies or viral spread, maintaining low case numbers is the safest strategy for long-term planning. This strategy i) prevents avoidable deaths during vaccine roll-out, ii) offers better preparedness should escape variants emerge, and iii) lowers the risk of further waves because local outbreaks are easier to contain with efficient TTI. Hence, low case numbers only have advantages for health, society, and the economy. Furthermore, a low case number strategy would greatly profit from an EU-wide commitment, and coordination [15]. Otherwise, strict border controls with testing and quarantine policies need to be installed as drastically different case numbers between neighboring countries or regions promote destabilization; infections could (and will) propagate between countries triggering a "ping-pong" effect, especially if restrictions are not jointly planned. Therefore, promoting a high vaccine uptake and low case numbers strategy should not only be a priority for each country but also for the whole European community.

In practice, there are several ways to lower case numbers to the capacity limit of TTI programs without the need to enact stringent NPIs immediately. For example, if restrictions are lifted gradually but marginally slower than the rate vaccination pace would allow, case numbers will still decline. Alternatively, restrictions could be relaxed initially to an intermediate level where case numbers do not grow exponentially while giving people some freedom. In such circumstances one can take advantage of the reduced susceptibility to drive case numbers down without the need of stringent NPIs (S5(E)–S5(H) Fig).

To conclude, the opportunity granted by the progressing vaccination should not only be used to lift restrictions carefully but also to bring case numbers down. This will significantly reduce fatalities, allow to lift all major restrictions gradually moving into summer 2021, and guard against newly-emerging variants or potential further waves in the EU.

Methods

Model overview

We model the spreading dynamics of SARS-CoV-2 following a SEIRD-ICU deterministic formalism through a system of delay differential equations. Our model incorporates age-stratified dynamics, ICU stays, and the roll-out of a 2-dose vaccine. For a graphical representation of the infection and core dynamics, see Fig 6. The contagion dynamics include the effect of externally
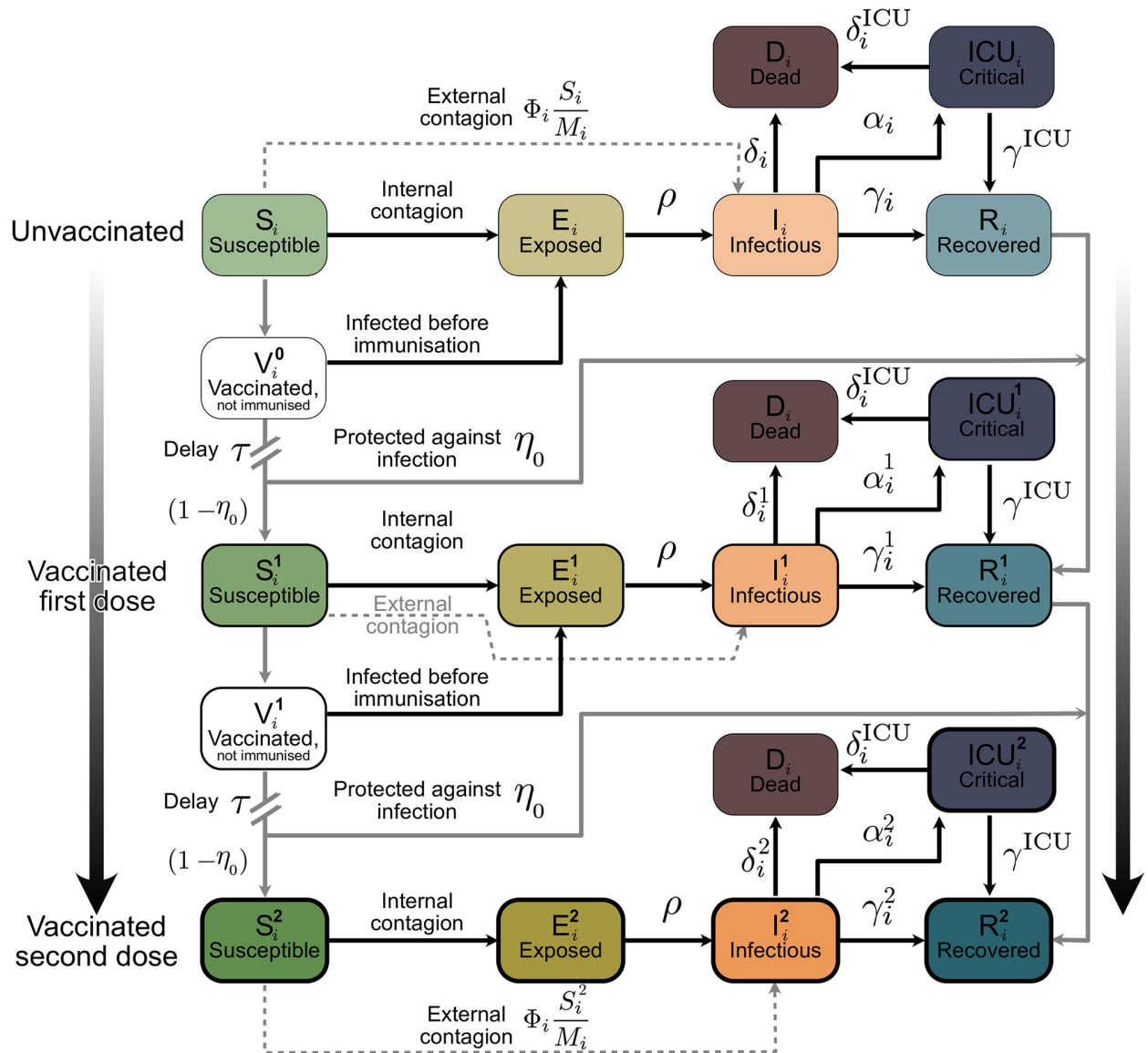
Fig 6. Scheme of our age-stratified SEIRD-ICU+vaccination model. The solid blocks in the diagram represent different SEIRD compartments. Solid black lines represent transition rates of the natural progression of the infection (contagion, latent period, and recovery). On the other hand, dashed lines account for external factors and vaccination. Solid gray lines represent non-linear transfers of individuals between compartments, e. g. through scheduled vaccination. From top to bottom, we describe the progression from unvaccinated to vaccinated, with stronger color and thicker edges indicating more protection from the virus. Subscripts *i* indicate the age groups, while superscripts represent the number of vaccine doses that have successfully strengthened immune response in individuals receiving them. Contagion can occur internally, where an individual from age group *i* can get infected from an infected person from any age group, or externally, e. g., abroad on vacation. If the contagion happens externally, we assume that the latent period is already over when the infected returns and, hence, they are immediately put into the infectious compartments I_i^v.

acquired infections as a non-zero influx Φ_i based on the formalism previously developed by our group [18, 19]: susceptible individuals of a given age group i (S_i) can acquire the virus from infected individuals from any other age group j and subsequently progress to the exposed ($S_i \rightarrow E_i$) and infectious ($E_i \rightarrow I_i$) compartments. They can also acquire the virus externally. However, in this case, they progress directly to the infectious compartment ($S_i \rightarrow I_i$), i.e., they get infected abroad, and by the time they return, the latent period is already over. Individuals exposed to the virus (E_i) become infectious after the latent period and thus progress from the exposed to the infectious compartments (I_i) at a rate ρ ($E_i \rightarrow I_i$). The infectious compartment has three different possible transitions: i) direct recovery ($I_i \rightarrow R_i$), ii) progression to ICU ($I_i \rightarrow$ ICU$_i$) or iii) direct death ($I_i \rightarrow D_i$). Individuals receiving ICU treatment can either recover (ICU$_i \rightarrow R_i$) or decease (ICU$_i \rightarrow D_i$).

A contact matrix weights the infection probability between age groups. We investigated three different settings for the contact structure to assess its impact on the spreading dynamics of COVID-19: i) Interactions between age groups are proportional to the group size, i.e., the whole population is mixed perfectly homogeneously, ii) interactions are proportional to pre-COVID contact patterns in the EU population [28], and iii) interactions are proportional to "almost" pre-COVID contact patterns [28], i.e., the contact intensity in the youngest age group (0–19 years) is halved. This accounts for some preventive measures kept in place in schools, e.g., regular rapid testing or smaller class sizes. Scenario iii) is the default scenario unless explicitly stated. However, figures for Scenarios i) and ii) are provided in S9–S14 Figs. We scale all the contact structures by a linear factor, which increases or decreases the stringency of NPIs so that the settings are comparable. However, the scaling above does not account for heterogeneous NPIs acting only on contacts between specific age groups, such as workplace or school restrictions.

Our model includes the effect of vaccination, where vaccines are administered with an age-stratified two-dosage delivery scheme. The scheme does not discriminate on serological status, i.e., recovered individuals with natural antibodies may also access the vaccine when offered to them. Immunization, understood as the development of proper antibodies against SARS-CoV-2, does not occur immediately after receiving the vaccination dose. Thus, newly vaccinated individuals get temporarily put into extra compartments (V_i^0 and V_i^1 for the first and second dose respectively) where, if infected, they would progress through the disease stages as if they would not have received that dose. For modeling purposes, we assume that a sufficient immune response is build up τ days after being vaccinated ($V_i^0 \rightarrow S_i^1$ and $V_i^1 \rightarrow S_i^2$), and that a fraction $p_i(t)$ of those individuals that received the dose acquire the infection before being immunized. Furthermore, there is some evidence that the vaccines partially prevent the infection with and transmission of the disease [40, 41]. Our model incorporates the effectiveness against infection following an 'all-or-nothing' scheme, removing a fraction of those vaccinated individuals to the recovered compartments ($V_i^0 \rightarrow R_i^1$ and $V_i^1 \rightarrow R_i^2$), thus assuming that they would not participate in the spreading dynamics. However, we consider those vaccinated individuals with a breakthrough infection have a lower probability of going to ICU or to die than unvaccinated individuals, i.e., effectiveness against severe disease follows a 'leaky' scheme. Furthermore, we assume those individuals carry a lower viral load and thus are less infectious by a factor of two [25]. All parameters and values are listed in Table 2.

We model the mean-field interactions between compartments by transition rates, determining the timescales involved. These transition rates can implicitly incorporate both the time course of the disease and the delays inherent to the case-reporting process. In the different scenarios analyzed, we include a non-zero influx Φ_i, i.e., new cases that acquired the virus from outside. Even though this influx makes a complete eradication of SARS-CoV-2 impossible,

Table 2. Model parameters. The range column either describes the range of values used in the various scenarios, or if values depend on the age group (indexed by *i*), the lowest and highest value across age-groups.

Parameter	Meaning	Value (default)	Range	Units	Source
R_t	Reproduction number (gross)	1.00	0–3.5	—	Assumed
η	Vaccine protection against transmission	0.75	0.5–0.85	—	[24, 40, 41]
κ	Vaccine efficacy (against severe disease)	0.9	0.7–0.95	—	[23, 57]
σ^v	Relative virulence of unvaccinated and vaccinated individuals	[1.0, 0.5, 0.5]	0.5–1	—	[25]
τ	Immunization delay	7	—	days	[24, 31]
v_r	Random vaccination fraction	0.35	—	—	[64, 65]
M_i	Population group size	Table 4	—	people	[43]
u_i	Vaccine uptake	Table 4	—	—	[6]
ρ	Transition rate $E \rightarrow I$	0.25	—	day^{-1}	[66, 67]
γ_i^v	Recovery rate from I_i^v	Table 5	0.088–0.1	day^{-1}	[54–56]
γ_i^{ICU}	Recovery rate from ICU$_i^v$	Table 5	0.08–0.2	day^{-1}	[50, 52, 68]
δ_i^v	Death rate from I_i^v	Table 5	10^{-6}–0.005	day^{-1}	[50, 52, 68]
δ_i^{ICU}	Death rate from ICU$_i^v$	Table 5	0.0055–0.083	day^{-1}	[50, 52, 68]
α_i^v	Transition rate $I \rightarrow$ ICU	Table 5	10^{-5}–0.007	day^{-1}	[50, 52, 68]
Φ_i	Infections from external sources	1	—	cases day^{-1} per million	Assumed
$p_i(t)$	Fraction of individuals getting infected before acquiring antibodies	—	—	—	Eq (34)
$\bar{\gamma}$	Effective removal rate from infectious compartment	—	—	day^{-1}	$(\gamma_i^v + \alpha_i^v + \delta_i^v)$
$f_i^1(t), f_i^2(t)$	Administered 1$^{\mathrm{st}}$ and 2$^{\mathrm{nd}}$ vaccine doses	—	—	doses/day	Eqs (19) and (20)

different outcomes in the spreading dynamics might arise depending on both contact intensity and TTI [18]. Additionally, we include the effects of non-compliance and unwillingness to be vaccinated as well as the effects of the TTI capacities from health authorities, building on [19]. Throughout the manuscript, we do not make explicit differences between symptomatic and asymptomatic infections. However, we implicitly consider asymptomatic infections by accounting for their effect on modifying the reproduction number R_t and all other epidemiological parameters. To assess the lifting of restrictions in light of progressing vaccinations, we use a Proportional-Derivative (PD) control approach to adapt the internal reproduction number R_t targeting controlled case numbers or ICU occupancy.

Model equations

The contributions of the spreading dynamics and the age-stratified vaccination strategies are summarized in the equations below. They govern the infection dynamics between the different age groups, each of which is represented by their susceptible-exposed-infectious-recovered-dead-ICU (SEIRD+ICU) compartments for all three vaccination statuses. We assume a regime that best resembles the situation in Germany at the beginning of March 2021, and we estimate the initial conditions for the different compartments of each age group accordingly. Furthermore, we assume that neither post-infection immunity [42] nor the immunization obtained through the different dosages of the vaccine vanish significantly in the considered time frames. The spreading parameters completely determine the resulting dynamics (characterized by the different age- and dose-dependent parameters, together with the gross reproduction number R_t) and the vaccination logistics.

All of the following parameters and compartments are shortly described in Tables 2 and 3. Some of these are elaborated in more detail in the following sections. Subscripts *i* in the equations denote the different age groups, while superscripts denote the vaccination status:

Table 3. Model variables. Subscripts i denote the ith age group, superscripts the vaccination status (unvaccinated, immunized by one dose, by two doses).

Variable	Meaning	Units	Explanation
S_i, S_i^1, S_i^2	Susceptible pools	people	Non-infected people that may acquire the virus.
V_i^0, V_i^1	Vaccinated pools	people	Non-infected people that have been vaccinated but have not developed antibodies yet, thus may acquire the virus.
E_i, E_i^1, E_i^2	Exposed pools	people	Infected people in latent period. Cannot spread the virus.
I_i, I_i^1, I_i^2	Infectious pools	people	Currently infectious people.
ICU_i, ICU_i^1, ICU_i^2	ICU pools	people	Infected people receiving ICU treatment, isolated.
D_i, D_i^1, D_i^2	Dead pools	people	Dead people.
R_i, R_i^1, R_i^2	Recovered pools	people	Recovered/immune people that have acquired post-infection or sterilizing vaccination immunity.
$\hat{N}^{\mathrm{obs}}$	Observed new infections	people day^{-1}	Daily new infections, including reporting delays. Eq (42)
$\hat{R}_t^{\mathrm{obs}}$	Observed reproduction number	–	The reproduction number that can be estimated only from the observed cases: $\hat{R}_t^{\mathrm{obs}} = \hat{N}^{\mathrm{obs}}(t)/\hat{N}^{\mathrm{obs}}(t-4)$.

unvaccinated (^{0} or none), immunized by one dose (^{1}), or by two doses (^{2}).

$$\frac{dS_i}{dt} = \underbrace{-\bar{\gamma} R_t S_i \sum_{j,v} C_{ji} \frac{\sigma^v I_j^v}{M_j}}_{\text{internal contagion}} - \underbrace{f_i^1(t) \frac{S_i}{S_i + R_i}}_{\text{administering first dose}} - \underbrace{\frac{S_i}{M_i} \Phi_i}_{\text{external contagion}} \tag{1}$$

$$\frac{dV_i^0}{dt} = \underbrace{-\bar{\gamma} R_t V_i^0 \sum_{j,v} C_{ji} \frac{\sigma^v I_j^v}{M_j}}_{\text{internal contagion}} + \underbrace{f_i^1(t) \frac{S_i}{S_i + R_i}}_{\text{administering first dose}} \cdots$$
$$\cdots - \underbrace{f_i^1(t-\tau) \frac{S_i}{S_i + R_i}\Big|_{t-\tau} (1 - p_i(t))}_{\text{first dose showing effect}} - \underbrace{\frac{V_i^0}{M_i} \Phi_i}_{\text{external contagion}} \tag{2}$$

$$\frac{dS_i^1}{dt} = \underbrace{-\bar{\gamma} R_t S_i^1 \sum_{j,v} C_{ji} \frac{\sigma^v I_j^v}{M_j}}_{\text{internal contagion}} - \underbrace{f_i^2(t) \frac{S_i^1}{S_i^1 + R_i^1}}_{\text{administering second dose}} \cdots$$
$$\cdots + \underbrace{(1 - \eta_0) f_i^1(t-\tau) \frac{S_i}{S_i + R_i}\Big|_{t-\tau} (1 - p_i(t))}_{\text{first dose (not immune)}} - \underbrace{\frac{S_i^1}{M_i} \Phi_i}_{\text{external contagion}} \tag{3}$$

$$\frac{dV_i^1}{dt} = \underbrace{-\bar{\gamma} R_t V_i^1 \sum_{j,v} C_{ji} \frac{\sigma^v I_j^v}{M_j}}_{\text{internal contagion}} + \underbrace{f_i^2(t) \frac{S_i^1}{S_i^1 + R_i^1}}_{\text{administering second dose}} \cdots$$
$$\cdots - \underbrace{f_i^2(t-\tau) \frac{S_i^1}{S_i^1 + R_i^1}\Big|_{t-\tau} (1 - p_i(t))}_{\text{second dose showing effect}} - \underbrace{\frac{V_i^1}{M_i} \Phi_i}_{\text{external contagion}} \tag{4}$$

$$\frac{dS_i^2}{dt} = \underbrace{-\bar{\gamma}R_t S_i^2 \sum_{j,v} C_{ji} \frac{\sigma^v I_j^v}{M_j}}_{\text{internal contagion}} + \underbrace{(1-\eta_0)f_i^2(t-\tau)\frac{S_i^1}{S_i^1+R_i^1}\bigg|_{t-\tau}(1-p_i(t))}_{\text{second dose (not immune)}} \cdots$$

$$\cdots - \underbrace{\frac{S_i^2}{M_i}\Phi_i}_{\text{external contagion}}$$

(5)

$$\frac{dE_i}{dt} = \underbrace{\bar{\gamma}R_t\left(S_i+V_i^0\right)\sum_{j,v}C_{ji}\frac{\sigma^v I_j^v}{M_j}}_{\text{internal contagion}} - \underbrace{\rho E_i}_{\text{end of latency}}$$

(6)

$$\frac{dE_i^1}{dt} = \underbrace{\bar{\gamma}R_t\left(S_i^1+V_i^1\right)\sum_{j,v}C_{ji}\frac{\sigma^v I_j^v}{M_j}}_{\text{internal contagion}} - \underbrace{\rho E_i^1}_{\text{end of latency}}$$

(7)

$$\frac{dE_i^2}{dt} = \underbrace{\bar{\gamma}R_t S_i^2 \sum_{j,v}C_{ji}\frac{\sigma^v I_j^v}{M_j}}_{\text{internal contagion}} - \underbrace{\rho E_i^2}_{\text{end of latency}}$$

(8)

$$\frac{dI_i}{dt} = \underbrace{\rho E_i}_{\text{end of latency}} - \underbrace{\bar{\gamma}I_i}_{\text{recovery, ICU admission, or death}} + \underbrace{\frac{S_i+V_i^0}{M_i}\Phi_i}_{\text{external contagion}}$$

(9)

$$\frac{dI_i^1}{dt} = \underbrace{\rho E_i^1}_{\text{end of latency}} - \underbrace{\bar{\gamma}I_i^1}_{\text{recovery, ICU admission, or death}} + \underbrace{\frac{S_i^1+V_i^1}{M_i}\Phi_i}_{\text{external contagion}}$$

(10)

$$\frac{dI_i^2}{dt} = \underbrace{\rho E_i^2}_{\text{end of latency}} - \underbrace{\bar{\gamma}I_i^2}_{\text{recovery, ICU admission, or death}} + \underbrace{\frac{S_i^2}{M_i}\Phi_i}_{\text{external contagion}}$$

(11)

$$\frac{d\text{ICU}_i^v}{dt} = \underbrace{-(\delta_i^{\text{ICU}}+\gamma_i^{\text{ICU}})\text{ICU}^v}_{\text{recovery or death}} + \underbrace{\alpha_i^v I_i^v}_{\text{ICU admission}}$$

(12)

$$\frac{dD_i}{dt} = \underbrace{\sum_v (\delta_i^{\text{ICU}}\text{ICU}_i^v+\delta_i^v I_i^v)}_{\text{total deaths}}$$

(13)

$$\frac{dR_i}{dt} = \underbrace{\gamma_i^{\text{ICU}}\text{ICU}_i+\gamma_i I_i}_{\text{recovery}} - \underbrace{f_i^1(t)\frac{R_i}{S_i+R_i}}_{\text{first dose}}$$

(14)

$$\frac{dR_i^1}{dt} = \underbrace{\gamma_i^{\mathrm{ICU}}\mathrm{ICU}_i^1 + \gamma_i^1 I_i^1}_{\text{recovery}} + \underbrace{f_i^1(t)\frac{R_i}{S_i + R_i}}_{\text{first dose after recovery}} \underbrace{- f_i^2(t)\frac{R_i^1}{S_i^1 + R_i^1}}_{\text{second dose}} \cdots$$

$$\cdots + \underbrace{\eta_0 f_i^1(t-\tau)\frac{S_i}{S_i + R_i}\bigg|_{t-\tau}(1 - p_i(t))}_{\text{first dose (sterilizing immunity))}} \tag{15}$$

$$\frac{dR_i^2}{dt} = \underbrace{\gamma_i^{\mathrm{ICU}}\mathrm{ICU}_i^2 + \gamma_i^2 I_i^2}_{\text{recovery}} + \underbrace{f_i^2(t)\frac{R_i^1}{S_i^1 + R_i^1}}_{\text{second dose after recovery}} \cdots$$

$$\cdots + \underbrace{\eta_0 f_i^2(t-\tau)\frac{S_i^1}{S_i^1 + R_i^1}\bigg|_{t-\tau}(1 - p_i(t))}_{\text{second dose (sterilizing immunity)}} \tag{16}$$

Contact structure and the effect of NPIs on the contact levels

We model the probability of a susceptible individual from age group i to get infected from an individual from age group j to be proportional to the –effective– incidence in that group $\left(\sum_v I_j^v \sigma^v\right)$ and the contact intensity between the two groups, given by the entries $(C)_{ij}$ of a contact matrix C scaled with the gross reproduction number R_t. The contact matrices are normalized to force their largest eigenvalue (i.e., their spectral radius) to be 1, so that, when multiplied with R_t, their spectral radius equals R_t. The total contact levels for different levels of NPIs are then just linearly scaled with R_t. We thus neglect any inhomogeneities in the NPIs that might affect contact between specific age groups more than others.

As described previously, we study three different configurations for the contact matrix C: i) a perfectly homogeneously mixed population, ii) pre-COVID structure in the EU population [28], and iii) "almost" pre-COVID contact structure [28], but with reduced potentially-contagious contacts in the youngest age group (0–19 years) accounting for some preventive measures kept in place in schools. If not explicitly stated otherwise, the default contact matrix we use in the main text is always the intermediate "almost" pre-COVID contact structure matrix. For the three scenarios, we analyze the demographics and contact structures in Germany, Finland, the Czech Republic, and Italy as a sample for varying demographics across the EU.

First scenario: Homogeneous contact structure. In this scenario, we consider that everyone has the same probability of meeting anyone from any other age group. The probability of meeting somebody from a given age group is thus proportional to the fraction of this age group within the whole population. Let f be the column vector collecting these fractions, $f_i = \frac{M_i}{M}$, the contact matrix for the n age-groups herein considered $C \in \mathbb{R}^{n \times n}$ is thus given by

$$(C)_{ij} = f_j, \forall j \tag{17}$$

and can be seen in Fig 7A, 7D, 7G and 7J, for the chosen demographics. Note that by this construction the largest eigenvalue of this C (i.e., its spectral radius) is automatically 1 for any demographics, i.e., for any f that fulfills $\sum_j f_j = 1$ (proof in S1 Supplementary Note).

Second scenario: Pre-COVID contact intensity, real-world contact structure. Here, we use the whole contact matrices from before the pandemic reported with one-year age resolution in [28], converted into the age brackets that we chose. We normalize them by their
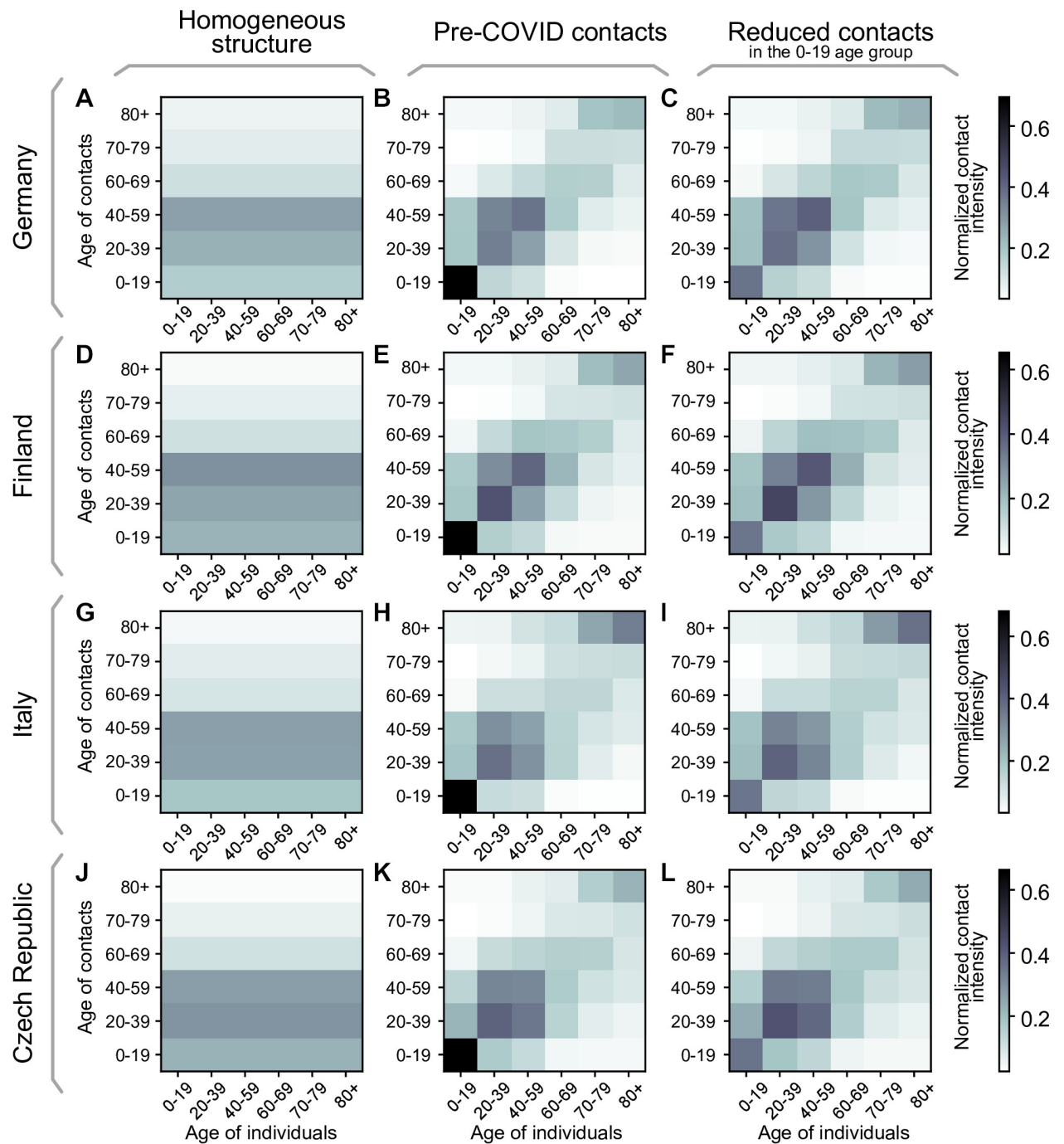
Fig 7. Contact structures for different EU countries in the three scenarios. The chosen contact matrices for i) homogeneous contact structure, ii) pre-COVID contact structure, and iii) "almost" pre-COVID structure with reduced potentially-contagious contacts in schools for Germany (**A-C**), Finland (**D-F**), Italy (**G-I**) and the Czech Republic (**J-L**). Entries of the matrices show the contact intensity between age groups normalized to give each matrix a spectral radius of 1.

spectral radius, leaving their internal contact structure intact. This scenario thus resembles completely homogeneous NPIs that affect every possible contact equally. The matrices are given in Fig Fig 7B, 7E, 7H and 7K for the chosen countries.

Third scenario: "Almost" pre-COVID contact intensity, real-world contact structure.
Finally, we again use the contact matrices from before the pandemic reported in [28] but adapt them to reduce the intensity of contacts of the youngest age group by half, accounting for those measures that remain in place to prevent contagion and mitigate outbreaks in school settings. Specifically, we halve the matrix element connecting the 0–19 age group with itself and normalize the obtained contact matrix C by its spectral radius. As can be seen in the resulting matrices, given in Fig 7C, 7F, 7I and 7L, this affects that the main contributions in the contacts are more evenly spread in the 0–59 year age groups. This serves as a first approximation to the contact structure with inhomogeneous NPIs targeting different age groups differently both in a complete lockdown, as well as some continued measures in schools.

Vaccination dynamics and logistics

In real-world settings, not every person accepts the vaccine when offered. Additionally, vaccine uptake is bounded because some vulnerable groups cannot be vaccinated because of health-related reasons. A systematic survey [26] estimates the vaccine uptake to be approximately 80% across the adult population in Germany, which we choose as our baseline. Due to a higher perception of the risk caused by an infection, we expect that the uptake is higher for elderly population. Thus, we set the uptake u_i to be age-group dependent. Besides the default 80%, we choose two more sets of uptakes averaging to a total of 70% and 90%, respectively. We suppose that an increase in the uptake is possible by education and information measures. They are listed in Table 4. We linearly interpolate between the three values to model arbitrary total vaccine uptakes.

Using official data of the German vaccine stock and stock projections [44, 45] we build up an estimated delivery function w_T that models the weekly number of doses delivered as a function of time. We assume it takes a logistic form, as we assume the number of daily doses increases strongly at the beginning until it reaches a stable level. Adapting the logistic function to the German stock projection (see Fig 8) yields:

$$w_T(week) = \frac{11 \times 10^6 \text{ doses}}{1 + \exp\left(-0.17(week - 21)\right)}, \tag{18}$$

where the parameters were chosen to roughly match past and projected deliveries, taking into account that some delays in the projections might appear because of logistic or manufacturing issues. Since the vaccine deliveries and distributions are done collectively and uniformly in the

Table 4. Parameters for the three main different vaccine uptake scenarios for Germany. The averages are to be understood across the vaccinable (16+) population. Slightly rescaled uptakes for Finnish, Italian and Czech age-demographics can be found in S1, S2 and S3 Tables.

Group ID	age group	eligible fraction	minimal uptake u_i	mid uptake u_i (default)	maximal uptake u_i	population fraction [43] M_i/M
1	0–19	0.2 (16+)	0.58	0.73	0.88	0.18
2	20–39	1.0	0.64	0.76	0.89	0.25
3	40–59	1.0	0.69	0.79	0.90	0.28
4	60–69	1.0	0.74	0.82	0.91	0.13
5	70–79	1.0	0.79	0.86	0.92	0.09
6	>80	1.0	0.85	0.89	0.93	0.07
average	—	—	0.70	0.80	0.90	—

https://doi.org/10.1371/journal.pcbi.1009288.t004
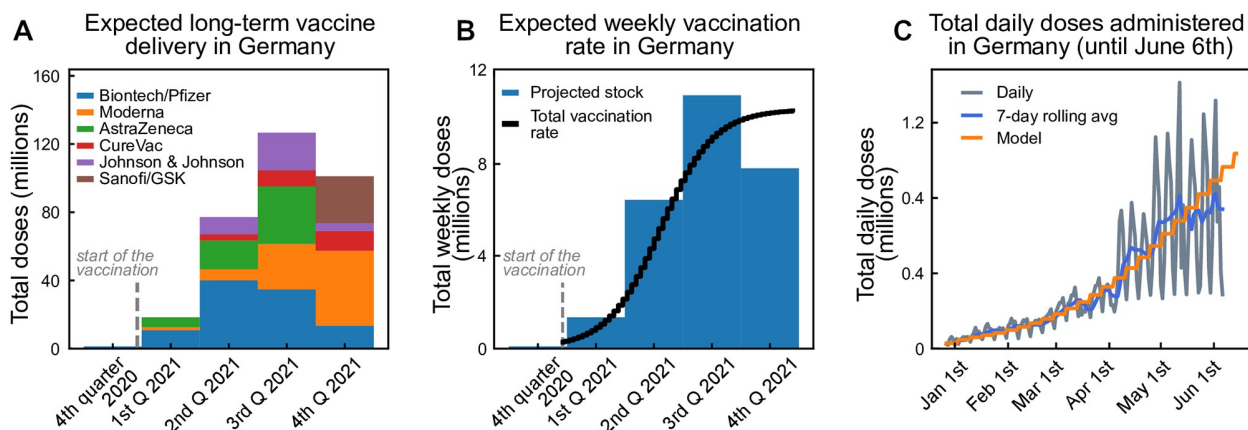
Fig 8. Estimated vaccination rates for Germany. From the announced vaccination stock, we estimate the vaccination delivery function. **A**: Total aggregated doses of different vaccine producers in Germany. **B**: Equivalent amount of 2-dose vaccines available per week in Germany, parameterized using a logistic function. **C**: Comparison between expected and observed vaccination progress in Germany.

EU, we scale this German projection by the respective population sizes for the other countries studied herein (Finland, Italy, Czech Republic). We further assume that because of logistic delays, the vaccination of the delivered doses occurs with some delay, which we model as a convolution with an empirical delay kernel given by $K = [0.6, 0.3, 0.1]$ (fraction of vaccines administered in the same, second and third week following delivery). With that, we get the total vaccination rates per week.

These doses are distributed among the age groups, taking into account that each individual requires two doses, spaced by at least four weeks, aware of the potential benefits of further delaying the two doses [46].

The vaccine prioritization order is the following:

1. First, to meet the demand of second doses, τ_{vac} weeks after the first dose.

2. Second, to distribute a fraction v_r of the remaining doses uniformly among age groups, to model the earlier vaccination of exposed occupations (health sector, first responders, among others).

3. Last, to plan the rest of the doses for the oldest age group that has not been fully vaccinated yet.

Exceptions to rule 3 are the low-risk groups 16–19, 20–39, and 40–59 that get vaccinated simultaneously. For each age group, only a fraction u_i is vaccinated because of limited willingness to get vaccinated (Table 4). In addition, the total number of vaccinations in the youngest age group 0–19 is further reduced since we consider only a fraction of around 20% (fraction of 16–19 year-old individuals in the group) to be *eligible* for vaccination (see Table 4). The uptake u_i in this age group is thus understood only among the eligible individuals.

This procedure results in the number of first $w_i^1(week)$ and second doses $w_i^2(week)$ vaccinated to the age group i as a function of the week. Dividing by 7 we obtain the daily administered first and second doses for age group i

$$f_i^1(t) = w_i^1(\lfloor t/7 \rfloor)/7 \quad \text{and} \tag{19}$$

$$f_i^2(t) = w_i^2(\lfloor t/7 \rfloor)/7. \tag{20}$$

Table 5. Age-dependent parameters.

Age group	ICU admission rate α_i (days^{-1})	Death rate in I δ_i (days^{-1})	Natural recovery rate γ_i (days^{-1})	Death rate in ICU δ_i^{ICU} (days^{-1})	ICU recovery rate γ_i^{ICU} (days^{-1})	Avg. duration in ICU $T_{\mathrm{res}}^{\mathrm{ICU}}$ (days)
0–19	0.000014	0.000002	0.09998	0.005560	0.194440	5
20–39	0.000204	0.000014	0.09978	0.007780	0.192220	5
40–59	0.001217	0.000111	0.09867	0.006164	0.084745	11
60–69	0.004031	0.000317	0.09565	0.009508	0.081401	11
70–79	0.005435	0.001422	0.09314	0.019756	0.091355	9
>80	0.007163	0.004749	0.08809	0.082433	0.084233	6

Age-stratified transition rates

Here, we will introduce the transition rates used in the model equations; details about their estimation are presented in the later sections.

The recovery rate γ_i of a given age group describes the recovery without the need for critical care. It is estimated from the literature. We expect this parameter to vary across age groups, mainly because of the strong correlation between the severity of symptoms and age. Age-resolved recovery rates estimated from data of the non-vaccinated population in Germany are listed in Table 5.

The ICU recovery rate γ_i^{ICU} is the rate of a given age group for leaving ICU care. This parameter varies across age groups, mainly because of the strong correlation between the severity of symptoms, age, and duration of ICU stay. Age-resolved ICU recovery rates estimated from data of the non-vaccinated population in Germany are listed in Table 5.

The ICU admission rate α_i of a given age group describes the transition from the infected compartment to the ICU compartment. It accounts for those cases developing symptoms where intensive care is required and is estimated from the literature. We expect this parameter to vary across age groups, mainly because of the strong correlation between the severity of symptoms and age. Age-resolved ICU-transition rates estimated from data of the non-vaccinated population in Germany are listed in Table 5. Further, we assume that anyone requiring intensive care would have access to ICU beds and care.

The death rate δ_i also varies across age groups, mainly because of the strong correlation between the severity of symptoms and age. This parameter accounts for those individuals dying because of COVID-19, but without being treated in the ICU. In that way, it is expected to be even smaller than the infection fatality ratio (IFR). Age-resolved death rates (outside ICU) estimated from data of the non-vaccinated population in Germany are listed in Table 5.

The death rate in ICU δ_i^{ICU} also varies across age groups, mainly because of the strong correlation between the severity of symptoms and age. In addition, this parameter accounts for those individuals dying because of COVID-19 when being treated in the ICU. In that way, it is expected to be even larger than the case fatality ratio CFR. Age-resolved ICU death rates estimated from data of the non-vaccinated population in Germany are listed in Table 5.

We estimate these age-dependent rates by combining hospitalization data with published IFR data. A comparison of ICU transition rates α_i^y across the EU is difficult as the definition of stationary treatment differs with regard to *hospitalization*, *ICU low* and *high-care*. In order to obtain sensible estimates for these rates, we need to consider the size of the unobserved pool in each age group. Our analysis of ICU transition rates is based on 14043 hospitalization reports collected in Germany between early 2020 and Oct. 26, 2020, as part of the official reporting data [47]. Those reports contain 20-year wide age strata but only represent a small sub-sample of all ICU-admissions ($n = 723$). A complete count of ICU-admissions is maintained by the

Deutsche Interdisziplinäre Vereinigung für Intensiv- und Notfallmedizin [48], without additional patient-data, like age. 19250 ICU admissions were reported throughout the same time frame. We estimated the number of ICU admissions in each 20-year wide age group by combining both sources, matching well with German studies on the first wave [49].

Throughout the first and second wave, the per age-group case-fatality rates (CFRs) in Germany are more than two times larger than the age-specific infection fatality rates (IFRs) estimated by [27, 50]. This difference indicates unobserved infections. Seroprevalence studies from Q3 2020 [51] confirm the existence of unobserved pools. The total number of infections in each age group is inferred from observed deaths assuming the age-specific IFR from [27]. α_i^v (*low-* and *high-care*) is calculated by dividing estimated ICU-admissions in each age group by the estimated total infections in each of those groups. A similar method is applied for the ICU-death-rate δ_i^{ICU} by taking hospitalization-deaths from [47] as a proxy for the age distribution.

The ICU-rates from the 10-year wide age-groups [52] based on French data (*high-care* only) were used to subdivide the 20-year wide age-group 60–79, replicating the French rate-ratio between 60–69 and 70–79 for the German ICU-ratios, while maintaining the German age-agnostic ICU-rate. Noteworthy, there is great variability between the reported ICU rates among different countries, and it seems to be more a problem of reporting criteria rather than differences in virus and host response [53]. Furthermore, as treatments become more effective compared to the first wave, the residence times have decreased in the second wave [30], thus modifying the transition rates.

We also considered the influence of our decision to use the IFR of O'Driscoll et al. [27] instead of Levin et al. [50]. The IFR from Levin et al. is about 50% larger and would lead to a lower level of infections overall in our scenarios, therefore reducing the fraction of natural immunity acquired at the end of the scenarios.

Estimation of general transition rates

After listing all transition rates that we consider in our work, we will now explain how we estimate them. Since we have to start somewhere, let us look at the ICU_i compartment first (see Fig 6 top right). The differential equation, without influx and including the initial condition ICU_0, is given by

$$ICU_i' = \underbrace{-\delta_i^{ICU}ICU_i}_{\text{to } D_i} - \underbrace{\gamma_i^{ICU}ICU_i}_{\text{to } R_i}, \qquad ICU_i(0) = ICU_0. \tag{21}$$

The solution of this ODE is known to be

$$ICU_i = ICU_0 \exp\left(-(\delta_i^{ICU} + \gamma_i^{ICU})t\right). \tag{22}$$

If we know the average ICU_i residence time T_{res}^{ICU}, we can obtain an expression for $(\delta_i^{ICU} + \gamma_i^{ICU})$:

$$\delta_i^{ICU} + \gamma_i^{ICU} = \frac{1}{T_{res}^{ICU}}. \tag{23}$$

Further, assuming that a fraction f_δ of those individuals being admitted to ICUs would die, we obtain an expression linking all rates:

$$f_\delta = \frac{\# \text{ people dead by } t = \infty}{\text{people entering ICU}_i \text{ at } t = 0} = \frac{\delta_i^{\text{ICU}} \cancel{\text{ICU}_0} \int_0^\infty \exp\left(-\frac{t}{T_{\text{res}}^{\text{ICU}}}\right) dt}{\cancel{\text{ICU}_0}} = \delta_i^{\text{ICU}} T_{\text{res}}^{\text{ICU}}. \tag{24}$$

Therefore, the transition rates are given by:

$$\delta_i^{\text{ICU}} = \frac{f_\delta}{T_{\text{res}}^{\text{ICU}}} \qquad \text{and} \qquad \gamma_i^{\text{ICU}} = \frac{(1 - f_\delta)}{T_{\text{res}}^{\text{ICU}}}. \tag{25}$$

Using this modeling approach, we implicitly assume the time scales at which people leave the ICU through recovery or death to be the same, i. e., the average ICU stay duration is independent of the outcome of the course of the disease.

Similarly, we can estimate the infected-to-death rate (δ_i), the infected-to-ICU transition rate (ICU admission rate α_i) and the infected-to-recovered rate (γ_i) based on these fractions and average times. If we assume that all the relevant median times are the same, we obtain the following expressions for the rates:

$$\delta_i = \frac{f_{I_i \to D_i}}{T_{\text{res}}^{\text{I}}}, \qquad \alpha_i = \frac{f_{\text{ICU}}}{T_{\text{res}}^{\text{I}}}, \qquad \gamma_i = \frac{(1 - (f_{I_i \to D_i} + f_{\text{ICU}}))}{T_{\text{res}}^{\text{I}}}. \tag{26}$$

As the average residence time in the I compartment is dominated by recoveries we assume $T_{\text{res}}^{\text{I}} = 10$ days [54–56].

Modeling vaccine efficacies

We assume the main effect of vaccinations on the individual to be twofold. A fraction η that has received both vaccine doses will develop total immunity and not contribute to the spreading dynamics. The rest may, in principle, be infected with the virus but still have some protection against a severe course of the illness, resulting in a lower probability of dying or going to ICU. Both effects combined give the total protection against severe infections seen in vaccine studies, which we will denote with κ. For current COVID-19 vaccines, efficacies against severe disease κ ranging from 70–99% [23, 31–33, 57–59] and infection blocking potentials η of 60–90% [24, 41, 60, 61] are reported. The roughly uniform distribution of vaccine types in the European Union (see also Fig 8), consists to a larger part of mRNA-type vaccines for which comparatively high values κ of 97–99% [33, 59] and η of 80–90% are reported. We thus chose the rather conservative 90% for κ and 75% for η as our default values. The explicit κ and η do not explicitly appear in our equations, but as parameters η_0 and κ_0, which we derive from the reported numbers as follows.

Due to the lack of solid evidence on the effects of the first dose, we assume that the fraction of individuals developing total immunity already after the first dose is given by η_0. We further assume that of the $(1 - \eta_0)$ people that do not develop the immunity after the first dose, the same fraction η_0 acquires it after the second dose, i. e. the total vaccination path of the people that do not develop total immunity after both doses is given by $S_i \xrightarrow{1 - \eta_0} S_i^1 \xrightarrow{1 - \eta_0} S_i^2$. η_0 can thus be

related to η by the formula

$$
\begin{aligned}
\eta \quad &= 1 - \frac{\text{not fully protected}}{\text{total vaccinated}} \\
&= 1 - (1 - \eta_0)^2 = \eta_0(2 - \eta_0).
\end{aligned}
\tag{27}
$$

For individuals vaccinated with both doses without total immunity, i. e., from S_i^2, we reduce the probabilities to die or go to ICU after infection to account for the reduced risk of severe symptoms due to the vaccine. Of the total number of people who get vaccinated the risk of going to ICU or dying is thus reduced by a factor

$$
1 - \kappa = (1 - \eta) \cdot (1 - \kappa_0),
\tag{28}
$$

from which we can deduce the value of κ_0.

Again, due to lack of solid data on the first doses we assume the risk of severe COVID-19 is reduced to a factor $\sqrt{(1 - \kappa)}$ when only a single dose has been received. From these assumptions we arrive at

$$
\delta_i^v = \left(\sqrt{1 - \kappa_0}\right)^v \delta_i,
\tag{29}
$$

$$
\alpha_i^v = \left(\sqrt{1 - \kappa_0}\right)^v \alpha_i,
\tag{30}
$$

$$
\gamma_i^v + \delta_i^v + \alpha_i^v = \bar{\gamma},
\tag{31}
$$

where $v = \{1, 2\}$ represents the dose of the vaccine for which an individual has successfully developed antibodies. Note that v is used as a super-index on the left-hand side of the equation but as an exponent on the right-hand side. Eq 31 enforces vaccination not to alter the total average timescale of the disease course.

The transition rates from ICU to death, δ_i^{ICU}, and from ICU to recovered, γ_i^{ICU}, are assumed to remain equal across doses. The reasons for this assumption are i) a lack of solid evidence for significant differences, and ii) once in ICU, it is reasonable to assume that the vaccine failed to work for this individual.

In addition to the effects of complete sterilizing immunity (η) and protection against severe disease (κ), we include a third effect of vaccines: Individuals that happen to have a break-through infection despite being vaccinated carry a lower viral load and are consequently less infectious than unvaccinated infected individuals. This has been shown already after the first dose [25, 60]. We include this effect by a factor σ in the contagion term (cf. (1)).

Individuals becoming infectious while developing antibodies

One special case that one has to consider is when individuals acquire the virus in the time frame between being vaccinated and developing an adequate antibody level. We assume that individuals share behavioral characteristics with the members of the corresponding susceptible compartment, so contagion follows the same dynamics. Let $X_i(s)$ be the fraction of susceptible individuals of a given age group vaccinated at time $s_0 < s$ and are not infected until time s. Assuming they can only leave the compartment by getting infected, the differential equation

governing their dynamics is:

$$\frac{dX_i}{ds} = -R_t X_i \sum_{j,v} C_{ji} \frac{\sigma^v I_j^v}{M_j} - \frac{X_i}{M_i} \Phi_i, \qquad \text{with } X_i(s_0) = 1.$$ (32)

The solution of (32) is given by

$$X_i(s) = \exp\left(-\int_{s_0}^{s} \sum_{j,v} R_{s'} C_{ji} \frac{\sigma^v I_j^v(s')}{M_j} ds' \right) \exp\left(-\frac{\Phi_i(s-s_0)}{M_i} \right).$$ Following the same formalism

for every batch of vaccinated individuals produced at time $t - \tau$, the ones that remain suscepti-ble by time t are given by:

$$X_i(t) = \exp\left(-\int_{t-\tau}^{t} \sum_{j,v} R_{t'} C_{ji} \frac{\sigma^v I_j^v(t')}{M_j} dt' \right) \exp\left(-\frac{\Phi_i \tau}{M_i} \right).$$ (33)

Therefore, we define the fraction of susceptible individuals acquiring the virus in the time-frame of antibodies development as

$$p_i(t) = 1 - \exp\left(-\int_{t-\tau}^{t} \sum_{j,v} R_{t'} C_{ji} \frac{\sigma^v I_j^v(t')}{M_j} dt' \right) \exp\left(-\frac{\Phi_i \tau}{M_i} \right).$$ (34)

This fraction is then subtracted in the transitions $V_i^v \rightarrow S_i^{v+1}$ from the vaccinated to the immunized pools in the differential equations.

Effect of test-trace-and-isolate

At low case numbers and moderate contact reduction, the spreading dynamics can be miti-gated through test-trace-and-isolate (TTI) policies [18, 19]. In such a regime, individuals can have slightly more contacts because the overall low amount of cases enables a diligent system to trace offspring infections and stop the contagion chains. In other words, efficient TTI would allow for having a larger gross reproduction number R_t without rendering the system unstable. The precise allowed increase in R_t is determined by i) the rate at which symptomatic individu-als are tested, ii) the probability of being randomly screened, and iii) the maximum capacity and fraction of contacts that health authorities can manually trace. When the different compo-nents of this meta-stable regime break down, we observe a self-accelerating growth in case numbers.

In our age-stratified model, we do not explicitly include TTI, given all the uncertainties that arise from the age-related modifying factors. However, we use our previous results to estimate the gross reproduction number R_t that would produce the same observed reproduction num-ber in the different regimes of i) no test or contact tracing, ii) strict testing criteria, iii) self-reporting, and iv) full TTI. Doing so, we build an empirical relation to evaluating the contex-tual stringency of the different strategies herein compared (namely, long-term stabilization at high or low case numbers).

In the phase diagram of Fig 9 we illustrate the conversion methodology. Two different R_t might produce the same observed reproduction number $\hat{R}_t^{\text{obs}}$, depending on the regime in which they operate. Fitting all curves to an exponential function, and assuming that the largest eigenvalue of the system (for all possibilities of testing and tracing) can be represented as a
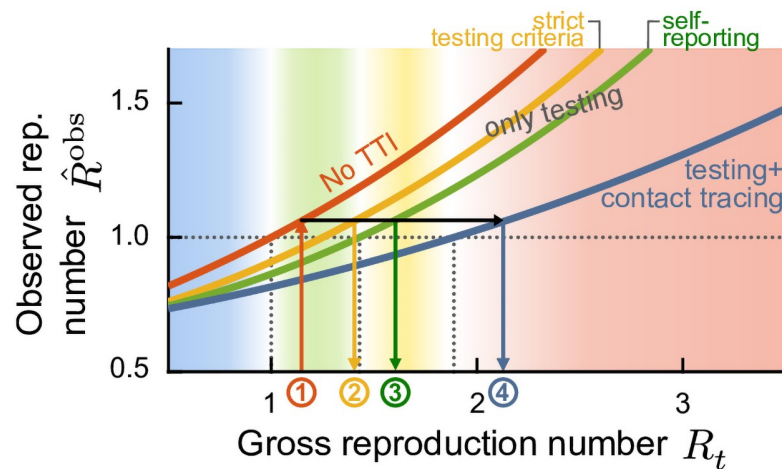
Fig 9. Test-trace-and-isolate (TTI) policies allow for greater freedom (quantified by the gross reproduction number R_t) while observing the same reproduction number $\hat{R}_t^{\text{obs}}$. Systematic efforts to slow down the spread of the disease, such as mass testing (random screening) and contact tracing, allow decreasing the observed reproduction number of the disease. For observing the same outcome in $\hat{R}_t^{\text{obs}}$, the gross reproduction number R_t would increase, or, in other words, individuals would be allowed to increase their potentially contagious contacts. Therefore, we extrapolate the R_t allowed in a full TTI setting at low case numbers and determine the equivalent R_t trends required to reach the same $\hat{R}_t^{\text{obs}}$ in different regimes, starting from the raw value considering no TTI (red curve). Assuming that the relationship between R_t and $\hat{R}_t^{\text{obs}}$ is exponential (Eq (35)), we can obtain the expected R_t trends in the low-case numbers TTI regime. Starting from the raw R_t curve (red, 1), we can obtain R_t in all the other possible regimes: under strict testing criteria (yellow, 2), self-reporting (green, 3), or full TTI (blue, 4). Adapted from [18].

https://doi.org/10.1371/journal.pcbi.1009288.g009

function of the gross reproduction number R_t, we obtain

$$\hat{R}_t^{\text{obs}} = a \exp\left(bR_t\right). \tag{35}$$

We then want to evaluate how to translate the values we get from our control problem (which has no testing nor tracing) to the equivalent in other regimes. Assuming that all strategies have the same $\hat{R}_t^{\text{obs}}$ (as schematized in Fig 9), we can relate their gross reproduction numbers in each regime through a simple equation:

$$R_t^i = \frac{1}{b_i}\left(\ln\left(\frac{a_0}{a_i}\right) + b_0 R_t\right), \tag{36}$$

which corresponds to a line, and where the subscript 0 represents the base scenario (with no testing or contact tracing) and the subscript i represents the other strategies. The exponential fit to the curves shown in Fig 9 gives to the following line equations:

$$R_t^{\text{test(ineff)}} = 1.0211 R_t + 0.2229, \tag{37}$$

$$R_t^{\text{test(eff)}} = 1.0756 R_t + 0.3272, \tag{38}$$

$$R_t^{\text{TTI}} = 1.6842 R_t + 0.1805. \tag{39}$$

Assuming smooth transitions for these conversions in R_t, which are related to certain values of the new daily cases N ($N_{\text{TTI}} < N_{\text{test(eff)}} < N_{\text{test(ineff)}} < N_{\text{no test}}$ respectively), we can define a

general conversion $R_t(N)$:

$$
R_t(N) = \begin{cases}
R_t^{\text{TTI}}, & \text{if } N < N_{\text{TTI}} \\[4pt]
R_t^{\text{test(eff)}}\phi_1 + R_t^{\text{TTI}}(1 - \phi_1), & \text{if } N_{\text{TTI}} \leq N < N_{\text{test(eff)}} \\[4pt]
R_t^{\text{test(ineff)}}\phi_2 + R_t^{\text{test(eff)}}(1 - \phi_2), & \text{if } N_{\text{test(eff)}} \leq N < N_{\text{test(ineff)}} \\[4pt]
R_t\phi_3 + R_t^{\text{test(ineff)}}(1 - \phi_3), & \text{if } N_{\text{test(ineff)}} \leq N < N_{\text{no test}} \\[4pt]
R_t, & \text{else,}
\end{cases}
\tag{40}
$$

where the ϕ parameters of each convex combination depend on N:

$$
\begin{aligned}
\phi_1 &= \frac{N - N_{\text{TTI}}}{N_{\text{test(eff)}} - N_{\text{TTI}}}, \\[6pt]
\phi_2 &= \frac{N - N_{\text{test(eff)}}}{N_{\text{test(ineff)}} - N_{\text{test(eff)}}}, \qquad \text{and} \\[6pt]
\phi_3 &= \frac{N - N_{\text{test(ineff)}}}{N_{\text{no test}} - N_{\text{test(ineff)}}}.
\end{aligned}
\tag{41}
$$

Default reference values for the N-related set-points are $N_{\text{TTI}} = 20$, $N_{\text{test(eff)}} = 100$, and $N_{\text{test(ineff)}} = 500$ and $N_{\text{no test}} = 10000$ new daily cases per million. When we plot and refer to the gross reproduction number R_t, it is always the value obtained from Eq (40).

Observed reproduction number

In real-world settings, the full extent of the disease spread can only be observed through testing and contact tracing. While the *true* number of daily infections N is a sum of all new infections, the *observed* number of daily infections $\hat{N}^{\text{obs}}$ is the number of new infections discovered by testing, tracing, and surveillance of the quarantined individuals' contacts. Thus, the observed number of daily infections is given by

$$
\hat{N}^{\text{obs}}(t) = \Bigg[\underbrace{\sum_{i,v} \rho E_i^v(t)}_{\text{end of latency}} + \underbrace{\sum_{i,v} \frac{S_i^v(t) + V_i^v(t)}{M_i}\Phi_i(t)}_{\text{ext. influx}} \Bigg] \circledast \underbrace{\mathcal{K}(t)}_{\text{delay kernel}}
\tag{42}
$$

where $\circledast$ denotes a convolution and $\mathcal{K}$ an empirical probability mass function that models a variable reporting delay, inferred from German data. As the Robert-Koch-Institute (RKI), the official body responsible for epidemiological control in Germany [62], reports the date the test is performed, the delay until the appearance in the database can be inferred. The laboratories obtain 50% of the sample results on the next day, 30% the second day, 10% the third day, and further delays complete the remaining 10%, which for simplicity we will truncate at day four. Considering that an extra day is needed for reporting the laboratory results, the probability mass function for days 0 to 5 is given by $\mathcal{K} = [0, 0, 0.5, 0.3, 0.1, 0.1]$.

The spreading dynamics are usually characterized by the observed reproduction number $\hat{R}_t^{\text{obs}}$, an estimator of the effective reproduction number, calculated from the observed number of new cases $\hat{N}^{\text{obs}}(t)$. We use the definition underlying the estimates that are published by the RKI, which defines the reproduction number as the relative change of daily new cases

separated by 4 days (the assumed serial interval of COVID-19 [63])

$$\hat{R}_t^{\text{obs}} = \frac{\hat{N}^{\text{obs}}(t)}{\hat{N}^{\text{obs}}(t-4)}.$$

(43)

In contrast to the original definition of $\hat{R}_t^{\text{obs}}$ [62], we do not need to remove real-world noise effects by smoothing this ratio. It should be noted that calling $\hat{N}^{\text{obs}}$ the observed case numbers is somewhat misleading since we do not model the hidden figure explicitly. However, as this is expected only to change slowly, it is still sufficiently accurate to obtain the observed reproduction number from Eq (43).

Keeping a steady number of daily infections with a PD control approach

With increasing immunity from the progressing vaccination program, keeping the spread of COVID-19 under control will require less and less effort by society. We can use this positive effect to lower the infections by upholding the same NPIs or gradually lifting restrictions to keep daily case numbers or ICU occupancy constant.

We model the optimal lifting of restrictions in the latter strategy using a Proportional Derivative (PD) control approach. The gross reproduction number R_t is changed at every day of the simulation depending on either the daily case numbers $\hat{N}^{\text{obs}}$ or the total ICU occupancy $\sum_{i,v}\text{ICU}_i^v$ such that the system is always driven towards a given set point. The change in R_t is negatively proportional to both the difference between the state and the setpoint as well as the change of that difference in time. The former dependence increases the number of infections if the case numbers drift down while the latter punishes rapid increases of the case numbers, keeping the system from overshooting the target value. We omit a dependence on the cumulative error, as is usually done in a PD controller, as that would enforce oscillations around the setpoint and because the PD has proven to be sufficient for our purposes.

Since both the case numbers and the ICU occupancy inherently only react to changes in R_t after a few days of delay, we can further improve the stability of the control by "looking into the future". The full procedure for every day t of the simulation then follows:

1. Run the system for a time span T using the current R_t.

2. Quantify the relative error $\Delta(t + T)$ of the system state at the end by the difference between the observed case numbers or the total ICU occupancy and the chosen set point divided by said set point.

3. Calculate R_t for the next day according to

$$R_{t+1\,\text{day}} = R_t - \left(k_p \cdot \Delta(t+T) + k_d \cdot \frac{d\Delta}{dt}(t+T) \right),$$

where k_p and k_d denote constant control parameters listed in Table 6.

Table 6. The PD control parameters depending on the objective.

control problem	preview time span T	proportional k_p	derivative k_d
$\hat{N}^{\text{obs}}$ (close to set point)	14 days	0.06	3.0
$\hat{N}^{\text{obs}}$ (away from set point)	14 days	0.06	1.2
$\sum_{i,v}\text{ICU}_i^v$ (close to set point)	14 days	0.2	15.0
$\sum_{i,v}\text{ICU}_i^v$ (away from set point)	14 days	0.2	7.0

4. Revert the system from the state at $t + T$ to $t + 1$ day and start again at 1.

We use the same control system to uphold the setpoint as we use to drive the system towards that state from the initial conditions. In a staged-control-like manner, we make the system more reactive to high slopes near the setpoint, i. e. increase k_d when within 10% of the target. In this way, the system can drive up quickly to the target while preventing overreactions to the gradual immunization changes while hovering at the fixed value.

Scenarios 2–4 in the main text consist of a chain of these control problems, changing from controlled case numbers to controlled ICU occupancy at one of the vaccination milestones (Fig 3).

Parameter choices

For the age stratification of the population and the ICU rates, we used numbers published for Germany (Table 4). We suppose that the quantitative differences to other countries are not so large that the result would differ qualitatively. When comparing ICU rates across countries, one has to bear in mind that the definition of what constitutes an intensive care unit can differ between countries. We chose our ICU limit of 65 per million as a conservative limit so that in Germany, around three-quarters of the capacity would still be available for non-COVID patients. This limit was reached during the second wave in Germany. Other countries in the EU might have fewer remaining beds for non-COVID patients at this limit, as Germany has a comparatively high *per capita* number of ICU beds available.

ICU-related parameters are calculated from 14043 hospitalizations reported by German institutions until October 26, 2020 Table 5, converted to transition rates from Table 1. All other epidemiological parameters, their sources, values, ranges, and units are listed in detail in Table 2.

The vaccine efficacy, as discussed previously, is modeled as a multiplicative factor of the non-vaccinated reference parameter. The dose-dependent multiplicative factor is chosen to be 90% in the default scenario, which is in the range of the 70 to 95% efficacy measured in phase 3 studies [57] of approved vaccines and in accordance with the 92% efficacy of the Pfizer vaccine found in a population study in Israel [23]. In addition, we analyzed different scenarios of vaccine uptake (namely, the overall compliance of people to get vaccinated according to the vaccination plan) because of its relevance to policymakers and different scenarios of the protection the vaccine grants against infections η. The latter has great relevance for assessing risks when evaluating restriction lifting.

Initial conditions

The initial conditions are chosen corresponding to the situation in Germany at the beginning of March 2021. We assume a seroprevalence of 10% because of post-infection immunity across all age groups, i.e., $R_i(0) = 0.1 \cdot M_i \, \forall i$. The vaccination at the beginning is according to the vaccination schedule introduced before, which leaves 5.1 million doses administered initially and an initial vaccination rate of 168 thousand doses per day. This compares to the 6.2 million total and the around 150 thousand daily administered doses at the time [26]. The initial number of daily new infections is at 200 per million, and the number of individuals treated in ICU is at 30 per million with an age distribution as observed during the first wave in Germany (taken from [47]). From these conditions and the total population sizes of the age groups (Table 4) we infer the initial size of each compartment.

Numerical calculation of solutions

The system of delay differential equations governing our model were numerically solved using a Runge-Kutta 4th order algorithm, implemented in Rust (version 1.48.0). The source code is available on GitHub https://github.com/Priesemann-Group/covid19_vaccination.

Supporting information

S1 Fig. Sensitivity analysis centered at default parameters (solid black lines), for the fourth scenario from the main text. We vary central parameters of the model individually, while keeping all others at their respective default value. For assessing the sensitivity to the TTI efficacy we scale all the capacity limits N_{TTI}, $N_{test(eff)}$, $N_{test(ineff)}$ and $N_{no\ test}$ (see Methods) by a common ratio.
(TIF)

S2 Fig. Contact structure can have a significant impact on the population immunity threshold. We assume that infections are kept stable at 250 daily infections until all age groups have been vaccinated. Then most restrictions are lifted, leading to a wave if vaccine uptake has not been high enough (see Fig 4A). We measure the severity of the wave (quantified by the duration of full ICUs) for varying uptake and vaccine efficacies for different contact structures (see Fig 7A–7C). **A-C**: The duration of the wave (measured by the duration of full ICUs) depends on the vaccine uptake and on the effectiveness of the vaccine measured by its efficacy at preventing infection (shades of purple) and severe illness (vaccine efficacy, full vs dashed vs dotted). **D-F**: If some NPIs are kept in place (such that the gross reproduction number goes up to $R_t = 2.5$), ICUs would be prevented from overflowing even in some cases of lower vaccine effectiveness. If precautionary measures are dropped in all age groups, including schools (A,D) the required uptake to prevent a further severe wave is increased by about 10% when compared to our default scenario of some continued measures to reduce the potential contagious contacts in school settings (B,E) or to completely homogeneous contacts (C,F). Not all combinations of vaccine effectiveness are possible as the vaccine efficacy against severe illness is by definition larger as the protection against any infection at all.
(TIF)

S3 Fig. EU countries with different demographics have very similar dynamics—But the required vaccine uptake to guard against further severe waves is most sensitive to the initial seroprevalence. Extended version of Fig 5, including more combinations of vaccine efficacies. **A–D**: If releasing all measures to pre-COVID contacts, keeping only some measures aiming to cup the reproduction number at 3.5. **E–H**: If releasing all measures to pre-COVID contacts, keeping only some measures aiming to cup the reproduction number at 3.5 and halving the contagiousness of contacts at school ages.
(TIF)

S4 Fig. Even with the emergence of the highly contagious B.1.1.7 variant vaccinations are a promising mid-term strategy against COVID-19. Staying at low case numbers can greatly increase the individual freedom, especially in the long-term. Schematic outlook into the effects of vaccination and the B.1.1.7 variant of SARS-CoV-2 on the societal freedom in the EU in 2021 compared to 2020 (see also the caption for Fig 1A). In 2020, seasonality effects and efficient test-trace-and-isolate (TTI) programs at low case numbers allowed for stable case numbers with only mild restrictions during summer, until about September. In 2021, vaccinations are expected to allow for greater freedom, but also a more contagious variant (B.1.1.7) is prevalent across the EU. Efficient TTI at low case numbers would thus help lifting major restrictions

earlier. The exact transition period between the wild type and B.1.1.7 (light purple shaded area) varies regionally.
(TIF)

S5 Fig. Lowering the case numbers without the most stringent restrictions opens a middle ground between freedom and fatalities and prevents a new wave in the long term. A–D: Variation of the fourth scenario from the main text (see Fig 3), where moderate restrictions are kept in place in the long term (letting the gross reproduction number go up to 2.5, compared to 3.5 in the default scenarios). **E–H**: Variation of the fifth scenario from the main text (see Fig 2) avoiding the strict initial restrictions. Keeping the gross reproduction number at a moderate level (1.5) until the everyone above 60 has been offered vaccination allows to decrease case numbers steadily. Over the summer a slight gradual increase in the contacts is allowed and all NPIs expect for test-trace-and-isolate (TTI) and enhanced hygiene are lifted when everyone received the vaccination offer (increasing the gross reproduction number to 3.5). **I**: The variation of the fourth scenario initially allows for the same increase in freedom as all the main scenarios, but needs more restrictions in the long term. The variation of the fifth scenario calls for stricter NPIs in the mid-term, but grants high freedom after summer. **J,K**: Both proposals lead to low number of infections and fatalities. **L**: Projected vaccination rates (see Fig 2).
(TIF)

S6 Fig. Long-term control strategies (low vaccine uptake, 70% among the vaccinable population) from main text Figs 2 and 3. Scenarios using default protection against infection $\eta =$ 0.75 and **low vaccine uptake of 70%** among the adult population.
(TIF)

S7 Fig. Long-term control strategies (default vaccine uptake, 80% among the vaccinable population) from main text Figs 2 and 3. Scenarios using default protection against infection $\eta = 0.75$ and **default vaccine uptake of 80%** among the adult population.
(TIF)

S8 Fig. Long-term control strategies (high vaccine uptake, 90% among the vaccinable population) from main text Figs 2 and 3. Scenarios using default protection against infection $\eta =$ 0.75 and **high vaccine uptake of 90%** among the adult population.
(TIF)

S9 Fig. Mirror of Fig 2, using a homogeneous contact structure.
(TIF)

S10 Fig. Mirror of Fig 3, using a homogeneous contact structure.
(TIF)

S11 Fig. Mirror of S5 Fig, using a homogeneous contact structure.
(TIF)

S12 Fig. Mirror of Fig 2, using an empirical pre-COVID contact structure.
(TIF)

S13 Fig. Mirror of Fig 3, using an empirical pre-COVID contact structure.
(TIF)

S14 Fig. Mirror of S5 Fig, an empirical pre-COVID contact structure.
(TIF)

S1 Table. Parameters for the three main different vaccine uptake scenarios for Finland. Uptakes and averages are to be understood across the eligible (16+) population. For German data see Table 2 in the main text. Italian and Czech data are to be found in S2 and S3 Tables respectively.
(XLSX)

S2 Table. Parameters for the three main different vaccine uptake scenarios for Italy. The averages are to be understood across the eligible (16+) population. For German data see Table 2 in the main text. Finnish and Czech data are to be found in S1 and S3 Tables respectively.
(XLSX)

S3 Table. Parameters for the three main different vaccine uptake scenarios for the Czech Republic. The averages are to be understood across the eligible (16+) population. For German data see Table 2 in the main text. Finnish and Italian data are to be found in S3 and S2 Tables respectively.
(XLSX)

S1 Supplementary Note. Eigenvalues of the homogeneous contact matrix. Here we demonstrate a general case for the eigenvalues of a homogeneous contact matrix, for which every column accounts for the fraction age-groups represent respect to the total population.
(PDF)

Author Contributions

Conceptualization: Simon Bauer, Sebastian Contreras, Jonas Dehning, Alvaro Olivera-Nappa, Viola Priesemann.

Data curation: Simon Bauer, Matthias Linden.

Formal analysis: Simon Bauer, Sebastian Contreras, Jonas Dehning, Matthias Linden.

Funding acquisition: Viola Priesemann.

Investigation: Simon Bauer, Sebastian Contreras, Emil Iftekhar, Sebastian B. Mohr.

Methodology: Simon Bauer, Sebastian Contreras, Jonas Dehning, Matthias Linden, Viola Priesemann.

Project administration: Viola Priesemann.

Software: Simon Bauer.

Supervision: Viola Priesemann.

Validation: Simon Bauer, Sebastian Contreras, Jonas Dehning, Matthias Linden, Sebastian B. Mohr, Alvaro Olivera-Nappa, Viola Priesemann.

Visualization: Simon Bauer, Sebastian Contreras.

Writing – original draft: Simon Bauer, Sebastian Contreras, Jonas Dehning, Sebastian B. Mohr.

Writing – review & editing: Simon Bauer, Sebastian Contreras, Jonas Dehning, Emil Iftekhar, Sebastian B. Mohr, Alvaro Olivera-Nappa, Viola Priesemann.

References

1. Contreras S, Priesemann V. Risking further COVID-19 waves despite vaccination. The Lancet Infectious Diseases. 2021. https://doi.org/10.1016/S1473-3099(21)00167-5 PMID: 33743848

2. Foy BH, Wahl B, Mehta K, Shet A, Menon GI, Britto C. Comparing COVID-19 vaccine allocation strategies in India: A mathematical modelling study. International Journal of Infectious Diseases. 2021; 103:431–438. https://doi.org/10.1016/j.ijid.2020.12.075 PMID: 33388436

3. Moore S, Hill EM, Tildesley MJ, Dyson L, Keeling MJ. Vaccination and non-pharmaceutical interventions for COVID-19: a mathematical modelling study. The Lancet Infectious Diseases. 2021. https://doi.org/10.1016/S1473-3099(21)00143-2 PMID: 33743847

4. Viana J, van Dorp CH, Nunes A, Gomes MC, van Boven M, Kretzschmar ME, et al. Controlling the pandemic during the SARS-CoV-2 vaccination rollout: a modeling study. Nature communications. 2021; 12 (3674):1–15.

5. Bubar KM, Reinholt K, Kissler SM, Lipsitch M, Cobey S, Grad YH, et al. Model-informed COVID-19 vaccine prioritization strategies by age and serostatus. Science. 2021. https://doi.org/10.1126/science.abe6959 PMID: 33479118

6. Wouters OJ, Shadlen KC, Salcher-Konrad M, Pollard AJ, Larson HJ, Teerawattananon Y, et al. Challenges in ensuring global access to COVID-19 vaccines: production, affordability, allocation, and deployment. The Lancet. 2021. https://doi.org/10.1016/S0140-6736(21)00306-8 PMID: 33587887

7. Davies NG, Abbott S, Barnard RC, Jarvis CI, Kucharski AJ, Munday JD, et al. Estimated transmissibility and impact of SARS-CoV-2 lineage B.1.1.7 in England. Science. 2021. https://doi.org/10.1126/science.abg3055 PMID: 33658326

8. Plante JA, Mitchell BM, Plante KS, Debbink K, Weaver SC, Menachery VD. The Variant Gambit: COVID's Next Move. Cell Host & Microbe. 2021. https://doi.org/10.1016/j.chom.2021.02.020

9. Van Egeren D, Novokhodko A, Stoddard M, Tran U, Zetter B, Rogers M, et al. Risk of rapid evolutionary escape from biomedical interventions targeting SARS-CoV-2 spike protein. PloS one. 2021; 16(4): e0250780. https://doi.org/10.1371/journal.pone.0250780 PMID: 33909660

10. Lavine JS, Bjornstad ON, Antia R. Immunological characteristics govern the transition of COVID-19 to endemicity. Science. 2021; 371(6530):741–745. https://doi.org/10.1126/science.abe6522 PMID: 33436525

11. Petherick A, Goldszmidt RG, Andrade EB, Furst R, Pott A, Wood A. A Worldwide Assessment of COVID-19 Pandemic-Policy Fatigue. Available at SSRN 3774252. 2021.

12. Van Bavel JJ, Baicker K, Boggio PS, Capraro V, Cichocka A, Cikara M, et al. Using social and behavioural science to support COVID-19 pandemic response. Nature Human Behaviour. 2020; p. 1–12.

13. Dehning J, Zierenberg J, Spitzner FP, Wibral M, Neto JP, Wilczek M, et al. Inferring change points in the spread of COVID-19 reveals the effectiveness of interventions. Science. 2020. https://doi.org/10.1126/science.abb9789 PMID: 32414780

14. Brauner JM, Mindermann S, Sharma M, Johnston D, Salvatier J, Gavenčiak T, et al. Inferring the effectiveness of government interventions against COVID-19. Science. 2020. https://doi.org/10.1126/science.abd9338 PMID: 33323424

15. Priesemann V, Brinkmann MM, Ciesek S, Cuschieri S, Czypionka T, Giordano G, et al. Calling for pan-European commitment for rapid and sustained reduction in SARS-CoV-2 infections. The Lancet. 2020. https://doi.org/10.1016/S0140-6736(20)32625-8 PMID: 33347811

16. Dorn F, Khailaie S, Stoeckli M, Binder SC, Lange B, Lautenbacher S, et al. The Common Interests of Health Protection and the Economy: Evidence from Scenario Calculations of COVID-19 Containment Policies. medRxiv. 2020; p. 2020.08.14.20175224.

17. Oliu-Barton M, Pradelski BS, Aghion P, Artus P, Kickbusch I, Lazarus JV, et al. SARS-CoV-2 elimination, not mitigation, creates best outcomes for health, the economy, and civil liberties. The Lancet. 2021. https://doi.org/10.1016/S0140-6736(21)00978-8

18. Contreras S, Dehning J, Loidolt M, Zierenberg J, Spitzner FP, Urrea-Quintero JH, et al. The challenges of containing SARS-CoV-2 via test-trace-and-isolate. Nature communications. 2021; 12(1):1–13. https://doi.org/10.1038/s41467-020-20699-8 PMID: 33452267

19. Contreras S, Dehning J, Mohr SB, Spitzner FP, Priesemann V. Low case numbers enable long-term stable pandemic control without lockdowns. medRxiv. 2020.

20. Kretzschmar ME, Rozhnova G, van Boven M. Isolation and Contact Tracing Can Tip the Scale to Containment of COVID-19 in Populations With Social Distancing. Frontiers in Physics. 2021; 8. https://doi.org/10.3389/fphy.2020.622485

21. Godara P, Herminghaus S, Heidemann KM. A control theory approach to optimal pandemic mitigation. PLOS ONE. 2021; 16(2):1–16. https://doi.org/10.1371/journal.pone.0247445 PMID: 33606802

22. Sharma M, Mindermann S, Rogers-Smith C, Leech G, Snodin B, Ahuja J, et al. Understanding the effectiveness of government interventions in Europe's second wave of COVID-19. medRxiv. 2021; p. 2021.03.25.21254330.

23. Dagan N, Barda N, Kepten E, Miron O, Perchik S, Katz MA, et al. BNT162b2 mRNA COVID-19 Vaccine in a Nationwide Mass Vaccination Setting. New England Journal of Medicine. 2021. https://doi.org/10.1056/NEJMoa2101765

24. Levine-Tiefenbrun M, Yelin I, Katz R, Herzel E, Golan Z, Schreiber L, et al. Initial report of decreased SARS-CoV-2 viral load after inoculation with the BNT162b2 vaccine. Nature medicine. 2021; 27 (5):790–792. https://doi.org/10.1038/s41591-021-01316-7 PMID: 33782619

25. Harris RJ, Hall JA, Zaidi A, Andrews NJ, Dunbar JK, Dabrera G. Effect of Vaccination on Household Transmission of SARS-CoV-2 in England. New England Journal of Medicine. 0;0(0):null.

26. Institute RK. COVID-19 Impfquoten-Monitoring in Deutschland (COVIMO) –1. Report; 2021. https://www.rki.de/DE/Content/InfAZ/N/Neuartiges_Coronavirus/Projekte_RKI/covimo_studie_bericht_1.pdf. Available from: https://www.rki.de/DE/Content/InfAZ/N/Neuartiges_Coronavirus/Projekte_RKI/covimo_studie_bericht_1.pdf?__blob=publicationFile.

27. O'Driscoll M, Ribeiro Dos Santos G, Wang L, Cummings DAT, Azman AS, Paireau J, et al. Age-specific mortality and immunity patterns of SARS-CoV-2. Nature. 2021; 590(7844):140–145. https://doi.org/10.1038/s41586-020-2918-0 PMID: 33137809

28. Mistry D, Litvinova M, y Piontti AP, Chinazzi M, Fumanelli L, Gomes MF, et al. Inferring high-resolution human mixing patterns for disease modeling. Nature communications. 2021; 12(1):1–12. https://doi.org/10.1038/s41467-020-20544-y PMID: 33436609

29. RKI. Corona-Monitoring bundesweit (RKI-SOEP-Studie): Überblick zu ersten Ergebnissen; 2021. https://www.rki.de/DE/Content/Gesundheitsmonitoring/Studien/lid/Ergebnisse.html?nn=14830934. Available from: https://www.rki.de/DE/Content/Gesundheitsmonitoring/Studien/lid/Ergebnisse.html?nn=14830934.

30. Karagiannidis C, Windisch W, McAuley DF, Welte T, Busse R. Major differences in ICU admissions during the first and second COVID-19 wave in Germany. The Lancet Respiratory Medicine. 2021. https://doi.org/10.1016/S2213-2600(21)00101-6 PMID: 33684356

31. Polack FP, Thomas SJ, Kitchin N, Absalon J, Gurtman A, Lockhart S, et al. Safety and Efficacy of the BNT162b2 mRNA COVID-19 Vaccine. New England Journal of Medicine. 2020; 383(27):2603–2615. https://doi.org/10.1056/NEJMoa2034577 PMID: 33301246

32. Voysey M, Clemens SAC, Madhi SA, Weckx LY, Folegatti PM, Aley PK, et al. Safety and efficacy of the ChAdOx1 nCoV-19 vaccine (AZD1222) against SARS-CoV-2: an interim analysis of four randomised controlled trials in Brazil, South Africa, and the UK. The Lancet. 2021; 397(10269):99–111. https://doi.org/10.1016/S0140-6736(20)32661-1 PMID: 33306989

33. Ministry of Health I. Effectiveness Data of the COVID-19 Vaccine Collected in Israel until 13.2.2021;. https://www.gov.il/en/departments/news/20022021-01.

34. Petter E, Mor O, Zuckerman N, Oz-Levi D, Younger A, Aran D, et al. Initial real world evidence for lower viral load of individuals who have been vaccinated by BNT162b2. medRxiv. 2021.

35. Altmann DM, Boyton RJ, Beale R. Immunity to SARS-CoV-2 variants of concern. Science. 2021; 371 (6534):1103–1104. https://doi.org/10.1126/science.abg7404 PMID: 33707254

36. Wang P, Nair MS, Liu L, Iketani S, Luo Y, Guo Y, et al. Antibody resistance of SARS-CoV-2 variants B. 1.351 and B. 1.1. 7. Nature. 2021; p. 1–6.

37. Garcia-Beltran WF, Lam EC, St Denis K, Nitido AD, Garcia ZH, Hauser BM, et al. Multiple SARS-CoV-2 variants escape neutralization by vaccine-induced humoral immunity. Cell. 2021. https://doi.org/10.1016/j.cell.2021.03.013

38. Tarke A, Sidney J, Methot N, Yu ED, Zhang Y, Dan JM, et al. Impact of SARS-CoV-2 variants on the total CD4+ and CD8+ T cell reactivity in infected or vaccinated individuals. Cell Reports Medicine. 2021; p. 100355. https://doi.org/10.1016/j.xcrm.2021.100355 PMID: 34230917

39. Hutt D. Why are Czechs among Europe's most sceptical over taking vaccines?; 2021. Available from: https://www.euronews.com/2021/01/06/coronavirus-why-are-czechs-among-europe-s-most-sceptical-when-it-comes-to-vaccines.

40. Mallapaty S. Can COVID vaccines stop transmission? Scientists race to find answers. Nature. 2021. PMID: 33608683

41. Hall VJ, Foulkes S, Saei A, Andrews N, Oguti B, Charlett A, et al. Effectiveness of BNT162b2 mRNA Vaccine Against Infection and COVID-19 Vaccine Coverage in Healthcare Workers in England, Multi-centre Prospective Cohort Study (the SIREN Study). Rochester, NY: Social Science Research Network; 2021. ID 3790399. Available from: https://papers.ssrn.com/abstract=3790399.

42. Dan JM, Mateus J, Kato Y, Hastie KM, Yu ED, Faliti CE, et al. Immunological memory to SARS-CoV-2 assessed for up to 8 months after infection. Science. 2021; 371 (6529). https://doi.org/10.1126/science.abf4063 PMID: 33408181

43. DESTATIS. 14. koordinierte Bevölkerungsvorausberechnung für Deutschland (Coordinated Population Projection for Germany); 2019. https://service.destatis.de/bevoelkerungspyramide/#!a=70,80&l=en&g. Available from: https://service.destatis.de/bevoelkerungspyramide/#!a=70,80&l=en&g.

44. RKI. Digitales Impfquotenmonitoring zur COVID-19-Impfung; 2021. https://www.rki.de/DE/Content/InfAZ/N/Neuartiges_Coronavirus/Daten/Impfquoten-Tab.html. Available from: https://www.rki.de/DE/Content/InfAZ/N/Neuartiges_Coronavirus/Daten/Impfquoten-Tab.html.

45. Der Spiegel. Impfstoff für 50 Millionen bis Ende Juni; 2021. Available from: https://www.spiegel.de/wirtschaft/soziales/corona-impfstoff-lieferungen-an-deutschland-vakzine-fuer-50-millionen-bis-ende-juni-a-c5a61e87-be51-4b79-8fd9-3be6d4201bee.

46. Maier BF, Burdinski A, Rose AH, Schlosser F, Hinrichs D, Betsch C, et al. Potential benefits of delaying the second mRNA COVID-19 vaccine dose; 2021.

47. Schilling J, Lehfeld A, Schumacher D, Ullrich A, Diercke M, et al. Krankheitsschwere der ersten COVID-19-Welle in Deutschland basierend auf den Meldungen gemäß Infektionsschutzgesetz. Journal of Health Monitoring. 2020; 5(S11):2–20.

48. Intensivregister-Team am RKI IT. Tagesreport aus dem DIVI-Intensivregister; 2020. https://doi.org/10.25646/7625.

49. Karagiannidis C, Mostert C, Hentschker C, Voshaar T, Malzahn J, Schillinger G, et al. Case characteristics, resource use, and outcomes of 10 021 patients with COVID-19 admitted to 920 German hospitals: an observational study. The Lancet Respiratory Medicine. 2020; 8(9):853–862. https://doi.org/10.1016/S2213-2600(20)30316-7 PMID: 32735842

50. Levin AT, Hanage WP, Owusu-Boaitey N, Cochran KB, Walsh SP, Meyerowitz-Katz G. Assessing the age specificity of infection fatality rates for COVID-19: systematic review, meta-analysis, and public policy implications. European Journal of Epidemiology. 2020. https://doi.org/10.1007/s10654-020-00698-1 PMID: 33289900

51. Santos-Hövener C, Busch MA, Koschollek C, Schlaud M, Hoebel J, Hoffmann R, et al. Seroepidemiological study on the spread of SARS-CoV-2 in populations in especially affected areas in Germany–Study protocol of the CORONA-MONITORING lokal study. Journal of Health. 2020.

52. Salje H, Kiem CT, Lefrancq N, Courtejoie N, Bosetti P, Paireau J, et al. Estimating the burden of SARS-CoV-2 in France. Science. 2020; 369(6500):208–211. https://doi.org/10.1126/science.abc3517 PMID: 32404476

53. Millar JE, Busse R, Fraser JF, Karagiannidis C, McAuley DF. Apples and oranges: international comparisons of COVID-19 observational studies in ICUs. The Lancet Respiratory Medicine. 2020; 8 (10):952–953. https://doi.org/10.1016/S2213-2600(20)30368-4 PMID: 32835653

54. He X, Lau EHY, Wu P, Deng X, Wang J, Hao X, et al. Temporal dynamics in viral shedding and transmissibility of COVID-19. Nature Medicine. 2020; p. 1–4.

55. Pan F, Ye T, Sun P, Gui S, Liang B, Li L, et al. Time course of lung changes on chest CT during recovery from 2019 novel coronavirus (COVID-19) pneumonia. Radiology. 2020; p. 200370.

56. Ling Y, Xu SB, Lin YX, Tian D, Zhu ZQ, Dai FH, et al. Persistence and clearance of viral RNA in 2019 novel coronavirus disease rehabilitation patients. Chinese medical journal. 2020. https://doi.org/10.1097/CM9.0000000000000774 PMID: 32118639

57. Mahase E. Covid-19: Where are we on vaccines and variants? BMJ. 2021; 372:n597. https://doi.org/10.1136/bmj.n597 PMID: 33653708

58. Bernal JL, Andrews N, Gower C, Robertson C, Stowe J, Tessier E, et al. Effectiveness of the Pfizer-BioNTech and Oxford-AstraZeneca vaccines on covid-19 related symptoms, hospital admissions, and mortality in older adults in England: test negative case-control study. bmj. 2021; 373.

59. Haas EJ, Angulo FJ, McLaughlin JM, Anis E, Singer SR, et al K F. Impact and effectiveness of mRNA BNT162b2 vaccine against SARS-CoV-2 infections and COVID-19 cases, hospitalisations, and deaths following a nationwide vaccination campaign in Israel: an observational study using national surveillance data. The Lancet. 2021; 397(10287):1819–1829. https://doi.org/10.1016/S0140-6736(21)00947-8 PMID: 33964222

60. Pritchard E, Matthews P, Stoesser N, et al. Impact of vaccination on new SARS-CoV-2 infections in the United Kingdom. Nature Medicine. 2021; p. 1546–170X. PMID: 34108716

61. Thompson MG, Burgess JL, Naleway AL, Tyner HL, Yoon SK, Meece J, et al. Interim estimates of vaccine effectiveness of BNT162b2 and mRNA-1273 COVID-19 vaccines in preventing SARS-CoV-2 infection among health care personnel, first responders, and other essential and frontline workers—eight US locations, December 2020–March 2021. Morbidity and Mortality Weekly Report. 2021; 70 (13):495. https://doi.org/10.15585/mmwr.mm7013e3 PMID: 33793460

62. an der Heiden M, Hamouda O. Schätzung der aktuellen Entwicklung der SARS-CoV-2- Epidemie in Deutschland—Nowcasting. Epidemiologisches Bulletin. 2020; 2020(17):10–15.

63. Lauer SA, Grantz KH, Bi Q, Jones FK, Zheng Q, Meredith HR, et al. The incubation period of coronavirus disease 2019 (COVID-19) from publicly reported confirmed cases: estimation and application. Annals of internal medicine. 2020. https://doi.org/10.7326/M20-0504 PMID: 32150748

64. Bundesministerium für Gesundheit BAnz, Verordnung zum Anspruch auf Schutzimpfung gegen das Coronavirus SARS-CoV-2 (Coronavirus-Impfverordnung – CoronaImpfV); 2021. Available from: https://www.bundesregierung.de/resource/blob/975226/1851894/e195f7a8ee3e463e5947c8254b6be1d5/2021-02-08-impfverordnung-neu-data.pdf?download=1.

65. Robert-Koch-Institut. Mitteilung der Ständigen Impfkommission am Robert-Koch-Institut. Beschluss der STIKO zur 2. Aktualisierung der COVID-19-Impfempfehlung und die dazugehörige wissenschaftliche Begründung; 2021. https://www.rki.de/DE/Content/Infekt/EpidBull/Archiv/2021/Ausgaben/05_21.pdf. Available from: https://www.rki.de/DE/Content/Infekt/EpidBull/Archiv/2021/Ausgaben/05_21.pdf?__blob=publicationFile.

66. Bar-On YM, Flamholz A, Phillips R, Milo R. Science Forum: SARS-CoV-2 (COVID-19) by the numbers. Elife. 2020; 9:e57309. https://doi.org/10.7554/eLife.57309 PMID: 32228860

67. Li R, Pei S, Chen B, Song Y, Zhang T, Yang W, et al. Substantial undocumented infection facilitates the rapid dissemination of novel coronavirus (SARS-CoV-2). Science. 2020; 368(6490):489–493. https://doi.org/10.1126/science.abb3221 PMID: 32179701

68. Linden M, Mohr SB, Dehning J, Mohring J, Meyer-Hermann M, Pigeot I, et al. Case numbers beyond contact tracing capacity are endangering the containment of COVID-19. Dtsch Arztebl International. 2020; 117(46):790–791. https://doi.org/10.3238/arztebl.2020.0790 PMID: 33533714

5

INTERPLAY BETWEEN RISK PERCEPTION, BEHAVIOR, AND COVID-19 SPREAD

This chapter is identical to the article [25]. The Supplementary Information can be found in Appendix C. The article is published in

Dönges, P., Wagner, J., Contreras, S., Iftekhar, E.N., Bauer, S., Mohr, S.B., Dehning, J., Calero Valdez, A., Kretzschmar, M., Mäs, M. et al., Interplay between risk perception, behavior, and COVID-19 spread, Frontiers in Physics, 10 (2022), under the terms of a Creative Common License (`http://creativecommons.org/licenses/by/4.0/`).

To this publication, I contributed equally with P. Dönges, J. Wagner, and S. Contreras. Roles: Methodology, Writing – original draft, Writing – review & editing.

Interplay Between Risk Perception, Behavior, and COVID-19 Spread

Philipp Dönges[1†], Joel Wagner[1†], Sebastian Contreras[1,2†], Emil N. Iftekhar[1†], Simon Bauer[1], Sebastian B. Mohr[1], Jonas Dehning[1], André Calero Valdez[3], Mirjam Kretzschmar[4], Michael Mäs[5], Kai Nagel[6] and Viola Priesemann[1,7]*

[1]Max Planck Institute for Dynamics and Self-Organization, Göttingen, Germany, [2]Centre for Biotechnology and Bioengineering, Universidad de Chile, Santiago, Chile, [3]Chair of Communication Science, RWTH Aachen University, Aachen, Germany, [4]University Medical Center Utrecht, Utrecht University, Utrecht, Netherlands, [5]Department of Sociology, Karlsruhe Institute of Technology, Karlsruhe, Germany, [6]Chair of Transport Systems Planning and Transport Telematics, Technische Universität Berlin, Berlin, Germany, [7]Institute for the Dynamics of Complex Systems, University of Göttingen, Göttingen, Germany

Pharmaceutical and non-pharmaceutical interventions (NPIs) have been crucial for controlling COVID-19. They are complemented by voluntary health-protective behavior, building a complex interplay between risk perception, behavior, and disease spread. We studied how voluntary health-protective behavior and vaccination willingness impact the long-term dynamics. We analyzed how different levels of mandatory NPIs determine how individuals use their leeway for voluntary actions. If mandatory NPIs are too weak, COVID-19 incidence will surge, implying high morbidity and mortality before individuals react; if they are too strong, one expects a rebound wave once restrictions are lifted, challenging the transition to endemicity. Conversely, moderate mandatory NPIs give individuals time and room to adapt their level of caution, mitigating disease spread effectively. When complemented with high vaccination rates, this also offers a robust way to limit the impacts of the Omicron variant of concern. Altogether, our work highlights the importance of appropriate mandatory NPIs to maximise the impact of individual voluntary actions in pandemic control.

Keywords: COVID-19, disease modeling, infodemic, human behavior, self-regulation, vaccine hesitancy, health policy and practice, Omicron variant (SARS-CoV-2)

1 INTRODUCTION

During the COVID-19 pandemic, the virus has played a central role in people's day-to-day conversations and the information they search for and consume [1]. The growing amount of news and specialized literature on COVID-19 can inform individual decisions in a wide range of situations and on various timescales [2]. For example, people decide multiple times every day how closely they follow mask-wearing regulations or meeting restrictions. However, if hesitant, they might take weeks or months to decide whether to accept a vaccine. These decisions impact the spreading dynamics of COVID-19 and ultimately determine the effectiveness of interventions and how smoothly we transit to SARS-CoV-2 endemicity.

While typical models of disease spread consider that individual behavior affects the spreading dynamics of an infectious disease, they often neglect that there is also a relation in the opposite causal direction. This feedback loop comprises that, e.g., mass media regularly updates individuals on the latest local developments of the pandemic, such as the current occupancy of intensive care units (ICUs). This information affects individuals' opinions and risk perceptions and, thus ultimately their actions [3]. For example, given high perceived risk, individuals reduce their non-essential contacts

FIGURE 1 | Interplay between risk perception and voluntary health-protective behavior. **(A)**: Sketch of the proposed age-stratified compartmental model of disease spread, which incorporates different stages for disease progression and immunological conditions of the susceptible population with their respective chances of being infected and developing a severe course (**Supplementary Figure S1**, Supplementary Information, for full model). The behavioral feedback (blue lines) changes individuals' contagious contact behavior, as well as their willingness to get vaccinated, and hence the effective spreading rate. **(B)**: We use the contact matrix of [12], which yields the contact rates at home, school, work and in the community for each age-group. For the subsequent scenarios, we adapt these contexts of contacts separately. Some of the contacts are by definition hard to reduce voluntarily (e.g., household contacts), while others (at school and work) strongly depend on current mandatory non-pharmaceutical interventions (**Supplementary Figure S3** for details).

decompose the overall contact structure into contextual contacts (**Figure 1B**) and for each context define a range in which voluntary action can be adapted according to individual risk-perception, given the level of mandatory non-pharmaceutical interventions (NPIs). To that end, we use the functional form identified in 1) (**Figure 2**). We explore different intervention scenarios in the face of adverse seasonality [9–11], using as reference the winter 2021/2022 in central Europe. Our analysis confirms that both extremes ("freedom day" or stringent measures throughout) bear large harms in the long run. However, when measures leave space for voluntary actions, people's adaptive behavior can efficiently contribute to breaking the wave and change the course of the pandemic.

2 RESULTS

2.1 Data-Derived Behavioral Feedback Loops

Throughout this manuscript, we investigate how the interplay between information about the COVID-19 pandemic and its spreading dynamics is mediated by the perception of risk. Risk perception modulates both, 1) people's immediate voluntary health-protective behavior, e.g., their level of contacts and their adherence to mask-wearing and hygiene recommendations, and 2) their willingness (or hesitancy) to receive vaccination (**Figure 1**). Individuals constantly receive information on the current COVID-19 incidence, ICU occupancy, and deaths (which are all closely related [13–15]) either via news outlets or because of reports about COVID-19 cases in their social circles. Hence, the risk they perceive depends on this evolving trend over time.

We tailor our approach to the situation of the COVID-19 pandemic, i.e., to a disease having the following characteristics: 1) high transmissibility, 2) relatively low infection fatality rate, 3) widespread vaccine hesitancy, 4) waning immunity, and 5) public attention and coverage. We differentiate from the approaches of [16–18] as we neither model the contagion of fear explicitly nor a direct coupling between incidence and fear. Instead, we assume that individuals build their perception of risk based on the ICU occupancy over time using a memory function, similar to the theoretical approach in [19, 20]. This is a sensible choice, as ICU occupancy signals 1) how likely governmental bodies are to re-implement emergency NPIs to prevent overwhelming healthcare facilities (and thereby limit individual freedoms), and 2) how likely it is that an individual's close contacts (or their contacts) would have been severely ill. Besides, our modeling framework constitutes a methodological advancement from that presented in [17], as we provide a detailed description of all epidemiologically relevant disease states and several external effects influencing its spread, such as seasonality, contextual contact networks and NPIs.

We assume that individuals base their decisions about heath-protective behavior on the recent developments of the pandemic. Following the ideas of Zauberman et al. about perception of time in decision-making [21], we consider that when individuals decide about behavior that only has immediate protective

beyond existing regulations and increase their willingness to accept vaccine offers accordingly, an effect observed in empirical research conducted with routine surveys in Germany [4] and other parts of the world [5–8]. However, to quantify the effect of individual voluntary actions on the dynamics of COVID-19, two questions remain open: 1) What is the relationship between risk perception and voluntary action, on the one hand, and the spread of the disease, on the other hand; and 2) what is the relative contribution of voluntary action when mandatory restrictions are in place?

In this work, we aim to quantify the impact of voluntary actions on disease spread while studying the questions mentioned above for the COVID-19 pandemic. 1) We analyze survey and COVID-19 vaccination data in European countries to uncover the relationship between the occupancy of ICUs—which determines the perceived risk—and voluntary immediate health-protective behavior as well as the willingness to get vaccinated. We then incorporate these effective feedback loops into a deterministic compartmental model (**Figure 1A**). 2) We

FIGURE 2 | Data-derived formulation of behavioral feedback loops. **(A)**: Reported contact reductions follow intensive care unit (ICU) occupancy in Germany. Survey participants were asked how likely they were to avoid private parties over the course of the pandemic on a discrete scale from 1 (never) to 5 (always) [4]. To decouple the effect of vaccination availability, we present 2020 (red) and 2021 (yellow) data separately. Ticks indicate the middle of the month. **(B)**: The survey data on contact reduction and the ICU occupancy are related. The piece-wise linear relationship shows the reduction of contacts with increasing ICU occupancy, and for even higher ICU occupancy a saturation. Red, yellow, and black represent fits to the data from 2020, 2021, and overall, respectively. **(C)**: In the model, the contact reduction and its dependency on ICU occupancy is implemented as a multiplicative reduction factor k that weighs the age-dependent contextual contact matrices (**Figure 1B**). **(D)**: Vaccine uptake increases with ICU occupancy in Romania (shown here) and other European countries (**Supplementary Figure S4**). **(E)**: Willingness to accept a vaccine offer is modeled using an exponentially-saturating function, ranging between a lower and upper bound of acceptance depending on ICU occupancy. The bounds represent that a fraction of people is willing to be vaccinated even at no immediate threat (no ICU occupancy), and another fraction is not willing or able to get vaccinated no matter the threat. **(F)**: Vaccines are delivered at a rate proportional to the number of people seeking a vaccine, i.e., the difference between the number of people willing to be vaccinated and those already vaccinated. Thus, when the number of already vaccinated equals the number of people willing to get vaccinated, no more vaccinations are carried out. The same functional shape describes the booster uptake.

effects, they consider only the current risk-level. For instance, when deciding whether or not to wear a mask in the supermarket on a given day, they only consider the most recently reported ICU occupancy. Decisions with longer-term protection, in contrast, are also based on a longer-term risk-assessment. When deciding whether or not to get a booster vaccine, for example, individuals do not only take into account the ICU-occupancy on the day of the decision but they are looking back at a longer period. We detail the assumptions about the perceived risk-level and the resulting health-protective behavior in the Methods section. In the following, we sketch the derivation of the feedback loops from this perceived risk to people's immediate voluntary health-protective behavior and willingness to get vaccinated.
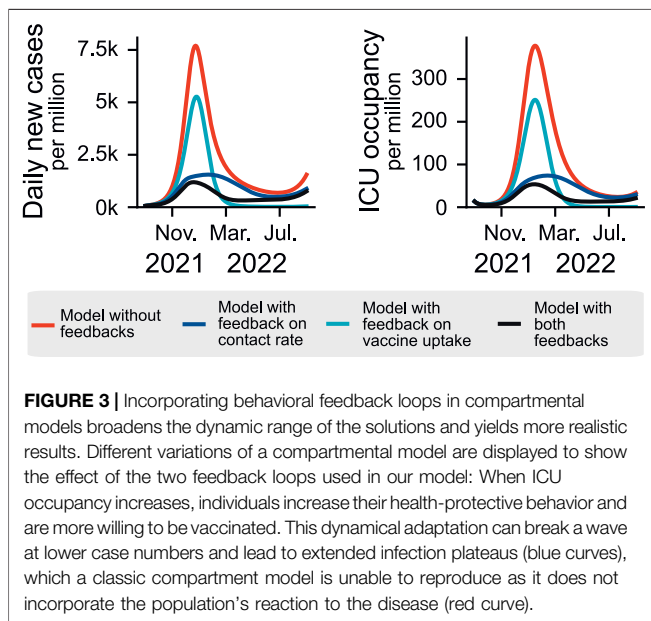
2.1.1 Feedback on Health-Protective Behavior
To determine the explicit relationship between the perceived level of risk and immediate voluntary health-protective behavior—which presents one of the feedback loops in our model—we exploit results from the German COSMO study, a periodic survey where participants are asked about their opinions and behavior regarding the COVID-19 pandemic and NPIs [4].

Their answers on adhering to health-protective behavior recommendations (avoiding private parties in this case) correlate with the ICU occupancy in Germany at the time (**Figure 2A**). However, at very high ICU occupancy, adoption of health-protective behavior seems to reach a plateau (**Figure 2B**); no further adoption seems to be feasible, arguably because those individuals willing to engage in health-protective behavior have done so already as far as they can, and those unwilling are insensitive to higher burden on ICUs. Hence, we fit a piece-wise linear function (with a rounded edge at the transition—called a softplus) to the COSMO data [Pearson correlation coefficient r = 0.64 for 2020–2021 (black), r = 0.81 for 2020 (red) and r = 0.53 for 2021 (yellow)] and use it for the feedback between information in terms of ICU occupancy and voluntary health-protective behavior (**Figure 2C** and Methods for details).

2.1.2 Feedback on Vaccination Behavior
The second feedback loop in our model describes the relationship between the level of perceived risk and vaccine hesitancy. To quantify it, we study the vaccination trends in different European countries and compare them with the trends in ICU occupancy

FIGURE 3 | Incorporating behavioral feedback loops in compartmental models broadens the dynamic range of the solutions and yields more realistic results. Different variations of a compartmental model are displayed to show the effect of the two feedback loops used in our model: When ICU occupancy increases, individuals increase their health-protective behavior and are more willing to be vaccinated. This dynamical adaptation can break a wave at lower case numbers and lead to extended infection plateaus (blue curves), which a classic compartment model is unable to reproduce as it does not incorporate the population's reaction to the disease (red curve).

(**Supplementary Figure S4**, Supplementary Information). The case of Romania (**Figure 2D**) illustrates the relation very clearly: Vaccination rates follow the ICU occupancy with a delay of a few weeks. By analyzing the correlation between vaccination rate and ICU occupancy with a variable delay, we reach the highest Pearson correlation coefficient (0.96) with a delay of 25 days. However, the specific reaction delay and magnitude of the effect differs between countries (**Supplementary Figure S4**). In our model, we propose that as ICU occupancy increases so does the willingness to get vaccinated (i.e., higher probability of accepting a vaccine offer when ICU occupancy is high). As not everybody in the population is willing to accept a vaccine offer, the willing fraction of the population is a function that saturates below 1 (**Figure 2E**). With this formulation, vaccinations are only carried out if the fraction of the population willing to get vaccinated is larger than the fraction of currently vaccinated (**Figure 2F** and Methods for details).

Our model can capture two features observed in real-world vaccination programs. First, when case numbers are low and vaccine uptake high, rational agents might have insufficient incentives for getting vaccinated. Assuming a high perceived risk of vaccine side effects, the agents would thus decline vaccination when offered. The above is known as the free-rider problem in game theory and economics [22]. Second, the two feedback loops in our model and the incorporation of waning immunity allows us to observe different incidence curve shapes and replicate recurrent waves of infections. The above is a necessary validity check, as real-world outbreaks exhibit a large variety of incidence curve shapes [23]. These may ultimately unveil universal patterns of disease spread that are consistent across countries [24].

2.2 Behavioral Feedback Loops Yield More Realistic Results than Classical Models
Classical SEIR-like compartmental models have found wide application in the first stages of the COVID-19 pandemic. In

these models, the different stages of disease progression are represented by separate compartments and individuals transit from one to another at a given (and typically constant) transition rate. In that way, an infectious disease outbreak will proliferate if the spreading rate of the disease is larger than the recovery rate and if a large-enough fraction of the population is susceptible to being infected. However, these simple models often tend to overestimate the size of an infectious disease outbreak or all possible trajectories for the incidence trends [23], as they do not incorporate mechanisms of dynamical adaptation of restrictions [25] or, as studied in this paper, behavior.
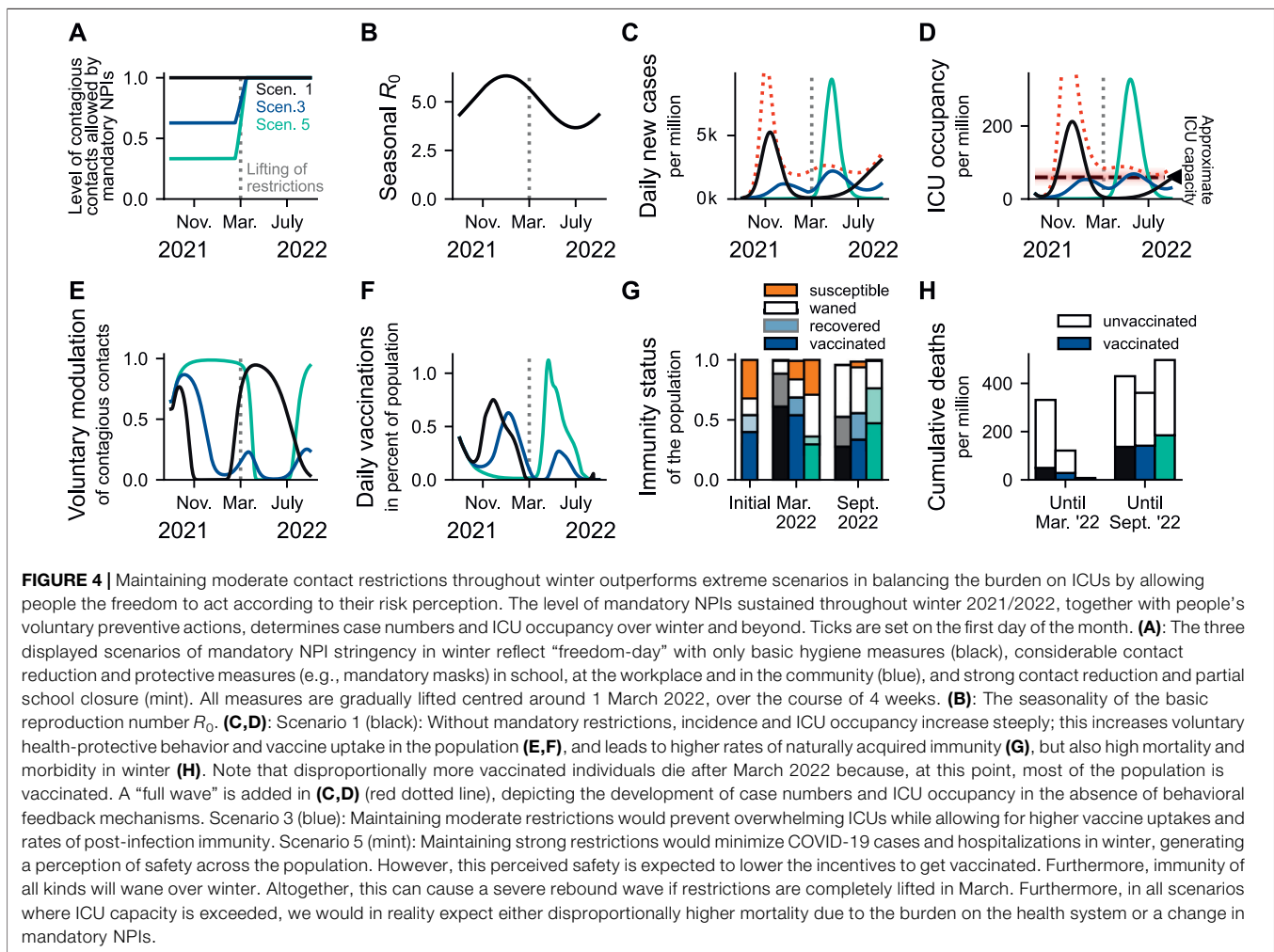
We observe that including the feedback loops described above reduces the peak in incidences and hospitalizations while keeping the timing of the wave almost unchanged (see **Figure 3**). More generally, these feedback loops break increasing and declining trends, resulting in long but flat infection plateaus or multiple waves. Compared to classical SEIR-like models, where two dynamical regimes are possible—exponential growth or decay of case numbers, when neglecting waning immunity—, our model captures a broader spectrum of dynamics by linking ICU occupancy with individuals' health-protective voluntary behavior and vaccine uptake.

2.3 Policies With Either too Weak or too Strong Interventions Throughout Winter Bear Higher Levels of Mortality and Morbidity
Using parameters obtained from surveys and other data sources (**Supplementary Table S3**, Supplementary Information), we analyze five scenarios of mandatory NPIs throughout winter (for all age-stratified results see **Supplementary Material**): 1) no NPIs at all, 2)-4) moderate NPIs and 5) strong NPIs (Methods for details). The stringency of the scenarios and the seasonal effects are depicted in **Figures 4A,B** and **Figures 5A,B**. As an example case, we assume a country with a total vaccination rate of 60% and a recovered fraction of 20%. Note that we include the possibility of overlaps between vaccinated and recovered. Thus, the total fraction of immune individuals does not add up to 80% but 68%. For more detail on the initial conditions, see **Supplementary Material**, **Supplementary Section S3.1**.

Without any mandatory NPIs throughout winter (Scenario 1, **Figure 4**, black lines), case numbers and hospitalizations will show a steep rise (**Figures 4C,D**). As a consequence, individuals voluntarily adapt their health-protective behavior and are more inclined to accept a vaccine offer (**Figures 4E–G**). Although this scenario features unrealistically high mortality and morbidity, modeling results in the absence of any behavior feedback mechanisms yield even higher levels (cf. **Figures 4C,D**, dotted red line).

In contrast, suppressing the seasonal wave through strong mandatory NPIs (Scenario 5, **Figure 4**, mint lines) and thereby maintaining low case numbers through winter only delays the wave to a later but inevitable date once restrictions

FIGURE 4 | Maintaining moderate contact restrictions throughout winter outperforms extreme scenarios in balancing the burden on ICUs by allowing people the freedom to act according to their risk perception. The level of mandatory NPIs sustained throughout winter 2021/2022, together with people's voluntary preventive actions, determines case numbers and ICU occupancy over winter and beyond. Ticks are set on the first day of the month. **(A)**: The three displayed scenarios of mandatory NPI stringency in winter reflect "freedom-day" with only basic hygiene measures (black), considerable contact reduction and protective measures (e.g., mandatory masks) in school, at the workplace and in the community (blue), and strong contact reduction and partial school closure (mint). All measures are gradually lifted centred around 1 March 2022, over the course of 4 weeks. **(B)**: The seasonality of the basic reproduction number R_0. **(C,D)**: Scenario 1 (black): Without mandatory restrictions, incidence and ICU occupancy increase steeply; this increases voluntary health-protective behavior and vaccine uptake in the population **(E,F)**, and leads to higher rates of naturally acquired immunity **(G)**, but also high mortality and morbidity in winter **(H)**. Note that disproportionally more vaccinated individuals die after March 2022 because, at this point, most of the population is vaccinated. A "full wave" is added in **(C,D)** (red dotted line), depicting the development of case numbers and ICU occupancy in the absence of behavioral feedback mechanisms. Scenario 3 (blue): Maintaining moderate restrictions would prevent overwhelming ICUs while allowing for higher vaccine uptakes and rates of post-infection immunity. Scenario 5 (mint): Maintaining strong restrictions would minimize COVID-19 cases and hospitalizations in winter, generating a perception of safety across the population. However, this perceived safety is expected to lower the incentives to get vaccinated. Furthermore, immunity of all kinds will wane over winter. Altogether, this can cause a severe rebound wave if restrictions are completely lifted in March. Furthermore, in all scenarios where ICU capacity is exceeded, we would in reality expect either disproportionally higher mortality due to the burden on the health system or a change in mandatory NPIs.
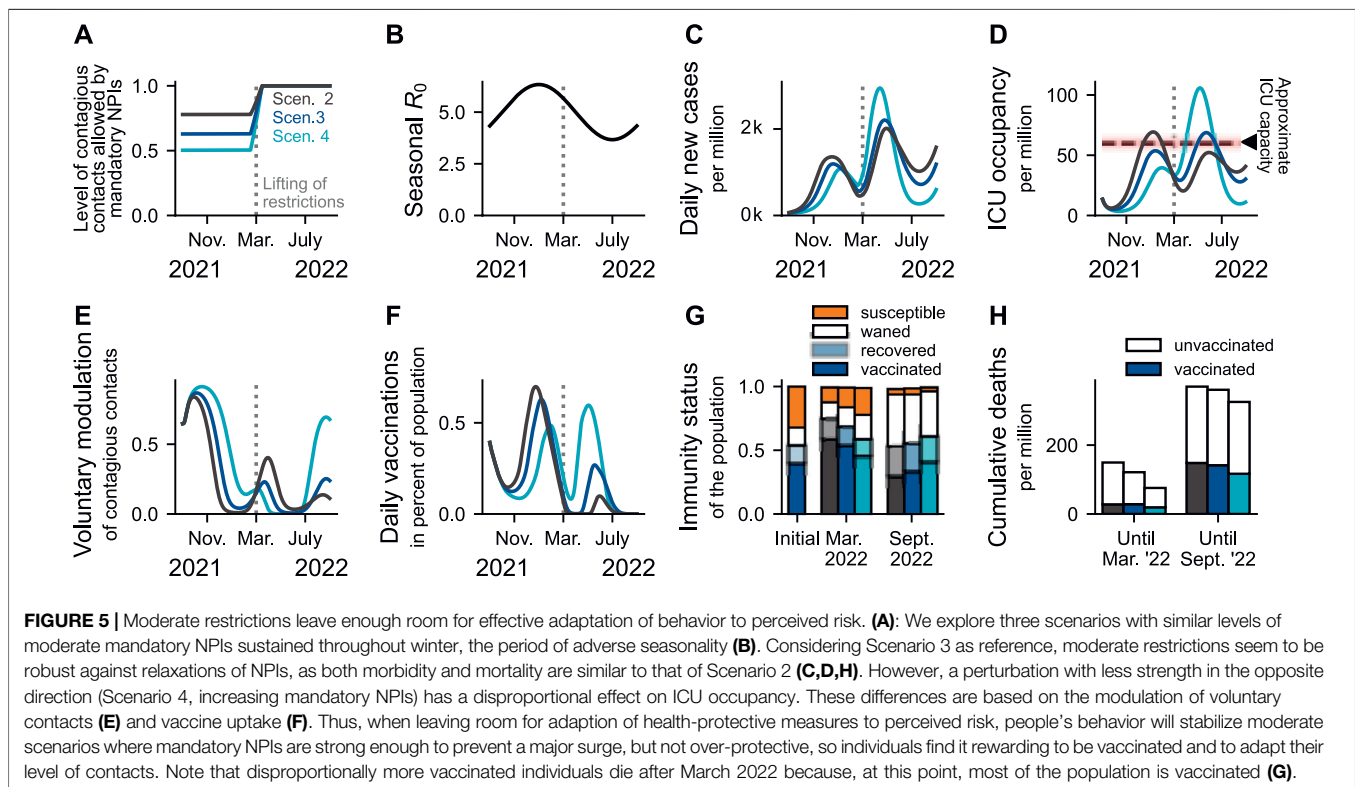
are lifted (**Figures 4C,D**). Low COVID-19 incidence throughout winter implies 1) low post-infection immunity, 2) little incentives for first or booster vaccination, 3) waning immunity, and 4) lower rates of "naturally" boosting immune memory upon re-exposure to the virus [26]. The resulting low immunity levels (**Figure 4G**) then fuel a higher rebound wave when restrictions are lifted in March 2022, despite favorable seasonality. Similar rebound waves have been observed for other seasonal respiratory viruses [27, 28].

Interestingly, the middle strategy, namely moderate NPIs during winter, prevents the high wave in winter as well as the rebound wave in spring that characterize the scenarios with no or with strong NPIs, respectively (Scenario 3, **Figure 4**, dark blue). Unlike in the extreme scenarios, the ICU capacity in Scenario 3 is not exceeded in any season, hence avoiding reduced health care quality and strong burden to health care workers. **Figure 4H** shows that the death toll in Scenario 3 is lower than in the other scenarios. In reality however, this difference would be much larger because Scenarios 1 and 5 surpass the assumed ICU capacity by far; that would imply disproportionally higher mortality, an effect we did not quantify in our model. Alternatively, emergency

mandatory NPIs would be introduced, which we do not model here.

2.4 Voluntary Actions can Dampen the Wave if Restrictions are Moderate

As presented in the previous section, extreme scenarios (Scenarios 1 and 5) bear high levels of morbidity and mortality. However, in scenarios with intermediate restriction levels (Scenarios 2–4, **Figure 5A**), voluntary preventive actions (**Figure 5E**) can compensate for slightly too low levels of mandatory NPIs, provided that these NPIs are strong enough to prevent a surge in COVID-19 incidence that might be too sudden or strong for individuals to voluntarily adopt health-protective behavior (**Figures 5C,D**). For example, while having different levels of mandatory NPIs, Scenarios 2 and 3 reach similar peaks in ICU occupancy (**Figure 5D**). Conversely, despite considering a proportional increase in the strength of NPIs (comparable to that from Scenario 2 to 3, **Figure 5A**), Scenario 4 is too protective: there are too few incentives to get vaccinated (**Figure 5F**) due to the low risk perception as well as too few infections (**Figure 5C**) and, hence, appropriate immunity

FIGURE 5 | Moderate restrictions leave enough room for effective adaptation of behavior to perceived risk. **(A)**: We explore three scenarios with similar levels of moderate mandatory NPIs sustained throughout winter, the period of adverse seasonality **(B)**. Considering Scenario 3 as reference, moderate restrictions seem to be robust against relaxations of NPIs, as both morbidity and mortality are similar to that of Scenario 2 **(C,D,H)**. However, a perturbation with less strength in the opposite direction (Scenario 4, increasing mandatory NPIs) has a disproportional effect on ICU occupancy. These differences are based on the modulation of voluntary contacts **(E)** and vaccine uptake **(F)**. Thus, when leaving room for adaption of health-protective measures to perceived risk, people's behavior will stabilize moderate scenarios where mandatory NPIs are strong enough to prevent a major surge, but not over-protective, so individuals find it rewarding to be vaccinated and to adapt their level of contacts. Note that disproportionally more vaccinated individuals die after March 2022 because, at this point, most of the population is vaccinated **(G)**.

levels are not reached (**Figure 5G**). As a consequence, a disproportionally larger off-seasonal wave in spring overwhelms ICUs (**Figure 5D**). Noteworthy, even though the nominal mortality is the lowest for Scenario 4 (**Figure 5H**), this value does not account for triage-induced over-mortality or novel necessary NPIs that would be likely be imposed and is thus invalid.

2.5 Case Study: Emergence of the Omicron Variant of Concern and its Effect on Case Numbers

A risk that cannot be neglected is the emergence of SARS-CoV-2 variants of concern (VOC), such as the Omicron VOC. This variant is rapidly replacing the Delta VOC, thus posing an imminent risk. Although there is substantial uncertainty about its epidemiological features, preliminary evidence shows: Compared to the Delta VOC, Omicron exhibits 1) an increased risk of reinfection or break-through infection [29–31], 2) a substantial reduction in antibody neutralization [32–38], 3) a reduction in vaccine effectiveness against infection [31, 37, 39–44], and 4) faster spread [30, 31, 45, 46] mainly due to immune escape [47].

Given this evidence, we analyze the impacts of a potential full replacement of the dominant Delta VOC by the Omicron VOC by 15th of January 2022. We incorporate the protection against infection by booster doses. As example scenario, we start with Scenario 3 (moderate mandatory NPIs), as it resembles a typical development in Europe. We then analyze four different possible

reactions to the Omicron VOC, i.e., starting to switch from Scenario 3 to Scenarios 1, 3, 4, or 5 before it takes over (**Figure 6A**). We evaluate three possibilities regarding the booster vaccine-protection against infection, 50, 65, and 80% (relative to the protection granted for Delta). This is consistent with available evidence suggesting Omicron's immune escape to reduce vaccine effectiveness against symptomatic disease to about 73% for freshly mRNA-boosted individuals [32]. Furthermore, we explore two possibilities of severity of infections after previous immunization: Either efficacy against severe course remains the same as with Delta, both for the immunized and immune-naive persons (**Figures 6B,E,H**), or protection is five times better for the immunized (**Figures 6C,F,I**).

As expected, the enhanced transmissibility resulting from the partial escape of the Omicron VOC breaks the decreasing trend in case numbers observed for Scenarios 3, 4, and 5 from the moment where the replacement takes place (**Figures 6A,D,G**). This results in a substantial surge in daily new cases in all scenarios except for Scenario 5 (most restrictive). Regarding ICU occupancy, our results depend strongly on the assumed protection against infection by recent vaccination or boosters. When the protection against infection granted by recently administered vaccines is above 50%, both Scenarios 4 (which has a more strict testing policy and further reduced contacts compared to Scenario 3) and 5 (in addition, group sizes in school are reduced) yield optimistic results for ICU occupancy. If Omicron infections lead to much less severe course of the disease for immunized or convalescent individuals, then even Scenario 3 can avoid severely overfilling intensive care units. We have represented Scenario 1
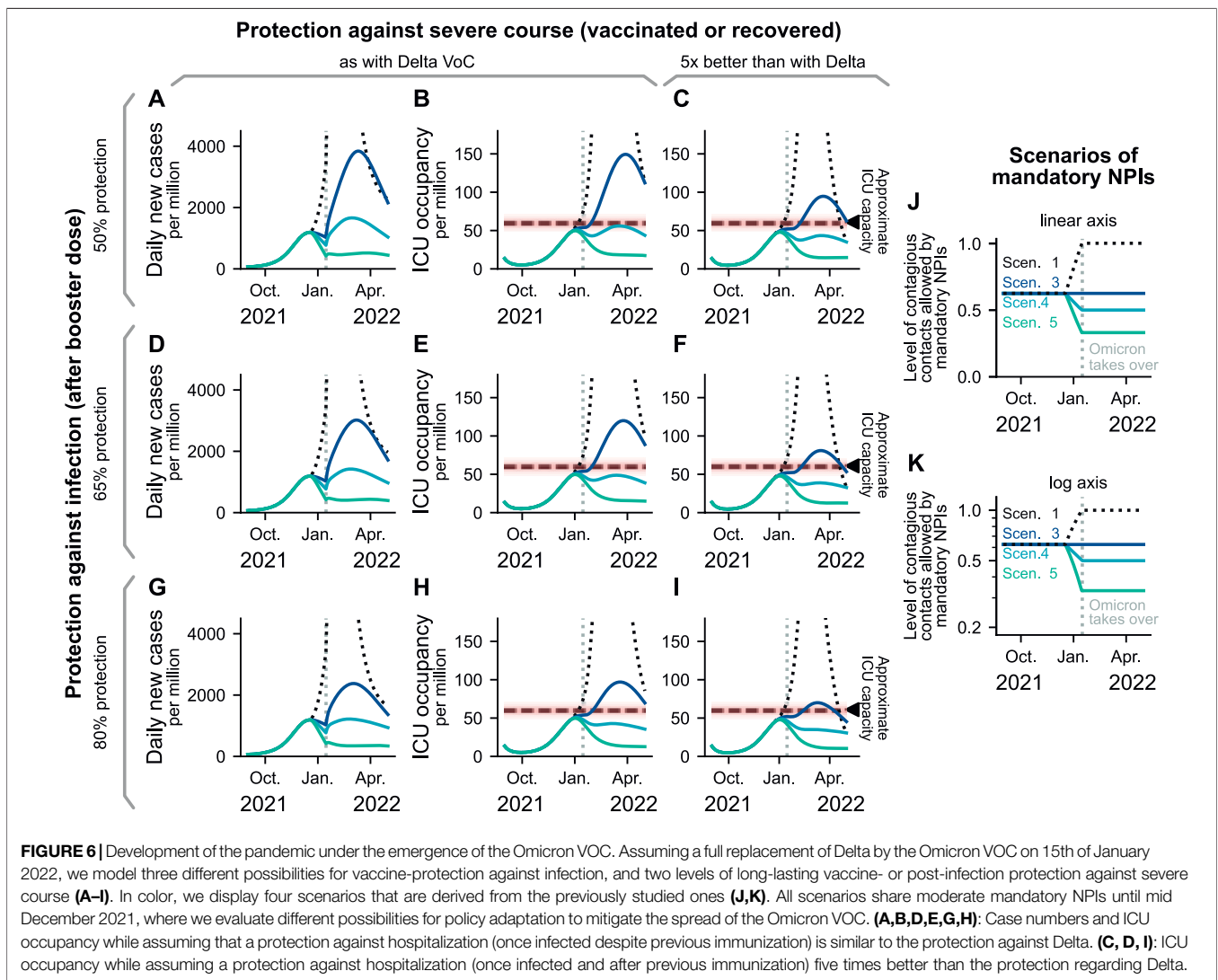
FIGURE 6 | Development of the pandemic under the emergence of the Omicron VOC. Assuming a full replacement of Delta by the Omicron VOC on 15th of January 2022, we model three different possibilities for vaccine-protection against infection, and two levels of long-lasting vaccine- or post-infection protection against severe course **(A–I)**. In color, we display four scenarios that are derived from the previously studied ones **(J,K)**. All scenarios share moderate mandatory NPIs until mid December 2021, where we evaluate different possibilities for policy adaptation to mitigate the spread of the Omicron VOC. **(A,B,D,E,G,H)**: Case numbers and ICU occupancy while assuming that a protection against hospitalization (once infected despite previous immunization) is similar to the protection against Delta. **(C, D, I)**: ICU occupancy while assuming a protection against hospitalization (once infected and after previous immunization) five times better than the protection regarding Delta.

(lifting all mandatory NPIs) with dashed lines, as it yields unrealistic results: Stricter NPIs would probably be reinstated if ICU occupancy becomes too high. The scenarios end in April, where we expect that an updated booster vaccine is developed and distributed. In that phase, lifting restrictions at the pace of vaccination and aiming for low case numbers would maximize freedom while minimizing mortality and morbidity [25, 48–50].

3 DISCUSSION

Modeling the interplay of human behavior and disease spread is one of the grand challenges of infectious disease modeling. While not being the first to model behavioral adaptation [17, 51–55], we incorporate data-driven insights into our modeling framework, inspiring the explicit functional dependency between risk and health-protective behavior as well as vaccine hesitancy in the context of the COVID-19 pandemic. Thereby, we can incorporate

self-regulation mechanisms into our scenario analysis, which best qualitatively describe what is to be expected in the future or in the event of the emergence of novel SARS-CoV-2 VOCs, such as the Omicron variant. We hence take a further step towards more empirically-grounded mathematical models.

Within our framework, a smooth transition to SARS-CoV-2 endemicity requires, besides a working and accepted vaccine, two ingredients. First, mandatory NPI levels should be high enough to prevent a surge in case numbers so fast that individuals could not react on time to prevent overwhelming ICUs. Second, mandatory NPIs should leave enough room so that individuals can effectively adopt voluntary preventive actions as a response to an increased perception of risk. Hence, governments must guarantee that the decision to, e.g., attend non-essential face-to-face activities that could be carried out remotely remains in the individual's hands. Under such circumstances, voluntary actions can dampen the wave and prevent overwhelming ICUs (Scenarios 2 and 3, **Figure 5**). Otherwise, irresponsible or overprotective measures would result in a wave that could surpass the healthcare capacity

in the short term or when lifting all measures (Scenarios 1, 4, and 5, **Figures 4**, **5**). In any case, people's awareness about the danger of a disease should ideally be driven by trust in scientific and governmental bodies instead of by the current burden to the healthcare system. Hence, it is crucial during a disease outbreak to engage in extensive, expert-guided, and audience-tailored risk communication [56] and to prevent the spread of mis- and disinformation that could damage general trust [57, 58].

Despite the empirical basis of our approach, the functional shape of the feedback mechanisms remains one of the main uncertainties in our model. The voluntary adoption of health-protective measures was inspired by survey data [4], and is thus bound to its limitations. Additionally, as ICU capacity was never extremely overwhelmed in Germany in the time frame of the COSMO survey, the study does not provide information on how people would act at very high levels of ICU occupancy; in principle, such emergency situations would trigger even stronger reactions in the population, and certainly also a change in NPI stringency (which we assumed to be constant throughout). Furthermore, when extrapolating our results to other countries, one should consider cultural differences or varying levels of trust in governmental bodies. Therefore, more empirical research to inform model assumptions and parameters remains crucial.

Vaccine uptake and coverage are critical parameters that determine mortality and morbidity levels. In line with what has been observed in high-income countries, we assume that vaccination rates are mostly limited by vaccine hesitancy instead of vaccine stocks or logistics. In that way, we can deal with emergent VOCs (as Omicron) with a healthy combination of mandatory NPIs aiming for low-case numbers while a working vaccine is developed and coverage is insufficient [25, 48] and by letting individuals decide on their own when the roll-out is complete. However, the core problem remains latent; wealthy countries concentrate resources while some countries cannot afford enough vaccines to protect even their population at risk [59]. As the latter countries are forced into accepting high-case numbers in order to keep their economies running, there are increased risks of breeding variants that could escape natural or vaccine-elicited protection [60]. Therefore, vaccine policy planning from an international perspective is critical for a smooth transition to SARS-CoV-2 endemicity.

Modeling the introduction and spread of different SARS-CoV-2 variants in a population is challenging. At the very least, modeling these dynamics would require having separate compartments for all the disease states of all circulating variants, disproportionally increasing the complexity of our model. In our approach, we take advantage of the extensive immune escape of the Omicron VOC to natural and vaccine-elicited neutralization [29, 31, 32, 45, 47], and assume that the replacement of Delta VOC occures very quickly (i.e., basically instantaneously) in mid-January. This simplification is not too distant from reality; replacement of Delta and other predominant sublineages for Omicron took only a few weeks in several countries [61]. For the spread of Omicron, we use the same basic reproduction number as for Delta but instead consider most individuals previously immunized to have lost protection against

infection, i.e., they are moved to the susceptible pool (Methods for details). Thereby, we can capture the explosive spread of Omicron VOC without increasing the base transmissibility. We furthermore include that those people having received a booster vaccine maintain some protection against infection with Omicron, which, however, also wanes. These assumptions are consistent with a large Danish cohort of households, where the secondary attack rate among unvaccinated was slightly higher for Delta infections than for Omicron [47], and with extensive experimental and observational studies [32, 38, 62, 63]. Despite the approximation we did for the transition to the Omicron variant, the mid- and long-term dynamics of the Omicron VOC should be reflected well.

In our work, the level of mandatory NPIs dictates the minimum and maximum level of voluntary health-protective behavior that individuals may adapt. For each scenario, we assume one specific, static level of mandatory NPIs, which best resembles real-world observations on compulsory measures aiming to reduce the probability of contagion (i.e., mask-wearing mandates, immunity passports, meeting restrictions, among others) and testing policy (as described in Methods). However, this static level can lead to unrealistically high waves of incidence and ICU occupancy, which 1) have not been seen so far and 2) would undoubtedly trigger the implementation of additional restrictions to prevent a major collapse in the health system. Nonetheless, we decided to incorporate this static mandatory NPI level because it illustrates a worst-case trajectory of each scenario. Besides, due to *pandemic fatigue* [64], we would expect the effectiveness of interventions and thus the imposed change in health-protective behavior in the different mandatory NPI scenarios to decay over time.

In summary, the way governments approach a pandemic situation when vaccines are available will shape long-term transmission dynamics by influencing the magnitude of information-behavior feedback loops. We show that the latter play a major role during the transition from epidemicity to endemicity. Thus most importantly, the challenge for authorities is to find ways to engage individuals with vaccination programs and health-protective behavior without requiring high case numbers for that. Here, clear communication and trust continues to be essential [65].

4 METHODS

4.1 Model Overview

We use an age-stratified compartmental model with compartments for susceptible-exposed-infected-recovered (SEIR) as well as for fatalities (D), receiving treatment in an ICU (ICU), and vaccination (first time and booster vaccines) (V) (**Supplementary Figure S1**). We also include waning immunity and seasonality effects (**Figures 4**, **5B**). To account for behavioral change induced by perceived risk of infection, we include a feedback loop between ICU occupancy, voluntary health-protective behavior and willingness to receive vaccination (**Figure 2** and **Supplementary Material**). Explicitly, we assume

that increases in ICU occupancy 1) decrease the contact rates among the population and thus the spreading rate of COVID-19 [4–7], and 2) increase vaccine acceptance among hesitant individuals [4, 8]. For the first feedback loop (voluntary health protective behavior), we assume that individuals adapt their contacts in different contexts depending on the risk they have perceived recently. The level of potentially contagious contacts is multiplied by a factor k that decreases with ICU occupancy between the minimum and maximum allowed by current mandatory NPIs (**Figure 2C**). Regarding the second feedback loop (related to vaccine uptake), we assume that a fraction of the population will always accept a vaccination offer, despite current ICU occupancy. From this minimum onward, vaccination willingness monotonically increases with ICU occupancy and saturates towards a maximum, accounting for a fraction of the population that will never accept the vaccine (**Figure 2E**). This means that we assume that there is a fraction in the population that is certainly not able or willing to be vaccinated. Given a fraction of people willing to be vaccinated, we determine the speed of the vaccination program using a linearly increasing function (**Figure 2F**). We model these two feedback loops to act on different timescales, as individuals can, e.g., decrease the number of contacts and contact intensity on a daily basis, while getting vaccinated takes longer. To capture this, we explicitly include memory kernels accounting for how individuals subjectively weigh events happening on different timescales when forming their perception of risk [21].

4.2 Memory on Perceived Risk
We assume that perceived risk regarding the disease depends on information about ICU occupancy that reaches individuals via media or affected social contacts. This perception of risk builds over time; people are not only aware of the occupancy numbers at the present moment but also of those in the recent past. To incorporate this into our model, we calculate the convolution of the ICU occupancy with a Gamma distribution (**Supplementary Figure S2**, Supplementary Information), effectively "weighting" the ICU occupancy numbers with their recency into a variable of risk perception which we call H_R. As a result, ICU occupancy numbers from a few days ago weigh more in people's memory and thus influence voluntary health-protective behavior at the present moment more than ICU occupancy that lies further in the past. We use this concept of ICU occupancy "with memory" to design the functions of the feedback loops (**Figures 2B,C,E,F**). The effect of the parameters chosen for the Gamma distribution on the model results as well as of all other model parameters is quantified in the sensitivity analysis, **Supplementary Section S4**, Supplementary Information.

4.3 NPI- and Risk-Induced Change in Health-Protective Behavior
When analyzing the joint effect of mandatory NPIs and voluntary measures to mitigate the spread of COVID-19, we find a strong overlap between them; mandatory NPIs limit the range of the measures that individuals could voluntarily take to protect themselves and their loved ones. For example, when large

private gatherings are officially forbidden, individuals cannot voluntarily choose not to meet. Additionally, when the engagement of the population in voluntary protective measures is very large, certain mandatory NPIs would not be required. We model the combined effect of mandatory NPIs and voluntary adoption of health-protective behavior as a function $k_{\text{NPI, self}}(H_R)$. Using the baseline of mandatory NPIs as an input, this function calculates the level of voluntary preventive action in dependence of the perceived risk H_R. To be precise, the value of $k_{\text{NPI, self}}(H_R) \in [0, 1]$ represents the level to which (potentially contagious) contacts of an average individual are reduced (**Figure 2C**), a factor that is multiplied onto the entries of a contact matrix separated by contexts (**Supplementary Figure S3**, Supplementary Information). For example, adaption of voluntary mask-wearing or a direct reduction of gatherings decreases the level of potentially contagious contacts and, thereby, $k_{\text{NPI, self}}(H_R)$. Furthermore, we distinguish between contacts made at home, in schools, in workplaces or during communal activities. We weight all the interactions with different $k_{\text{NPI,self}}^{\nu}(H_R)$ with $\nu \in \{$Households, Schools, Workplaces, Communities$\}$ that act on contextual contact matrices C_{ij}^{ν}, see **Supplementary Section S1.2** and **Figure 1**.

Inspired by the COSMO survey data [4] (**Figure 2B**), we suggest the following shape for $k_{\text{NPI,self}}^{\nu}(H_R)$: The level of (potentially) contagious contacts decreases linearly upon increases in the ICU-mediated perception of risk H_R below a threshold $H_R = H_{\max}$, from which point on no further reduction is possible (**Figure 2C**). This might represent 1) a fraction of the population agnostic to measures or unwilling to comply, or 2) limitations of voluntary preventive action imposed by practical constraints related to the current level of imposed restrictions, for example, having to make contacts in one's own household or having to go to work or school. We implement $k_{\text{NPI,self}}^{\nu}(H_R)$ as a softplus function, having a differentiable transition at $H_{\max}$. Each function (for each scenario) is defined by 3 parameters $H_{\max}$, $k_{\text{NPI,self}}^{\nu}(H_R = 0)$, and $k_{\text{NPI,self}}^{\nu}(H_R = H_{\max})$. $H_{\max} = 37$ is obtained by the fit to the COSMO data shown in **Figure 2** (black line) and used for the two other fits shown in **Figure 2** (red and yellow lines) as well as for the behavior parametrizations for the different scenarios (**Supplementary Figure S3**, Supplementary Information).

4.4 Different Mandatory NPI Scenarios
We choose to simulate five different scenarios, each having a different level of overall stringency. In the following we briefly describe the scenarios:

Scenario 1 ("Freedom day"): All mandatory restrictions are lifted, resulting in a factor of $k_{\text{NPI,self}}^{\nu}(H_R = 0) = 1 \,\forall \nu$. However, if ICU occupancy increases, we leave room for individuals' voluntary action based on perceived risk to reduce viral transmission: $k_{\text{NPI,self}}^{\nu}(H_R > 0) < 1$. We assume that communal activities and workplaces leave more room for voluntary preventive action than households and schools because of the possibility of working from home, avoiding non-essential gatherings etc. This difference is depicted in **Supplementary Figure S3**.

TABLE 1 | Different scenarios of mandatory NPIs. Listed are descriptions of the general measures imposed in each scenario as well as the input parameters to the function $k_{\mathrm{NPI,self}}^{\gamma}(H_R)$ that modulates the spread. The parameters act as multiplicative factors onto infection terms in our model, thus high parameter values (close to 1) translate to little reduction in infections and low parameters (close to 0) translate to strong reductions in infections. For each cell, the first parameter translates to a reduction at high ICUs ($k_{\mathrm{NPI,self}}^{\gamma}(H_R = H_{\max})$) and the second parameter to the corresponding reduction at empty ICUs ($k_{\mathrm{NPI,self}}^{\gamma}(H_R = 0)$), between which we linearly interpolate (**Supplementary Figure S3**).

Sc.	Name	Description of measures	$k^{\mathrm{Households}}$	k^{Schools}	$k^{\mathrm{Workplaces}}$	$k^{\mathrm{Communities}}$
1	"freedom day"	no mandatory measures	0.8–1	0.8–1	0.6–1	0.6–1
2	moderate NPIs A	increased stringency affecting risk of transmission in schools	0.8–1	0.25–0.5	0.5–0.9	0.5–0.9
3	moderate NPIs B	mild NPIs + reduction of transmission at workplaces	0.8–1	0.25–0.5	0.25–0.5	0.5–0.9
4	moderate NPIs C	moderate NPIs + enforcement of restrictions in communal activities	0.8–1	0.1–0.25	0.25–0.5	0.25–0.5
5	strong NPIs	strong NPIs + further restrictions wherever possible	0.8–1	0.1–0.25	0.25–0.5	0.1–0.2

Scenario 2 (Moderate NPIs A): Easy-to-follow measures are kept in place and potentially contagious contacts at school are reduced to $k_{\mathrm{NPI,self}}^{\mathrm{School}}(H_R = 0) = 0.5$.

Scenario 3 (Moderate NPIs B): Further measures at work (e.g., home office or testing) reduce $k_{\mathrm{NPI,self}}^{\mathrm{Workplaces}}(H_R = 0) = 0.5$.

Scenario 4 (Moderate NPIs C): Further reduction in potentially contagious school contacts and restrictions affecting communal contacts reduce $k_{\mathrm{NPI,self}}^{\mathrm{School}}(H_R = 0) = 0.25$ and $k_{\mathrm{NPI,self}}^{\mathrm{Communities}}(H_R = 0) = 0.5$.

Scenario 5 (Strong NPIs): Communal activities are further reduced to $k_{\mathrm{NPI,self}}^{\mathrm{Communities}}(H_R = 0) = 0.2$.

Table 1 lists all values for the different scenarios and contexts of interaction between individuals. The reduction of household contacts is assumed to remain the same for all scenarios. Note that, as the stringency of measures increases, room for voluntary adoption of health-protective behavior usually decreases: To give an example, without mandatory measures the level of contact reduction in communal activities lies in the range 1–0.6, whereas in a scenario with strong mandatory NPIs it lies in the range 0.2–0.1. The difference between the two bounds effectively measures the room for voluntary actions (0.4 for freedom day vs. 0.1 for strong NPIs). An exception are school contacts in which moderate restriction scenarios (2 and 3) display a wider range of possible voluntary action than the freedom day scenario. As health-protective behavior among children could be encouraged but not imposed, their adherence to rules constitutes a voluntary act.

4.5 Modeling the Introduction and Spread of the Omicron VOC

Modeling the introduction and spread of the Omicron VOC requires modifications to the model compartments, transition rates, and parameters. In particular, these modifications allow us to explore the effects of Omicron's 1) extensive immune escape and 2) potential reduced risk for severe course of the disease. We implemented the introduction of Omicron VOC as a total replacement of the previously dominating Delta VOC on 15 Jan 2022. At that moment, we rearrange the distribution of individuals between the "waned" and "immune" compartments, increase the rate of waning immunity to account for Omicron's immune escape, and

reduce the probability of having a severe course. Explicitly, before the introduction of the Omicron VOC, the immune population is tracked in additional pseudo-compartments V^o, R^o, $R^{v,o}$ with a faster waning rate. In that way, there are always less individuals in V^o, R^o, $R^{v,o}$ than in V, R, R^v. At the time of variant replacement, $V - V^o$, $R - R^o$, $R^v - R^{v,o}$ individuals are moved from the vaccinated and recovered compartments to the respective waned compartments; individuals previously protected against Delta would now be susceptible to Omicron. We model booster-vaccination protection against infection following a leaky scheme, thus boostered individuals have a probability of η of being entirely protected. With probability $1 - \eta$, individuals remain in their current compartment but are tracked as if the vaccine had worked successfully.

DATA AVAILABILITY STATEMENT

The original contributions presented in the study are included in the article/**Supplementary Material**. Source code for data generation and analysis is available online on GitHub https://github.com/Priesemann-Group/covid19_infoXpand_feedbackloop. Further inquiries can be directed to the corresponding author.

AUTHOR CONTRIBUTIONS

Conceptualization: PD, JW, SC, SB, JD, VP. Methodology: PD, JW, SC, SB, SM, EI, VP. Software: PD, JW. Formal analysis: PD, JW, SC, SB. Writing—Original Draft: all authors. Writing—Review and Editing: all authors. Visualization: PD, JW, SC. Supervision: SC, MK, MM, KN, AC, VP.

FUNDING

ACKNOWLEDGMENTS

SUPPLEMENTARY MATERIAL

The Supplementary Material for this article can be found online at: https://www.frontiersin.org/articles/10.3389/fphy.2022.842180/full#supplementary-material

REFERENCES

1. Casero-Ripolles A. Impact of COVID-19 on the media System. Communicative and Democratic Consequences of News Consumption during the Outbreak. *Epi* (2020) 29. doi:10.3145/epi.2020.mar.23

2. Kim HK, Ahn J, Atkinson L, Kahlor LA. Effects of COVID-19 Misinformation on Information Seeking, Avoidance, and Processing: A Multicountry Comparative Study. *Sci Commun* (2020) 42:586–615. doi:10.1177/1075547020959670

3. Ferrer RA, Klein WM. Risk Perceptions and Health Behavior. *Curr Opin Psychol* (2015) 5:85–9. doi:10.1016/j.copsyc.2015.03.012

4. Betsch C, Wieler LH, Habersaat K. Monitoring Behavioural Insights Related to Covid-19. *The Lancet* (2020) 395:1255–6. doi:10.1016/s0140-6736(20)30729-7

5. Imbriano G, Larsen EM, Mackin DM, An AK, Luhmann CC, Mohanty A, et al. Online Survey of the Impact of Covid-19 Risk and Cost Estimates on Worry and Health Behavior Compliance in Young Adults. *Front Public Health* (2021) 9:157. doi:10.3389/fpubh.2021.612725

6. Perrotta D, Grow A, Rampazzo F, Cimentada J, Del Fava E, Gil-Clavel S, et al. Behaviours and Attitudes in Response to the Covid-19 Pandemic: Insights from a Cross-National Facebook Survey. *EPJ Data Sci* (2021) 10:17–3. doi:10.1140/epjds/s13688-021-00270-1

7. Druckman JN, Klar S, Krupnikov Y, Levendusky M, Ryan JB. Affective Polarization, Local Contexts and Public Opinion in america. *Nat Hum Behav* (2021) 5:28–38. doi:10.1038/s41562-020-01012-5

8. Salali GD, Uysal MS. Effective Incentives for Increasing Covid-19 Vaccine Uptake. *Psychol Med* (2021) 1–3. doi:10.1017/s0033291721004013

9. Gavenčiak T, Monrad JT, Leech G, Sharma M, Mindermann S, Brauner JM, et al. Seasonal Variation in Sars-Cov-2 Transmission in Temperate Climates. *medRxiv* (2021). doi:10.1101/2021.06.10.21258647

10. Moriyama M, Hugentobler WJ, Iwasaki A. Seasonality of Respiratory Viral Infections. *Annu Rev Virol* (2020) 7:83–101. doi:10.1146/annurev-virology-012420-022445

11. Sajadi MM, Habibzadeh P, Vintzileos A, Shokouhi S, Miralles-Wilhelm F, Amoroso A. Temperature and Latitude Analysis to Predict Potential Spread and Seasonality for COVID-19. Available at SSRN 3550308 (2020).

12. Mistry D, Litvinova M, y Piontti AP, Chinazzi M, Fumanelli L, Gomes MF, et al. Inferring High-Resolution Human Mixing Patterns for Disease Modeling. *Nat Commun* (2021) 12:1–12. doi:10.1038/s41467-020-20544-y

13. Olivieri A, Palù G, Sebastiani G. Covid-19 Cumulative Incidence, Intensive Care, and Mortality in Italian Regions Compared to Selected European Countries. *Int J Infect Dis* (2021) 102:363–8. doi:10.1016/j.ijid.2020.10.070

14. Bravata DM, Perkins AJ, Myers LJ, Arling G, Zhang Y, Zillich AJ, et al. Association of Intensive Care Unit Patient Load and Demand with Mortality Rates in Us Department of Veterans Affairs Hospitals during the Covid-19 Pandemic. *JAMA Netw Open* (2021) 4:e2034266. doi:10.1001/jamanetworkopen.2020.34266

15. Linden M, Mohr SB, Dehning J, Mohring J, Meyer-Hermann M, Pigeot I, et al. Case Numbers beyond Contact Tracing Capacity Are Endangering the Containment of COVID-19. *Dtsch Arztebl Int* (2020) 117:790–1. doi:10.3238/arztebl.2020.0790

16. Epstein JM, Parker J, Cummings D, Hammond RA. Coupled Contagion Dynamics of Fear and Disease: Mathematical and Computational Explorations. *PLoS One* (2008) 3:e3955. doi:10.1371/journal.pone.0003955

17. Epstein JM, Hatna E, Crodelle J. Triple Contagion: a Two-Fears Epidemic Model. *J R Soc Interf* (2021) 18:20210186. doi:10.1098/rsif.2021.0186

18. Bauch CT. Imitation Dynamics Predict Vaccinating Behaviour. *Proc R Soc B* (2005) 272:1669–75. doi:10.1098/rspb.2005.3153

19. d'Onofrio A, Manfredi P. Information-related Changes in Contact Patterns May Trigger Oscillations in the Endemic Prevalence of Infectious Diseases. *J Theor Biol* (2009) 256:473–8.

20. d'Onofrio A, Manfredi P, Salinelli E. Vaccinating Behaviour, Information, and the Dynamics of Sir Vaccine Preventable Diseases. *Theor Popul Biol* (2007) 71:301–17.

21. Zauberman G, Kim BK, Malkoc SA, Bettman JR. Discounting Time and Time Discounting: Subjective Time Perception and Intertemporal Preferences. *J Marketing Res* (2009) 46:543–56. doi:10.1509/jmkr.46.4.543

22. Bauch CT, Bhattacharyya S. Evolutionary Game Theory and Social Learning Can Determine How Vaccine Scares Unfold. *Plos Comput Biol* (2012) 8: e1002452. doi:10.1371/journal.pcbi.1002452

23. Tkachenko AV, Maslov S, Wang T, Elbana A, Wong GN, Goldenfeld N. Stochastic Social Behavior Coupled to Covid-19 Dynamics Leads to Waves, Plateaus, and an Endemic State. *eLife* (2021) 10:e68341. doi:10.7554/eLife.68341

24. Dankulov MM, Tadic B, Melnik R. Worldwide Clustering and Infection Cycles as Universal Features of Multiscale Stochastic Processes in the Sars-Cov-2 Pandemic. *medRxiv* (2021). doi:10.1101/2021.12.20.21268095

25. Bauer S, Contreras S, Dehning J, Linden M, Iftekhar E, Mohr SB, et al. Relaxing Restrictions at the Pace of Vaccination Increases freedom and Guards against Further Covid-19 Waves. *Plos Comput Biol* (2021) 17:e1009288. doi:10.1371/journal.pcbi.1009288

26. Brown EL, Essigmann HT. Original Antigenic Sin: the Downside of Immunological Memory and Implications for Covid-19. *Msphere* (2021) 6: e00056-21. doi:10.1128/mSphere.00056-21

27. Gomez GB, Mahé C, Chaves SS. Uncertain Effects of the Pandemic on Respiratory Viruses. *Science* (2021) 372:1043–4. doi:10.1126/science.abh3986

28. Sanz-Muñoz I, Tamames-Gómez S, Castrodeza-Sanz J, Eiros-Bouza JM, de Lejarazu-Leonardo RO. Social Distancing, Lockdown and the Wide Use of Mask; a Magic Solution or a Double-Edged Sword for Respiratory Viruses Epidemiology? *Vaccines* (2021) 9:595. doi:10.3390/vaccines9060595

29. Viana R, Moyo S, Amoako DG, Tegally H, Scheepers C, Lessells RJ, et al. Rapid Epidemic Expansion of the Sars-Cov-2 Omicron Variant in Southern Africa. *Nature* (2021). doi:10.1038/d41586-021-03832-5

30. Pulliam JR, van Schalkwyk C, Govender N, von Gottberg A, Cohen C, Groome MJ, et al. Increased Risk of Sars-Cov-2 Reinfection Associated with Emergence of the Omicron Variant in south africa. *medRxiv* (2021). doi:10.1101/2021.11.11.21266068

31. Ferguson N, Ghani A, Cori A, Hogan A, Hinsley W, Volz E. Report 49: Growth, Population Distribution and Immune Escape of the Omicron in england. *Imperial College London* (2021). doi:10.25561/93038

32. Cele S, Jackson L, Khoury DS, Khan K, Moyo-Gwete T, Tegally H, et al. Omicron Extensively but Incompletely Escapes Pfizer Bnt162b2 Neutralization. *Nature* (2021). doi:10.1038/s41586-021-04387-1

33. Wilhelm A, Widera M, Grikscheit K, Toptan T, Schenk B, Pallas C, et al. Reduced Neutralization of Sars-Cov-2 Omicron Variant by Vaccine Sera and Monoclonal Antibodies. *medRxiv* (2021). doi:10.1101/2021.12.07.21267432

34. Cameroni E, Bowen JE, Rosen LE, Saliba C, Zepeda SK, Culap K, et al. Broadly Neutralizing Antibodies Overcome Sars-Cov-2 Omicron Antigenic Shift. *Nature* (2021) 1–9. doi:10.1038/s41586-021-04386-2

35. Roessler A, Riepler L, Bante D, von Laer D, Kimpel J. Sars-cov-2 B. 1.1. 529 Variant (Omicron) Evades Neutralization by Sera from Vaccinated and Convalescent Individuals. *medRxiv* (2021). doi:10.1101/2021.12.08.21267491

36. Hoffmann M, Krüger N, Schulz S, Cossmann A, Rocha C, Kempf A, et al. The Omicron Variant Is Highly Resistant against Antibody-Mediated Neutralization–Implications for Control of the Covid-19 Pandemic. *Cell* (2021). doi:10.1016/j.cell.2021.12.032

37. Gardner BJ, Kilpatrick AM. Estimates of Reduced Vaccine Effectiveness against Hospitalization, Infection, Transmission and Symptomatic Disease of a New Sars-Cov-2 Variant, Omicron (B. 1.1. 529), Using Neutralizing Antibody Titers. *medRxiv* (2021). doi:10.1101/2021.12.10.21267594

38. Pérez-Then E, Lucas C, Monteiro VS, Miric M, Brache V, Cochon L, et al. Immunogenicity of Heterologous Bnt162b2 Booster in Fully Vaccinated Individuals with Coronavac against Sars-Cov-2 Variants delta and Omicron: The dominican republic Experience. *medRxiv* (2021). doi:10.1101/2021.12.27.21268459

39. Gruell H, Vanshylla K, Tober-Lau P, Hillus D, Schommers P, Lehmann C, et al. Mrna Booster Immunization Elicits Potent Neutralizing Serum Activity against the Sars-Cov-2 Omicron Variant. *Nat. Med.* (2022). doi:10.1038/s41591-021-01676-0

40. Kuhlmann C, Mayer CK, Claassen M, Maponga TG, Sutherland AD, Suliman T, et al. Breakthrough Infections with Sars-Cov-2 Omicron Variant Despite Booster Dose of Mrna Vaccine. Available at SSRN 3981711 (2021).

41. Nemet I, Kliker L, Lustig Y, Zuckerman N, Erster O, Cohen C, et al. Third Bnt162b2 Vaccination Neutralization of SARS-CoV-2 Omicron Infection. *New Engl J Med* (2021). doi:10.1056/nejmc2119358

42. Basile K, Rockett RJ, McPhie K, Fennell M, Johnson-Mackinnon J, Agius J, et al. Improved Neutralization of the Sars-Cov-2 Omicron Variant after Pfizer-Biontech Bnt162b2 Covid-19 Vaccine Boosting. *bioRxiv* (2021). doi:10.1101/2021.12.12.472252

43. Garcia-Beltran WF, St Denis KJ, Hoelzemer A, Lam EC, Nitido AD, Sheehan ML, et al. mRNA-based COVID-19 Vaccine Boosters Induce Neutralizing Immunity Against SARS-CoV-2 Omicron Variant. *Cell* (2022). doi:10.1016/j.cell.2021.12.033

44. Andrews N, Stowe J, Kirsebom F, Toffa S, Rickeard T, Gallagher E, et al. Effectiveness of Covid-19 Vaccines against the Omicron (B. 1.1. 529) Variant of Concern. *medRxiv* (2021). doi:10.1101/2021.12.14.21267615

45. Torjesen I. Covid Restrictions Tighten as Omicron Cases Double Every Two to Three Days. *BMJ* (2021) 375. doi:10.1136/bmj.n3051

46. Barnard RC, Davies NG, Pearson CA, Jit M, John W, Edmunds WJ. Projected epidemiological consequences of the Omicron SARS-CoV-2 variant in England. *medRxiv* (2021). doi:10.1101/2021.12.15.21267858

47. Lyngse FP, Mortensen LH, Denwood MJ, Christiansen LE, Møller CH, Skov RL, et al. Sars-cov-2 Omicron Voc Transmission in Danish Households. *medRxiv* (2021). doi:10.1101/2021.12.27.21268278

48. Contreras S, Dehning J, Mohr SB, Bauer S, Spitzner FP, Priesemann V. Low Case Numbers Enable Long-Term Stable Pandemic Control without Lockdowns. *Sci Adv* (2021) 7:eabg2243. doi:10.1126/sciadv.abg2243

49. Oliu-Barton M, Pradelski BSR, Aghion P, Artus P, Kickbusch I, Lazarus JV, et al. SARS-CoV-2 Elimination, Not Mitigation, Creates Best Outcomes for Health, the Economy, and Civil Liberties. *The Lancet* (2021) 397:2234–6. doi:10.1016/s0140-6736(21)00978-8

50. Czypionka T, Iftekhar EN, Prainsack B, Priesemann V, Bauer S, Calero Valdez A, et al. The Benefits, Costs and Feasibility of a Low Incidence Covid-19 Strategy. *The Lancet Reg Health - Europe* (2022) 13:100294. doi:10.1016/j.lanepe.2021.100294

51. Funk S, Salathé M, Jansen VAA. Modelling the Influence of Human Behaviour on the Spread of Infectious Diseases: a Review. *J R Soc Interf* (2010) 7:1247–56. doi:10.1098/rsif.2010.0142

52. Verelst F, Willem L, Beutels P. Behavioural Change Models for Infectious Disease Transmission: a Systematic Review (2010-2015). *J R Soc Interf* (2016) 13:20160820. doi:10.1098/rsif.2016.0820

53. Weston D, Hauck K, Amlôt R. Infection Prevention Behaviour and Infectious Disease Modelling: a Review of the Literature and Recommendations for the Future. *BMC public health* (2018) 18:336–16. doi:10.1186/s12889-018-5223-1

54. Bedson J, Skrip LA, Pedi D, Abramowitz S, Carter S, Jalloh MF, et al. A Review and Agenda for Integrated Disease Models Including Social and Behavioural Factors. *Nat Hum Behav* (2021) 1–13. doi:10.1038/s41562-021-01136-2

55. Buonomo B, Della Marca R. Effects of Information-Induced Behavioural Changes during the Covid-19 Lockdowns: the Case of italy. *R Soc Open Sci* (2020) 7:201635. doi:10.1098/rsos.201635

56. Priesemann V, Balling R, Bauer S, Beutels P, Valdez AC, Cuschieri S, et al. Towards a European Strategy to Address the Covid-19 Pandemic. *The Lancet* (2021) 398:838–9. doi:10.1016/s0140-6736(21)01808-0

57. Cinelli M, Quattrociocchi W, Galeazzi A, Valensise CM, Brugnoli E, Schmidt AL, et al. The Covid-19 Social media Infodemic. *Sci Rep* (2020) 10:16598–10. doi:10.1038/s41598-020-73510-5

58. Banerjee D, Meena K. Covid-19 as an "Infodemic" in Public Health: Critical Role of the Social media. *Front Public Health* (2021) 9:231. doi:10.3389/fpubh.2021.610623

59. Contreras S, Olivera-Nappa Á, Priesemann V. Rethinking Covid-19 Vaccine Allocation: it Is Time to Care about Our Neighbours. *The Lancet Reg Health–Europe* (2022) 12, 100277. doi:10.1016/j.lanepe.2021.100277

60. Thompson RN, Hill EM, Gog JR. SARS-CoV-2 Incidence and Vaccine Escape. *Lancet Infect Dis* (2021) 21:913–4. doi:10.1016/s1473-3099(21)00202-4

61. Ritchie H, Mathieu E, Rodés-Guirao L, Appel C, Giattino C, Ortiz-Ospina E, et al. *Coronavirus Pandemic (Covid-19)*. Our World in Data (2020). Available at: Https://ourworldindata.org/coronavirus.

62. Viana J, van Dorp CH, Nunes A, Gomes MC, van Boven M, Kretzschmar ME, et al. Controlling the Pandemic during the SARS-CoV-2 Vaccination Rollout. *Nat Commun* (2021) 12:3674–15. doi:10.1038/s41467-021-23938-8

63. Lu L, Mok BW-Y, Chen L-L, Chan JM-C, Tsang OT-Y, Lam BH-S, et al. Neutralization of SARS-CoV-2 Omicron Variant by Sera from BNT162b2 or Coronavac Vaccine Recipients. *Clinical Infectious Diseases* (2021). doi:10.1093/cid/ciab1041

64. Petherick A, Goldszmidt R, Andrade EB, Furst R, Hale T, Pott A, et al. A Worldwide Assessment of Changes in Adherence to Covid-19 Protective Behaviours and Hypothesized Pandemic Fatigue. *Nat Hum Behav* (2021) 5:1145–60. doi:10.1038/s41562-021-01181-x

65. Iftekhar EN, Priesemann V, Balling R, Bauer S, Beutels P, Calero Valdez A, et al. A Look into the Future of the COVID-19 Pandemic in Europe: an Expert Consultation. *Lancet Reg Health - Europe* (2021) 8:100185. doi:10.1016/j.lanepe.2021.100185

6

IMPACT OF THE EURO 2020 CHAMPIONSHIP ON THE SPREAD OF COVID-19

This chapter is identical to the article [26]. The Supplementary Information can be found in Appendix D. The article is published in

Dehning, J., Mohr, S.B., Contreras, S., Dönges, P., Iftekhar, E.N., Schulz, O., Bechtle, P., Priesemann, V. 2023, Impact of the Euro 2020 championship on the spread of COVID-19, Nature Communications, 14 (2023)

under the terms of a Creative Common License (http://creativecommons.org/licenses/by/4.0/).

Roles: Visualisation, Writing – original draft, Writing – review & editing.

Impact of the Euro 2020 championship on the spread of COVID-19

Jonas Dehning [1,6], Sebastian B. Mohr [1,6], Sebastian Contreras [1], Philipp Dönges [1], Emil N. Iftekhar [1], Oliver Schulz [2], Philip Bechtle [3] & Viola Priesemann [1,4,5]

Large-scale events like the UEFA Euro 2020 football (soccer) championship offer a unique opportunity to quantify the impact of gatherings on the spread of COVID-19, as the number and dates of matches played by participating countries resembles a randomized study. Using Bayesian modeling and the gender imbalance in COVID-19 data, we attribute 840,000 (95% CI: [0.39M, 1.26M]) COVID-19 cases across 12 countries to the championship. The impact depends non-linearly on the initial incidence, the reproduction number R, and the number of matches played. The strongest effects are seen in Scotland and England, where as much as 10,000 primary cases per million inhabitants occur from championship-related gatherings. The average match-induced increase in R was 0.46 [0.18, 0.75] on match days, but important matches caused an increase as large as +3. Altogether, our results provide quantitative insights that help judge and mitigate the impact of large-scale events on pandemic spread.

Passion for competitive team sports is widespread worldwide. However, the tradition of watching and celebrating popular matches together may pose a danger to coronavirus disease 2019 (COVID-19) mitigation, especially in large gatherings and crowded indoor settings (see, e.g., refs. [1–6]). Interestingly, sports events taking place under substantial contact restrictions had only a minor effect on COVID-19 transmission[7–11]. However, large events with massive media coverage, stadium attendance, increased travel, and viewing parties can play a major role in the spread of COVID-19—especially if taking place in settings with few COVID-19-related restrictions. This was the case for the UEFA Euro 2020 Football Championship (Euro 2020 in short), staged from June 11 to July 11, 2021. While stadium attendance might only have a minor effect[12–14], it increases TV viewer engagement[15–17], and encourages additional social gatherings[18]. These phenomena and previous observational analyses[19] suggest that the Euro 2020's impact may have been considerable. Therefore, we used this championship as a case study to quantify the impact of large events on the spread of

COVID-19. Counting with quantitative insights on the impact of these events allows policymakers to determine the set of interventions required to mitigate it.

Two facts make the Euro 2020 especially suitable for the quantification. First, the Euro 2020 resembles a randomized study across countries: The time-points of the matches in a country do not depend on the state of the pandemic in that country and how far a team advances in the championship has a random component as well[20]. This independence between the time-points of the match and the COVID-19 incidence allows quantifying the effect of football-related social gatherings without classical biasing effects. This is advantageous compared to classical inference studies quantifying the impact of non-pharmaceutical interventions (NPIs) on COVID-19 where implementing NPIs is a typical reaction to growing case numbers[21–23]. Second, the attendance at match-related events, and thus the cases associated with each match, is expected to show a gender imbalance[24]. This was confirmed by news outlets and early studies[25–28]. Hence, the gender

[1]Max Planck Institute for Dynamics and Self-Organization, Am Faßberg 17, 37077 Göttingen, Germany. [2]Max Planck Institute for Physics, Föhringer Ring 6, 80805 München, Germany. [3]Physikalisches Institut, Universität Bonn, Nußallee 12, 53115 Bonn, Germany. [4]Institute for the Dynamics of Complex Systems, University of Göttingen, Friedrich-Hund-Platz 1, 37077 Göttingen, Germany. [5]Institute of Computer Science and Campus Institute Data Science, University of Göttingen, Goldschmidtstraße 7, 24118 Göttingen, Germany. [6]These authors contributed equally: Jonas Dehning, Sebastian B. Mohr. ✉e-mail: bechtle@physik.uni-bonn.de; viola.priesemann@ds.mpg.de

imbalance presents a unique opportunity to disentangle the impact of the matches from other effects on pathogen transmission rates.

Here we build a Bayesian model to quantify the effect large-scale sports events on the spread of COVID-19, using the Euro 2020 as case study. In the following, we use "case" to refer to a confirmed case of a severe acute respiratory syndrome coronavirus 2 (SARS-CoV-2) infection in a human and "case numbers" to refer to the number of such cases. Not all infections are detected and represented in the cases and cases come with a delay after the actual infection. Our model simulates COVID-19 spread in each country using a discrete renewal process[22,29] for each gender separately, such that the effect of matches can be assessed through the gender imbalance in case numbers. This is defined as "(male incidence – female incidence)/total incidence", and through the temporal association of cases to match dates of the countries' teams. Regarding the expected gender imbalance at football-related gatherings, we chose a prior value of 33% (95% percentiles [18%, 51%]) female participants, which is more balanced than the values reported for national leagues (about 20%)[24]. However, this agrees with the expected homogeneous and broad media attention of events like the Euro 2020. For the effective reproduction number R_{eff} we distinguish three additive contributions; the base, NPI-, and behavior-dependent reproduction number R_{base}, a match-induced boost on it $\Delta R_{football}$, and a noise term ΔR_{noise}, such that $R_{eff} = R_{base} + \Delta R_{football} + \Delta R_{noise}$. We assume R_{base} to vary smoothly over time, while the effect of single matches $\Delta R_{football}$ is concentrated on one day and allows for a gender imbalance. The term ΔR_{noise} allows the model to vary the relative reproduction number for each gender independent of the football events smoothly over time. We analyzed data from all participating countries in the Euro 2020 that publish daily gender-resolved case numbers ($n = 12$): England, the Czech Republic, Italy, Scotland, Spain, Germany, France, Slovakia, Austria, Belgium, Portugal, and the Netherlands (ordered by resulting effect size). We retrieved datasets directly from governmental institutions or the

COVerAGE-DB[30]. See Supplementary Section S1 for a list of data sources. Our analyses were carried out following FAIR[31] principles; all code, including generated datasets, are publicly available (https://github.com/Priesemann-Group/covid19_soccer).

Results

The main impact arises from the subsequent infection chains

We quantified the impact of the Euro 2020 matches on the reproduction number for the 12 analyzed countries (Fig. 1a) and for every single match (Supplementary Fig. S8). On average, a match increases the reproduction number R by 0.46 (95% CI [0.18, 0.75]) (Fig. 1a and Supplementary Table S4) for a single day. In other words, when a country participated in a match of the Euro 2020 championship, every individual of the country infected on average ΔR_{match} extra persons (see Supplementary Section S2 for more details). The cases resulting from these infections occurring at gatherings on the match days are referred to as primary cases.

However, primary cases are only the tip of the iceberg; any of these cases can initiate a new infection chain, potentially spreading for weeks (see Supplementary Section S2 for more details). We included all subsequent cases until July 31, which is about two weeks after the final. As expected, subsequent cases outnumber the primary cases considerably at a ratio of about 4:1 on average (Supplementary Table S3). As a consequence, on average, only 3.2% [1.3%, 5.2%] of new cases are directly associated with the match-related social gatherings throughout that analysis period (Fig. 1b). This surge of subsequent cases highlights the long-lasting impact of potential single events on the COVID-19 spread (see Supplementary Table S2).

We find an increase in COVID-19 spread at the Euro 2020 matches in all countries we analyzed, except for the Netherlands. In the Netherlands, a "freedom day" coincided with the analysis period[32] and was accompanied by the opposite gender imbalance compared to the football matches, thereby apparently inverted the football effect.
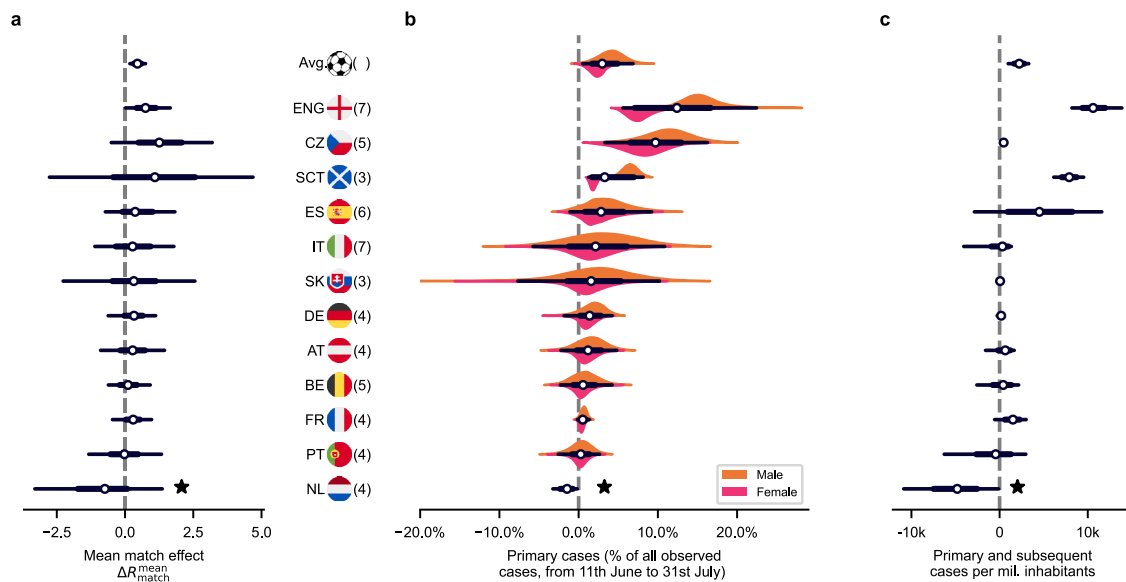
Fig. 1 | Quantifying the impact of the Euro 2020 on COVID-19 spread. a Using Bayesian inference and an SEIR-like model, we infer the mean increase on the reproduction number associated with Euro 2020 matches, ΔR_{match}^{mean}, in each analyzed country ($n = 12$ countries). Almost all countries show a median of the mean increase larger than zero (cf. Supplementary Table S4). Note that in the Netherlands (★) a complete lifting of restrictions was implemented on June 26 2021 ("freedom day"). Apparently, its impact also had the opposite gender imbalance, making it hard for the model to extract the Euro 2020's effect (Supplementary Fig. S31). **b** The ΔR_{match}^{mean} enables us to quantify the primary cases, i.e., cases associated directly with the match days (as percentage of all cases from June 11 to July 31 2021). **c** Any primary infection at a match can start an infection chain. The total number of primary and subsequent cases that were inferred to be causally related to the Euro 2020 from its start until 31 July depend on the COVID-19 prevalence and the base spread during the analysis period. In parentheses are the number of matches played by the respective team. White dots represent median values, black bars and whiskers correspond to the 68% and 95% credible intervals (CI), respectively, and the distributions in color (truncated at 99% CI) represent the differences by gender (Supplementary Table S2). The Netherlands is left out from the average calculations and subsequent analyses.
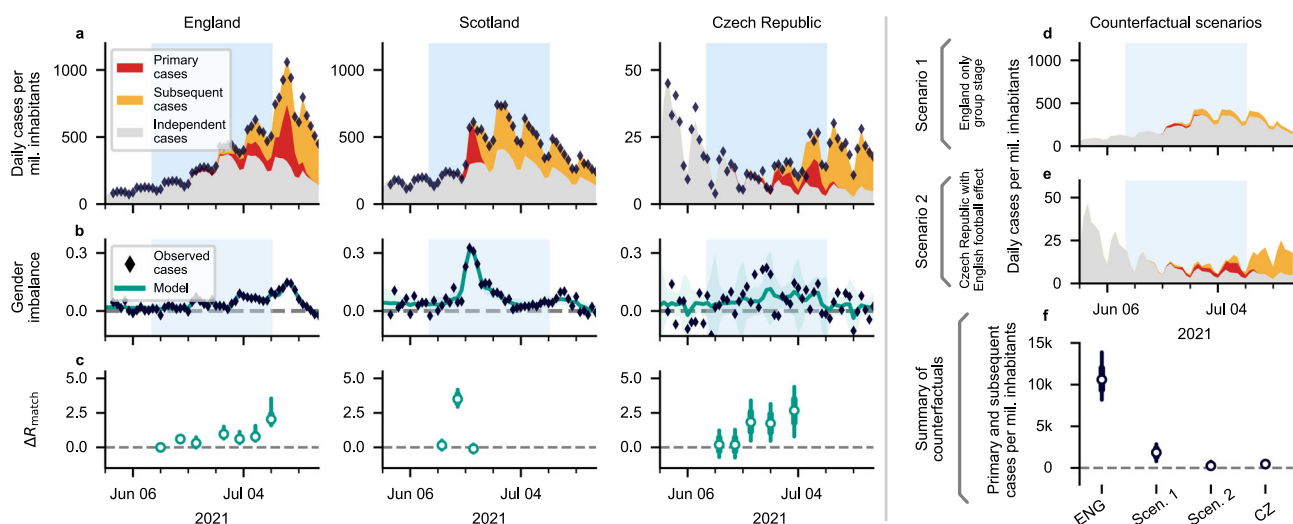
Fig. 2 | Example cases illustrate that the spread associated with the Euro 2020 can encompass a substantial fraction of the observed cases. a The model enables one to split the observed incidence (black diamonds) into: cases independent of Euro 2020 matches (gray area), primary cases (directly associated with Euro 2020 matches, red area), and subsequent cases (additional infection chains started by primary cases, orange area). See Supplementary Information for all countries (Supplementary Figs. S24–S36). Here and in all following figures, the light blue shaded area signifies the time span of the Euro 2020. **b** Football-related gatherings, and hence the case numbers, show a gender imbalance. This facilitates the inference of the football-related increase in COVID-19 spread. Here the turquoise shaded areas correspond to 95% CI. **c** The effect of social gatherings at match days is modeled as a single additive increase in the reproduction number

ΔR_{match} concentrated on the day of each match. For example, $\Delta R_{match} = 2$ means that, on the day of the match, each infected individual on average infected two additional persons (on top of the base trend). **d, e** The counterfactual scenario assumes that England would not have reached the knockout phase (**d**, Scen. 1), or that the Czech fans and matches would have been equal to the English (i.e., reaching the final, and Czech people doing the same football-related gatherings as the English by their impact on disease spread; **e**, Scen. 2). **f** In the counterfactual scenarios, the Euro 2020 would have had much smaller impact with fewer matches (Scen. 1), or with an overall more favorable pandemic situation as in the Czech Republic (Scen. 2). White dots represent median values, bars and whiskers correspond to the 68% and 95% credible intervals (CI).

Therefore, we exclude the Netherlands from general averages and correlation studies, but still display the results for completeness.

The primary and subsequent cases on average amounted to 2200 (95% CI [986, 3308]) cases per million inhabitants (Fig. 1c and Supplementary Table S2). This amounts to about 0.84 million (CI: [0.39M, 1.26M]) cases related to the Euro 2020 in the 12 countries (cf. Supplementary Table S3). With the case fatality risk of that period, this corresponds to about 1700 (CI: [762, 2470]) deaths, assuming that the primary and subsequent spread affects all ages equally. Most likely this is slightly overestimated since the age groups most at risk from COVID-19-related death are probably underrepresented in football-related social activities and thus more unlikely to be affected by primary championship-related infections. However, the overall number of primary and subsequent cases attributed to the championship is dominated by the subsequent cases, and the mixing of individuals of different age-groups then mitigates this bias. Individually, three countries, England, the Czech Republic, and Scotland showed a significant increase in COVID-19 incidence associated with the Euro 2020, and Spain and France show an increase at the one-sided 90% significance threshold. In other countries such as Germany, only a relatively small contribution of primary cases was associated with the Euro 2020 championship, and a small gender imbalance was observed. Low COVID-19 incidence during the championship or imprecise temporal association between infection and confirmation of it as a case can lead to a loss of sensitivity and hinder the detection of an effect, as can be seen from the large width of several posterior distributions (e.g., Italy and Slovakia, which had particularly low incidence).

**The strongest effect is observed in England and Scotland**
Overall, the effect of the Euro 2020 was quite diverse across the participating countries, ranging from almost no additional infections to up to 1% of the entire population being infected (i.e., from Portugal to England, Fig. 1). To illustrate this diversity, the comparison between England, Scotland, and the Czech Republic is particularly illustrative

(Fig. 2). For all countries, we disentangled the cases that are considered to happen independently of the Euro 2020 (Fig. 2a, gray), the primary cases directly associated with gatherings on the days of the matches (red), and the subsequent infection chains started by the primary cases (orange; see Supplementary Figs. S24–S36 for all countries).

England, being the runner-up of the championship and thus played the maximum number of matches, displays the strongest effect over the longest duration, with a substantial increase in reproduction number ΔR_{match} towards the last matches of the championship. This reflects the increasing popularity of the later matches, as e.g., quantified by the increase of the search term on Google (Supplementary Fig. S20). Scotland shows a particularly strong effect of a single match (Scotland vs England) staged in London during the group phase, with $\Delta R_{match} = 3.5$ [2.9, 4.2] (Fig. 2c). This means that on average over the total Scottish population, every single person infected additional 3.5 persons at or around that single day. These are very strong effects. As a consequence, in Scotland the subsequent cases from the single match accounted for about 30% of the cases in the following weeks, illustrating the impact of such gatherings on public health.

Low overall incidence prevents large match-related spread
In the Czech Republic, the situation was different compared to England and Scotland, although the analyses point to similarly strong gatherings on the match days (i.e., large ΔR_{match}, Fig. 1a). However, because of the overall low incidence much fewer people were infected throughout the championship. The advantage of low incidence or fewer games is illustrated in two counterfactual scenarios. Even under the assumption that the Czech team had continued to the final and the population had gathered exactly like the English (i.e., showing the same ΔR_{match} in the matches they played), the total number of cases (per million) would have been more than 40 times lower than in England, owing to the lower base incidence and a lower base reproduction number (Fig. 2d). Assuming, as a counterfactual scenario, that England had dropped out in the group stage, the number of cases associated with the Euro 2020
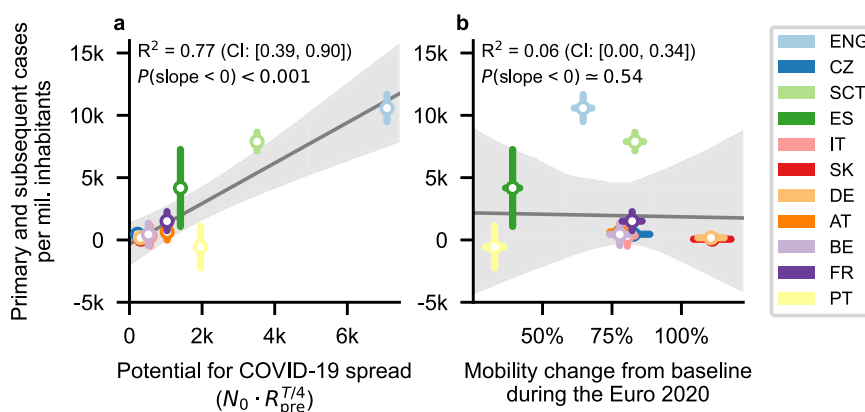
Fig. 3 | Which variables can predict the extent of the impact of Euro 2020 matches? a The potential for spread, i.e., the number of COVID-19 cases that would be expected during the time T a country is playing in the Euro 2020 ($N_0 \cdot R_{pre}^{T/4}$), is strongly correlated with the number of Euro 2020-related cases. Therefore, policymakers should simultaneously consider the initial incidence N_0, reproduction number prior to the event R_{pre}, and expected duration of an event T to assess whether it is pertinent to allow it (The correlation is not significant if England and Scotland are left out, but the slope is still consistent with this result.). **b** Mobility changes from baseline during the Euro 2020 are not correlated with the number of COVID-19 cases associated with the championship in each country. Furthermore, the direction of the effect of mobility per se in this context is unclear. The gray line and area are the median and 95% CI of the linear regression ($n = 11$ countries; The Netherlands was excluded for this analysis). Whiskers denote one standard deviation.

would have been much lower. This suggests that both the success in the championship and the base incidence and behavior in a country influence the public health impact of such large-scale events.

To better understand the impact of the Euro 2020, we quantified the determinants of the spread across countries. From theory, we expect the absolute number of infections generated by Euro 2020 matches to depend non-linearly on a country's base incidence N_0, which determines the probability to meet an infected person, and on the effective reproduction number prior to the championship R_{pre}, as a gauge for the underlying infection dynamics generating the subsequent cases, which determines how strongly an additional infection spreads in the population. We can then define the potential for COVID-19 spread as the number of COVID-19 cases that would be expected during the time T a country is playing in the Euro 2020 ($N_0 \cdot R_{pre}^{T/4}$), assuming a generation interval of 4 days. Indeed, we find a clear correlation between the observed and the expected incidence Fig. 3a, $R^2 = 0.77$ (95% CI [0.39,0.9]), $p < 0.001$, with a slope of 1.62 (95% CI [1.0, 2.26]). The strong significance of this correlation relies mainly on England and Scotland. However, the observed slope in an analysis without these two countries (0.76, 95% CI: [−1.46, 3.04]), while not significant at the 95% confidence level, is consistent with the findings including all countries. This is shown in Supplementary Fig. S7.

Furthermore, quantifying correlations between N_0 and R_{pre} and the number of primary and subsequent cases related to the Euro 2020, we see a trend for each (Supplementary Fig. S6a, b). However, these are weak and statistically significant only for R_{pre}. Altogether, our data suggest that a favorable pandemic situation (low R_{pre} and low N_0) before the gatherings, and low R_{base} during the period of gatherings jointly minimize the impact of the Euro 2020 on community contagion. A prerequisite for this is that the known preventive measures, such as reducing group size, imposing preventive measures, and minimizing the number of encounters remain encouraged.

Independently on the epidemic situation, Euro 2020's effect might be influenced by people's prudence and the team's popularity and success during the championship. While we do not observe any obvious effect of local mobility as a measure of the prudence of people (Fig. 3b, $R^2 = 0.06$ (95% CI [0.00, 0.34]), $p = 0.54$, and Supplementary Fig. S4), the potential popularity −represented by the number of matches played and hosted by a given country− had a more notable trend (Supplementary Fig. S6c). Still, this correlation was not statistically significant. Moreover, we found no relationship between the effect size and the Oxford governmental response tracker[33] (Supplementary Fig. S5).

Discussion

Large international-scale sports events like the Euro 2020 Football Championship have the potential to gather people like no other type of event. Our quantitative insights on the impact of such gatherings on COVID-19 spread provide policymakers with tools to design the portfolio of interventions required for mitigation (using, e.g., results of refs. 22,23,34). Thereby, our quantification can support society in carefully weighing the positive social, psychological, and economic effects of mass events against the potential negative impact on public health[35]. Our analysis attributes about 0.84 million (95% CI: [0.39M, 1.26M]) additional infected persons to the Euro 2020 championship. Assuming that the primary and subsequent spread affects all ages equally, this corresponds across the 12 countries to about 1700 (CI: [762, 2470]) deaths. Thus, the public health impact of the EURO 2020 was not negligible.

To prevent the impacts of these events, measures, such as promoting vaccination, enacting mask mandates, and limiting gathering sizes, can be helpful. Besides, the effectiveness of such interventions has already been quantified in different settings (e.g., refs. 22,23) so that policymakers can weigh them according to specific targets and priorities. Furthermore, focused measures that aim to mitigate disease spread in situ, such as testing campaigns and requiring COVID passports to attend sport-related gatherings and viewing parties, present themselves as helpful options. In addition, one could encourage participants of a large gathering to self-quarantine and test themselves afterward. Moreover, the championship distribution of matches every 4−5 days coincides with the mean incubation period and generation interval of COVID-19. This means that individuals who get infected watching a match can turn infectious by the subsequent while potentially pre-symptomatic. Such resonance effects between gathering intervals and incubation time can increase the spread considerably[34]. It thus depends on the design of the championships, on the precautionary behavior of individuals, and on the basic infection situation how much large-scale events threaten public health, even if the reproduction number is transiently increased during these events.

Previous studies that evaluated the impact of sports events on the spread of COVID-19 and considered the spectator gatherings at match venues were not conclusive[7,8,36]. This agrees with our results as we find the impact of hosting a match to be small to non-existent (Supplementary Fig. S9). However, location having little effect may well be specific to the Euro 2020, where matches were distributed across different countries. In the traditional settings of the UEFA European

Football Championship or the FIFA World Cup, a single country or a small group of countries hosts the entire championship, and the championship is accompanied by elaborate supporting events, public viewing, and extensive travel of international guests. Hence, for other championships, such as, e.g., the FIFA World Cup 2022 in Qatar or the Euro 2024 in Germany, the impact of location might be considerably larger.

Our model accounts for slow changes in the transmission rates that are unrelated to football matches through the gender-independent reproduction number R_{base}. We find R_{base} to increase at least transiently during the championship in all 12 countries except for England and Portugal (Supplementary Figs. S24–S35). The above may suggest that our estimate of the match effect ΔR_{match} is conservative: The overall increase of COVID-19 spread might in part be attributed to R_{base}, but will not be incorrectly associated with football matches. Our results might further be biased if the incidence and the teams' progression in the Euro 2020 are correlated. It is conceivable that high incidence would negatively correlate with team progression through ill or quarantined team members. However, there were only few such cases during the Euro 2020[37], and the correlation might also be positive: At higher case numbers the team might be more careful. Hence, the correlation is unclear and probably negligible.

The COVID-19 spread obviously depends on many factors. However, many of those parameters, such as the vaccination rate, the contact behavior or motivation to be tested, are changing slowly over time and hence can be absorbed into the slowly changing base reproduction rate R_{base} and the gender-asymmetric noise ΔR_{noise}; other parameters, like social and regional differences, age-structure or specific contact networks are expected to be constant over time and average out across a country. To further test the robustness of our model, we systematically varied the prior assumptions on the central model parameters, among them the delay (Supplementary Fig. S12), the width of the delay kernel (Supplementary Fig. S13), the change point interval (Supplementary Fig. S14), the generation interval (Supplementary Fig. S16) and a range of other priors (Supplementary Fig. S17). Furthermore, when using wider prior ranges for the gender imbalance, football-related COVID-19 cases remain unchanged but the uncertainty increases (Supplementary Fig. S15), thus validating our choice. Even for the case of prior symmetric gender imbalance assumptions, the posterior distribution of the female participation converges for the three most significant countries to median values between 20 and 45%. As last cross-check, we made sure that we found no effect when shifting the match dates by 2 weeks relative to the case numbers (Supplementary Fig. S10) nor by shifting match dates outside the championship range, by more than ±30 days (Supplementary Fig. S11).

Besides quantifying the impact of matches on the reproduction number, our methodology allowed us to estimate the delay between infections and confirmation of positive tests D without a requirement to identify the source of each infection (Supplementary Fig. S19). Our estimates for D in the participating countries were around 3-5 days (England: 4.5 days (95% CI [4.3, 5]), Scotland: 3.5 days (95% CI [3.3, 3.8]), Supplementary Figs. S24 and S33g and Supplementary Table S4). This agrees with available literature and is an encouraging signal for the feasibility of containing COVID-19 with test-trace-and-isolate[38–42]. However, we expect that some individuals would actively get tested right after a match, thereby increasing the case finding and reporting rates. This can slightly affect our estimates for the delay distribution D and would require additional information to be corrected. Altogether, analyzing large-scale events with precise timing and substantial impact on the spread presents a promising, resource-efficient complement to classical quantification of delays.

Understanding how popular events with major in-person gatherings affect the spreading dynamics of COVID-19 can help us design better strategies to prevent new outbreaks. The Euro 2020 had a

pronounced impact on the spread despite considerable awareness of the risks of COVID-19. We estimate that, e.g., about 48% of all cases in England until July 31 are related to the championship. In future, with declining awareness about COVID-19 but potentially better immunity, similar mass events, such as the football world cups, the Super Bowl, or the Olympics, will still unfold their impact. Acute, long-COVID-19 and post-COVID-19 will continue to pose a challenge to societies in the years to come. Our analysis suggest that a combination of low R_{pre} and low initial incidence at the beginning of the event, together with the known preventive measures, can strongly reduce the impact of these events on community contagion. Fulfilling these preconditions and increasing health education in the general population can substantially reduce the adverse health effects of future mass events.

Methods

To estimate the effect of the championship in different countries, we constructed a Bayesian model that uses the reported case numbers in 12 countries. Ethical approval was not sought as we only worked with openly available data. A graphical overview of the inference model is given in Fig. 4 and model variables, prior distributions, indices, country-dependent priors, and sampling performance are summarized in Tables 1, 2, 3, 4 and 5, respectively.

Modeling the spreading dynamics, including gender imbalance

The model simulates the spread of COVID-19 in each country separately using a discrete renewal process[22,29,43]. We infer a time-dependent effective reproduction number with gender interactions between genders g and g', $R_{eff,g,g'}(t)$, for each country[21].

Even though participation of women in football fan activity has increased in the last decades[44], football fans are still predominantly male[24]. Hence one expects a higher infection probability at the days of the match for the male compared to the female population. Integrating this information into the model by using gender resolved case numbers, allows improved inference of the Euro 2020's impact. In the following, genders "male" and "female" are denoted by the subscripts $\bullet_{g=1}$ and $\bullet_{g=2}$, respectively. Furthermore, we modeled the spreading dynamics of COVID-19 in each country separately.

In the discrete renewal process for disease dynamics of the respective country, we define for each gender g a susceptible pool S_g and an infected pool I_g. With N denoting the population size, the spreading dynamics with daily time resolution t reads as

$$I_g(t) = \frac{S_g(t)}{N} \sum_{g'=1}^{2} \mathbf{R}_{eff,g,g'}(t) \sum_{\tau=0}^{10} I_{g'}(t-1-\tau)\, G(\tau), \quad (1)$$

$$S_g(t) = S_g(t-1) - E_g(t-1), \quad (2)$$

$$G(\tau) = \text{Gamma}(\tau; \mu=4, \sigma=1.5). \quad (3)$$

We apply a discrete convolution in Eq. (1) to account for the latent period and subsequent infection (red box in Fig. 4). This generation interval (between infections) is modeled by a Gamma distribution $G(\tau)$ with a mean μ of four days and standard deviation σ of one and a half days. This is a little longer than the estimates of the generation interval of the Delta variant[45,46], but shorter than the estimated generation interval of the original strain[47,48]. The impact of the choice of generation interval has negligible impact on our results (Supplementary Fig. S16). The infected compartment (commonly I) is not modeled explicitly as a separate compartment, but implicitly with the assumed generation interval kernel.

The effective spread in a given country is described by the country-dependent effective reproduction numbers for infections of
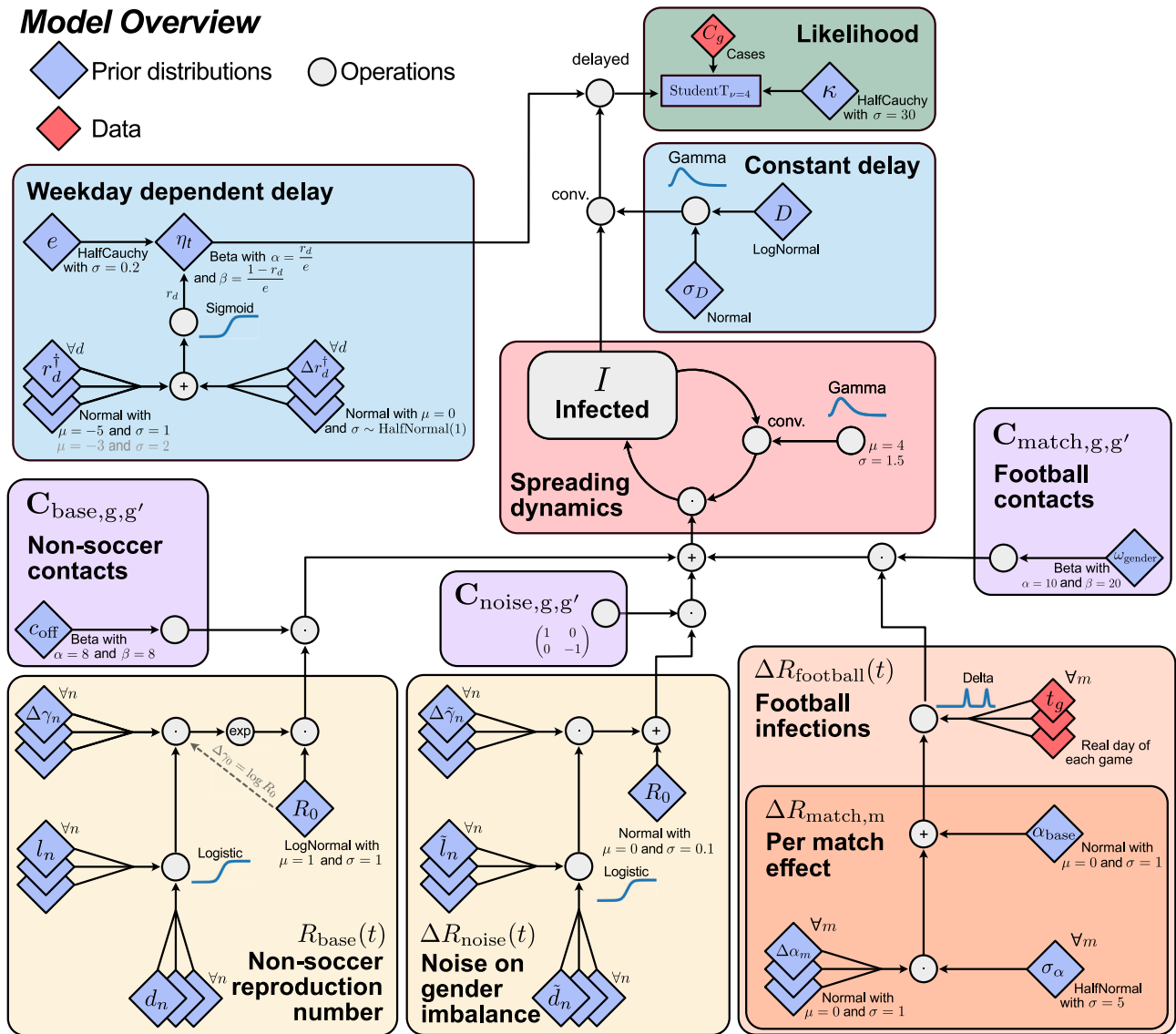
Fig. 4 | Model overview illustrating the relationship between the chosen prior distributions and the disease dynamics. Boxes in the flowchart are color-coded according to what they describe. Light blue boxes: delay modulations. Green boxes: likelihoods. Red boxes: spreading dynamics. Purple boxes: contact matrices. Yellow boxes: effects independent of football matches. Orange boxes: effects of the football matches. Diamonds show prior distributions (blue) or incorporated data (red), and gray circles denote any mathematical operation.

individuals of gender g by individuals of gender g'

$$\mathbf{R}_{\text{eff},g,g'}(t) = R_{\text{base}}(t)C_{\text{base},g,g'} + \Delta R_{\text{football}}(t)C_{\text{match},g,g'} + \Delta R_{\text{noise}}(t)C_{\text{noise},g,g'},$$ (4)

where $C_{\text{base},g,g'}$, $C_{\text{match},g,g'}$, and $C_{\text{noise},g,g'}$ describe the entries of the contact matrices $\mathbf{C}_{\text{base}}$, $\mathbf{C}_{\text{match}}$, $\mathbf{C}_{\text{noise}}$ respectively (purple boxes in Fig. 4).

This effective reproduction number is a function of three different reproduction numbers (yellow and orange boxes in Fig. 4):

1. A slowly changing base reproduction number R_{base} (22) that has the same effect on both genders; besides incorporating the epidemiological information given by the basic reproduction number R_0, it represents the day-to-day contact behavior, including the impact of non-pharmaceutical interventions (NPIs), voluntary preventive measures, immunity status, etc.

2. The reproduction number associated with social gatherings in the context of a football match $R_{\text{match}}(t)$ (11); this number is only different from zero on days with matches that the respective country's team participates in and it has a larger effect on men than on women.

3. A slowly changing noise term $\Delta R_{\text{noise}}(t)$ (31), which subsumes all additional effects which might change the incidence ratio between males and females (gender imbalance).

The interaction between persons of specific genders is implemented by effective contact matrices $\mathbf{C}_{\text{match}}$, $\mathbf{C}_{\text{base}}$ and $\mathbf{C}_{\text{noise}}$. All three are assumed to be symmetric.

$\mathbf{C}_{\text{base}}$ describes non-football related contacts outside the context of Euro 2020 matches (left purple box in Fig. 4):

$$\mathbf{C}_{\text{base}} = \begin{pmatrix} 1 - c_{\text{off}} & c_{\text{off}} \\ c_{\text{off}} & 1 - c_{\text{off}} \end{pmatrix},$$ (5)

with $c_{\text{off}} \sim \text{Beta}(\alpha = 8, \beta = 8)$. (6)

Table 1 | The intermediate variables of the model and their meaning

Variable	Meaning	Equation
$R_{\mathrm{eff},g,g'}(t)$	Effective reproduction number between genders g and g'	(4)
$S_g(t)$	Number of susceptible persons of gender g	(2)
$I_g(t)$	Number of infected persons of gender g	(1)
N	Population size	
$G(\tau)$	Generation interval (Gamma kernel)	(3)
$R_{\mathrm{base}}(t)$	Base reproduction number	(22)
$\Delta R_{\mathrm{football}}(t)$	Time dependent additive reproduction number due to football matches	(11)
$\Delta R_{\mathrm{noise}}(t)$	Time dependent additive reproduction number due other non-balanced transmission	(31)
$\Delta R_{\mathrm{match},m}$	Additive reproduction number of match m	(13)
$\mathbf{C}_{\mathrm{base}}$	Base contact matrix between genders	(5)
$\mathbf{C}_{\mathrm{match}}$	Contact matrix for football related gatherings	(8)
$\mathbf{C}_{\mathrm{noise}}$	Contact matrix for other non-balanced transmission	(10)
t_m	Day of match m	
α_{prior}	Vector encoding country participation in matches	
β_{prior}	Vector encoding whether country hosted matches	
$\Delta\alpha_m$	Difference of the effect of individual matches m (the country participated in) to mean effect of such matches	(15)
$\Delta\beta_m$	Difference of the effect of individual matches m (the country hosted) to mean effect of such matches	(20)
$\gamma_n(t)$	Time-dependent base reproduction number in log-space between change point n and $n+1$	(24)
$\Delta\gamma_n$	Effect of the change point n	(25)
$\tilde{\gamma}_n(t)$	Additive reproduction number due other non-balanced transmission between change point n and $n+1$	(33)
$\Delta\tilde{\gamma}_n$	Effect of the change point n on the non-balanced transmission	(34)
$C_g^{\dagger}(t)$	Delayed number of infected persons of gender g	(40)
$\bar{D}_{\mathrm{country}}$	Country dependent reporting delay	Table 4
$\hat{C}_g(t)$	Modeled number of cases of gender g	(44)
η_t	Fraction of daily delayed cases	(45)
r_d	Average value of the fraction of delayed cases on weekday d	(46)
$r_d^{\dagger}$	Logit-transformed average value of the fraction of delayed cases on weekday d	(47)
$\Delta r_d^{\dagger}$	Deviation from the prior value of the fraction of delayed cases on weekday d	(50)
$C_g(t)$	Measured number of cases of gender g	(53)
R_{pre}	Reproduction number two weeks prior to the start of the Euro 2020	Used in Fig. 3
I_{primary}	Number of primary infected persons due to football matches	(65)
$I_{\mathrm{subsequent}}$	Number of subsequent infected persons due to football matches	(67)
I_{none}	Number of infected persons without considering football matches	(67)

Here, we have the prior assumption that contacts between women, contacts between men, and contacts between women and men are equally probable. Hence, we chose the parameters for the Beta distribution such that c_{off} has a mean of 50% with a 2.5th and 97.5th percentile of [27%, 77%]. This prior is chosen such that it is rather uninformative. As shown in Supplementary Fig. S17, this and other priors of auxiliary parameters do not affect the parameter of interest if their width is varied within a factor of 2 up and down.

$\mathbf{C}_{\mathrm{match}}$ describes the contact behavior in the context of the Euro 2020 football matches (right purple box in Fig. 4). Here, we assume as a prior that the female participation in football-related gatherings accounts for $\simeq 33\%$ (95% percentiles [18%,51%]) of the total participation. Hence, we get the following contact matrix

$$\mathbf{C}_{\mathrm{match,unnorm.}} = \begin{pmatrix} (1-\omega_{\mathrm{gender}})^2 & \omega_{\mathrm{gender}}(1-\omega_{\mathrm{gender}}) \\ \omega_{\mathrm{gender}}(1-\omega_{\mathrm{gender}}) & \omega_{\mathrm{gender}}^2 \end{pmatrix} \quad (7)$$

$$\mathbf{C}_{\mathrm{match}} = \frac{\mathbf{C}_{\mathrm{match,unnorm.}}}{|\mathbf{C}_{\mathrm{match,unnorm.}} \cdot (0.5,0.5)^T|_2} \quad (8)$$

$$\omega_{\mathrm{gender}} \sim \mathrm{Beta}(\alpha=10, \beta=20). \quad (9)$$

The prior beta distribution of ω_{gender} is bounded between at 0 and 1 and with the parameter values of $\alpha=10$ and $\beta=20$ has the expectation value of 1/3. The robustness of the choice of this parameter is explored in Supplementary Fig. S15. $\mathbf{C}_{\mathrm{match}}$ is normalized such that for balanced case numbers (equal case numbers for men and women) and an additive reproduction number $R_{\mathrm{match}}=1$ will lead to a unitary increase of total case numbers. The reproduction number of women will therefore increase by $2\omega_{\mathrm{gender}}\Delta R_{\mathrm{match}}(t)$ on match days whereas the one of men will increase by $2(1-\omega_{\mathrm{gender}})\Delta R_{\mathrm{match}}$, assuming balanced case numbers beforehand.

$\mathbf{C}_{\mathrm{noise}}$ describes the effect of an additional noise term, which changes gender balance without being related to football matches (middle purple box in Fig. 4). For simplicity, it is implemented as

$$\mathbf{C}_{\mathrm{noise}} = \begin{pmatrix} 1 & 0 \\ 0 & -1 \end{pmatrix}, \quad (10)$$

whereby we center the diagonal elements such that the cases introduced by the noise term sum up to zero, i.e. $\sum_{i,j} R_{\mathrm{noise}} \cdot C_{\mathrm{noise},i,j} = 0$.

Football-related effect
Our aim is to quantify the number of cases (or equivalently the fraction of cases) associated with the Euro 2020, Γ_g^{Euro}. To that end we assume

Table 2 | Prior distributions

Variable	Meaning	Prior distribution	Equation
c_{off}	Off-diagonal term of non-football related interaction matrix	Beta($\alpha = 8, \beta = 8$)	(6)
ω_{gender}	The fraction of female participation in football related gatherings compared to the total participation	Beta($\alpha = 10, \beta = 20$)	(9)
ΔR_{match}^{mean}	Mean gathering-related match effect	$\mathcal{N}(\mu = 0, \sigma = 5)$	(14)
$\Delta R_{stadium}^{mean}$	Mean effect of hosting a match at the stadium	$\mathcal{N}(\mu = 0, \sigma = 5)$	(19)
σ_α	Prior value of the deviation from the mean match effect	HalfNormal($\sigma = 5$)	(16)
σ_β	Prior value of the deviation from the mean stadium effect	HalfNormal($\sigma = 5$)	(21)
R_O	Value of $R_{base}(t)$ at $t = 0$	LogNormal($\mu = 1, \sigma = 1$)	(23)
$\sigma_{\Delta\gamma}$	Prior value of the effect of the change points of the base reproduction number	HalfCauchy(0.5)	(26)
l_n	Length of the change point n	$\log(1 + \exp(\mathcal{N}(4,1)))$	(27)
d_n	Date of the change point n	27th May 2021 $+ 10 \cdot n + \mathcal{N}(0, 3.5)$	(29)
$\Delta R_{O,noise}$	Value of $\Delta R_{noise}(t)$ at $t = 0$	$\mathcal{N}(\mu = 0, \sigma = 0.1)$	(32)
$\sigma_{\Delta\bar{\gamma}}$	Prior value of the effect of the change points of the reproduction number of other non-balanced transmission	HalfCauchy(0.2)	(35)
$\bar{l}_n$	Length of the non-balanced transmission change point n	$\log(1 + \exp(\mathcal{N}(4,1)))$	(36)
$\bar{d}_n$	Date of the non-balanced transmission change point n	27th May 2021 $+ 10 \cdot n + \mathcal{N}(0, 3.5)$	(38)
D	Median of the latent period and reporting delay kernel	$\log(\mathcal{N}(\mu = \exp(\bar{D}_{country}), \sigma = \sigma_{\log \bar{D}}))$	(41)
σ_D	Standard deviation of the delay kernel	$\mathcal{N}(\mu = 0.2 \cdot \bar{D}_{country}, \sigma = 0.08 \cdot \bar{D}_{country})$	(43)
$r_{base,d}^\dagger$	Prior fraction of the logit-transformed weekday dependent delay		(48), (49)
σ_r	Prior deviation of the different weekdays from the prior of the fraction of delayed cases	HalfCauchy(1)	(51)
e	Prior deviation of each day from the weekday dependent delay	HalfCauchy(0.2)	(52)
κ	Overdispersion of the observed cases around the expected number of cases	HalfCauchy(20)	(54)

These are all the prior distributions and their meaning in our main model.

Table 3 | Indices

Index	Meaning	Values
$\cdot_g$	Gender	1 = male; 2 = female
$\cdot_m$	Match	
$\cdot_n$	Change point	
$\cdot_t$	Time (in days)	
$\cdot_d$	Weekday	Monday, ..., Sunday

We use these standardized indices in our model.

Table 4 | Country-dependent priors on the delay structure

Country	Reporting convention	Prior delay ($\bar{D}_{country}$)	Scale of prior delay ($\sigma_{\log \bar{D}}$)
England	Symptom onset	4 days	0.1
Scotland	Symptom onset	4 days	0.1
Germany	Reporting date	7 days	0.1
France	Symptom onset	4 days	0.1
Austria	Unknown	5 days	0.15
Belgium	Unknown	5 days	0.15
The Czech Republic	Unknown	5 days	0.15
Italy	Unknown	5 days	0.15
The Netherlands	Symptom onset	4 days	0.1
Portugal	Unknown	5 days	0.15
Slovakia	Unknown	5 days	0.15
Spain	Unknown	5 days	0.15

These priors depend on the definition of the date in the daily case numbers, which for some countries refers to symptom onset, sample collection or sample analysis.

that infections can occur at public or private football screenings in the two countries participating in the respective match m (parameterized by $\Delta R_{match,m}$). Note that for the Euro 2020 not a single country, but a set of 11 countries hosted the matches. The participation of a team or the staging of a match in a country may have different effect sizes. Thus, we define the football related additive reproduction number as

$$\Delta R_{football}(t) = \sum_m \Delta R_{match,m} \cdot \delta(t_m - t). \quad (11)$$

We assume the effect of each match to only be effective in a small time window centered around the day of a match m, t_m (light orange box in Fig. 4). Thus, we apply an approximate delta function $\delta(t_m - t)$. To guarantee differentiability and hence better convergence of the model, we did not use a delta distribution but instead a narrow normal distribution centered around t_m, with a standard deviation of one day:

$$\delta(t) = \frac{1}{\sqrt{2\pi}} \exp\left(-\frac{t^2}{2}\right). \quad (12)$$

We distinguish between the effect size of each match m on the spread of COVID-19. For modeling the effect $\Delta R_{match,m}$, associated with public or private football screenings in the home country, we introduce one base effect ΔR_{match}^{mean} and a match specific offset $\Delta\alpha_m$ for a typical hierarchical modeling approach (dark orange box in Fig. 4). As

prior we assume that the base effect ΔR_{match}^{mean} is centered around zero, which means that in principle also a negative effect of the football matches can be inferred:

$$\Delta R_{match,m} = \alpha_{prior,m}\left(\Delta R_{match}^{mean} + \Delta\alpha_m\right) \quad (13)$$

$$\Delta R_{match}^{mean} \sim \mathcal{N}(0,5) \quad (14)$$

$$\Delta\alpha_m \sim \mathcal{N}\left(0, \sigma_\alpha\right) \quad (15)$$

$$\sigma_\alpha \sim \text{HalfNormal}(5). \quad (16)$$

Table 5 | Maximal $\mathcal{R}$-hat values[51]

Country	Max. $\mathcal{R}$-hat of relevant variables	Max. $\mathcal{R}$-hat of all variables
England	1.07	1.98
The Czech Republic	1.00	1.16
Scotland	1.01	1.10
Spain	1.05	2.24
Italy	1.01	1.10
Slovakia	1.00	1.15
Germany	1.01	1.42
Austria	1.00	1.15
Belgium	1.01	1.22
France	1.01	1.82
Portugal	1.00	1.14
The Netherlands	1.03	1.83

The convergence is good (≈1) for the relevant variables, which are the variables that encode the reproduction number.

$\alpha_{\mathrm{prior},m}$ is the m-th element of the vector that encodes the prior expectation of the effect of a match on the reproduction number. If a country participated in a match, the entry is 1 and otherwise 0. The robustness of the results with respect to the hyperprior σ_α is explored in Supplementary Fig. S17.

For Supplementary Fig. S9, we expand the model by including the effect of infections happening in stadiums and in the vicinity of it as well as during travel towards the venue of the match. In detail, we add to the football related additive reproduction number (Eq. (11)) an additive effect $\Delta R_{\mathrm{stadium},m}$:

$$\Delta R_{\mathrm{football}}(t) = \sum_m (\Delta R_{\mathrm{match},m} + \Delta R_{\mathrm{stadium},m}) \cdot \delta(t_m - t). \quad (17)$$

Analogously to the gathering-related effect we apply the same hierarchy to the effect caused by hosting a match in the stadium – but change the prior of the day of the effect:

$$\Delta R_{\mathrm{stadium},m} = \beta_{\mathrm{prior},m} (\Delta R_{\mathrm{stadium}}^{\mathrm{mean}} + \Delta \beta_m) \quad (18)$$

$$\Delta R_{\mathrm{stadium}}^{\mathrm{mean}} \sim \mathcal{N}(0,5) \quad (19)$$

$$\Delta \beta_m \sim \mathcal{N}(0,\sigma_\beta) \quad (20)$$

$$\sigma_\beta \sim \mathrm{HalfNormal}(5). \quad (21)$$

$\beta_{\mathrm{prior},m}$ encodes whether or not a match was *hosted* by the respective country, i.e equates 1 if the match took place in the country and otherwise equates 0.

Non-football-related reproduction number

To account for effects not related to the football matches, e.g., non-pharmaceutical interventions, vaccinations, seasonality or variants, we introduce a slowly changing reproduction number $R_{\mathrm{base}}(t)$, which is identical for both genders and should map all other not specifically modeled gender independent effects (left yellow box in Fig. 4):

$$R_{\mathrm{base}}(t) = R_0 \exp\left(\sum_n \gamma_n(t)\right) \quad (22)$$

$$R_0 \sim \mathrm{LogNormal}(\mu = 1, \sigma = 1) \quad (23)$$

This base reproduction number is modeled as a superposition of logistic change points $\gamma(t)$ every 10 days, which are parameterized by the transient length of the change points l, the date of the change point d and the effect of the change point $\Delta \gamma_n$. The subscripts n denotes the discrete enumeration of the change points:

$$\gamma_n(t) = \frac{1}{1 + e^{-4/l_n \cdot (t - d_n)}} \cdot \Delta \gamma_n \quad (24)$$

$$\Delta \gamma_n \sim \mathcal{N}(0, \sigma_{\Delta\gamma}) \,\forall n \quad (25)$$

$$\sigma_{\Delta\gamma} \sim \mathrm{HalfCauchy}(0.5) \quad (26)$$

$$l_n = \log\left(1 + \exp(l_n^\dagger)\right) \quad (27)$$

$$l_n^\dagger \sim \mathcal{N}(4,1) \,\forall n \,(\text{unit is days}) \quad (28)$$

$$d_n = 27^{\mathrm{th}}\,\mathrm{May}\,2021 + 10 \cdot n + \Delta d_n \text{ for } n = 0, \ldots, 9 \quad (29)$$

$$\Delta d_n \sim \mathcal{N}(0,3.5) \,\forall n \,(\text{unit is days}). \quad (30)$$

The idea behind this parameterization is that $\Delta \gamma_n$ models the change of R-value, which occurs at times d_n. These changes are then summed in Eq. (24). Change points that have not occurred yet at time t do not contribute in a significant way to the sum as the sigmoid function tends to zero for $t \ll d_n$. The robustness of the results regarding the spacing of the change-points d_n is explored in Supplementary Fig. S14 and the robustness of the choice of the hyperprior $\sigma_{\Delta\gamma}$ is explored in Supplementary Fig. S17.

Similarly, to account for small changes in the gender imbalance, the noise on the ratio between infections in men and women is modeled by a slowly varying reproduction number (middle yellow box in Fig. 4), parameterized by series of change points every 10 days:

$$\Delta R_{\mathrm{noise}}(t) = \Delta R_{0,\mathrm{noise}} + \left(\sum_n \tilde{\gamma}_n(t)\right) \quad (31)$$

$$\Delta R_{0,\mathrm{noise}} \sim \mathcal{N}(\mu = 0, \sigma = 0.1) \quad (32)$$

$$\tilde{\gamma}_n(t) = \frac{1}{1 + e^{-4/\tilde{l}_n \cdot (t - \tilde{d}_n)}} \cdot \Delta \tilde{\gamma}_n \quad (33)$$

$$\Delta \tilde{\gamma}_n \sim \mathcal{N}(0, \sigma_{\Delta\tilde{\gamma}}) \quad (34)$$

$$\sigma_{\Delta\tilde{\gamma}} \sim \mathrm{HalfCauchy}(0.2) \quad (35)$$

$$\tilde{l}_n = \log\left(1 + \exp(\tilde{l}_n^\dagger)\right) \quad (36)$$

$$\tilde{l}_n^\dagger \sim \mathcal{N}(4,1) \,\forall n \,(\text{unit is days}) \quad (37)$$

$$\tilde{d}_n = 27^{\mathrm{th}}\,\mathrm{May}\,2021 + 10 \cdot n + \Delta \tilde{d}_n \text{ for } n = 0, \ldots, 9 \quad (38)$$

$$\Delta \tilde{d}_n \sim \mathcal{N}(0, 3.5) \; \forall n \; (\text{unit is days}). \tag{39}$$

Delay

Modeling the delay between the time of infection and the reporting of it is an important part of the model (blue boxes in Fig. 4); it allows for a precise identification of changes in the infection dynamics because of football matches and the reported cases. We split the delay into two different parts: First we convolved the number of newly infected people with a kernel, which delays the cases between 4 and 7 days. Second, to account for delays that occur because of the weekly structure (some people might delay getting tested until Monday if they have symptoms on Saturday or Sunday), we added a variable fraction that delays cases depending on the day of the week.

Constant delay. To account for the latent period and an eventual apparition of symptoms we apply a discrete convolution, a Gamma kernel, to the infected pool (right blue box in Fig. 4). The prior delay distribution D is defined by incorporating knowledge about the country specific reporting structure: If the reported date corresponds to the moment of the sample collection (which is the case in England, Scotland and France) or if the reported date corresponds to the onset of symptoms (which is the case in the Netherlands), we assumed 4 days as the prior median of the delay between infection and case. If the reported date corresponds to the transmission of the case data to the authorities, we assumed 7 days as prior median of the delay. If we do not know what the published date corresponds to, we assumed a median $\bar{D}_{\text{country}}$ of 5 days, with a larger prior standard deviation $\sigma_{\log \bar{D}}$ (see Table 4):

$$C_g^\dagger(t) = \sum_{\tau=1}^{T} E_g(t - \tau) \cdot \text{Gamma}(\tau; \mu = D, \sigma = \sigma_D) \tag{40}$$

$$D = \log(D^\dagger) \tag{41}$$

$$D^\dagger \sim \mathcal{N}\left(\mu = \exp\left(\bar{D}_{\text{country}}\right), \sigma = \sigma_{\log \bar{D}}\right) \tag{42}$$

$$\sigma_D \sim \mathcal{N}\left(\mu = 0.2 \cdot \bar{D}_{\text{country}}, \sigma = 0.08 \cdot \bar{D}_{\text{country}}\right). \tag{43}$$

Here, Gamma represents the delay kernel. We obtain a delayed number of infected persons $C_g^\dagger$ by delaying the newly infected number of persons $I_g(t)$ of gender g from Eq. (1). The robustness of the choice of the width of the delay kernel σ_D is explored in Supplementary Fig. S17.

Weekday-dependent delay. Because of the different availability of testing resources during a week, we further delay a fraction of persons, depending on the day of the week (left blue box in Fig. 4). We model the fraction η_t of delayed tests on a day t in a recurrent fashion, meaning that if a certain fraction gets delayed on Saturday, these same individuals can still get delayed on Sunday (Eq. (44)). The fraction η_t is drawn separately for each individual day. However, the prior is the same for certain days of the week d (Eq. (45)): we assume that few tests get delayed on Tuesday, Wednesday, and Thursday, using a prior with mean 0.67% (Eq. (48)), whereas we assume that more tests might be delayed on Monday, Friday, Saturday and Sunday. Hence compared to $C_g^\dagger$, we obtain slightly more delayed numbers of cases $\hat{C}_g$, which now include a weekday-dependent delay:

$$\hat{C}_g(t) = (1 - \eta_t) \cdot \left(C_g^\dagger(t) + \eta_{t-1} \hat{C}_g(t-1)\right) \text{ with } \hat{C}_g(0) = C_g^\dagger(0) \tag{44}$$

$$\eta_t \sim \text{Beta}\left(\alpha = \frac{r_d}{e}, \beta = \frac{1 - r_d}{e}\right) \text{ with } d = \text{Monday}, \dots, \text{Sunday} \tag{45}$$

$$r_d = \text{sigmoid}\left(r_d^\dagger\right) \tag{46}$$

$$r_d^\dagger = r_{\text{base},d}^\dagger + \Delta r_d^\dagger \tag{47}$$

$$r_{\text{base},d}^\dagger \sim \mathcal{N}(-5, 1) \text{ for } d = \text{Tuesday, Wednesday, Thursday} \tag{48}$$

$$r_{\text{base},d}^\dagger \sim \mathcal{N}(-3, 2) \text{ for } d = \text{Friday, Saturday, Sunday, Monday} \tag{49}$$

$$\Delta r_d^\dagger \sim \mathcal{N}(0, \sigma_r) \tag{50}$$

$$\sigma_r \sim \text{HalfNormal}(1) \tag{51}$$

$$e \sim \text{HalfCauchy}(0.2). \tag{52}$$

The parameter r_d is defined such that it models the mean of the Beta distribution of Eq. (45), whereas e models the scale of the Beta distribution. r_d is then transformed to an unbounded space by the sigmoid $f(x) = \frac{1}{1 + \exp(-x)}$ (Eq. (46)). This allows to define the hierarchical prior structure for the different weekdays. We chose the prior of $r_{\text{base},d}^\dagger$ for Tuesday, Wednesday, and Thursday such that only a small fraction of cases are delayed during the week. The chosen prior in Eq. (48) corresponds to a 2.5th and 97.5th percentile of r_d of [0%; 5%]. For the other days (Friday, Saturday, Sunday, Monday), the chosen prior leaves a lot of freedom for inferring the delay. Equation (49) corresponds to a 2.5th and 97.5th percentile of r_d of [0%; 72%]. The robustness of the other priors σ_r and e is explored in Supplementary Fig. S17.

Likelihood

Next we want to define the goodness of fit of our model to the sample data. The likelihood of that is modeled by a Student's t-distribution, which allows for some outliers because of its heavier tails compared to a Normal distribution (green box in Fig. 4). The error of the Student's t-distribution is proportional to the square root of the number of cases, which corresponds to the scaling of the errors in a Poisson or Negative Binomial distribution:

$$C_g(t) \sim \text{StudentT}_{\nu=4}\left(\mu = \hat{C}_g(t), \sigma = \kappa \sqrt{\hat{C}_g(t) + 1}\right) \tag{53}$$

$$\kappa \sim \text{HalfCauchy}(\sigma = 30). \tag{54}$$

Here $C_g(t)$ is the measured number of cases in the population of gender g as reported by the respective health authorities, whereas $\hat{C}_g(t)$ is the modeled number of cases (Eq. (44)). The robustness of the prior κ is explored in Supplementary Fig. S17.

Average effect across countries

In order to calculate the mean effect size across countries (Fig. 1b, c), we average the individual effects of each country. To be consistent in our approach, we build an hierarchical Bayesian model accounting for the individual uncertainties of each country estimated from the width of the posterior distributions. As effect size, we use the fraction of primary cases associated with football matches during the championship. Then our estimated mean effect size $\hat{l}_g$ across all countries c (except the Netherlands) for the gender g is inferred with the following

model:

$$\hat{I}_g \sim \text{Normal}(\mu = 0, \sigma = 2) \quad \text{with } g = \{\text{male, female}\} \tag{55}$$

$$\tau_g \sim \text{HalfCauchy}(\beta = 10) \tag{56}$$

$$I^\dagger_{c,g} \sim \text{Normal}(\mu = \hat{I}_g, \sigma = \tau_g) \tag{57}$$

$$\hat{\sigma}_{c,g} \sim \text{HalfCauchy}(\beta = 10) \tag{58}$$

$$I_{s,c,g} \sim \text{StudentT}_{\nu=4}\left(\mu = I^\dagger_{c,g}, \sigma = \hat{\sigma}_{c,g}\right). \tag{59}$$

The estimated effect size of each country (the fraction of primary cases) is denoted by $I^\dagger_{c,g}$ and the effect size of individual samples s from the posterior of the main model is denoted by $I_{s,c,g}$.

We applied a similar hierarchical model but without gender dimensions and with slightly different priors to calculate the average mean match effect $\Delta R^{\text{mean}}_{\text{match}}$ (Fig. 1a). Here by reusing the same notation:

$$\hat{I} \sim \text{Normal}(\mu = 0, \sigma = 10) \tag{60}$$

$$\tau \sim \text{HalfCauchy}(\beta = 10) \tag{61}$$

$$I^\dagger_c \sim \text{Normal}(\mu = \hat{I}, \sigma = \tau) \tag{62}$$

$$\hat{\sigma}_c \sim \text{HalfCauchy}(\beta = 10) \tag{63}$$

$$\Delta R^{\text{mean}}_{\text{match},c,s} \sim \text{StudentT}_{\nu=4}\left(\mu = I^\dagger_c, \sigma = \hat{\sigma}_c\right), \tag{64}$$

where $\Delta R^{\text{mean}}_{\text{match},c,s}$ are the posterior samples from the main model runs of the $\Delta R^{\text{mean}}_{\text{match}}$ variable.

Calculating the primary and subsequent cases

We compute the number of primary football related infected $I_{\text{primary},g}(t)$ as the number of infections happening at football related gathering. The percentage of primary cases f_g is then computed by dividing by the total number of infected $I_g(t)$.

$$I_{\text{primary},g}(t) = \frac{S(t)R_{\text{football}}(t)}{N}\sum_{g'}I_{g'}(t)\mathbf{C}_{\text{football},g'g} \tag{65}$$

$$f_g = \sum_t \frac{I_{\text{primary},g}(t)}{I_g(t)} \quad t \in [\text{11th June, 31st July}] \tag{66}$$

To obtain the subsequent infected $I_{\text{subsequent},g}(t)$, we subtract infected obtained from a hypothetical scenario without football games $I_{\text{none},g}(t)$ from the total number of infected.

$$I_{\text{subsequent},g} = I_g(t) - I_{\text{primary},g}(t) - I_{\text{none},g}(t) \tag{67}$$

Specific, we consider a counterfactual scenario, where we sample from our model leaving all inferred parameters the same expect for the football related reproduction number $R_{\text{football},g}(t)$, which we set to zero.

Sampling

The sampling was done using PyMC3[49]. We use a NUTS sampler[50], which is a Hamiltonian Monte-Carlo sampler. As random initialization often leads to some chains getting stuck in local minima, we run 32 chains for 500 initialization steps and chose the 8 chains with the highest unnormalized posterior to continue tuning and sampling. We then let these chains tune for additional 2000 steps and draw 4000 samples. The maximum tree depth was set to 12.

The quality of the mixing was tested with the $\mathcal{R}$-hat measure[51] (Table 5). The $\mathcal{R}$-hat value measures how well chains with different starting values mix; optimal are values near one. We measured twice: (1) for all variables and (2) for the subset of variables encoding the reproduction number. Variables modeling the reproduction number are the central part of our model (lower half of Fig. 4). As such, we are satisfied if the $\mathcal{R}$-hat values is sufficiently good for these variables, which it is ($\leq$1.07). The high $\mathcal{R}$-hat when calculated over all variables is mostly due to the weekday-dependent delay, which we assume is not central to the results we are interested in.

Robustness tests

In the base model for each country, we only consider the matches in which the respective country participated. It is reasonable to ask whether the matches of foreign countries occurring in local stadium have an effect on the case numbers, caused by transmission in and around the stadium and related travel. To investigate this question we ran a model with an additional parameter (in-country effect) associating the case numbers to the in-country matches (Eq. (17)). In some countries the in-country effect parameter and the original fan gathering effect are covariant, as a large number of matches are played by the country at home, whereas in other countries the additional parameter had no significant effect (Supplementary Fig. S9).

We checked that the inferred fractions of football related cases are robust against changes in the priors of the width σ_D of the delay parameter D (see Supplementary Fig. S13) and the intervals of change points of R_{base} (Supplementary Fig. S14). The results are also, to a very large degree, robust against a more uninformative prior on the fraction of female participants in the fan activities dominating the additional transmission ω_{gender} (Supplementary Fig. S15). To reduce CO_2 emissions, we performed fewer runs for these robustness tests: We only ran the models for which the original posterior distributions might indicate that one could find a significant effect. Each country required eight cores for about 10 days to finish sampling.

In order to further test the robustness of the association between individual matches and infections, we varied the dates of the matches, i.e., shifted them forward and backward in time. The results for the twelve countries under investigation are shown in Supplementary Figs. S10 and S12. In the countries where sensitivity to a championship-related case surge exists, a stable association is obtained for shifts by up to 2 days. As shown for the examples of England and Scotland in Fig. S19, such a shift is compensated by the model by a complementary adjustment of the delay parameter D. For larger shifts, the model might associate other matches to the increase of cases, as matches took place approximately every 4 days.

Correlations

In order to calculate the correlation between the effect size and various explainable variables (Fig. 3 and Supplementary Figs. S4 and S6), we built a Bayesian regression model, using the previously computed posterior samples from the individual runs of each country. Let us denote the previously computed cumulative primary and subsequent cases related to the Euro 2020 by $Y_{s,c}$, for every sample s and analyzed country c, and the explainable variable from auxiliary data by X_c. We used a simple linear model to check for pairwise correlation between $Y_{s,c}$ and X_c:

$$\hat{Y}_c = \beta_0 + \beta_1\hat{X}_c \tag{68}$$

$$\beta_0 \sim \text{Normal}(\mu = 0, \sigma = 10000) \tag{69}$$

$$\beta_1 \sim \text{Normal}(\mu = 0, \sigma = 100000) \tag{70}$$

We used every sample s obtained from the main analysis to incorporate uncertainties on the variable Y_c from our prior results. The auxiliary data X_c might also have errors ϵ_c, which we model using a Normal distribution. Additionally, we allow our estimate for the effect size $\hat{Y}_c$ to have an error for each country c in a typical hierarchical manner and choose uninformative priors for the scale hyper-parameter τ. As prior we considered 10k a reasonable choice for the β parameter as our data X_c is normally in a range multiple magnitudes smaller:

$$\hat{X}_c \sim \text{Normal}(\mu = X_c, \sigma = \epsilon_c) \, \forall c \tag{71}$$

$$\tau \sim \text{HalfCauchy}(\beta = 10000) \tag{72}$$

$$Y_c^\dagger \sim \text{Normal}(\mu = \hat{Y}_c, \sigma = \tau) \, \forall c. \tag{73}$$

Again using uninformative priors for the error, the likelihood to obtain our results given the individual country effect size estimate $Y_c^\dagger$ from the hierarchical linear model is

$$Y_{s,c} \sim \text{StudentT}_{\nu = 4}\left(\mu = Y_c^\dagger, \sigma = \hat{\sigma}_c\right) \, with \tag{74}$$

$$\hat{\sigma}_c \sim \text{HalfCauchy}(\beta = 10000). \tag{75}$$

Therefore, our regression model includes the "measurement error" $\hat{\sigma}_c$, which models the heteroscadistic effect size of every country, and an additional model error τ which models the homoscedastic deviations of the country effect sizes from the linear model. In the plots, we plot the regression line $\hat{Y}_c$ with its shaded 95% CI, and data points $(\hat{X}_c, Y_c^\dagger)$ where the whiskers correspond to the one standard deviation, modeled here by ϵ_c and $\hat{\sigma}_c$.

The coefficient of determination, R^2, is calculated following the procedure suggested by Gelman and colleagues[52]. Their R^2 measure is intended for Bayesian regression models as it notably uses the expected data variance given the model instead of the observed data variance. For our model, it is defined as

$$R^2 = \frac{\text{Explained variance}}{\text{Residual variance} + \text{Explained variance}} = \frac{\frac{1}{n_c - 1}\sum_c \hat{Y}_c^2}{\tau^2 + \frac{1}{n_c - 1}\sum_c \hat{Y}_c^2}, \tag{76}$$

where n_c is the number of countries. With this formula, one obtains the posterior distribution of R^2 by evaluating it for every sample.

As auxiliary data, we used:

1. *Mobility data*: We use the mobility index $m_{c,t}$ provided by the "Google COVID-19 Community Mobility Reports"[53] for each country c at day t during the Euro 2020 ($t \in$ [June 11 2021, July 11 2021]), where N denotes the number of days in the interval. The error is the standard deviation of the mean:

$$X_c = \frac{1}{N}\sum_t m_{c,t} \tag{77}$$

$$\epsilon_c = \sqrt{\frac{1}{N^2}\sum_t (m_{c,t} - X_c)^2} \tag{78}$$

2. *Reproduction number*: We use the base reproduction number $R_{\text{pre},c}$ for each country c as inferred from our model 2 weeks prior to the Euro 2020 ($t \in$ [May 28 2021, June 11 2021]).

$$X_c = \frac{1}{N}\sum_t R_{\text{pre},c}(t) \tag{79}$$

$$\epsilon_c = \sqrt{\frac{1}{N}\sum_t (R_{\text{pre},c}(t) - X_c)^2} \tag{80}$$

3. *Cumulative reported cases*: From the daily reported cases $C(t)$ two weeks prior to the Euro 2020 ($t \in$ [May 28 2021, June 11 2021]), we computed the cumulative reported cases normalized by the number of inhabitants p_c in each country c. Note: We also used reported cases without gender assignment here.

$$X_c = \frac{\sum_t C(t)}{p_c} \tag{81}$$

$$\epsilon_c = \vec{0} \tag{82}$$

4. *Potential for COVID-19 spread*: As for the cumulative cases we used the daily reported cases $C(t)$ two weeks prior to the Euro 2020 ($t \in$ [May 28 2021, June 11 2021]), and we computed the cumulative reported cases normalized by the number of inhabitants p_c in each country c. Furthermore, we used the base reproduction number $R_{\text{base}}(t)$ 2 weeks prior to the Euro 2020, as well as the duration of a country participating in the championship T_c (Table S5) to compute the potential for spread:

$$N_0 = \frac{\sum_t C(t)}{p_c} \tag{83}$$

$$X_c = N_0 \cdot \frac{\sum_t R_{\text{pre},c}^{T_c/4}(t)}{N} \tag{84}$$

$$\epsilon_c = \vec{0} \tag{85}$$

5. *Proxy for popularity*: To represent popularity of the Euro 2020 in country c, we used the union of the number of matches played by each country $n_{\text{match},c}$ and the number of matches hosted by each country $n_{\text{hosted},c}$ (Table S5). By "union" we mean the sum without the overlap, i.e., we take the sum of these numbers and subtract the number of home matches $n_{\text{home},c}$

$$X_c = n_{\text{match},c} + n_{\text{hosted},c} - n_{\text{home},c} \tag{86}$$

$$\epsilon_c = \vec{0} \tag{87}$$

Reporting summary
Further information on research design is available in the Nature Portfolio Reporting Summary linked to this article.

Data availability

Code availability

All code to reproduce the analysis and figures shown in the manuscript as well as in the Supplementary Information is available online on GitHub https://github.com/Priesemann-Group/covid19_soccer or via https://doi.org/10.5281/zenodo.7386313[54].

References

1. Chau, N. V. V. et al. Superspreading event of SARS-CoV-2 infection at a Bar, Ho Chi Minh City, Vietnam. *Emerg. Infect. Dis.* **27**, 310 (2021).
2. Bernheim, B. D., Buchmann, N., Freitas-Groff, Z. & Otero, S. The effects of large group meetings on the spread of COVID-19: the case of Trump rallies. https://siepr.stanford.edu/publications/working-paper/effects-large-group-meetings-spread-covid-19-case-trump-rallies (2020).
3. Wang, L. et al. Inference of person-to-person transmission of COVID-19 reveals hidden super-spreading events during the early outbreak phase. *Nat. Commun.* **11**, 1–6 (2020).
4. Dave, D., McNichols, D. & Sabia, J. J. The contagion externality of a superspreading event: the Sturgis Motorcycle Rally and COVID-19. *South Econ. J.* **87**, 769–807 (2021).
5. Leclerc, Q. J. et al. What settings have been linked to SARS-CoV-2 transmission clusters?*Wellcome Open Res.* **5**, 83 (2020).
6. Nordsiek, F., Bodenschatz, E. & Bagheri, G. Risk assessment for airborne disease transmission by poly-pathogen aerosols. *PLoS ONE* **16**, e0248004 (2021).
7. Fischer, K. Thinning out spectators: did football matches contribute to the second COVID-19 wave in Germany? *Ger. Econ. Rev.* **23**, 595–640 (2022).
8. Toumi, A., Zhao, H., Chhatwal, J., Linas, B. P. & Ayer, T. The effect of NFL and NCAA football games on the spread of COVID-19 in the United States: an empirical analysis. Preprint at *medRxiv* https://doi.org/10.1101/2021.02.15.21251745 (2021).
9. Olczak, M., Reade, J. & Yeo, M. Mass outdoor events and the spread of an airborne virus: English football and Covid-19. https://doi.org/10.2139/ssrn.3682781 (2021).
10. Alfano, V. COVID-19 diffusion before awareness: the role of football match attendance in Italy. *J. Sports Econ.* **23**, 503–523 (2022).
11. Gómez, J.-P. & Mironov, M. Using soccer games as an instrument to forecast the spread of covid-19 in europe. *Financ. Res. Lett.* **43**, 101992 (2021).
12. Jones, B. et al. SARS-CoV-2 transmission during rugby league matches: do players become infected after participating with SARS-CoV-2 positive players? *Br. J. Sports Med.* **55**, 807–813 (2021).
13. Schumacher, Y. O. et al. Resuming professional football (soccer) during the COVID-19 pandemic in a country with high infection rates: a prospective cohort study. *Br. J. Sports Med.* **55**, 1092–1098 (2021).
14. Egger, F., Faude, O., Schreiber, S., Gärtner, B. C. & Meyer, T. Does playing football (soccer) lead to SARS-CoV-2 transmission? - a case study of 3 matches with 18 infected football players. *Sci. Med. Footb.* **5**, 2–7 (2021).
15. Oh, T., Sung, H. & Kwon, K. D. Effect of the stadium occupancy rate on perceived game quality and visit intention. *Int. J. Sports Mark. Spons.* **18**, 166–179 (2017).
16. Herold, E., Boronczyk, F. & Breuer, C. Professional clubs as platforms in multi-sided markets in times of COVID-19: the role of spectators and atmosphere in live football. *Sustainability* **13**, 2312 (2021).
17. Horky, T. No sports, no spectators - no media, no money? The importance of spectators and broadcasting for professional sports during covid-19. *Soccer Soc.* **22**, 96–102 (2021).
18. Yim, B. H., Byon, K. K., Baker, T. A. & Zhang, J. J. Identifying critical factors in sport consumption decision making of millennial sport fans: mixed-methods approach. *Eur. Sport Manag. Q.* **21**, 484–503 (2021).
19. Cuschieri, S., Grech, S. & Cuschieri, A. An observational study of the covid-19 situation following the first pan-european mass sports event. *Eur. J. Clin. Investig.* **52**, e13743 (2022).
20. Feder, T. Soccer obeys bessel-function statistics. *Phys. Today* **59**, 26 (2006).
21. Dehning, J. et al. Inferring change points in the spread of COVID-19 reveals the effectiveness of interventions. *Science* **369**, eabb9789 (2020).
22. Brauner, J. M. et al. Inferring the effectiveness of government interventions against COVID-19. *Science* **371**, eabd9338 (2020).
23. Sharma, M. et al. Understanding the effectiveness of government interventions against the resurgence of COVID-19 in Europe. *Nat. Commun.* **12**, 1–13 (2021).
24. Lagaert, S. & Roose, H. The gender gap in sport event attendance in Europe: the impact of macro-level gender equality. *Int. Rev. Sociol. Sport* **53**, 533–549 (2018).
25. Shah, S. A. et al. Predicted COVID-19 positive cases, hospitalisations, and deaths associated with the Delta variant of concern, June–July, 2021. *Lancet Digital Health* **3**, e539–e541 (2021).
26. Marsh, K., Griffiths, E., Young, J. J., Gibb, C.-A. & McMenamin, J. Contributions of the EURO 2020 football championship events to a third wave of SARS-CoV-2 in Scotland, 11 June to 7 July 2021. *Euro Surveill.* **26**, 2100707 (2021).
27. Riley, S. et al. REACT-1 round 13 interim report: acceleration of SARS-CoV-2 Delta epidemic in the community in England during late June and early July 2021. Preprint at *medRxiv* https://doi.org/10.1101/2021.07.08.21260185 (2021).
28. Roxby, P. Covid: watching Euros may be behind rise in infections in men. *BBC News* (8 July 2021).
29. Fraser, C. Estimating individual and household reproduction numbers in an emerging epidemic. *PLoS ONE* **2**, e758 (2007).
30. Riffe, T. & Acosta, E. Data resource profile: COVerAGE-DB: a global demographic database of COVID-19 cases and deaths. *Int. J. Epidemiol.* **50**, 390–390f (2021).
31. Wilkinson, M. D. et al. The fair guiding principles for scientific data management and stewardship. *Sci. Data* **3**, 1–9 (2016).
32. Government of The Netherlands. Reopening society step by step. https://web.archive.org/web/20210627222056/https://www.government.nl/topics/coronavirus-covid-19/plan-to-reopen-society (2022).
33. Hale, T. et al. A global panel database of pandemic policies (Oxford COVID-19 Government Response Tracker). *Nat. Hum. Behav.* **5**, 529–538 (2021).
34. Zierenberg, J., Spitzner, F. P., Priesemann, V., Weigel, M. & Wilczek, M. How contact patterns destabilize and modulate epidemic outbreaks. Preprint at *arXiv* https://arxiv.org/abs/2109.12180 (2021).
35. Iftekhar, E. N. et al. A look into the future of the COVID-19 pandemic in Europe: an expert consultation. *Lancet Regional Health Eur.* **8**, 100185 (2021).
36. Heese, H. et al. Results of the enhanced COVID-19 surveillance during UEFA EURO 2020 in Germany. *Epidemiol. Infect.* **150**, 1–7 (2022).
37. Reuters. Euro 2020 players affected by COVID-19. https://www.reuters.com/article/soccer-euro-coronavirus-idUKL5N2NS2ED (2021).
38. Kretzschmar, M. E., Rozhnova, G. & van Boven, M. Isolation and contact tracing can tip the scale to containment of COVID-19 in populations with social distancing. *Front. Phys.* https://doi.org/10.3389/fphy.2020.622485 (2021).
39. Kerr, C. C. et al. Controlling COVID-19 via test-trace-quarantine. *Nat. Commun.* **12**, 1–12 (2021).
40. Contreras, S. et al. The challenges of containing SARS-CoV-2 via test-trace-and-isolate. *Nat. Commun.* **12**, 1–13 (2021).

41. Contreras, S. et al. Low case numbers enable long-term stable pandemic control without lockdowns. *Sci. Adv.* **7**, eabg2243 (2021).

42. Salathé, M. et al. COVID-19 epidemic in Switzerland: on the importance of testing, contact tracing and isolation. *Swiss Med. Wkly.* **150**, w20225 (2020).

43. Flaxman, S. et al. Estimating the effects of non-pharmaceutical interventions on COVID-19 in Europe. *Nature* **584**, 257–261 (2020).

44. Meier, H. E., Strauss, B. & Riedl, D. Feminization of sport audiences and fans? Evidence from the German men's national soccer team. *Int. Rev. Sociol. Sport* **52**, 712–733 (2017).

45. Zhang, M. et al. Transmission dynamics of an outbreak of the COVID-19 Delta variant B.1.617.2 - Guangdong Province, China, May-June 2021. *China CDC Wkly.* **3**, 584–586 (2021).

46. Hart, W. S. et al. Generation time of the alpha and delta SARS-CoV-2 variants: an epidemiological analysis. *Lancet Infect. Dis.* **22**, 603–610 (2022).

47. Hu, S. et al. Infectivity, susceptibility, and risk factors associated with SARS-CoV-2 transmission under intensive contact tracing in Hunan, China. *Nat. Commun.* **12**, 1533 (2021).

48. Ferretti, L. et al. Quantifying SARS-CoV-2 transmission suggests epidemic control with digital contact tracing. *Science* **368**, eabb6936 (2020).

49. Salvatier, J., Wiecki, T. V. & Fonnesbeck, C. Probabilistic programming in Python using PyMC3. *PeerJ Comput. Sci.* **2**, e55 (2016).

50. Hoffman, M. D. & Gelman, A. The No-U-Turn sampler: adaptively setting path lengths in Hamiltonian Monte Carlo. *J. Mach. Learn. Res.* **15.1**, 1593–1623 (2014).

51. Vehtari, A., Gelman, A., Simpson, D., Carpenter, B. & Bürkner, P.-C. Rank-normalization, folding, and localization: An improved $\hat{R}$ for assessing convergence of MCMC. *Bayesian Analysis*16 (2021).

52. Gelman, A., Goodrich, B., Gabry, J. & Vehtari, A. R-squared for Bayesian Regression Models. *Am. Stat.* **73**, 307–309 (2019).

53. Google. COVID-19 community mobility reports. https://www.google.com/covid19/mobility/ (2022).

54. Dehning, J. et al. Software: impact of the Euro 2020 championship on the spread of COVID-19. github https://github.com/PriesemannGroup/covid19_soccer; zenodo https://doi.org/10.5281/zenodo.7386313 (2022).

Acknowledgements

Author contributions

Conceptualization: V.P., S.B.M., J.D., S.C., P.D. Methodology: S.B.M., J.D., V.P., P.B., O.S. Software: S.B.M., J.D. Validation: S.B.M., J.D. Formal analysis: S.B.M., J.D. Investigation: S.B.M., J.D., O.S., P.B. Data curation: S.B.M., J.D., P.D., O.S. Writing—original draft: all. Writing—review and editing: all. Visualization: S.B.M., J.D., P.D., S.C., E.I. Supervision: V.P., P.B., O.S., J.D. Funding acquisition: V.P., P.B., O.S.

Funding

Competing interests

V.P. is a member of the ExpertInnenrat of the German federal government on COVID and is also advising other governmental and non-governmental entities. The other authors declare no competing interests.

Additional information

Supplementary information The online version contains supplementary material available at https://doi.org/10.1038/s41467-022-35512-x.

Correspondence and requests for materials should be addressed to Philip Bechtle or Viola Priesemann.

Peer review information *Nature Communications* thanks the anonymous reviewer(s) for their contribution to the peer review of this work. Peer reviewer reports are available.

Reprints and permissions information is available at http://www.nature.com/reprints

Publisher's note Springer Nature remains neutral with regard to jurisdictional claims in published maps and institutional affiliations.

7

THE BENEFITS, COSTS AND FEASIBILITY OF A LOW INCIDENCE COVID-19 STRATEGY

The benefits, costs and feasibility of a low incidence COVID-19 strategy

Thomas Czypionka,[a,*] Emil N. Iftekhar,[b] Barbara Prainsack,[c,*] Viola Priesemann,[d] Simon Bauer,[e] André Calero Valdez,[f] Sarah Cuschieri,[g] Enrico Glaab,[h] Eva Grill,[i] Jenny Krutzinna,[j] Christos Lionis,[k] Helena Machado,[l] Carlos Martins,[m] George N. Pavlakis,[n] Matjaž Perc,[o] Elena Petelos,[p] Martyn Pickersgill,[q] Alexander Skupin,[r] Eva Schernhammer,[s] Ewa Szczurek,[t] Sotirios Tsiodras,[u] Peter Willeit,[v] and Paul Wilmes[w]

[a]Institute for Advanced Studies, Vienna, Austria, and London School of Economics and Political Science, London, UK
[b]Max Planck Institute for Dynamics and Self-Organization, Göttingen, Germany
[c]University of Vienna, Vienna, Austria
[d]Max Planck Institute for Dynamics and Self-Organization, Göttingen, Germany
[e]Max Planck Institute for Dynamics and Self-Organization, Göttingen, Germany
[f]RWTH Aachen University, Aachen, Germany
[g]Faculty of Medicine and Surgery, University of Malta, Msida, Malta
[h]University of Luxembourg, Esch-sur-Alzette, Luxembourg
[i]Ludwig-Maximilians University, Munich, Germany
[j]University of Bergen, Bergen, Norway
[k]Clinic of Social and Family Medicine, Faculty of Medicine, University of Crete, Heraklion, Greece and Institute of Health and Medicine, University of Linkoping, Linkoping, Sweden
[l]University of Minho, Minho, Portugal
[m]Department of Community Medicine, Health Information and Decision Sciences of the Faculty of Medicine of the University of Porto, Porto, Portugal
[n]National Cancer Institute, Bethesda, USA
[o]University of Maribor, Maribor, Slovenia, and Department of Medical Research, China Medical University Hospital, China Medical University, Taichung, Taiwan
[p]Clinic of Social and Family Medicine, Faculty of Medicine, University of Crete, Heraklion, Greece and Faculty of Health, Medicine and Life Sciences, Maastricht University, Maastricht, The Netherlands
[q]The University of Edinburgh, Edinburgh, UK
[r]University of Luxembourg, Esch-sur-Alzette, Luxembourg
[s]Medical University of Vienna, Vienna, Austria
[t]University of Warsaw, Warsaw, Poland
[u]National and Kapodistrian University of Athens Medical School, Athens, Greece
[v]Medical University of Innsbruck, Innsbruck, Austria, and University of Cambridge, Cambridge, UK
[w]University of Luxembourg, Esch-sur-Alzette, Luxembourg

Summary

In the summer of 2021, European governments removed most NPIs after experiencing prolonged second and third waves of the COVID-19 pandemic. Most countries failed to achieve immunization rates high enough to avoid resurgence of the virus. Public health strategies for autumn and winter 2021 have ranged from countries aiming at low incidence by re-introducing NPIs to accepting high incidence levels. However, such high incidence strategies almost certainly lead to the very consequences that they seek to avoid: restrictions that harm people and economies. At high incidence, the important pandemic containment measure 'test-trace-isolate-support' becomes inefficient. At that point, the spread of SARS-CoV-2 and its numerous harmful consequences can likely only be controlled through restrictions. We argue that all European countries need to pursue a low incidence strategy in a coordinated manner. Such an endeavour can only be successful if it is built on open communication and trust.

*Correspondence to: Thomas Czypionka, Josefstaedterstrasse 39, 1080 Vienna, Austria. Phone: +431599911127.
E-mail address: thomas.czypionka@ihs.ac.at (T. Czypionka).

Introduction

In light of decreasing COVID-19 infection rates in early summer 2021, governments in many European countries removed most non-pharmaceutical interventions (NPIs) aimed at controlling the pandemic. In addition to the growing (deceptive) sense of complete safety that

the progress in vaccination programmes conveys, there is also considerable pressure on policymakers to "give people back their freedom". This pressure is rising amidst growing frustration about the protracted pandemic and loss of public trust in governments.[1,2]

While the rate of fully vaccinated people is not sufficient to interrupt infection chains and reduce infection rates in most European countries, especially in the East and among young people, and emerging variants of concern (VOCs) show partial immune escape, lifting certain NPIs means living with a relatively high incidence of cases. Such high incidence means hundreds of cases per week per 100,000 people. While in some countries case numbers have begun to drop, the first 18 months of the pandemic have taught us that it is extremely difficult, if not impossible, to maintain stable incidence at intermediate levels, especially given the increased reproduction number of the Delta variant. Pursuing a low-incidence strategy consequently seems warranted for the winter, especially when people spend more time indoors. *However, achieving a low COVID-19 incidence across Europe will continue to be impossible without good communication, public trust, and a coordinated pan-European approach.*[3,30]

Search strategy and selection criteria

Work for this study has emerged from a previous Delphi study led by Viola Priesemann and Emil Iftekhar.[4] The scientific procedure of the Delphi study consisted of bias-avoiding discussions between scientists of various disciplines and European countries. These discussions were guided, summarised, and synthesized by facilitators. For the insights of this work, the participants of said Delphi study analysed different public health policy strategies against the backdrop of the advantages and disadvantages of different possible scenarios developed in the Delphi study. The considered content arose from three iterations of the authors providing input and evidence and subsequent evaluation by the main authors.

Hastily reducing all NPIs means accepting high COVID-19 incidence

NPIs encompass a wide range of measures and policies, from practices with little impact on personal freedom (e.g., regular disinfection of public spaces) to those that many people consider highly restrictive or invasive (e.g., restrictions on movement). In many countries politicians felt compelled to abolish mask mandates the moment infection numbers declined.

Examples from Israel and Singapore suggest, however, that even in countries with high vaccination rates, especially when colliding with waning immunity, lifting all NPIs will contribute to high incidence and associated undesirable effects.[5-8] Other factors contributing to rising incidence in the winter months include travel and cross-border commutes in and out of regions with high incidence; disadvantageous seasonality effects[9-11]; insufficient support for people to enable self-isolation; lowered risk perception, and inadequate governmental communication around harm reduction[10,11]; and the emergence of VOCs with partial immune escape, such as Delta.[6,12,13]

Against this backdrop, repealing most NPIs appears to be a risky strategy. At incidence levels exceeding 50 cases per 100,000 people per week, test-trace-isolate-support systems (TTIS) capacity is quickly exceeded. This makes it impossible to detect and break many chains of infection. A further rapid increase in incidence to the point of complete loss of control over transmission can then potentially result.[12,13] Exempting vaccinated people from NPIs, such as mask wearing or testing, poses further challenges to containment. This is because these individuals may still get infected and transmit the virus; given frequent exemption of testing requirements for vaccinated people on the basis of European Union's Digital Covid Certificate, their role in transmission chains needs to be assessed in terms of contribution to the spread of VOCs, particularly given Delta's higher transmissibility. Without effective TTIS systems, infections will rise unreported, and many infection chains will not be detected and broken in time. If this happens in winter 2021/2022, incidence could reach levels as high as 500 cases per week per 100,000 people.[16]

The costs of high incidence

The first 18 months of the pandemic have taught us that accepting a high incidence of COVID-19 is unwise - even since vaccines have been available. First, a high incidence incurs direct harm to the health of considerable parts of the population - particularly the most vulnerable, including economically deprived and/or socially marginalised populations,[17] who tend to be less well-served by vaccination programmes and campaigns.[18] The harms include a higher COVID-19 associated mortality and more cases of Long COVID, including pulmonary, cardiovascular, and renal sequelae.[19,20] Many people either cannot be vaccinated for health reasons or show poor immune response to the vaccine (e.g., people with weakened immune systems), and thus remain at risk.[21]

Second, a high incidence also has negative impacts on the workforce; when people fall ill or need to isolate or quarantine, others need to do their work. This additional workload increases the likelihood of burnout, as has become evident especially among healthcare workers.[22] Assuming an incidence of 100 new infected persons per 100,000 per week among the working population, and a quarantine period of ten days, then on average 1% of the population will be off work on any given workday. An additional >1% would need to self-isolate due to being a close contact of an infected

person. Consequently, high incidence makes it unlikely that quarantine orders can and will be adhered to or would even be mandated by some governments. Consequently, the effectiveness of this vital means to mitigate viral transmission is diminished.

Third, in the domain of education, infected children and their close contacts are excluded from attending school or childcare. In this manner, a high incidence also harms children and their education, even if schools remain open. This adds to the existing harms that children have already experienced during the pandemic.[23]

Fourth, a high incidence coupled with only part of the population being vaccinated or naturally immune after disease gives the virus more opportunities to mutate and increases evolutionary pressure on it to escape such immunity. This increases the probability of new VOCs emerging and spreading unnoticed in Europe.[24] This is compounded by the fact that vaccinated people are unlikely to maintain the same vigilance levels regarding potential SARS-CoV-2 transmission as during the first phase of lockdowns.[25] A VOC that renders existing vaccines less effective taking a foothold in Europe would prolong the pandemic and potentially cost even more lives and livelihoods.

Fifth, a central challenge is to avoid hospitals reaching and exceeding capacity. Assuming a slow COVID-19 incidence increase, largely effective vaccines, and fast progress in vaccination (including boosters where appropriate), hospitalization rates are unlikely to reach the levels of winter 2020/2021 (Figure 1). However, even if COVID-19-related hospitalizations remain substantially fewer than in previous waves, additional burdens will be placed on health systems: (a) With NPIs lifted and lowered risk perception, influenza, Respiratory Syncytial Virus, and pneumonia cases are likely to be more than last year[26] and (b) due to postponement of surgeries and routine care during the pandemic there is a large backlog of patients in need of care.[27] Indeed, if incidence increases before a sufficient proportion of people has been vaccinated (against COVID-19 and influenza), health systems may reach capacity limits (Figure 1) - with all this implies for quality of care and patient safety.

Finally, the economic, social, and health related burdens of NPIs should not be neglected either.[30,31] Many of these burdens hit vulnerable and disadvantaged groups particularly hard. Maintaining and achieving low incidence is likely to reduce the need for the kinds of restrictions that are most harmful. Nevertheless, unintended negative consequences to ostensibly laudable measures are well characterised in the history of public health. As such, the role of NPIs in producing harm must be closely and carefully monitored.

In sum, strategies that seek to accommodate or accept high incidence at the current pandemic stage ironically lead to the very consequences they set out to prevent: With rising incidence, more invasive NPIs, potentially even lockdowns, become necessary. This, in turn, increases the negative effects both of the virus itself as well as the harms incurred by NPIs and other pandemic prevention and containment measures. Moreover, the zig-zag courses that pandemic measures inevitably take when too many NPIs are dropped too quickly make it more difficult to communicate to the public and for people and businesses to plan ahead. This adversely impacts upon the psychological wellbeing, whilst simultaneously eroding public trust.[28]

A low incidence strategy to avoid illness, deaths, and lockdowns

An alternative to accepting a high COVID-19 incidence is to achieve and maintain a low incidence by combining increasing population immunization with moderate NPIs in the winter and progressive social and economic policy measures to enhance public health.[16,29] The rationale for this recommendation rests on the following three pillars: First, when incidence is high, retaining control over viral transmission is much more difficult. At low incidence, in contrast, TTIS systems can function effectively.[14,15] Second, as population vaccination coverage progresses - including younger age groups for whom vaccines are newly approved or authorised, the effective reproduction number R_{eff} is continuously reduced, necessitating only moderate NPIs to keep R_{eff} below 1. Finally, a key aim of low incidence is to avoid the more restrictive measures that would follow spikes in infection rates, consequently lessening the harms incurred by NPIs. For this reason, a strategy successfully maintaining a low incidence provides more stability and helps to protect from the manifold social, psychological, and economic harms of such more restrictive measures (see Table 1).

Overall, a pan-European commitment is crucial. The core pillars necessary to achieve and maintain low incidence include a clear political commitment across all Europe to rapidly achieve high vaccination coverage, the close and systematic monitoring of the spread of SARS-CoV-2 and its VOCs across regions and countries, and a systematic and representative sampling of SARS-CoV-2 infection among asymptomatic and symptomatic carriers together with monitoring of new variants presenting an early warning system. Should a new Delta wave occur in the winter, or should novel VOCs that can evade vaccines emerge, coordinated timing of NPIs across Europe will be essential to avoid the 'ping-pong' effects of cross-border spread.[29] The better (and earlier) less-invasive NPIs such as the use of masks, the prohibition of mass gatherings, or good testing regimes are maintained, the lower is the risk that more invasive NPIs will be needed. Last but not least, a common European strategy is needed to share vaccines with countries that do not have sufficient supply. Coordinated global cooperation will greatly facilitate the pursuit of a low

Incidence	About ten per week per 100,000	Several hundred per week per 100,000
Conditions	low transmission for vaccinated, high overall vaccination, European coordination, sufficient NPIs to compensate for the other conditions	high virus transmission also for vaccinated (e.g., given new VOC with partial immune-escape); low risk of severe disease course for most vaccinated
Implications	✗more restrictions at first ✓lower morbidity, mortality and disabilities ✓lower additional burden to the health care system ✓TTIS works effectively ✓lower risk for new VOC emergence ✓protection of vulnerable ✓less workforce in quarantine ✓less strict NPIs in total ✓open schools	✓fewer NPIs in the beginning ✗more morbidity, mortality and disabilities ✗hospital capacity limit might be reached (threshold depends on effective protection against severe course of the disease) ✗Tracing and quarantine of contact persons loses its meaning: too many people would need to be quarantined ✗loss of workforce (especially in the health system, where infected personnel poses a risk to patients) ✗stricter NPIs might be necessary to stabilize case numbers at some point (including school closures)

Table 1: Conditions and implications of corner scenarios for two hypothetical incidence regimes in Europe.

COVID-19 incidence strategy, and thus indirectly the suppression of the emergence of new VOCs. This would allow control of the pandemic and the discussed risks of the high-incidence scenario would be avoided.

In sum, at low incidence, further damage to health, economy and society could be prevented. Unlike in 2020, European countries now have the ability to effectively implement moderate NPIs (e.g., indoor facemasks, lateral-flow testing). We have a better understanding of the effectiveness of different NPIs than a year ago. This means that societies are, now, in a better position to choose the minimum and least invasive set of NPIs necessary to reach and maintain low incidence, alongside social and economic policy measures (such as easily accessible payments to enable self-isolation) that will likewise play a vital role in keeping cases low.

Implementing a low incidence strategy - communication and trust

It remains critical that policies to mitigate and recover from the pandemic define a clear, timely, and accurate communication strategy early on, and include a sufficient degree of democratic involvement and coordination involving all stakeholders. Aside from the democratic imperative to do so, the effectiveness of rules and recommendations largely depends on the willingness and ability of populations to adhere to them.[31] Opaque and ambiguous communication has been identified as an important reason for declining public trust and falling public commitment to pandemic measures.[1,3] The importance of clear communication strategies that include scientific evidence and openly acknowledge uncertainties, are key to public trust.[32]

Faster progress should also be made on establishing mechanisms of actively tackling misinformation and systematically developing counter arguments regarding COVID-19 vaccines and NPIs.[33] The support of locally respected persons, primary healthcare with strong links to communities, and the use of culturally adapted strategies can greatly contribute to sound messaging, with sincerity, openness, and empathy, to enhance public awareness and adherence.[34,35] In addition, those residing in countries where measures are in place should have resources available to them for adherence to be economically and psychologically viable.[4,36]

Conclusion

Despite important progress in vaccination coverage, and the ability to reach low incidence across many European countries over the summer months of 2021, there is a risk of a resurgence of COVID-19 cases in winter. This is especially important if vaccination rates among the most vulnerable groups of the population are insufficient. Decision makers should think ahead and take decisive measures to avoid the failures of 2020: Evidence-based proactive and effective regulations, instead of knee-jerk reactions, across Europe are needed, alongside bold and imaginative social and economic policy to support and enhance public health. With uncertainty regarding children and vulnerable groups, such as those immunocompromised, and, especially, with the catastrophically low availability of vaccines in the Global South, a high incidence in Europe will have global implications that will ultimately adversely impact everyone.

We have yet to overcome the pandemic, but an end is at least conceivable. Until then, the goal is to minimize the cost, emerging from the virus directly, and from measures to prevent its spread, to our communities and societies in Europe and across the world. The way to achieve this is with coordinated European commitment and cooperation, including a Pan-European voice within the global multilateral dialogue, to effectively control the transmission of SARS-CoV-2.

Key Messages

- While at this point of the pandemic incidence levels have a different meaning (due to vaccination), they remain very relevant for policymaking. For example, they correlate with the risk of long COVID, determine the effectiveness of test-trace-isolate-support programs, and predict the proportion of serious cases requiring hospitalisation.

- A high incidence strategy may seem the easiest route for political decision makers, but it is fraught with risks, provides less stability, and ultimately incurs higher costs.

- A low-incidence strategy in Europe seems achievable and more advantageous for public health, society, and for the economy.

- To achieve low incidence, a moderate and targeted set of NPIs should be maintained or re-introduced alongside progressive social and economic policy that enables social practices aligned with the goal of decreasing the impacts of the pandemic until vaccination coverage is sufficient.

- Pan-European commitment and cooperation is key to the success of this strategy.

Author contributions

Most authors were part of a Delphi study on the future of the Covid-19 pandemic and a follow-up opinion piece.[4,35] The idea for this article emerged from these discussions. TC, ENI, BP, VP conceived the article, wrote the first draft, and are first authors. All authors provided expertise from their respective fields and were involved in writing, review, and editing. TC, ENI, and BP coordinated the shaping of the paper.

References

1. Devine D, Gaskell J, Jennings W, Stoker G. Trust and the Coronavirus Pandemic: What are the Consequences of and for Trust? An Early Review of the Literature. *Political Studies Review* 2021;**19**:274–85.
2. Schernhammer E, Weitzer J, Laubichler MD, et al. Correlates of COVID-19 vaccine hesitancy in Austria: trust and the government. *J Public Health (Oxf)* 2021. https://doi.org/10.1093/pubmed/fdab122. published online May 5.
3. Harring N, Jagers SC, Löfgren Å. COVID-19: Large-scale collective action, government intervention, and the importance of trust. *World Development* 2020. https://doi.org/10.1016/j.worlddev.2020.105236.
4. Iftekhar EN, Priesemann V, Balling R, et al. A look into the future of the COVID-19 pandemic in Europe: an expert consultation. *Lancet Reg Health Eur* 2021;**8**:100185.
5. Siggins MK, Thwaites RS, Openshaw PJ. Durability of immunity to SARS-CoV-2 and other respiratory viruses. *Trends in Microbiology* 2021 Apr 8.
6. Harder T, Külper-Schiek W, Reda S, Treskova-Schwarzbach M, Koch J, Vygen-Bonnet S, Wichmann O. Effectiveness of COVID-19 vaccines against SARS-CoV-2 infection with the Delta (B. 1.617. 2) variant: second interim results of a living systematic review and meta-analysis, 1 January to 25 August 2021. *Eurosurveillance* 2021 Oct 14;**26**(41):2100920.
7. Wadman M. Israel's struggles to contain COVID-19 may be a warning for other nations. *Science* 2021. (published online Sep 21) (accessed Oct 28, 2021). https://www.science.org/content/article/israel-s-struggles-contain-covid-19-may-be-warning-other-nations.
8. Aravindan A. Analysis: Vaccinated Singapore shows zero-COVID countries cost of reopening. *Reuters* 2021. (published online Oct 22) (accessed Oct 28, 2021). https://www.reuters.com/world/asia-pacific/vaccinated-singapore-shows-zero-covid-countries-cost-reopening-2021-10-22/.
9. Merow C, Urban MC. Seasonality and uncertainty in global COVID-19 growth rates. *Proc Natl Acad Sci U S A* 2020;**117**:27456–64.
10. Anastasiou OE, Hüsing A, Korth J, et al. Seasonality of Non-SARS, Non-MERS Coronaviruses and the Impact of Meteorological Factors. *Pathogens* 2021;**10**:187.
11. Byun WS, Heo SW, Jo G, et al. Is coronavirus disease (COVID-19) seasonal? A critical analysis of empirical and epidemiological studies at global and local scales. *Environ Res* 2021;**196**:110972.
12. Planas D, Veyer D, Baidaliuk A, et al. Reduced sensitivity of SARS-CoV-2 variant Delta to antibody neutralization. *Nature* 2021;**596**:276–80.
13. Mlcochova P, Kemp S, Dhar MS, et al. SARS-CoV-2 B.1.617.2 Delta variant replication and immune evasion. *Nature* 2021: 1–8.
14. Contreras S, Dehning J, Loidolt M, et al. The challenges of containing SARS-CoV-2 via test-trace-and-isolate. *Nature Communications* 2021;**12**:378.
15. Kretzschmar M, Rozhnova G, van boven M. Isolation and Contact Tracing Can Tip the Scale to Containment of COVID-19 in Populations With Social Distancing. *Frontiers in Physics* 2021;**8**. https://doi.org/10.3389/fphy.2020.622485.
16. Bauer S, Contreras S, Dehning J, et al. Relaxing restrictions at the pace of vaccination increases freedom and guards against further COVID-19 waves. *PLOS Computational Biology* 2021;**17**:e1009288.
17. Bambra C, Riordan R, Ford J, Matthews F. The COVID-19 pandemic and health inequalities. *J Epidemiol Community Health* 2020;**74**:964–8.
18. Barry V, Dasgupta S, Weller DL, et al. Patterns in COVID-19 Vaccination Coverage, by Social Vulnerability and Urbanicity - United States, December 14, 2020-May 1, 2021. *MMWR Morb Mortal Wkly Rep* 2021;**70**:818–24.
19. Phillips S, Williams MA. Confronting Our Next National Health Disaster — Long-Haul Covid. *New England Journal of Medicine* 2021;**385**:577–9.
20. Nalbandian A, Sehgal K, Gupta A, et al. Post-acute COVID-19 syndrome. *Nat Med* 2021;**27**:601–15.
21. Monin L, Laing AG, Muñoz-Ruiz M, et al. Safety and immunogenicity of one versus two doses of the COVID-19 vaccine BNT162b2 for patients with cancer: interim analysis of a prospective observational study. *Lancet Oncol* 2021;**22**:765–78.
22. Khosravi M, Ghiasi Z, Ganjali A. A narrative review of research on healthcare staff's burnout during the COVID-19 pandemic. In: In: Proceedings of Singapore Healthcare; 2021. 20101058211040575.
23. Ravens-Sieberer U, Kaman A, Erhart M, Devine J, Schlack R, Otto C. Impact of the COVID-19 pandemic on quality of life and mental health in children and adolescents in Germany. *Eur Child Adolesc Psychiatry* 2021. https://doi.org/10.1007/s00787-021-01726-5. published online Jan 25.
24. Interim guidance on the benefits of full vaccination against COVID-19 for transmission and implications for non-pharmaceutical interventions. *European Centre for Disease Prevention and Control* 2021. (published online April 21) (accessed Oct 28, 2021). https://www.ecdc.europa.eu/en/publications-data/interim-guidance-benefits-full-vaccination-against-covid-19-transmission.
25. Rahamim-Cohen D, Gazit S, Perez G, et al. Survey of Behaviour Attitudes Towards Preventive Measures Following COVID-19 Vaccination. 2021 DOI:10.1101/2021.04.12.21255304.
26. Gomez GB, Mahé C, Chaves SS. Uncertain effects of the pandemic on respiratory viruses. *Science* 2021. (published online June 4) (accessed Oct 28, 2021). https://www.science.org/doi/abs/10.1126/science.abh3986.
27. Topriceanu C, Wong A, Moon JC, et al. Evaluating access to health and care services during lockdown by the COVID-19 survey in five UK national longitudinal studies. *BMJ Open* 2021;**11**:e045813. https://doi.org/10.1136/bmjopen-2020-045813.
28. Saqr M, Wasson B. COVID-19: Lost opportunities and lessons for the future. *Int J Health Sci (Qassim)* 2020;**14**:4–6.
29. Viana J, van Dorp CH, Nunes A, et al. Controlling the pandemic during the SARS-CoV-2 vaccination rollout. *Nat Commun* 2021;**12**:3674.
30. Priesemann V, Balling R, Brinkmann MM, et al. An action plan for pan-European defence against new SARS-CoV-2 variants. *Lancet* 2021;**397**:469–70.
31. Prainsack B. Solidarity in Times of Pandemics. *Democratic Theory* 2020;**7**:124–33.
32. Lee Y, Li JQ. The role of communication transparency and organizational trust in publics' perceptions, attitudes and social distancing behaviour: A case study of the COVID-19 outbreak. *Journal of Contingencies and Crisis Management* 2021. https://doi.org/10.1111/1468-5973.12354. published online Feb 7.
33. Krause N, Freiling I, Beets B, Brossard D. Fact-checking as risk communication: the multi-layered risk of misinformation in times of COVID-19. *Journal of Risk Research* 2020;**23**:1–8.

34 Béhague D, Ortega F. Mutual aid, pandemic politics, and global social medicine in Brazil. *Lancet* 2021;**398**:575–6.

35 Lionis C, Papadakaki M, Saridaki A, Dowrick C, O'donnell CA, Mair FS, Van Den Muijsenbergh M, Burns N, De Brún T, De Brún MO, van Weel-Baumgarten E. Engaging migrants and other stakeholders to improve communication in cross-cultural consultation in primary care: a theoretically informed participatory study. *BMJ open* 2016 Jul 1;**6**(7):e010822.

36 Priesemann V, Balling R, Bauer S, et al. Towards a European strategy to address the COVID-19 pandemic. *Lancet* 2021;**398**:838–9.

Part III

DISCUSSION

LESSONS FOR RESPONDING TO PANDEMICS

This thesis leverages concepts and tools from physics and dynamical systems theory to further the quantitative modeling of infectious disease transmission, with a focus on gaining insights into the COVID-19 pandemic. Collectively, the works included demonstrate the power of complex-systems-inspired mathematical modeling for not only deepening our theoretical understanding of epidemics, but also generating actionable evidence to inform public health policy making during crisis events like COVID-19. Beyond analyzing specific topics like non-pharmaceutical interventions and vaccination, the thesis emphasizes the critical need to incorporate psychological, social, and policy dimensions beyond purely epidemiological factors.

In chapter 3, we performed an expert consultation to inform our quantitative work. We identified key control parameters and regime shifts for our analyses: population immunity and vaccination, the emergence and prevalence of variants of concern, and public responses to pandemic policy. We further elucidated predictions for the pandemic that highlighted key uncertainties, guiding the further research questions of this thesis.

Building on this, chapter 4 focused on reopening strategies as vaccination campaigns progressed in 2021. Using an extended SIR model incorporating vaccination rollout, we quantified sustainable rates of lifting non-pharmaceutical interventions (NPIs) based on immunization pace. We found that a slow lifting of restrictions at the pace of the vaccine roll-out offered the best trade-off between preventing resurgences and restoring freedoms. This demonstrated the value of data-driven models in mapping out acute complex policy trade-offs.

In chapter 5, we incorporated additional real-world evidence by linking intensive care unit (ICU) occupancy to individuals' voluntary health-protective behaviour and vaccine acceptance. Our model estimated that moderate NPIs balancing perceived risk and freedom enable behavioral adaptation that helps stabilize control. Neither a "full freedom" nor a more restrictive approach appeared optimal. This underlined the need for nuanced behavioral insights alongside epidemiological modeling.

Shifting focus, chapter 6 leveraged the "natural experiment" of the Euro 2020 football championship to statistically estimate its impact on

transmission. By modeling male/female case imbalance and the timing of matches, we inferred a significant growth in infections associated with the events. This data-driven approach demonstrated the value of studies utilising unique circumstances to quantify epidemiological impacts in a complex world.

Finally, chapter 7 synthesized multi-disciplinary expert opinions and some of this thesis' findings for health policy recommendations. We argued that coordinated efforts across Europe to maintain low incidence outperform a high-incidence accepting alternative on various dimensions.

In synthesis, the insights of chapter 3 inspired the complex systems models in chapter 4, chapter 5 and chapter 6 that provided quantitative insights about real-world COVID-19 pandemic response and also guided policy recommendations, e.g., in chapter 7.

While developing sophisticated dynamical models grounded in epidemiological mechanisms, we also emphasized designing scenarios or studies to specifically inform policy questions. Football matches and ICU occupancy provided natural experiments to quantify gathering impacts and behavioral adaptation (chapter 6 and chapter 5, respectively). In chapter 3, expert forecasts synthesized qualitative and big-picture insights to complement mechanistic models. This demonstrated the importance of not just theoretical modeling but embedding models within data and domain context.

Beyond mathematically modeling governmental interventions, a methodological contribution was representing COVID-19 transmission through a nonlinear dynamics perspective focused on regime shifts. This approach illuminated, e.g., how feedback loops between disease spread and human intervention make the difference between controlled epidemics and explosive spread when passing critical tipping points. Such nonlinear phenomena like infection plateaus and multi-wave dynamics emerged from the models but cannot easily be captured by simple SIR approaches. Hence, our work elucidated how factors like voluntary behavioral changes and responsive policies can help maintain desirable regimes and prevent uncontrolled epidemics. From a physics viewpoint, epidemic modeling benefits tremendously from thinking in terms of dynamical systems.

In the following, we will discuss some of the overarching insights of this thesis in more detail and in the context of other scientific evidence.

8.1 MAINTAINING LOW INCIDENCE: THE BEST STRATEGY?

A key insight is that, under certain conditions, a low incidence strategy for COVID-19 causes less public health and other societal damage than accepting high incidence (chapter 3, chapter 4, chapter 6 and chapter 7).

A key containment measure, test-trace-isolate (TTI), is most effective when the incidence is low (chapter 1, chapter 3, and chapter 4). Furthermore, there will always be some incidence that will be deemed too high by society, e.g., when hospitals, intensive care units or health care systems would collapse, or when too many people would be too sick to ensure that essential infrastructure is running smoothly (chapter 7 and chapter 4). At the latest by then, containment measures would be needed. Hence, to minimise the amount of intrusive measures in such a system, it is optimal to choose a low incidence strategy, where TTI can replace other more intrusive measures and enable containment, mitigation or control. This way, there is not only less direct public health damage through fewer infections, hospitalisation, long-COVID and deaths (chapter 4), but also less other damage to society because, ultimately, fewer non-pharmaceutical interventions have to be introduced (chapter 7).

We further find that the necessary mitigation of spread does not have to be achieved through mandatory measures alone (chapter 5). Additional voluntary health protective behaviour has the ability to close the gap to protect health systems, while still leaving the population with some agency to minimise the negative impacts of the pandemic on their lives. For example, if mandates are in place that effectively allow home-office, people can make use of the home-office option if they perceive it to be the appropriate thing to do. This benefit of joint voluntary and mandatory behaviour was also found in other compartmental modelling work (e.g. [28, 29]). Complementing these complex systems modelling results, statistical work finds that the effect of NPIs on disease spread is also derived from voluntary behaviour [30] and that voluntary behaviour in the absence of mandatory measures can even have the same order of magnitude of effect as mandatory behaviour change [31]. Given that health-protective behaviour through mandatory measures (in part) replaces voluntary health-protective behaviour [32], finding the right balance between mandatory and voluntary behaviour to achieve low incidence is key.

The benefit of a low incidence strategy goes so far as to enable countries to hold large-scale events with minimal public health damage (chapter 6). In line with other work (e.g. [33–36]), we find that most

of the additional cases caused by such events arise from secondary infections, i.e. when people get infected during the event and afterwards infect others in their surroundings. Together with the previous findings, this allows us to connect the dots and suggest an interpretation: In a low incidence regime (and with low reproduction number), TTI is able to stop most infection chains, which would make up the majority of the public health damage, and thereby leads to a much safer event. The large impact of preventing secondary infections arising from superspreading events has also been found in theoretical stochastic modelling work (e.g. [37]).

8.1.1   *Low incidence less attractive if hospitals are never overwhelmed*

However, once the situation changes, it is necessary to re-evaluate the costs and benefits of a strategy. In a different situation, one of the underlying assumptions may not hold anymore. Let us consider for example the assumption that it will be necessary to implement severe NPIs at some point to avert health system or infrastructure collapse. If such NPI implementation will not happen in any plausible scenario, TTI at peak effectiveness is not required anymore to complement less intrusive measures in mitigating the spread sufficiently. Then, a low incidence strategy is not required to achieve better control and may not be the best option anymore. So, which pandemic situation changes would make implementing severe NPIs at any point obsolete? We illustrate the multiple pathways here with a SIHR model, i.e. a SIR model where people may be hospitalised in case of severe disease, before they recover (Figure 8.1**A**).

The baseline scenario is chosen such that the number of COVID-19 hospitalisations during a wave would exceed maximum hospital capacity by far (Figure 8.1**B**, gray dashed line). For this scenario, let us consider that only NPIs that are in tendency perceived as less intrusive are implemented, such as mask wearing. If the goal is to make more intrusive NPIs obsolete, one option to ensure that hospitals are not overwhelmed is to increase the maximum hospital capacity. This was done to some extent at the beginning of the COVID-19 pandemic [38]. However, often high enough hospital capacity is only possible in high-income countries [39], and only to a certain extent: While it may be possible to set up more hospital beds or acquire treatment material, it is difficult to hire more healthcare workers quickly [40]. Hence, if it is
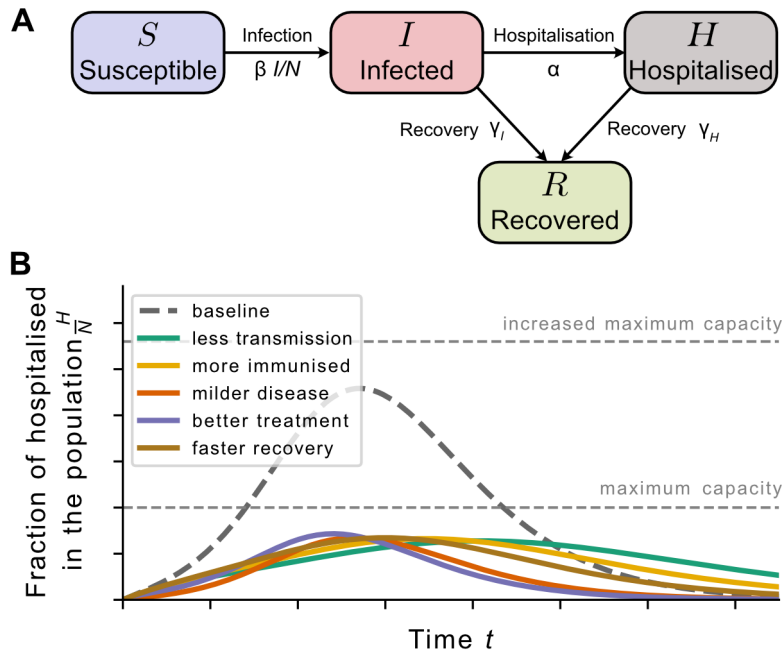
Figure 8.1: **Multiple developments avoid hospital overload. A:** We illustrate
this with a SIHR model. Compared to the classical SIR model, the SIHR
model allows infected people to get hospitalised due to a severe disease
course and recover afterwards. **B:** The baseline scenario (gray dashed line)
is calculated with $\beta = 0.2$, $\gamma_I = 0.1$, $\alpha = 0.01$ and $\gamma_H = 0.1$. If hospital
capacities are large enough, hospitals are not overwhelmed even with a
full wave. Else, different developments can cause fewer hospitalisations:
via fewer infections through less transmission, i.e. smaller $\beta = 0.14$ (green
line), more immunised or recovered R and thereby fewer susceptible S
in the population, i.e. only 73% suscpeptible in the beginning instead of
99% (yellow line), milder disease, i.e. smaller $\alpha = 2.5 \cdot 10^{-3}$ (red line),
shorter hospital stays through better treatment, i.e. larger $\gamma_H = 0.35$
(blue line), and faster recovery before the disease becomes severe, i.e.
larger $\gamma_I = 0.145$ (brown line).

not possible to increase hospital capacities sufficiently, the number of hospitalisations needs to decrease somehow.

First, it is possible that the transmission probability decreases, leading to fewer infections and, thus, hospitalisations (Figure 8.1**B**, green line). This could for example happen through new kinds of measures or technologies that, e.g., increase indoor air quality and, thereby, reduce infections indoors [41]. Or it could happen through (partly) sterilising immunity, i.e. that immune individuals do not spread the disease (as much) [42].

After a COVID-19 infection or vaccination, people are temporarily immune against infection. In consequence, the susceptible compartment gets smaller, which also reduces the number of infections and thereby of hospitalisations (Figure 8.1**B**, yellow line). We have also seen that in chapter 4 and chapter 5. Even if the immunity wanes over time, the severity of COVID-19 after re-infection decreases (chapter 4 and chapter 5), lowering the probability of hospitalisation (Figure 8.1**B**, red line). In the context of the SIHR model, a lower hospitalisation probability would also be caused by a new variant of SARS-CoV-2 that induces less severe disease. This was the case with the Omicron variant. During the work regarding chapter 5, there was still a lot of uncertainty regarding the properties of Omicron. However, by now it is clear that it induces less severe disease than previous prevalent variants (e.g [43]). On the other hand, it also increases the probability of breakthrough infections, i.e. it is more likely to evade existing immunity (e.g [44]), and induces weaker immunity in persons it infected (e.g. [45]). Thereby, the decrease in hospitalisations is to some extent counteracted through the mechanism represented by the green and red lines in Figure 8.1**B**. However, the protecting effect of vaccinations is not completely cancelled (e.g. [46]), which ultimately contributed to a better controlled pandemic and better health outcomes (e.g. [47]).

Next, the number of hospital patients would be reduced if the patients tended to recover faster in hospitals (Figure 8.1**B**, blue line). This could also be a result of a new variant, but also of better hospital care and treatment. In fact, it has become clear that oxygen supplementation and mechanical ventilation improve COVID-19 patient outcomes (e.g. [48]) and antiviral drugs have become available as well (e.g. [49]).

Lastly, if there is medicine that facilitates recovery even before hospitalisation, hospitalisations would decrease as well (Figure 8.1**B**, brown line).

To summarise, any one or any combination of these mechanisms is principally able to achieve a situation where the COVID-19 pandemic

does not overwhelm hospitals without too intrusive measures, making a low incidence strategy obsolete. At the time of writing, a combination of said mechanisms is thereby actually decreasing the advantages of a low incidence strategy.

8.1.2 *Health-protective behaviour at low incidence?*

There is one potential difficulty of the low incidence strategy that has not been discussed yet: the social, economic and psychological barriers to implementing a low incidence strategy.

We have seen that voluntary behaviour is dependent on incidence through mechanisms such as risk perception (chapter 5). Risk-perception and information based behaviour change has also been used in other COVID-19 modelling work (e.g. [29, 50]). Accordingly, most people would not voluntarily engage in health-protective behaviour at too low incidence. Hence, there would be no voluntary behaviour contribution to spread mitigation at low incidence.

Furthermore, we have learned that adherence to mandatory measures needs to be facilitated as well (chapter 3). If the cost of adhering to measures is too high compared to the perceived benefit, mandatory measures also lose their effectiveness. A low incidence might give the momentary impression that the benefit of adhering to measures is not large enough and thereby would nullify the mandatory contribution to the mitigation of the spread as well.

Hence, our findings suggest that if there is no voluntary health-protective behaviour and no adherence to mandatory measures at low incidence, one can only wait until incidence, the related public health damage, risk perception, and health-protective behaviour increases again, before one can implement more intrusive NPIs. Under such circumstances it would not be possible to rely on a low incidence strategy.

However, by now empirical evidence has accumulated, suggesting that health-protective behaviour is not as strongly and clearly dependent on the pandemic state and would, thus, not need to undermine a low incidence strategy: Even though adherence to health-protective measures is empirically found to be dependent on risk perception (e.g. [51–54]), the correlation between risk perception and behaviour varies over time [55] and risk perception does not seem to correlate well with incidence [54]. In fact, prosocial tendencies, values and worldviews, trust in institutions and perceptions about efficacy of measures and strategies

matter for health-protective behaviour as well (e.g. [56, 57]), according to some empirical studies even more than risk perception and incidence [55, 58]. Especially if the objective risk is low, risk perception plays a subordinate role besides factors such as trust [59]. And if the risk is perceived as high, while the efficacy of measures is perceived as low, it even disincentivises health-protective behaviour [53].

These findings also have implications for the validity of our work in chapter 5: The self-regulation of the population's health-protective behaviour dependent on the pandemic state may not be as effective in controlling the spread as modelled. Therefore, empirical validation of this feedback between disease spread and behaviour is warranted. First statistical quantitative analyses, partially including complex psychological models, do infer this feedback loop in two European countries [60, 61]. A further global and more detailed analysis is also being conducted within the infoXpand research consortium that I was also a part of and supported by [62]. Hence, the answer to the question of whether a low incidence strategy is feasible from a psychological perspective remains unclear until more evidence is gathered.

In conclusion, a low COVID-19 incidence strategy offers public health benefits by enabling effective test-trace-isolate and avoiding overwhelming hospitals, thereby minimizing the need for stringent NPIs. However, sustaining low incidence has costs and may become unnecessary if hospitals are not overwhelmed regardless of NPIs or if people do not engage sufficiently in health-protective behaviour at low incidence.

8.2   VACCINATION

8.2.1   *Heterogeneity and vaccinating superspreaders*

As explained in Section 8.1.1, we find that sufficient vaccination coverage greatly reduces the need for NPIs (chapter 3, chapter 4, and chapter 5). This is in line with other analyses (e.g. [63–65]). Like others (e.g. [65, 66]), we model the vaccination roll-out starting with the oldest most vulnerable age groups and ending with the youngest age groups (chapter 4). Under the assumption that older age groups are vaccinated with a higher proportion and with the higher vulnerability of older age groups to disease, said vaccination strategy leads to better pandemic control (chapter 4 and chapter 5). Similar modelling work has equivalent findings (e.g. [65, 66]).

However, we hint at the fact that the spread mitigating effect of vaccination does not simply linearly scale with the total coverage (chapter 4): The contact behaviour and network structure matter as well, affecting what would be the optimal vaccination strategy. Indeed, other modelling research suggests that population immunity may be reached at a lower threshold and faster if younger age groups are vaccinated first (e.g. [67]). This is because there is heterogeneity in disease spread: younger age groups tend to have more contacts and may thereby be able to infect more people and are more likely to be infected as well (e.g. [68]). The conditions for this mechanism to hold, however, are high enough vaccine effectiveness [69] and sufficient vaccine coverage [70]. Furthermore, while incidence might come under control faster by vaccinating younger populations earlier, the number of deaths could be higher compared to the alternative [70–72].

In general, heterogeneity in exposure, susceptibility, infectivity or other contact behaviour leads to a lower population immunity threshold compared to the homogeneous counterfactual (e.g. [73–76]). This is especially the case if, e.g., susceptibility and infectivity is correlated [77]. In other words, a good vaccination strategy might be one that vaccinates network hubs and thereby minimises the impact of super-spreaders (e.g. [78, 79]).

If the vaccination roll-out coincides with the implementation of NPIs, it is important to note that the exact results of the impact depend on how the heterogeneity is modelled. For example, degree heterogeneity lowers the population immunity threshold if interventions are modelled as a change in transmission rate. However, if modelled as a change in the contact network, the threshold is lowered less because highly connected nodes may be shielded and stay susceptible [80]. Therefore, population immunity thresholds strongly depend on the mathematical model of disease spread, vaccination and NPIs.

In practice, it might be politically feasible to vaccinate younger populations first. However, targeting network hubs specifically is difficult because it is not easy to assess which people are the most important network hubs. Modelling studies find that vaccinating essential workers in high-contact occupations first is promising in this regard [81–83]. Nonetheless, deciding what counts as 'essential' may be controversial, making it hard to design a fair and non-discriminatory policy for a vaccination program that focuses on people with more contacts.

In the end, the trade-off between different vaccination strategies depends on various considerations and factors [70, 71].

8.2.2 *Vaccine uptake, hesitancy and barriers*

Regardless of the strategy of the vaccination program, it will only be successful if the vaccine uptake is as high as planned, i.e. if people actually get vaccinated.

Like others (e.g. [84, 85]), we model that vaccination uptake rises and falls with the number of people in intensive care through mechanisms such as risk perception (chapter 5). In Section 8.1.2, we discuss that health-protective behaviour is also – and maybe even more so – dependent on factors other than risk perception. The same applies to getting vaccinated, which is an example of health-protective behaviour: Vaccine hesitancy is, e.g., correlated with concerns about vaccine safety and side effects (e.g. [86–88]), a lack of trust (e.g. [86, 88]) and perceived low efficacy of getting vaccinated (e.g. [86–88]). Marginalised groups tend to be affected even stronger, also due to being mistreated and neglected by official institutions in other circumstances as well (e.g [89, 90]). Community-based interventions, monetary incentives, and digital health literacy interventions have been found to address some these problems and reduce vaccine hesitancy (e.g. [91]), along with supportive political leadership (e.g. [92]). In chapter 3, we considered the possibility of a vaccination mandate; but due to being contrary to people's desire to make an informed individual decision to vaccinate, a general vaccination mandate for COVID-19 is not recommended (e.g. [93]). Instead, strengthening pro-social values such as solidarity is put forward (e.g. [3, 94]).

Beyond vaccine hesitancy, there are further barriers that diminish vaccine uptake. As is done in other models (e.g. [84, 85]), we assume that everyone who wants to get vaccinated, gets vaccinated (chapter 4 and chapter 5). However, in reality, there are systemic issues that pose structural barriers to uptake: a lack of time, missing transportation options, high costs, or a lack of clinics or outlet locations can prevent people from getting vaccinated (e.g. [95, 96]). In general, accessibility and convenience play a large role in uptake (e.g. [96, 97]). Barriers are especially high for ethnic minorities and migrants, with added language and communication issues, fear of deportation, lack of specific guidelines and knowledge of health-care professionals, as well as reduced physical, legal and bureaucratic access (e.g. [89, 98–100]). Hence, more attention, awareness and inclusive action are called for (e.g. [99]).

Another level of barriers are supply-side barriers that low- and middle-income countries have had and still have to face. Low- and middle-income countries have little vaccine production, have trouble procuring high-

quality vaccines due to their costs, got pushed to the end of the cue in the global vaccine procurement, lack infrastructure and resources for vaccine storage and distribution, and have sub-optimal vaccine delivery and administration (e.g. [101]). The COVID-19 Vaccines Global Access (COVAX) initiative was meant to solve the issue through a joint and equitable international procurement mechanism; however, "its impact was undermined by [vaccine] donors' and industry's pursuit of national security, diplomatic and commercial interests" [102]. In response, international cooperation, rethinking issues around intellectual property and globally diversifying vaccine production are suggested (e.g. [103, 104]).

In summary, achieving sufficient COVID-19 vaccine uptake faces multiple challenges. Vaccine hesitancy driven by various factors besides risk-perception can only be overcome through communication, community engagement, and more systemic political action. Uptake barriers like limited accessibility, especially for marginalized groups, would also need to be addressed through systemic improvements. Also, global inequities in vaccine access highlight the need for international cooperation and supply-side solutions. Comprehensively tackling willingness, access, and availability is key to realizing the public health potential of vaccines. These issues remain important to be tackled as waning immunity against COVID-19, other diseases such as influenza and potential new pandemics keep the need for successful vaccination programs high. The models presented in this thesis and other models in the literature simplify these complex dynamics, but integrating social and policy perspectives remains vital for proper pandemic analysis and response.

8.3 GLOBAL PERSPECTIVE

In part ii, we model and discuss the COVID-19 pandemic from a European perspective. We suggest that strategies may not work well if only implemented nationally but that international cooperation and coordination on at least an European level is crucial (chapter 3 and chapter 7). For example, coordinated implementation or relaxation of NPIs across Europe could greatly contribute to mitigation of disease spread [105]. Otherwise, mobility and the introduction of new cases and perhaps even new variants of concern diminish the feasibility of, e.g., a low incidence strategy. In fact, multi-seeding independent outbreaks through mobility is shown to increase incidence non-linearly [106]. Hence,

we have used some of these results to evidence science communication to call for pan-European action [4, 107–109].

However, for a global pandemic, solely regional cooperation is not enough: SARS-CoV-2 and later variants of concerns emerged in various continents but spread worldwide (e.g. [110]). Globalised supply chains were affected by national COVID-19 policies as well (e.g. [111]). Global international cooperation can be a solution to this problem. After insufficient cooperation during the COVID-19 pandemic, "governments are [at the time of writing] negotiating a new pandemic treaty and revising the International Health Regulations" [112]. As discussed in previous Section 8.2.2, this could, e.g., contribute to global vaccine equity.

We have also seen the important role of data in modelling and pandemic response. The complex models in chapter 4, chapter 5 and chapter 6 as well as a lot of the modelling literature cited above were heavily informed by various kinds of data and data sources. Our and other rigorous statistical analyses would not have been possible at all if not for the ample database in a few countries (e.g. [5, 6, 26, 63]). Unfortunately, such good data were rarely available in a lot of low- and middle-income countries. One might argue that model results such as the ones of this thesis are completely transferable internationally and answer the key pandemic response questions of every country. However, results, such as the public health outcomes of specific mitigation strategies, already vary between countries in Europe (e.g. [5, 24, 63]). On a global level, the variety in contact patterns, age structures, cultural norms, political and socio-economic circumstances, and seasonality demand different models and yield different results and conclusions. Besides that, data is also in itself essential to understand the state of the pandemic. Hence, the unavailability of data for modelling, monitoring, and analysis is another important factor undermining successful global coordination and equity. For pandemic preparedness and future response, robust funding for disease surveillance systems and data platforms are thus crucial [113].

In summary, while the models in this thesis focus on Europe, the COVID-19 pandemic demands global cooperation and equitable access. Pathogens ignore borders, and variants emerging anywhere endanger principally everyone everywhere. Regional coordination like in Europe helps, but fully containing pandemics necessitates worldwide collaboration on travel restrictions, data sharing, vaccine distribution, and more. Moreover, limited model generalisability makes tailoring insights to local contexts essential and highlights the problem of insufficient data from

low- and middle-income countries. By supporting global surveillance
and response capacity along with international partnerships, pandemic
preparedness will improve. But the fundamental reality is that the world
is interconnected — locally optimizing alone cannot solve global crises.

THE ROLE OF COMPLEX SYSTEMS MODELLING IN PANDEMIC RESPONSE

The COVID-19 pandemic has demonstrated the immense value of using complex systems approaches to model infectious disease transmission dynamics. Framing epidemiology as a complex dynamical system enables a clear qualitative and detailed quantitative understanding of public health emergencies. Specifically, this thesis illustrates several key strengths of the complex systems perspective for informing pandemic response:

First, it articulates core conceptual arguments and mechanistic hypotheses about disease spread, behavioral changes, and policy impacts through formal mathematical models. The presented models act as theoretical representations to test assumptions. Think back for example to the analysis of the test-trace-isolate intervention in, e.g., chapter 1 or to the illustration of the relevance of the feedback loop between disease spread and human behaviour (chapter 5). Even simple prototypes can elucidate first-order effects and trade-offs, such as the existence of a disease spread tipping point (chapter 2) or the effects of higher immunity or new virus variants on hospitalisations (chapter 8).

Second, incorporating real-world data into the models facilitates estimating rough magnitudes and outcomes. With care, useful projections can inform preparedness and evaluation of response measures. For example, chapter 4 shows us that an immediate lifting of restrictions at the considered time would not even be the option with "the most freedom". Furthermore, we illustrate that no measures at all would have been catastrophic in the winter of 21/22, but also that too many measures would have been counter-productive (chapter 5). Hence, models act as virtual laboratories grounded by observations.

Third, complex system models can explicitly analyse mechanics that are not directly observable and trade-offs arising from feedbacks and non-linearities inherent to epidemiology. In chapter 5, we are able to consider the impacts of multiple such trade-offs: On the one hand, more mandatory measures in winter cause fewer severe cases of COVID-19 while implemented. On the other hand, this leads to less immunity in the population in spring through two mechanisms at the same time: less post-infection immunity through the lower incidence and less vaccination

coverage due to the behavioural feedback. To understand whether this would mean another uncontrolled wave in spring, one even needs to take favourable seasonality into account. Without a quantitative approach like in this thesis, understanding the relative impact of these different mechanistic contributions would not be feasible. Thereby, models aid systematic exploration of such dynamics.

Finally, simpler mathematical models efficiently search the phase space and identify key mechanisms. Their findings in turn inform detailed agent-based and computational models. Hence, complex systems modeling provides the theoretical scaffolding for data-driven forecasting and also post-factual statistical analyses (e.g. chapter 6). In the SIR-type framework including more complex dynamics through, e.g., reporting delays, we are able to accurately quantify the impact of real-world event on the pandemic.

However, models alone cannot suffice. Interdisciplinary communication is vital to ensure models capture relevant mechanisms from across the health sciences, social sciences, and humanities (e.g. [114]). Models must be embedded in policy contexts through communication as well. And even the best models cannot foretell unprecedented events or control messy real-world dynamics. Humility remains essential.

In summary, a dynamical systems perspective generates critical insights, guides intuition, estimates outcomes, and informs decisions. Alongside domain knowledge and political acumen, it is an invaluable tool for understanding and responding to pandemics. But one needs to keep in mind that it is only one complementary tool among many required to safeguard public health in a complex world.

BIBLIOGRAPHY

[1] James Clerk Maxwell. *Matter and motion.* Cambridge University Press, 1888. DOI: https://doi.org/10.1017/CBO9780511709326.

[2] Yaneer Bar-Yam. "General features of complex systems." In: *Encyclopedia of Life Support Systems (EOLSS), UNESCO, EOLSS Publishers, Oxford, UK* 1 (2002).

[3] Emil N. Iftekhar, Viola Priesemann, Rudi Balling, Simon Bauer, Philippe Beutels, André Calero Valdez, Sarah Cuschieri, Thomas Czypionka, Uga Dumpis, Enrico Glaab, et al. "A look into the future of the COVID-19 pandemic in Europe: an expert consultation." In: *The Lancet Regional Health–Europe* 8 (2021). DOI: https://doi.org/10.1016/j.lanepe.2021.100185.

[4] Viola Priesemann, Melanie M. Brinkmann, Sandra Ciesek, Sarah Cuschieri, Thomas Czypionka, Giulia Giordano, Deepti Gurdasani, Claudia Hanson, Niel Hens, Emil N. Iftekhar, et al. "Calling for pan-European commitment for rapid and sustained reduction in SARS-CoV-2 infections." In: *The Lancet* 397.10269 (2021), pp. 92–93. DOI: https://doi.org/10.1016/S0140-6736(20)32625-8.

[5] Seth Flaxman, Swapnil Mishra, Axel Gandy, H Juliette T Unwin, Thomas A Mellan, Helen Coupland, Charles Whittaker, Harrison Zhu, Tresnia Berah, Jeffrey W Eaton, et al. "Estimating the effects of non-pharmaceutical interventions on COVID-19 in Europe." In: *Nature* 584.7820 (2020), pp. 257–261.

[6] Jan M Brauner, Sören Mindermann, Mrinank Sharma, David Johnston, John Salvatier, Tomáš Gavenčiak, Anna B Stephenson, Gavin Leech, George Altman, Vladimir Mikulik, et al. "Inferring the effectiveness of government interventions against COVID-19." In: *Science* 371.6531 (2021), eabd9338.

[7] Sebastian Contreras, Jonas Dehning, Matthias Loidolt, Johannes Zierenberg, F Paul Spitzner, Jorge H Urrea-Quintero, Sebastian B Mohr, Michael Wilczek, Michael Wibral, and Viola Priesemann. "The challenges of containing SARS-CoV-2 via test-trace-and-isolate." In: *Nature communications* 12.1 (2021), p. 378.

[8]   D. Arrowsmith and C.M. Place. *Dynamical Systems: Differential Equations, Maps, and Chaotic Behaviour*. Chapman Hall/CRC Mathematics Series. Taylor & Francis, 1992. ISBN: 9780412390807. URL: https://books.google.ch/books?id=8qCcP7KNaZ0C.

[9]   William Ogilvy Kermack and Anderson G McKendrick. "A contribution to the mathematical theory of epidemics." In: *Proceedings of the royal society of london. Series A, Containing papers of a mathematical and physical character* 115.772 (1927), pp. 700–721.

[10]   Odo Diekmann, Hans Heesterbeek, and Tom Britton. *Mathematical tools for understanding infectious disease dynamics*. Vol. 7. Princeton University Press, 2013.

[11]   Salihu S Musa, Shi Zhao, Maggie H Wang, Abdurrazaq G Habib, Umar T Mustapha, and Daihai He. "Estimation of exponential growth rate and basic reproduction number of the coronavirus disease 2019 (COVID-19) in Africa." In: *Infectious diseases of poverty* 9.1 (2020), pp. 1–6.

[12]   Shiva Moein, Niloofar Nickaeen, Amir Roointan, Niloofar Borhani, Zarifeh Heidary, Shaghayegh Haghjooy Javanmard, Jafar Ghaisari, and Yousof Gheisari. "Inefficiency of SIR models in forecasting COVID-19 epidemic: a case study of Isfahan." In: *Scientific reports* 11.1 (2021), p. 4725.

[13]   René Thomas, Denis Thieffry, and Marcelle Kaufman. "Dynamical behaviour of biological regulatory networks—I. Biological role of feedback loops and practical use of the concept of the loop-characteristic state." In: *Bulletin of mathematical biology* 57 (1995), pp. 247–276.

[14]   Peter M Cox, Richard A Betts, Chris D Jones, Steven A Spall, and Ian J Totterdell. "Acceleration of global warming due to carbon-cycle feedbacks in a coupled climate model." In: *Nature* 408.6809 (2000), pp. 184–187.

[15]   Anne S Warlaumont, Jeffrey A Richards, Jill Gilkerson, and D Kimbrough Oller. "A social feedback loop for speech development and its reduction in autism." In: *Psychological science* 25.7 (2014), pp. 1314–1324.

[16]   Safieddine Bouali. "Feedback loop in extended Van der Pol's equation applied to an economic model of cycles." In: *International Journal of Bifurcation and Chaos* 9.04 (1999), pp. 745–756.

[17]   David N Ford. "A behavioral approach to feedback loop domi-
       nance analysis." In: *System Dynamics Review: The Journal of
       the System Dynamics Society* 15.1 (1999), pp. 3–36.

[18]   Brahim Haraoubia. "2 - Low-frequency Oscillators." In: *Non-
       linear Electronics 1*. Ed. by Brahim Haraoubia. Elsevier, 2018,
       pp. 83–123. ISBN: 978-1-78548-300-4. DOI: https://doi.org/
       10.1016/B978-1-78548-300-4.50002-6. URL: https://www.
       sciencedirect.com/science/article/pii/B9781785483004500026.

[19]   Erik Plahte, Thomas Mestl, and Stig W Omholt. "Feedback
       loops, stability and multistationarity in dynamical systems." In:
       Journal of Biological Systems 3.02 (1995), pp. 409–413.

[20]   Simone Pigolotti, Sandeep Krishna, and Mogens H Jensen. "Os-
       cillation patterns in negative feedback loops." In: *Proceedings of
       the National Academy of Sciences* 104.16 (2007), pp. 6533–6537.

[21]   Xavier Rodet and Christophe Vergez. "Nonlinear dynamics in
       physical models: Simple feedback-loop systems and properties."
       In: *Computer Music Journal* 23.3 (1999), pp. 18–34.

[22]   Michael A Johnson and Mohammad H Moradi. *PID control.*
       Springer, 2005.

[23]   Aldo Ianni and Nicola Rossi. "SIR-PID: a proportional–integral–
       derivative controller for COVID-19 outbreak containment." In:
       Physics 3.3 (2021), pp. 459–472.

[24]   Simon Bauer, Sebastian Contreras, Jonas Dehning, Matthias
       Linden, Emil N. Iftekhar, Sebastian B. Mohr, Alvaro Olivera-
       Nappa, and Viola Priesemann. "Relaxing restrictions at the
       pace of vaccination increases freedom and guards against further
       COVID-19 waves." In: *PLoS computational biology* 17.9 (2021),
       e1009288. DOI: https://doi.org/10.1371/journal.pcbi.
       1009288.

[25]   Philipp Dönges, Joel Wagner, Sebastian Contreras, Emil N.
       Iftekhar, Simon Bauer, Sebastian B. Mohr, Jonas Dehning, An-
       dré Calero Valdez, Mirjam Kretzschmar, Michael Mäs, et al.
       "Interplay Between Risk Perception, Behavior, and COVID-19
       Spread." In: *Frontiers in Physics* 10 (2022). ISSN: 2296-424X.
       DOI: 10.3389/fphy.2022.842180.

[26]   Jonas Dehning, Sebastian B. Mohr, Sebastian Contreras, Philipp
       Dönges, Emil N. Iftekhar, Oliver Schulz, Philip Bechtle, and
       Viola Priesemann. "Impact of the Euro 2020 championship on the

spread of COVID-19." In: *Nature Communications* 14.1 (2023), p. 122. ISSN: 2041-1723. DOI: 10.1038/s41467-022-35512-x.

[27] Thomas Czypionka, Emil N. Iftekhar, Barbara Prainsack, Viola Priesemann, Simon Bauer, Andre Calero Valdez, Sarah Cuschieri, Enrico Glaab, Eva Grill, Jenny Krutzinna, et al. "The benefits, costs and feasibility of a low incidence COVID-19 strategy." In: *The Lancet Regional Health–Europe* 13 (2022). DOI: https://doi.org/10.1016/j.lanepe.2021.100294.

[28] Alexandra Teslya, Thi Mui Pham, Noortje G Godijk, Mirjam E Kretzschmar, Martin CJ Bootsma, and Ganna Rozhnova. "Impact of self-imposed prevention measures and short-term government-imposed social distancing on mitigating and delaying a COVID-19 epidemic: A modelling study." In: *PLoS medicine* 17.7 (2020), e1003166.

[29] Bruno Buonomo and Rossella Della Marca. "Effects of information-induced behavioural changes during the COVID-19 lockdowns: the case of Italy." In: *Royal Society open science* 7.10 (2020), p. 201635.

[30] Lun Liu, Zhu Zhang, Hui Wang, Shenhao Wang, Shengsheng Zhuang, and Jishan Duan. "Comparing modelling approaches for the estimation of government intervention effects in COVID-19: Impact of voluntary behavior changes." In: *Plos one* 18.2 (2023), e0276906.

[31] Julian C Jamison, Donald Bundy, Dean T Jamison, Jacob Spitz, and Stéphane Verguet. "Comparing the impact on COVID-19 mortality of self-imposed behavior change and of government regulations across 13 countries." In: *Health services research* 56.5 (2021), pp. 874–884.

[32] Youpei Yan, Amyn A Malik, Jude Bayham, Eli P Fenichel, Chandra Couzens, and Saad B Omer. "Measuring voluntary and policy-induced social distancing behavior during the COVID-19 pandemic." In: *Proceedings of the National Academy of Sciences* 118.16 (2021), e2008814118.

[33] Kaiyuan Sun, Wei Wang, Lidong Gao, Yan Wang, Kaiwei Luo, Lingshuang Ren, Zhifei Zhan, Xinghui Chen, Shanlu Zhao, Yiwei Huang, et al. "Transmission heterogeneities, kinetics, and controllability of SARS-CoV-2." In: *Science* 371.6526 (2021), eabe2424.

[34]   Max SY Lau, Bryan Grenfell, Michael Thomas, Michael Bryan, Kristin Nelson, and Ben Lopman. "Characterizing superspreading events and age-specific infectiousness of SARS-CoV-2 transmission in Georgia, USA." In: *Proceedings of the National Academy of Sciences* 117.36 (2020), pp. 22430–22435.

[35]   Liang Wang, Xavier Didelot, Jing Yang, Gary Wong, Yi Shi, Wenjun Liu, George F Gao, and Yuhai Bi. "Inference of person-to-person transmission of COVID-19 reveals hidden super-spreading events during the early outbreak phase." In: *Nature communications* 11.1 (2020), p. 5006.

[36]   Agus Hasan, Hadi Susanto, Muhammad Firmansyah Kasim, Nuning Nuraini, Bony Lestari, Dessy Triany, and Widyastuti Widyastuti. "Superspreading in early transmissions of COVID-19 in Indonesia." In: *Scientific reports* 10.1 (2020), p. 22386.

[37]   Benjamin M Althouse, Edward A Wenger, Joel C Miller, Samuel V Scarpino, Antoine Allard, Laurent Hébert-Dufresne, and Hao Hu. "Superspreading events in the transmission dynamics of SARS-CoV-2: Opportunities for interventions and control." In: *PLoS biology* 18.11 (2020), e3000897.

[38]   Ruth McCabe, Nora Schmit, Paula Christen, Josh C D'Aeth, Alessandra Løchen, Dheeya Rizmie, Shevanthi Nayagam, Marisa Miraldo, Paul Aylin, Alex Bottle, et al. "Adapting hospital capacity to meet changing demands during the COVID-19 pandemic." In: *BMC medicine* 18.1 (2020), pp. 1–12.

[39]   Brendon Sen-Crowe, Mason Sutherland, Mark McKenney, and Adel Elkbuli. "A closer look into global hospital beds capacity and resource shortages during the COVID-19 pandemic." In: *Journal of Surgical Research* 260 (2021), pp. 56–63.

[40]   Cecilia Vindrola-Padros, Lily Andrews, Anna Dowrick, Nehla Djellouli, Harrison Fillmore, Elysse Bautista Gonzalez, Dena Javadi, Sasha Lewis-Jackson, Louisa Manby, Lucy Mitchinson, et al. "Perceptions and experiences of healthcare workers during the COVID-19 pandemic in the UK." In: *BMJ open* 10.11 (2020), e040503.

[41]   Nehul Agarwal, Chandan Swaroop Meena, Binju P Raj, Lohit Saini, Ashok Kumar, N Gopalakrishnan, Anuj Kumar, Nagesh Babu Balam, Tabish Alam, Nishant Raj Kapoor, et al. "Indoor air quality improvement in COVID-19 pandemic." In: *Sustainable Cities and Society* 70 (2021), p. 102942.

[42]   Ilka Wahl and Hedda Wardemann. "Sterilizing immunity: understanding COVID-19." In: *Immunity* 55.12 (2022), pp. 2231–2235.

[43]   Claudia Sievers, Benedikt Zacher, Alexander Ullrich, Matthew Huska, Stephan Fuchs, Silke Buda, Walter Haas, Michaela Diercke, Matthias An der Heiden, and Stefan Kröger. "SARS-CoV-2 Omicron variants BA. 1 and BA. 2 both show similarly reduced disease severity of COVID-19 compared to Delta, Germany, 2021 to 2022." In: *Eurosurveillance* 27.22 (2022), p. 2200396.

[44]   Laura A VanBlargan, John M Errico, Peter J Halfmann, Seth J Zost, James E Crowe Jr, Lisa A Purcell, Yoshihiro Kawaoka, Davide Corti, Daved H Fremont, and Michael S Diamond. "An infectious SARS-CoV-2 B. 1.1. 529 Omicron virus escapes neutralization by therapeutic monoclonal antibodies." In: *Nature medicine* 28.3 (2022), pp. 490–495.

[45]   Venice Servellita, Abdullah M Syed, Mary Kate Morris, Noah Brazer, Prachi Saldhi, Miguel Garcia-Knight, Bharath Sreekumar, Mir M Khalid, Alison Ciling, Pei-Yi Chen, et al. "Neutralizing immunity in vaccine breakthrough infections from the SARS-CoV-2 Omicron and Delta variants." In: *Cell* 185.9 (2022), pp. 1539–1548.

[46]   Sophia T Tan, Ada T Kwan, Isabel Rodríguez-Barraquer, Benjamin J Singer, Hailey J Park, Joseph A Lewnard, David Sears, and Nathan C Lo. "Infectiousness of SARS-CoV-2 breakthrough infections and reinfections during the Omicron wave." In: *Nature Medicine* 29.2 (2023), pp. 358–365.

[47]   Farhina Mozaffer, Philip Cherian, Sandeep Krishna, Brian Wahl, and Gautam I Menon. "Effect of hybrid immunity, school reopening, and the Omicron variant on the trajectory of the COVID-19 epidemic in India: a modelling study." In: *The Lancet Regional Health-Southeast Asia* 8 (2023).

[48]   Vrishali S Salian, Jessica A Wright, Peter T Vedell, Sanjana Nair, Chenxu Li, Mahathi Kandimalla, Xiaojia Tang, Eva M Carmona Porquera, Krishna R Kalari, and Karunya K Kandimalla. "COVID-19 transmission, current treatment, and future therapeutic strategies." In: *Molecular pharmaceutics* 18.3 (2021), pp. 754–771.

[49] John H Beigel, Kay M Tomashek, Lori E Dodd, Aneesh K Mehta, Barry S Zingman, Andre C Kalil, Elizabeth Hohmann, Helen Y Chu, Annie Luetkemeyer, Susan Kline, et al. "Remdesivir for the treatment of Covid-19." In: *New England Journal of Medicine* 383.19 (2020), pp. 1813–1826.

[50] Folashade B Agusto, Igor V Erovenko, Alexander Fulk, Qays Abu-Saymeh, Daniel Romero-Alvarez, Joan Ponce, Suzanne Sindi, Omayra Ortega, Jarron M Saint Onge, and A Townsend Peterson. "To isolate or not to isolate: The impact of changing behavior on COVID-19 transmission." In: *BMC Public Health* 22.1 (2022), pp. 1–20.

[51] Xin Yu Yang, Rui Ning Gong, Samuel Sassine, Maxime Morsa, Alexandra Sonia Tchogna, Olivier Drouin, Nicholas Chadi, and Prévost Jantchou. "Risk perception of COVID-19 infection and adherence to preventive measures among adolescents and young adults." In: *Children* 7.12 (2020), p. 311.

[52] Mohammad Rayani, Saba Rayani, and Fatemeh Najafi-Sharjabad. "COVID-19-related knowledge, risk perception, information seeking, and adherence to preventive behaviors among undergraduate students, southern Iran." In: *Environmental Science and Pollution Research* 28 (2021), pp. 59953–59962.

[53] Richard Brown, Lynne Coventry, and Gillian Pepper. "COVID-19: the relationship between perceptions of risk and behaviours during lockdown." In: *Journal of Public Health* 31.4 (2023), pp. 623–633.

[54] Anna Petherick, Rafael Goldszmidt, Eduardo B Andrade, Rodrigo Furst, Thomas Hale, Annalena Pott, and Andrew Wood. "A worldwide assessment of changes in adherence to COVID-19 protective behaviours and hypothesized pandemic fatigue." In: *Nature Human Behaviour* 5.9 (2021), pp. 1145–1160.

[55] Claudia R Schneider, Sarah Dryhurst, John Kerr, Alexandra LJ Freeman, Gabriel Recchia, David Spiegelhalter, and Sander van der Linden. "COVID-19 risk perception: a longitudinal analysis of its predictors and associations with health protective behaviours in the United Kingdom." In: *Journal of Risk Research* 24.3-4 (2021), pp. 294–313.

[56] Lucia Savadori and Marco Lauriola. "Risk perception and protective behaviors during the rise of the COVID-19 outbreak in Italy." In: *Frontiers in psychology* (2021), p. 3822.

[57] Pablo Cabrera-Álvarez, Matthew J Hornsey, and Josep Lobera. "Determinants of self-reported adherence to COVID-19 regulations in Spain: social norms, trust and risk perception." In: *Health Promotion International* 37.6 (2022), daac138.

[58] Lilian Kojan, Laura Burbach, Martina Ziefle, and André Calero Valdez. "Perceptions of behaviour efficacy, not perceptions of threat, are drivers of COVID-19 protective behaviour in Germany." In: *Humanities and Social Sciences Communications* 9.1 (2022), pp. 1–15.

[59] Ricci P H Yue, Bobo HP Lau, Cecilia LW Chan, and Siu-Man Ng. "Risk perception as a double-edged sword in policy compliance in COVID-19 pandemic? A two-phase evaluation from Hong Kong." In: *Journal of Risk Research* 25.9 (2022), pp. 1131–1145.

[60] Viktor K Jirsa, Spase Petkoski, Huifang Wang, Marmaduke Woodman, Jan Fousek, Cornelia Betsch, Lisa Felgendreff, Robert Bohm, Lau Lilleholt, Ingo Zettler, et al. "Integrating psychosocial variables and societal diversity in epidemic models for predicting COVID-19 transmission dynamics." In: *PLOS Digital Health* 1.8 (2022), e0000098.

[61] Andreas Koher, Frederik Jørgensen, Michael Bang Petersen, and Sune Lehmann. "Epidemic modelling of monitoring public behavior using surveys during pandemic-induced lockdowns." In: *Communications Medicine* 3.1 (2023), p. 80.

[62] *infoXpand – Interaction between infodemics and pandemics. Modeling Network for Severe Infectious Diseases.* https://webszh.uk-halle.de/monid/?page_id=2004&lang=en. Accessed: 21.11.2023.

[63] Yong Ge, Wen-Bin Zhang, Xilin Wu, Corrine W Ruktanonchai, Haiyan Liu, Jianghao Wang, Yongze Song, Mengxiao Liu, Wei Yan, Juan Yang, et al. "Untangling the changing impact of non-pharmaceutical interventions and vaccination on European COVID-19 trajectories." In: *Nature Communications* 13.1 (2022), p. 3106.

[64] Oguzhan Alagoz, Ajay K Sethi, Brian W Patterson, Matthew Churpek, Ghalib Alhanaee, Elizabeth Scaria, and Nasia Safdar. "The impact of vaccination to control COVID-19 burden in the United States: A simulation modeling approach." In: *PloS one* 16.7 (2021), e0254456.

[65] Sam Moore, Edward M Hill, Michael J Tildesley, Louise Dyson, and Matt J Keeling. "Vaccination and non-pharmaceutical interventions for COVID-19: a mathematical modelling study." In: *The lancet infectious diseases* 21.6 (2021), pp. 793–802.

[66] Kate M Bubar, Kyle Reinholt, Stephen M Kissler, Marc Lipsitch, Sarah Cobey, Yonatan H Grad, and Daniel B Larremore. "Model-informed COVID-19 vaccine prioritization strategies by age and serostatus." In: *Science* 371.6352 (2021), pp. 916–921.

[67] Joan Saldaña and Caterina Scoglio. "Influence of heterogeneous age-group contact patterns on critical vaccination rates for herd immunity to SARS-CoV-2." In: *Scientific Reports* 12.1 (2022), p. 2640.

[68] Tom Britton, Frank Ball, and Pieter Trapman. "A mathematical model reveals the influence of population heterogeneity on herd immunity to SARS-CoV-2." In: *science* 369.6505 (2020), pp. 846–849.

[69] Laura Matrajt, Julia Eaton, Tiffany Leung, and Elizabeth R Brown. "Vaccine optimization for COVID-19: Who to vaccinate first?" In: *Science Advances* 7.6 (2021), eabf1374.

[70] Nuru Saadi, Y-Ling Chi, Srobana Ghosh, Rosalind M Eggo, Ciara V McCarthy, Matthew Quaife, Jeanette Dawa, Mark Jit, and Anna Vassall. "Models of COVID-19 vaccine prioritisation: a systematic literature search and narrative review." In: *BMC medicine* 19 (2021), pp. 1–11.

[71] Cong Yang, Yali Yang, and Yang Li. "Assessing vaccination priorities for different ages and age-specific vaccination strategies of covid-19 using an seir modelling approach." In: *Plos one* 16.12 (2021), e0261236.

[72] Chao Zuo, Zeyang Meng, Fenping Zhu, Yuzhi Zheng, and Yuting Ling. "Assessing vaccination prioritization strategies for COVID-19 in South Africa based on age-specific compartment model." In: *Frontiers in public health* 10 (2022), p. 876551.

[73] Antonio Montalbán, Rodrigo M Corder, and M Gabriela M Gomes. "Herd immunity under individual variation and reinfection." In: *Journal of Mathematical Biology* 85.1 (2022), p. 2.

[74] M Gabriela M Gomes, Marcelo U Ferreira, Rodrigo M Corder, Jessica G King, Caetano Souto-Maior, Carlos Penha-Gonçalves, Guilherme Gonçalves, Maria Chikina, Wesley Pegden, and Ricardo Aguas. "Individual variation in susceptibility or exposure

to SARS-CoV-2 lowers the herd immunity threshold." In: *Journal of theoretical biology* 540 (2022), p. 111063.

[75]   Fan Bai. "Effect of population heterogeneity on herd immunity and on vaccination decision making process." In: *Journal of theoretical biology* 526 (2021), p. 110795.

[76]   Elamin H Elbasha and Abba B Gumel. "Vaccination and herd immunity thresholds in heterogeneous populations." In: *Journal of mathematical biology* 83.6-7 (2021), p. 73.

[77]   Yaron Oz, Ittai Rubinstein, and Muli Safra. "Heterogeneity and superspreading effect on herd immunity." In: *Journal of Statistical Mechanics: Theory and Experiment* 2021.3 (2021), p. 033405.

[78]   Istvan Szapudi. "Heterogeneity in SIR epidemics modeling: superspreaders and herd immunity." In: *Applied Network Science* 5.1 (2020), p. 93.

[79]   Tarcísio M Rocha Filho, José FF Mendes, Thiago B Murari, Aloísio S Nascimento Filho, Antônio JA Cordeiro, Walter M Ramalho, Fúlvio A Scorza, Antônio-Carlos G Almeida, and Marcelo A Moret. "Optimization of COVID-19 vaccination and the role of individuals with a high number of contacts: A model based approach." In: *Plos one* 17.3 (2022), e0262433.

[80]   Francesco Di Lauro, Luc Berthouze, Matthew D Dorey, Joel C Miller, and István Z Kiss. "The Impact of Contact Structure and Mixing on Control Measures and Disease-Induced Herd Immunity in Epidemic Models: A Mean-Field Model Perspective." In: *Bulletin of Mathematical Biology* 83 (2021), pp. 1–25.

[81]   Nicola Mulberry, Paul Tupper, Erin Kirwin, Christopher McCabe, and Caroline Colijn. "Vaccine rollout strategies: The case for vaccinating essential workers early." In: *PLOS Global Public Health* 1.10 (2021), e0000020.

[82]   Md Rafiul Islam, Tamer Oraby, Audrey McCombs, Mohammad Mihrab Chowdhury, Mohammad Al-Mamun, Michael G Tyshenko, and Claus Kadelka. "Evaluation of the United States COVID-19 vaccine allocation strategy." In: *PloS one* 16.11 (2021), e0259700.

[83]   Hendrik Nunner, Arnout van de Rijt, and Vincent Buskens. "Prioritizing high-contact occupations raises effectiveness of vaccination campaigns." In: *Scientific reports* 12.1 (2022), p. 737.

[84] Chao Zuo, Fenping Zhu, and Yuting Ling. "Analyzing COVID-19 vaccination behavior using an seirm/v epidemic model with awareness decay." In: *Frontiers in Public Health* 10 (2022), p. 817749.

[85] Bruno Buonomo, Rossella Della Marca, Alberto d'Onofrio, and Maria Groppi. "A behavioural modelling approach to assess the impact of COVID-19 vaccine hesitancy." In: *Journal of theoretical biology* 534 (2022), p. 110973.

[86] Gianmarco Troiano and Alessandra Nardi. "Vaccine hesitancy in the era of COVID-19." In: *Public health* 194 (2021), pp. 245–251.

[87] Junjie Aw, Jun Jie Benjamin Seng, Sharna Si Ying Seah, and Lian Leng Low. "COVID-19 vaccine hesitancy—A scoping review of literature in high-income countries." In: *Vaccines* 9.8 (2021), p. 900.

[88] Md Rafiul Biswas, Mahmood Saleh Alzubaidi, Uzair Shah, Alaa A Abd-Alrazaq, and Zubair Shah. "A scoping review to find out worldwide COVID-19 vaccine hesitancy and its underlying determinants." In: *Vaccines* 9.11 (2021), p. 1243.

[89] Mohammed Abba-Aji, David Stuckler, Sandro Galea, and Martin McKee. "Ethnic/racial minorities' and migrants' access to COVID-19 vaccines: A systematic review of barriers and facilitators." In: *Journal of migration and health* 5 (2022), p. 100086.

[90] Ebrahim Payberah, Daniel Payberah, Ashish Sarangi, and Jayasudha Gude. "COVID-19 vaccine hesitancy in patients with mental illness: strategies to overcome barriers—a review." In: *Journal of the Egyptian Public Health Association* 97.1 (2022), pp. 1–6.

[91] Prem Singh, Pritu Dhalaria, Satabdi Kashyap, Gopal Krishna Soni, Partha Nandi, Shreeparna Ghosh, Mrinal Kar Mohapatra, Apurva Rastogi, and Divya Prakash. "Strategies to overcome vaccine hesitancy: a systematic review." In: *Systematic reviews* 11.1 (2022), pp. 1–13.

[92] Rina Fajri Nuwarda, Iqbal Ramzan, Lynn Weekes, and Veysel Kayser. "Vaccine hesitancy: contemporary issues and historical background." In: *Vaccines* 10.10 (2022), p. 1595.

[93] Amelia Fiske, Franziska Schönweitz, Johanna Eichinger, Bettina Zimmermann, Nora Hangel, Anna Sierawska, Stuart McLennan, and Alena Buyx. "The COVID-19 Vaccine: Trust, doubt, and hope for a future beyond the pandemic in Germany." In: *PloS one* 17.4 (2022), e0266659.

[94]   Barbara Prainsack. "Solidarity in times of pandemics." In: *Democratic theory* 7.2 (2020), pp. 124–133.

[95]   Rebecca J Fisk. "Barriers to vaccination for coronavirus disease 2019 (COVID-19) control: experience from the United States." In: *Global Health Journal* 5.1 (2021), pp. 51–55.

[96]   Anuli Njoku, Marcelin Joseph, and Rochelle Felix. "Changing the narrative: structural barriers and racial and ethnic inequities in COVID-19 vaccination." In: *International journal of environmental research and public health* 18.18 (2021), p. 9904.

[97]   George T Nawas, Rana S Zeidan, Cole A Edwards, and Rania H El-Desoky. "Barriers to COVID-19 vaccines and strategies to improve acceptability and uptake." In: *Journal of pharmacy practice* 36.4 (2023), pp. 900–904.

[98]   Atiya Kamal, Ava Hodson, and Julia M Pearce. "A rapid systematic review of factors influencing COVID-19 vaccination uptake in minority ethnic groups in the UK." In: *Vaccines* 9.10 (2021), p. 1121.

[99]   Alison F Crawshaw, Anna Deal, Kieran Rustage, Alice S Forster, Ines Campos-Matos, Tushna Vandrevala, Andrea Würz, Anastasia Pharris, Jonathan E Suk, John Kinsman, et al. "What must be done to tackle vaccine hesitancy and barriers to COVID-19 vaccination in migrants?" In: *Journal of travel medicine* 28.4 (2021), taab048.

[100]   Alison F Crawshaw, Yasmin Farah, Anna Deal, Kieran Rustage, Sally E Hayward, Jessica Carter, Felicity Knights, Lucy P Goldsmith, Ines Campos-Matos, Fatima Wurie, et al. "Defining the determinants of vaccine uptake and undervaccination in migrant populations in Europe to improve routine and COVID-19 vaccine uptake: a systematic review." In: *The Lancet Infectious Diseases* (2022).

[101]   Eunice Twumwaa Tagoe, Nurnabi Sheikh, Alec Morton, Justice Nonvignon, Abdur Razzaque Sarker, Lynn Williams, and Itamar Megiddo. "COVID-19 vaccination in lower-middle income countries: national stakeholder views on challenges, barriers, and potential solutions." In: *Frontiers in Public Health* 9 (2021), p. 709127.

[102]   Antoine de Bengy Puyvallée and Katerini Tagmatarchi Storeng. "COVAX, vaccine donations and the politics of global vaccine inequity." In: *Globalization and Health* 18.1 (2022), pp. 1–14.

[103]   Matthew M Kavanagh, Luis Gil Abinader, and Amanda Banda. *Equity and technology in the pandemic treaty.* 2023.

[104]   Bavesh D Kana, Patrick Arbuthnot, Benjamin K Botwe, Yahya E Choonara, Fatima Hassan, Hechmi Louzir, Precious Matsoso, Penny L Moore, Apollo Muhairwe, Kubendran Naidoo, et al. "Opportunities and challenges of leveraging COVID-19 vaccine innovation and technologies for developing sustainable vaccine manufacturing capabilities in Africa." In: *The Lancet Infectious Diseases* (2023).

[105]   Nick Warren Ruktanonchai, JR Floyd, Shengjie Lai, Corrine Warren Ruktanonchai, Adam Sadilek, Pedro Rente-Lourenco, Xue Ben, Alessandra Carioli, Joshua Gwinn, JE Steele, et al. "Assessing the impact of coordinated COVID-19 exit strategies across Europe." In: *Science* 369.6510 (2020), pp. 1465–1470.

[106]   Mattia Mazzoli, Emanuele Pepe, David Mateo, Ciro Cattuto, Laetitia Gauvin, Paolo Bajardi, Michele Tizzoni, Alberto Hernando, Sandro Meloni, and José J Ramasco. "Interplay between mobility, multi-seeding and lockdowns shapes COVID-19 local impact." In: *PLoS computational biology* 17.10 (2021), e1009326.

[107]   Viola Priesemann, Rudi Balling, Melanie M Brinkmann, Sandra Ciesek, Thomas Czypionka, Isabella Eckerle, Giulia Giordano, Claudia Hanson, Zdenek Hel, Pirta Hotulainen, et al. "An action plan for pan-European defence against new SARS-CoV-2 variants." In: *The Lancet* 397.10273 (2021), pp. 469–470.

[108]   Viola Priesemann, Rudi Balling, Simon Bauer, Philippe Beutels, André Calero Valdez, Sarah Cuschieri, Thomas Czypionka, Uga Dumpis, Enrico Glaab, Eva Grill, et al. "Towards a European strategy to address the COVID-19 pandemic." In: *The Lancet* 398.10303 (2021), pp. 838–839. DOI: https://doi.org/10.1016/S0140-6736(21)01808-0.

[109]   André Calero Valdez, Emil N. Iftekhar, Miquel Oliu-Barton, Robert Böhm, Sarah Cuschieri, Thomas Czypionka, Uga Dumpis, Giulia Giordano, Claudia Hanson, Zdenek Hel, et al. "Europe must come together to confront omicron." In: *BMJ* (2022). DOI: https://doi.org/10.1136/bmj.o90.

[110]   Finlay Campbell, Brett Archer, Henry Laurenson-Schafer, Yuka Jinnai, Franck Konings, Neale Batra, Boris Pavlin, Katelijn Vandemaele, Maria D Van Kerkhove, Thibaut Jombart, et al. "Increased transmissibility and global spread of SARS-CoV-2

variants of concern as at June 2021." In: *Eurosurveillance* 26.24 (2021), p. 2100509.

[111]   I Nyoman Pujawan and Alpha Umaru Bah. "Supply chains under COVID-19 disruptions: literature review and research agenda." In: *Supply Chain Forum: An International Journal*. Vol. 23. 1. Taylor & Francis. 2022, pp. 81–95.

[112]   Matthew M Kavanagh, Clare Wenham, Elize Massard da Fonseca, Laurence R Helfer, Elvin Nyukuri, Allan Maleche, Sam F Halabi, Adi Radhakrishnan, and Attiya Waris. "Increasing compliance with international pandemic law: international relations and new global health agreements." In: *The Lancet* 402.10407 (2023), pp. 1097–1106.

[113]   Global Preparedness Monitoring Board. *A Fragile State of Preparedness: 2023 Report on the State of the World's Preparedness.* Licence: CC BY-NC-SA 3.0 IGO. Geneva, 2023.

[114]   Jamie Bedson, Laura A Skrip, Danielle Pedi, Sharon Abramowitz, Simone Carter, Mohamed F Jalloh, Sebastian Funk, Nina Gobat, Tamara Giles-Vernick, Gerardo Chowell, et al. "A review and agenda for integrated disease models including social and behavioural factors." In: *Nature human behaviour* (2021), pp. 1–13.

APPENDICES A-D

APPENDIX A: SUPPLEMENTARY INFORMATION TO CHAPTER 3: "A LOOK INTO THE FUTURE OF THE COVID-19 PANDEMIC IN EUROPE: AN EXPERT CONSULTATION"

Methods

The methodology to generate and compile the content of this manuscript is inspired by the Delphi method.[1] It describes a process for facilitating discussions or forecasts by groups of people. Key characteristics of this method are that (a) the participants do not communicate directly with each other while formulating their opinions and that (b) the synthesis of the content is moderated by designated facilitators. One advantage of the Delphi method is that it reduces some common group biases.[2] The facilitators in this case were Viola Priesemann, Emil Iftekhar, Sebastian Mohr, and Simon Bauer (all affiliated with the Max Planck Institute for Dynamics and Self-Organization, Göttingen, Germany). The precise individual steps of the process were the following:

1. Formulating instructions for the collaborators

The facilitators drafted general instructions and sets of guiding questions to send out to the collaborators (see supplementary material "questions.zip"). The guiding questions were formulated with the aim of serving as inspiration only. The facilitators prepared four different sets of questions, structured along five general headings:

1. On general aspects of COVID-19
2. What is the perspective for the coming summer?
3. What is the perspective for the coming winter?
4. What is the perspective for the coming 3-5 years?
5. Mitigating the effects of the COVID-19 pandemic

Each questionnaire included general questions and questions regarding a specific field of research: epidemiology and dynamics, public health, social sciences, and virology. The initial outline of this methodology and the guiding questions were refined with the help of some experts (see Table 1) and finalized by the facilitators.

Name	Country of affiliation	Field of expertise
Peter Klimek	Austria	Mathematical modeling
Barbara Prainsack	Austria	Political science, bioethics
Eva Schernhammer	Austria	Public health, medicine
Carlos Martins	Portugal	Family medicine
Mirjam Kretzschmar	The Netherlands	Infectious disease dynamics

Table 1: List of experts contributing to the design of the methodology and the formulation of the instructions for the rest of the collaborators.

2. Choosing the collaborators

The facilitators chose the collaborators for the Delphi study such that all four selected fields were about evenly represented and that as many European countries as possible were represented. The prospective collaborators were largely selected from the facilitators' existing professional networks or based on recommendations by colleagues. As a result, 98 experts from 31 countries were contacted. As the invitations were via email, it is possible that the invitations did not reach a few of them due to spam filtering. Of the experts that were contacted, 30 people from 17 European countries replied and subsequently contributed to the study as collaborators (see Table 2 and Figure 4). Note that three of the collaborators were also involved in refining the questionnaires and methods. Even though this is not a strict division of labor between facilitators and collaborators, we deem the thereby-introduced influence on the content as negligible.

Figure 4: Country affiliations of the collaborators (marked in yellow).

Name	Country of affiliation	Questionnaire assigned by facilitators
Thomas Czypionka	Austria	Social sciences
Peter Klimek	Austria	Epidemiology and dynamics
Eva Schernhammer	Austria	Epidemiology and dynamics
Peter Willeit	Austria	Epidemiology and dynamics
Philippe Beutels	Belgium	Epidemiology and dynamics
Steven Van Gucht	Belgium	Virology
Pirta Hotulainen	Finland	Epidemiology and dynamics
Eva Grill	Germany	Public health, virology
Gérard Krause	Germany	Epidemiology and dynamics
Armin Nassehi	Germany	Social sciences
André Calero Valdez	Germany	Social sciences
Elena Petelos	Greece	Public health
Sotirios Tsiodras	Greece	Virology
Anthony Staines	Ireland	Public health
Uga Dumpis	Latvia	Virology
Rudi Balling	Luxembourg	Virology
Enrico Glaab	Luxembourg	Virology
Sarah Cuschieri	Malta	Public health

Jenny Krutzinna	Norway	Social sciences
Tyll Krüger	Poland	Epidemiology and dynamics
Ewa Szczurek	Poland	Epidemiology and dynamics
Helena Machado	Portugal	Social sciences
Matjaž Perc	Slovenia	Epidemiology and dynamics
Claudia Hanson	Sweden	Public health
Joacim Rocklöv	Sweden	Epidemiology and dynamics
Nicola Low	Switzerland	Epidemiology and dynamics
Mirjam Kretzschmar	The Netherlands	Epidemiology and dynamics
Sebastian Funk	UK	Epidemiology and dynamics
Martin McKee	UK	Public health
Martyn Pickersgill	UK	Social sciences

Table 2: List of collaborators participating in the Delphi-survey and their respective countries of affiliation. The third column indicates which of the four field-specific questionnaires the collaborator received from the facilitators.

3. Writing the document

All collaborators (see Table 2) were invited to take part in this Delphi forecast on the long-term perspective regarding the COVID-19 pandemic in Europe. They were provided (a) an explanation of the steps of the process, (b) the general instructions and (c) at least one set of questions related to their field of expertise. The collaborators were asked to send their input separately to facilitators and to not communicate with each other. Though provided with guiding questions, answering them was communicated to be optional and the collaborators were welcomed to make further points.

After receiving all inputs, the facilitators summarised and synthesized the inputs into one document. The resulting document was sent out to the collaborators, along with all single replies of the collaborators. This was followed by two rounds of revisions; in each round, (1) the collaborators were asked to send their comment separately to the facilitators, (2) the facilitators incorporated the comments, and (3) presented the updated document to the collaborators. The contributions of the collaborators included references to pertinent scientific literature to support and evidence their statements. In the second step of incorporating the collaborators' comments, the facilitators added additional references to some statements in the manuscript. These additional references were then accepted, amended, or corrected by the collaborators. As a last step, the collaborators were able to suggest minor corrections in a shared online document and were asked to confirm their authorship after the finalization of the draft. The process of writing the document started on March 8, 2021, and ended on May 6, 2021.

References

1.   Brown BB. Delphi process: a methodology used for the elicitation of opinions of experts. Rand Corp Santa Monica CA; 1968.
2.   Linstone HA, Turoff M. The delphi method. Reading, MA: Addison-Wesley; 1975.

APPENDIX B: SUPPLEMENTARY INFORMATION TO CHAPTER 4:
"RELAXING RESTRICTIONS AT THE PACE OF VACCINATION
INCREASES FREEDOM AND GUARDS AGAINST FURTHER COVID-
19 WAVES"

APPENDIX B: SUPPLEMENTARY INFORMATION TO CHAPTER 4:
"RELAXING RESTRICTIONS AT THE PACE OF VACCINATION
INCREASES FREEDOM AND GUARDS AGAINST FURTHER COVID-
19 WAVES"

S1 Eigenvalues of the homogeneous contact matrix

Here we will demonstrate a general case for the eigenvalues of a homogeneous contact matrix, for which every column accounts for the fraction age-groups represent respect to the total population.

Theorem S1.1. *Let C be a square $n \times n$ matrix, such that all columns are identical, i.e., $C_{i,\bullet} = f_i$, $f \in \mathbb{R}^n$, and $\sum_i f_i \neq 0$. Then C is diagonalizable and has a single non-zero eigenvalue $\lambda = \sum_i f_i$.*

Proof. First, we note that the dimension of the kernel of $T : \mathbb{R}^n \to \mathbb{R}^n$, $T(u) = Cu$, i.e, the vector space $\ker(T) = \{u | Cu = 0\}$ is $n-1$. Thus, there are $n-1$ linearly independent vectors associated to the eigenvalue $\lambda = 0$, which algebraic multiplicity has therefore to be equal or larger than $n-1$. Then, we study the nature of the characteristic polynomial:

$$p(\lambda) = \det(C - \lambda I) \tag{1}$$

$$= \begin{vmatrix} f_1 - \lambda & f_1 & \cdots & f_1 \\ f_2 & f_2 - \lambda & \cdots & f_2 \\ \vdots & \vdots & \ddots & \vdots \\ f_n & f_n & \cdots & f_n - \lambda \end{vmatrix} \tag{2}$$

$$\xrightarrow{\text{column } j - \text{ column } 1, \forall j > 1} = \begin{vmatrix} f_1 - \lambda & \lambda & \lambda & \cdots & \lambda \\ f_2 & -\lambda & 0 & \cdots & 0 \\ f_3 & 0 & -\lambda & \cdots & 0 \\ \vdots & \vdots & \vdots & \ddots & \vdots \\ f_n & 0 & 0 & \cdots & -\lambda \end{vmatrix} \tag{3}$$

$$\xrightarrow{\text{row } 1 + \text{ row } j, \forall j > 1} = \begin{vmatrix} \sum_i f_i - \lambda & 0 & 0 & 0 & 0 \\ f_2 & -\lambda & 0 & \cdots & 0 \\ f_3 & 0 & -\lambda & \cdots & 0 \\ \vdots & \vdots & \vdots & \ddots & \vdots \\ f_n & 0 & 0 & \cdots & -\lambda \end{vmatrix} \tag{4}$$

The highlighted zone in the determinant corresponds to $-\lambda I_{n-1}$, with I_{n-1} the identity matrix in $\mathbb{R}^{n-1 \times n-1}$. Let $\tilde{I}_{n-1}^j$ be I_{n-1}, but with the j'th row replaced by a row of zeros. Using that $|aA| = a^n |A|$ for an $n \times n$ arbitrary matrix, and that $|D| = \prod d_{ii}$ for a diagonal matrix, we calculate $p(\lambda)$ by minor determinants:

$$p(\lambda) = \left(\sum_i f_i - \lambda\right) |-\lambda I_{n-1}| + \sum_{i=2}^{n} (-1)^{i-1} f_i \left| \tilde{I}_{n-1}^j \right| \tag{5}$$

$$= \left(\sum_i f_i - \lambda\right) (-1)^{n-1} \lambda^{n-1}. \tag{6}$$

As we found the last eigenvalue, and, by definition, it has at least one eigenvector, we completed the required set of n eigenvectors and concluded the demonstration. $\square$

Corollary S1.1.1. *When C is a contact matrix as defined in theorem S1.1 and f accounts for the fraction age-groups represent respect to the total population, the largest eigenvalue of matrix C is 1.*
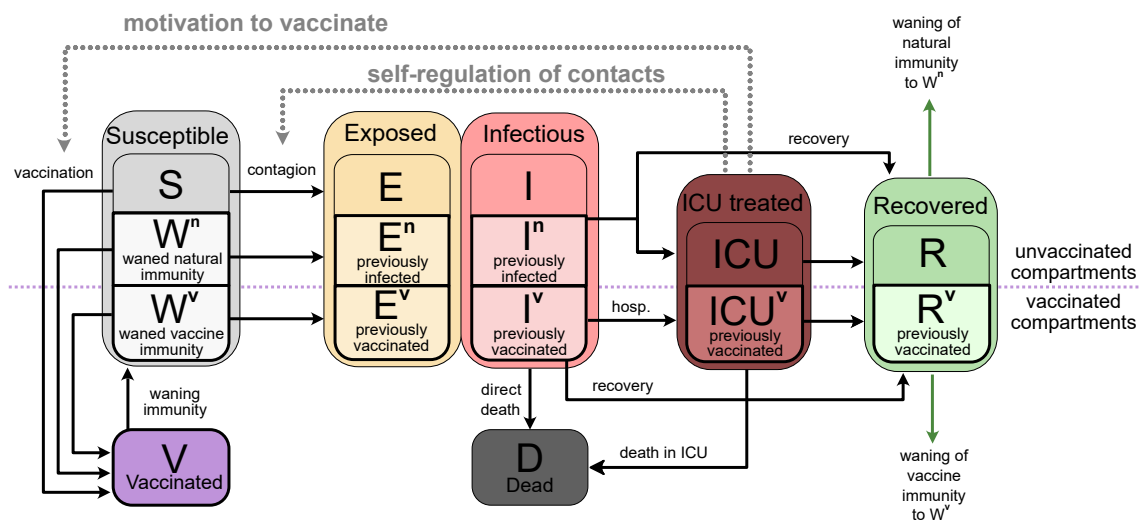
Proof. Direct from theorem S1.1, knowing that $\sum_i f_i = 1$. $\square$

APPENDIX C: SUPPLEMENTARY INFORMATION TO CHAPTER 5:
"INTERPLAY BETWEEN RISK PERCEPTION, BEHAVIOR, AND
COVID-19 SPREAD"

APPENDIX C: SUPPLEMENTARY INFORMATION TO CHAPTER 5:
"INTERPLAY BETWEEN RISK PERCEPTION, BEHAVIOR, AND
COVID-19 SPREAD"

Supplementary Material

SUPPLEMENTARY INFORMATION
S1   MODEL

Supplementary Figure S1: **Age-stratified SEIRD-ICU compartmental model with vaccination and feedback loops for the interplay between information and disease spread.** Besides considering relevant compartments to capture COVID-19 dynamics, we explicitly incorporate mechanisms of voluntary preventive action through behavioural changes in response to information and individual perception of risks. We incorporate two mechanisms of voluntary action: (i) individuals can voluntarily adapt their immediate health-protective behaviour, adapting it according to their possibilities and the risk they perceive, and (ii) adapt their willingness regarding vaccination, being likelier to accept vaccine offers when feeling at risk for prolonged periods. Transition rates and other variables are listed in Tables S3 and S5, but omitted in the figure for clarity purposes.

We model the spreading dynamics of SARS-CoV-2 by a deterministic age-stratified compartmental model. Our model incorporates disease spreading dynamics (SEIRD), intensive care unit stays (ICU), the roll-out of a single-dose equivalent vaccine and boosters thereof (V), the protection from which wanes over time, and the interplay between risk perception and disease spread through the self-regulation of voluntary health-protective behaviour. We assume that health-protective behaviour is modulated by the perception of risk. When perceiving risks, humans tend to weigh more recent developments more heavily as well as put more weight on developments in the timescale relevant for the decision to be made (i.e., shorter timescales for immediate actions and longer ones for one-time decisions with sustained consequences) Zauberman et al. (2009). Explicitly, if perceiving increased risk, individuals can (i) adapt their level of potentially contagious contacts they have

and (ii) adapt their willingness towards seeking vaccination. For a graphical representation of the dynamics see Fig. S1.

In our model, susceptible (S) individuals can acquire the virus from infected individuals and subsequently progress to the exposed ($S \rightarrow E$) and, after the latent period, to the infectious ($E \rightarrow I$) compartment. Vaccinated and recovered individuals can be infected after their immunity has waned. Alternatively, our model can be interpreted such that waning immunity increases the probability of breakthrough infections. Individuals whose natural or vaccine-induced immunity has waned are modelled via two compartments (W^n and W^v, respectively), which feature no protection against infection but against a severe course of the disease, i.e., have reduced probabilities of requiring intensive care or dying. If infected, they transit to different exposed (E^n, E^v) and infectious (I^n, I^v) compartments so that vaccinated and unvaccinated individuals are separated.

The infectious compartments have three different possible transitions: i) direct recovery ($I, I^n \rightarrow R$ and $I^v \rightarrow R^v$) with rate γ, ii) admission to ICU ($I, I^n \rightarrow \mathrm{ICU}$ and $I^v \rightarrow \mathrm{ICU}^v$) with rate δ (reduced by a factor $(1 - \kappa)$ for I^n, I^v) or iii) direct death ($I, I^n, I^v \rightarrow D$) with rate θ (reduced by a factor $(1 - \kappa)$ for I^n, I^v). We assume the recovery and death rate in ICU to be independent of immunisation status. That way, individuals receiving ICU treatment either recover at a rate γ_{ICU} ($\mathrm{ICU} \rightarrow R$ and $\mathrm{ICU}^v \rightarrow R^v$) or die at a rate θ_{ICU} ($\mathrm{ICU}, \mathrm{ICU}^v \rightarrow D$). Note that the probability to get admitted to an ICU is reduced for infected individuals with waned immunity. However, their death rate in ICU is equal to that of those infected for the first time. We use two ICU compartments to separate the vaccinated from the unvaccinated compartments to keep track of individuals who can still receive a vaccine after recovering.

Each compartment is split into sub-compartments for the age groups that interact with each other following the contact matrix described in Sec. S1.2. Full age-structured model equations are presented in Sec. S3. Apart from the transmission-relevant interactions, the effect of having different age groups is incorporated into our vaccine feedback (described in Sec. S2.1) as well as in the transition rates between compartments (described in Sec. S2.2).

S1.1   Memory kernel

In this section we specify the memory kernel that measures how risk perception builds on past development of the ICU occupancy. These memory kernels (Fig. S2) relate to two processes occurring on different timescales. Voluntary adaption of health-protective behaviour depends on the perceived risk in the recent past, $H_R(t)$, defined as:

$$H_R(t) := \mathrm{ICU}^{\mathrm{tot}} * \mathcal{G}_{p_R, b_R} = \int_{-\infty}^{t} \mathrm{d}t' \, \mathrm{ICU}^{\mathrm{tot}}(t') \, \mathcal{G}_{p_R, b_R}(-t' + t) \,. \tag{1}$$

$\mathrm{ICU}^{\mathrm{tot}}(t)$ is the sum of all patients in ICU treatment at time t: $\mathrm{ICU}^{\mathrm{tot}}(t) = \sum_i \mathrm{ICU}_i(t) + \mathrm{ICU}_i^v(t)$. The arguments of the Gamma distribution $\mathcal{G}_{p_R, b_R}$ are set to $p_R = 0.7$ (shape) and $b_R = 4$ (rate), resulting in a curve that peaks at around four days in the past (Fig. S2a). Depending on $H_R(t)$, individuals reduce their potentially contagious contacts in different contexts by a weighting factor $k_{\mathrm{NPI,self}}$ (Fig. 2, main text) within thresholds determined by current mandatory NPIs (Fig. S3). See Sec. S4 for a sensitivity analysis on parameter choices.
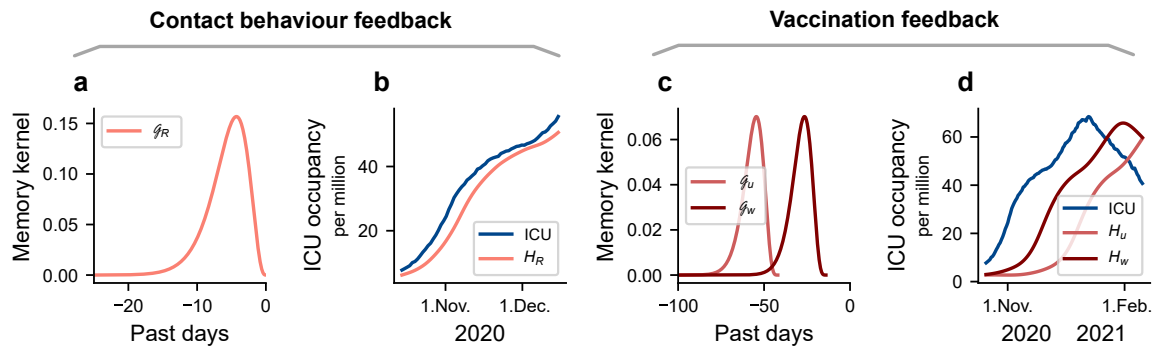
Supplementary Figure S2: **Modelling the relationship between perceived risk and pandemic developments.** Based on the information that individuals receive on the recent developments of the pandemic (e.g., ICU occupancy), they form their perception of risk. The way individuals perceive these temporal trends is biased towards recent developments, prioritising them over past developments for their decisions Zauberman et al. (2009). Furthermore, we assume a delay in individuals' reactions to ICU occupancy because of (i) delays inherent to the information spreading dynamics, and (ii) need for recurrent stimuli and various sources for accepting new information. Therefore, we convolve the ICU occupancy time series with a Gamma delay kernel (**a**), which captures both the delay related to information delivery and the subjective perception of time described above. Vaccine dynamics require a further delay related to the time required to build up immunity: Individuals whose immunity takes effect at a certain time made their decision and got vaccinated some time ago. The length of this delay depends on whether it is a first time or booster vaccination (**c**). **b,d:** Once convoluted with ICU occupancy (German example shown here), we obtain a measure for perceived risk H_R, H_u and H_w, respectively, for the voluntary adaption of immediate health-protective behaviour, first-time vaccination, and booster vaccination. In comparison with the actual ICU development, the variables H_* are smoother and delayed in time, representing non-instantaneous decisions based on individuals' perception of the recent ICU occupancy.

Time memory for vaccination willingness is assumed to work in the same way, but with different Gamma distributions, for two reasons. Firstly, there is a delay τ_u or τ_w between the decision to be vaccinated and the onset of immunity. Secondly, vaccination willingness is assumed to depend more strongly on past ICU occupancy compared to more immediate health-protective behaviour. Combined, it translates into a Gamma distribution $\mathcal{G}_{p_{\text{vac}}, b_{\text{vac}}}$ that is shifted in time and is flatter (Fig. S2c), which is characterised by the parameters τ_u, τ_w, $p_{\text{vac}} = 0.4$ and $b_{\text{vac}} = 6$:

$$H_{u,w}(t) := \text{ICU}^{\text{tot}} * \mathcal{G}_{p_{\text{vac}}, b_{\text{vac}}} = \int_{-\infty}^{t} \mathrm{d}t' \, \text{ICU}^{\text{tot}}(t') \, \mathcal{G}_{p_{\text{vac}}, b_{\text{vac}}}(-t' - \tau_{u,w} + t). \tag{2}$$

The subscripts u and w indicate first and booster doses, respectively. Booster doses are usually only a single dose so τ_w is just the delay between administration of the dose and onset of immunity, which we assume to be 2 weeks. The parameter τ_u is larger than τ_w because we include the delay of around 6 weeks for most vaccines that need two doses. For the initial conditions of H_R and $H_{u,w}$, ICU and ICU^v are set to a constant $\text{ICU}(t < 0) = \text{ICU}(t = 0)$ (same for ICU^v) in the past.

S1.2 Spreading dynamics

In our model, the spreading dynamics are governed by the sizes of the infectious compartments I, I^n, I^v and the compartments S, W^n, W^v, from which a transition to an infected state is possible. We include the effects of (i) mandatory non-pharmaceutical interventions (NPIs), (ii) individuals voluntarily adapting their health-protective behaviour based on perceived risk, and (iii) seasonality. Each is represented by a factor k that acts as a multiplicative reduction or increase on the spreading dynamics.

Seasonality is described by the factor $k_{\text{seasonality}}$ (see Equation 7 below). Mandatory NPIs and individuals' voluntary preventive actions are represented by $k_{\text{NPI,self}}(H_R)$. It does not factorise into single contributions of mandatory NPIs and voluntary preventive action because we assume the level of NPIs and voluntary behaviour to be coupled.

We introduce an infection term $\sum_j C_{ji}\mathcal{I}_j$ that governs the spreading between age groups i and j. The term is present in all differential equations that include transmissions, i.e., the transitions

$$
\begin{aligned}
S_i &\to E_i &&\text{non vaccinated, non infected} \\
W_i^n &\to E_i^n &&\text{waned infected (unvaccinated)} \\
W_i^v &\to E_i^v &&\text{waned vaccinated (potentially infected previously)}
\end{aligned}
\tag{3}
$$

include a term proportional to $\sum_j C_{ji}\mathcal{I}_j$, which is subtracted from the susceptible and waned and added to the exposed states.

C_{ij} is the overall contact matrix, which we describe below, and $\mathcal{I}_i$ is a term describing the infectiousness of age group i. We define it as

$$
\mathcal{I}_i := \beta \cdot k_{\text{seasonality}} \cdot \frac{I_i^{\text{eff}}}{M_i} \quad \text{with} \quad I_i^{\text{eff}} := (I_i + I_i^n + I_i^v + \Psi M_i) .
\tag{4}
$$

β is the spreading rate, I^{eff} is the effective size of the infectious compartments, M_i is the total population size of age group i, and Ψ is an external influx of infections, which we assume to be distributed equally over the population, e.g., being the largest for the largest age group.

The coupling between age groups is represented by a pre-COVID-19 contact matrix C_{ij}. This matrix represents the static, non-ICU-dependent contact behaviour of the different age groups (age group i potentially infecting age group j). It can be interpreted as the sum of various layers of contextual contacts (work-, school-, community-, and household-related contacts) Mistry et al. (2021). For a graphical representation of the contextual layers, see Fig. 1, main text, and Fig. S3. Depending on the context, some of these contacts can be voluntarily reduced according to individuals' perception of risk. Hence, we use each of the contextual layers of the matrix C_{ij}^ν separately and weigh each layer with reduction factors $k_{\text{NPI,self}}^\nu(H_R)$. We use H_R as an effective measure of the ICU occupancy that reflects the population's perceived risk (see subsection S1.1). Finally, we normalise the overall contact matrix C_{ij} by its spectral radius when its values are not reduced because of mandatory NPIs or voluntary protective behaviour, i.e., at $k_{\text{NPI,self}} = 1$ and $H_R = 0$. That way, the largest eigenvalue of the contact matrix $C_{ij} = \sum_\nu C_{ij}^\nu$ equals one in the absence of mandatory NPIs and voluntary measures.

The resulting infection term present in all transmission-related differential equations for age group i is thus

$$
\sum_j C_{ji}\mathcal{I}_j = \beta \cdot k_{\text{seasonality}} \sum_j \left(\sum_\nu C_{ji}^\nu \cdot k_{\text{NPI,self}}^\nu \right) \frac{I_j^{\text{eff}}}{M_j} ,
\tag{5}
$$

with j counting age groups and ν counting layers of the contact matrix. Having a normalised contact matrix C_{ij}, we can approximate the seasonal reproduction number $R_{0,\text{seasonal}}(t)$, which is defined as the largest eigenvalue of the next generation matrix Diekmann et al. (2010), at $H_R = 0$. By assuming that $\delta, \theta \ll \gamma$, we get

$$R_{0,\text{seasonal}}(t) \approx k_{\text{seasonality}}(t)\frac{\beta}{\gamma}\,, \tag{6}$$

with $\gamma = \sum_i \gamma_i M_i$. Postulating that $R_0 = 5$ at $k_{\text{seasonality}} = 1$, we can use this formula to calculate the spreading rate β. Note that this only holds true if seasons are long compared to the duration of an infection. With the latent period being $\frac{1}{\rho} = 4$ days and the duration in the infected compartment approximately $\frac{1}{\gamma} = 10$ days, the duration of an infection is roughly two weeks which is shorter than the time scale over which seasonality varies significantly.

We incorporate the effect of seasonality $k_{\text{seasonality}}$ as a time-dependent sinusoidal modulation factor, as proposed in Gavenčiak et al. (2021):

$$k_{\text{seasonality}} = 1 + \mu \cos\left(2\pi\frac{t + d_0 - d_\mu}{360}\right), \tag{7}$$

where μ is the sensitivity to seasonality, d_0 the starting day of the simulation, and d_μ the day with the highest effect on seasonality. We set $d_\mu = 0$, corresponding to January 1st. For simplicity, we assume that one month has 30 days and a full year, thus, 360 days. This approximation does not affect the results in the observed time horizon.

S1.3 Contact matrices

In our model, individuals can adapt the level of contagious contacts based on their perception of risk. Explicitly, we consider the contact matrices for the German population reported in Mistry et al. (2021), which differentiate between four different contexts (Households, Schools, Workplaces, and Communities). These matrices are represented in Fig. S3a, c, e, g. Then, depending on the perception of risk, the scenario of mandatory NPIs, and how much freedom these allow for in different contexts, we calculate a weighting factor $k_{\text{min}} \leq k_{\text{NPI,self}}^\nu(H) \leq k_{\text{max}}$ that multiplies each matrix (Fig. S3b, d, f, h). Scenario-dependent threshold values for the weighting factors are reported in Table 1 and explained in the Methods Section, main text.

The contact matrix for the Community context is equally distributed, meaning that each individual ("x-axis") has the same probability of being infected by any contact ("y-axis"), independent of age. Because the age groups are different in size, a horizontal pattern emerges; it is likelier to be infected by an individual part of a larger age group.

Although straightforward to understand, the household layer of contacts applied to our mean-field model may lead to unrealistic results in some situations. For example, consider an ideal full lockdown policy where any transmissions between households were perfectly eliminated. Obviously, in such a theoretical scenario, the pandemic would quickly end as infected individuals would not transmit the virus any further than to contacts within their household. However, under a mean-field

compartmental model, the distinction between people in one's household and another household cannot be made, which would lead to a viral spread even under such a scenario. To solve this issue, the factor $k_{\text{NPI,self}}^{\text{Households}}(H)$ is scaled by a factor which is the average of the other reductions: $\frac{1}{3}\sum_{\nu} k_{\text{NPI,self}}^{\nu}(H), \nu \in \{\text{Schools, Workplaces, Communities}\}$. In that way, eliminating all contacts in contexts aside from households should end the pandemic.
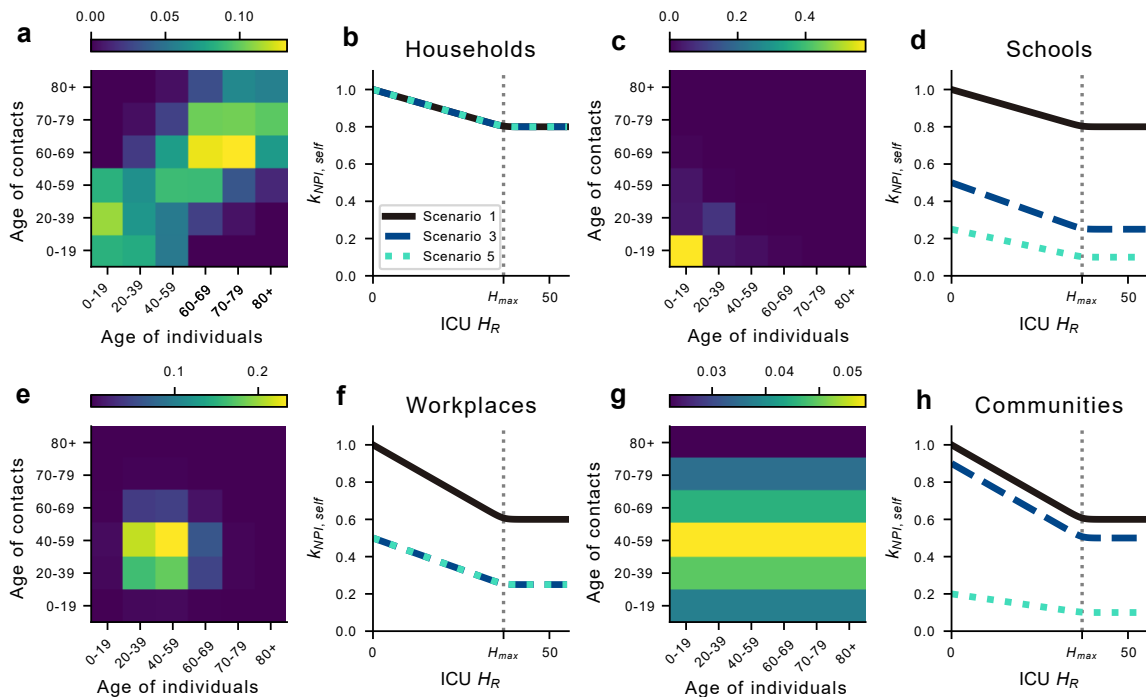
Supplementary Figure S3: **The mechanism of the reduction of potentially contagious contacts.** The contact matrix for interactions within households, schools, workplaces and communal activities (**a,c,e,g**) and the ICU-occupancy-dependent reduction $k_{\text{NPI,self}}^{\nu}(H_R)$ (**b,d,f,h**) for scenarios 1,3, and 5. Each matrix entry is multiplied by the value of $k_{\text{NPI,self}}^{\nu}(H_R)$ (**b,d,f,h**), which decreases linearly with perceived ICU occupancy H_R up to the point $H_{max} = 37$ where no further reduction is taken as motivated by Fig. 2, main text.

S1.4 Vaccination effects and waning immunity

Our model includes the effect of vaccination, where vaccines are for simplicity administered with a single-dosage delivery scheme. Vaccinated individuals cannot be infected while being in the vaccinated compartment, but will proceed to the waned immunity compartment W^v at a rate Ω Thomas et al. (2021); Puranik et al. (2021). The same applies to recovered individuals, who also lose their post-infection immunity at rate Ω Turner et al. (2021). Hence, people transition from compartment R_i to compartment W_i^n and from R_i^v and V_i to W_i^v at rate Ω.

We assume the emptying of the immune compartments to be exponential with rate Ω or, equivalently, with half-life period $T_{1/2} = \ln(2)/\Omega$. In other words, we assume that after $T_{1/2}$, half of the immune individuals have completely waned immunity and the other half is still fully immune. Within the mean-field approximation, this corresponds to all individuals in the immune compartments having halfway waned immunity after $T_{1/2}$. This time, when the effectiveness against infection η reduces to 50%, equals to about 5 months according to empirical data (for vaccination)

Tartof et al. (2021). Hence, the waning immunity rate is given by

$$\Omega = \frac{\ln(2)}{T_{1/2}} \approx \frac{\ln(2)}{5 \cdot 30 \, \text{days}} \approx \frac{1}{225} \frac{1}{\text{days}}. \tag{8}$$

As soon as individuals enter one of the waned compartments they can be infected with the same probability as individuals never infected or vaccinated before. However, we assume that robustness against a severe course of the disease remains high Tartof et al. (2021); Chemaitelly et al. (2021); Pegu et al. (2021); Naaber et al. (2021) which leads to a reduction of $(1 - \kappa)$ to the probability of requiring treatment in ICUs or dying directly. The parameter κ is estimated using κ_{obs}, which denotes the full protection against hospitalisation as in observed studies. The parameter κ used in our model is lower than κ_{obs} because it is the effectiveness against hospitalisation once an individual is already infected. We estimate it via

$$(1 - \eta)(1 - \kappa) = (1 - \kappa_{\text{obs}}) \tag{9}$$

with η being the vaccine effectiveness against an infection. According to Tartof et al. (2021) it holds that $\eta = 0.5$ and $\kappa_{\text{obs}} = 0.9$ (both after five months). Thus, we estimate $\kappa \approx 0.8$ and approximate it to be independent of the time after vaccination.

S1.5 Vaccine uptake

The age group dependent vaccine uptake is described by two different functions: one for susceptible individuals (ϕ_i) and one for individuals whose immunity has waned (φ_i). The core idea is to vaccinate only if willingness for vaccine uptake is larger than the fraction of already vaccinated; if the fraction of individuals who are willing to be vaccinated with a first dose (u^{willing}) is larger than the fraction of already vaccinated (u^{current}), vaccinations are carried out at a rate proportional to the difference of the two.

Willingness to be vaccinated depends on the past development of the ICU occupancy numbers. u^{willing} can shift between a minimum and a maximum value (u^{base} and $u^{\text{max}} = 1 - \chi_u$), representing the general observed acceptance for the first dose and people who are strictly opposed to vaccines or cannot be immunised because of age or other preconditions (making up χ_u), respectively. The sensitivity constant α_u determines how sensitive to ICU occupancy the vaccine hesitancy is (see Sec. S1.5.1). The willingness to receive the first dose of the vaccine is then described by

$$u_i^{\text{willing}} = u_i^{\text{base}} + \left(u_i^{\text{max}} - u_i^{\text{base}} \right) \left(1 - \exp\left(-\alpha_u H_u \right) \right). \tag{10}$$

Hence, u_i^{willing} is a fraction for each age group i between zero and one and the total number of people willing to be vaccinated in each age group i is thus $u_i^{\text{willing}} M_i$. For the differences in the parameters u_i^{base} and $u_{i,\text{max}}$ between age groups, see Sec. S2.1 and for a graphical example representation of u^{willing} see Fig.2e, main text.

The function that determines the rate at which first time vaccines are administered is denoted by ϕ. It determines the transition away from S_i and W_i^n, is age group dependent, and is described via a softplus function:

$$\phi_i(H_u) = \frac{1}{t_u} \cdot \frac{S_i + W_i^n}{M_i(1 - u_i^{\text{current}})} \cdot \epsilon \ln\left(\exp\left(1 + \frac{1}{\epsilon}\left(u_i^{\text{willing}}(H_u) - u_i^{\text{current}}\right)\right)\right), \qquad (11)$$

where ϵ is a curvature parameter. Multiplying by $\frac{S_i + W_i^n}{M_i(1 - u_i^{\text{current}})}$ ensures that we only vaccinate if people are actually present in S or W^n. Dividing by t_u smoothens the transition between the state of vaccinating and not vaccinating, the physical explanation being that people require time (of the order of t_u days) to organise a vaccine, which reduces the vaccination rate after crossing the threshold. t_u is assumed to be constant here. However, when there is a lot of demand for vaccine uptake, t_u is likely larger in reality due to administrative and logistical problems. For the implementation of ϕ_i into the model equations, see Sec. S3. In the term $\frac{dS_i}{dt}$ we multiply ϕ by $\frac{S_i}{S_i + W_i^n}$ and in the term $\frac{dW_i^n}{dt}$ we multiply by $\frac{W_i^n}{S_i + W_i^n}$, effectively splitting up the vaccinations among the two groups.

The administration of booster doses works in a similar way. First, we define a function for the age group dependent willingness to accept a booster dose:

$$w_i^{\text{willing}} = w_i^{\text{base}} + \left(w_i^{\text{max}} - w_i^{\text{base}}\right)\left(1 - \exp\left(-\alpha_w H_w\right)\right). \qquad (12)$$

The function for booster doses φ can then be written as

$$\varphi_i(H_w) = \frac{1}{t_w} \cdot \frac{W_i^v}{M_i(u_i^{\text{current}} - w_i^{\text{current}})} \cdot \epsilon \ln\left(\exp\left(1 + \frac{1}{\epsilon}\left(w_i^{\text{willing}}(H_w)u_i^{\text{current}} - w_i^{\text{current}}\right)\right)\right), \quad (13)$$

We only vaccinate if willingness among those who received a first dose is larger than the fraction of already boostered people, i.e. u_i^{current} is the upper limit for w_i^{current}.

S1.5.1   Assessment of sensitivity to ICU occupancy for vaccination dynamics

In our model, we assume the willingness in the total population to be vaccinated for the first time to range between threshold values u^{base} and u^{max}. The difference $u^{\text{max}} - u^{\text{base}}$ is the fraction of people that, initially hesitant, decide to accept the vaccine offer based on their perception of risk. In order to estimate how sensitive this group is to risk perception in the form of awareness about the ICU occupancy, we proceed as follows. If we estimate the ICU occupancy at which half of the people belonging to this initially hesitant group accepts a vaccination, we can calculate the sensitivity parameter α_u: Let $H_{1/2}$ be this ICU occupancy. We then have to solve

$$u^{\text{base}} + \frac{1}{2}\left(u^{\text{max}} - u^{\text{base}}\right) \overset{!}{=} u^{\text{base}} + \left(u^{\text{max}} - u^{\text{base}}\right)\left(1 - \exp\left(-\alpha_u H_{1/2}\right)\right), \qquad (14)$$

which reduces to

$$\alpha_u = \frac{\log 2}{H_{1/2}}. \tag{15}$$

We assume $H_{\max}$, i.e., the threshold at which no further adaption of health-protective behaviour occurs, as a first estimate for $H_{1/2}$ to obtain an approximate value for the sensitivity as $\alpha_u = \frac{\log 2}{H_{\max}} = \frac{\log 2}{37} \approx 0.02$. The quantified effect that this parameter has on the results is explored in Sec. S4.

S1.5.2   Tracking vaccinated individuals

Transition rates between the susceptible (S_i) and waned (W_i^n, W_i^v) compartments due to vaccination depend on the difference between willingness to be vaccinated and the fraction of currently vaccinated. Thus, it is necessary to keep track of how many people have received a first and booster dose, respectively. This is modelled by integrating over the vaccination rates. It translates into two additional differential equations:

$$\frac{d}{dt}u_i^{\text{current}} = \phi_i(H_u) \quad \text{and} \quad \frac{d}{dt}w_i^{\text{current}} = \varphi_i(H_w), \tag{16}$$

where u^{current} and w^{current} are the fraction of people who received a first and booster dose, respectively. The initial conditions for u_i^{current} and w_i^{current} are the total reported numbers of administered vaccine doses Ritchie et al. (2021).

S1.6   Exploring vaccination rate and ICU occupancy trends in different European countries

The main assumption underlying the vaccination feedback is that vaccination willingness follows ICU occupancy. In the case of Romania this relation is evident (Figure S4): Approaching winter 2021, case numbers and ICU occupancy had a steep rise, arguably due to insufficient immunity among the population, as vaccine coverage was under 30% Ritchie et al. (2021). Under such circumstances, there was a lot of "room for improvement" within the unvaccinated population not strictly opposed to vaccines, which led to a steep surge in administered doses (Fig. S4). Note that there might also be other underlying causes for increased vaccine uptake: For example, imposing restrictions only onto unvaccinated might motivate vaccine uptake. While this is a governmental choice not considered in our model, such enforcements usually follow high levels of ICU occupancy and are thus indirectly accounted for.

In countries other than Romania, the trend is less visible (Fig. S4). Several countries show an increase in vaccine uptake in October 2021; however, it is unclear whether this is mainly motivated by voluntary behaviour following an increase in ICU occupancy. Concurrently, requests for launching country-wide booster campaigns were on the rise, which might have been the leading cause of increased vaccine uptake. However, whether the causes are voluntary behaviour or institutional recommendations regarding vaccinations, both follow perceived risk (on individual level vs governmental level) and lead to the same effect: increased ICU occupancy leads to increased vaccine uptake. Apart from Estonia and Belgium, we do not observe countries in which a rise in ICU occupancy is not followed by a rise in vaccinations. If the contrary is the case, i.e., vaccines

rising despite ICU occupancy staying low, this could be attributed to external motivations and would require further country-specific investigation.

In countries where we observe increasing vaccines following ICU occupancy, we should note that the delay between the two varies a lot. While in Romania and Bulgaria, the delay seems to be of the order of one month, we observe that in Germany, Austria and the Czech Republic, there does not seem to be any relevant delay. Note that the vaccination curve measures daily administered vaccines and not the onset of immunity (which the kernel in our model represents). The effect of the delay incorporated in our model is quantified in the sensitivity analysis S4.
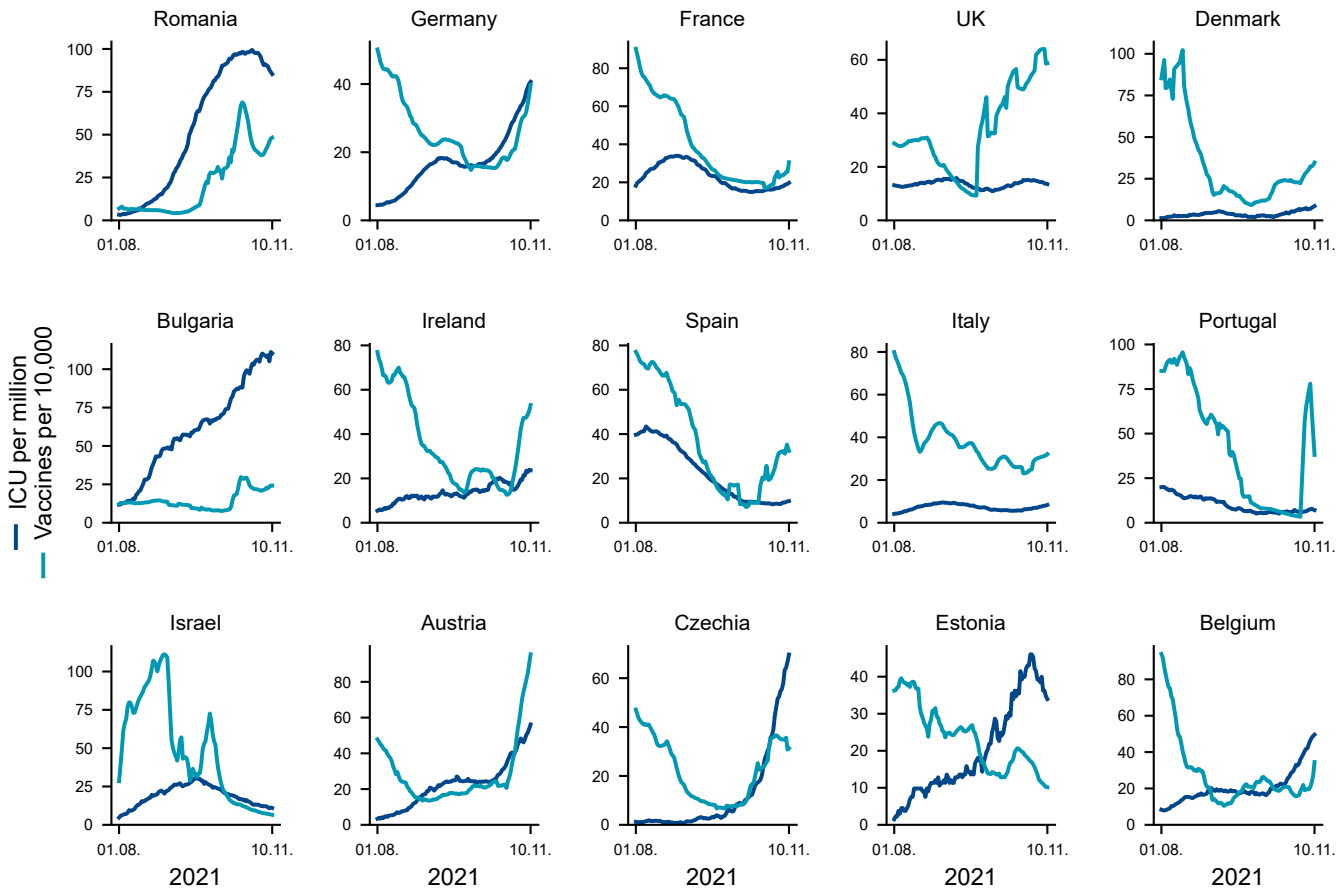
Supplementary Figure S4: **Vaccination rate and ICU occupancy trends across selected countries.** ICU occupancy per million inhabitants and daily vaccinations per 10,000 inhabitants for several European countries and Israel. Booster doses and first time doses are added together.

S2   AGE STRATIFICATION

S2.1   Age-dependent vaccine uptake

Although there are vaccines accredited for children below 12 years in the European Union, we assume that these age groups will have much lower uptakes, affecting our parameters u_i^{max} (maximum vaccine uptake) and w_i^{max} (maximum booster uptake). Furthermore, due to likelier side effects of vaccines for the young, but lesser consequences of an infection, we assume that these parameters as well as the baseline acceptances for vaccines increase with age. Thus, u_i^{base}, w_i^{base}, u_i^{max} and w_i^{max}

become age-dependent. All vaccine-related parameters are listed in Table S1. Note that $w_i^{\max}$ is a fraction of u_i^{current} and not of M_i, thus it is no contradiction if $w_i^{\text{base}} > u_i^{\text{base}}$.

Table S1. Different age groups and age-dependent parameters related to vaccine uptake.

Group ID	age group	fraction of population M_i/M	$u_i^{\max}$	$w_i^{\max}$	u_i^{base}	w_i^{base}
1	0-19	0.18	0.35	0.76	0.2	0.1
2	20-39	0.25	0.9	0.8	0.5	0.25
3	40-59	0.28	0.92	0.84	0.55	0.275
4	60-69	0.13	0.94	0.88	0.6	0.3
5	70-79	0.09	0.96	0.92	0.65	0.325
6	80+	0.07	0.98	0.96	0.7	0.35

S2.2 Age-dependent transition rates

Differing disease severity after a SARS-CoV-2 infection for different age groups translates into age-dependent transition rates between our model compartments. More specifically, we include age-dependent parameters for the natural recovery rate γ, the ICU admission rate δ, the death rate θ and the recovery as well as death rates from ICU, γ_{ICU} and θ_{ICU}, respectively. Table S2 lists the different parameters as reported in Bauer et al. (2021).

Table S2. Age-dependent transition parameters related to the ICU-, death- and recovery rates. All parameters are given in units of days^{-1}.

ID	Age group	Recovery rate $\gamma_i \left[\text{day}^{-1}\right]$	ICU adm. rate $\delta_i \left[\text{day}^{-1}\right]$	Death rate $\theta_i \left[\text{day}^{-1}\right]$	ICU rec. rate $\gamma_{\text{ICU},i} \left[\text{day}^{-1}\right]$	ICU death rate $\delta_{\text{ICU},i} \left[\text{day}^{-1}\right]$
1	0-19	0.09998	0.000014	0.000002	0.19444	0.00556
2	20-39	0.09978	0.000204	0.000014	0.19222	0.00778
3	40-59	0.09867	0.001217	0.000111	0.084745	0.006164
4	60-69	0.09565	0.004031	0.000317	0.081401	0.009508
5	70-79	0.09314	0.005435	0.001422	0.091355	0.019756
6	80+	0.08809	0.007163	0.004749	0.084233	0.082433

S3 MODEL EQUATIONS

The combined contributions of the infection-spreading and vaccination dynamics are represented by the set of equations below. The time evolution of our model is then completely determined by the initial conditions of the system. The first-order transition rates between compartments are given by the probability for an individual to undergo this transition divided by the average transition time, e.g., the recovery rate γ is the probability that an individual recovers from the disease divided by the time span of the recovery process. Note that in principle γ should be different for the I and I^B compartment, as the probability to recover is larger for individuals previously immunised. We neglect this difference as it is negligible within the margin of error since the probability to recover is close to 1 in both cases. The subscripts i denote the sub-compartments for each age group and C_{ij} the contact matrix that describes the interactions within the age groups.

$$I_i^{\text{eff}} = \underbrace{(I_i + I_i^n + I_i^v + \Psi M_i)}_{\text{effective incidence}} \tag{17}$$

$$\mathcal{I}_i = \underbrace{\beta \, k_{\text{seasonality}} \frac{I_i^{\text{eff}}}{M_i}}_{\text{effective infection rate}} \tag{18}$$

$$C_{ij} = \underbrace{\sum_\nu C_{ij}^\nu \, k_{\text{NPI,self}}^\nu}_{\text{sub-matrices times reductions}} \tag{19}$$

$$\frac{dS_i}{dt} = - \underbrace{S_i \sum_j C_{ji} \mathcal{I}_j}_{\text{unvaccinated infections}} - \underbrace{M_i \phi_i(H_u) \frac{S_i}{S_i + W_i^n}}_{\text{first vaccinations}} \tag{20}$$

$$\frac{dW_i^n}{dt} = - \underbrace{W_i^n \sum_j C_{ji} \mathcal{I}_j}_{\text{waned infections}} - \underbrace{M_i \phi_i(H_u) \frac{W_i^n}{S_i + W_i^n}}_{\text{first vaccinations}} + \underbrace{\Omega R_i}_{\text{waning natural immunity}} \tag{21}$$

$$\frac{dW_i^v}{dt} = - \underbrace{W_i^v \sum_j C_{ji} \mathcal{I}_j}_{\text{waned infections}} - \underbrace{M_i u_i^{\text{current}} \varphi_i(H_w)}_{\text{booster vaccinations}} + \underbrace{\Omega V_i + \Omega R_i^v}_{\text{waning immunity}} \tag{22}$$

$$\frac{dV_i}{dt} = \underbrace{M_i \left(\phi_i(H_u) + u_i^{\text{current}} \varphi_i(H_w) \right)}_{\text{vaccinations}} - \underbrace{\Omega V_i}_{\text{waning vaccine immunity}} \tag{23}$$

$$\frac{dE_i}{dt} = \underbrace{S_i \sum_j C_{ji} \mathcal{I}_j}_{\text{unvaccinated exposed}} - \underbrace{\rho E_i}_{\text{end of latency}} \tag{24}$$

$$\frac{dE_i^n}{dt} = \underbrace{W_i^n \sum_j C_{ji} \mathcal{I}_j}_{\text{unvaccinated waned exposed}} - \underbrace{\rho E_i^n}_{\text{end of latency}} \tag{25}$$

$$\frac{dE_i^v}{dt} = \underbrace{W_i^v \sum_j C_{ji} \mathcal{I}_j}_{\text{vaccinated waned exposed}} - \underbrace{\rho E_i^v}_{\text{end of latency}} \tag{26}$$

$$\frac{dI_i}{dt} = \underbrace{\rho E_i}_{\text{start of infectiousness}} - \underbrace{(\gamma_i + \delta_i + \theta_i) \, I_i}_{\rightarrow \text{recovery, ICU, and death}} \tag{27}$$

$$\frac{dI^n}{dt} = \underbrace{\rho E_i^n}_{\text{start of infectiousness}} - \underbrace{(\gamma_i + (\delta_i + \theta_i)(1 - \kappa)) \, I_i^n}_{\substack{\rightarrow \text{recovery, ICU (reduced),} \\ \text{and death (reduced)}}} \tag{28}$$

$$\frac{dI_i^v}{dt} \quad = \quad \underbrace{\rho E_i^v}_{\text{start of infectiousness}} \quad - \underbrace{\left(\gamma_i + (\delta_i + \theta_i)(1-\kappa)\right) I_i^v}_{\substack{\rightarrow\text{recovery, ICU (reduced),} \\ \text{and death (reduced)}}} \tag{29}$$

$$\frac{d\text{ICU}_i}{dt} = \underbrace{\delta_i \left(I_i + (1-\kappa)I_i^n\right)}_{\text{nonvaccinated ICU}} \quad - \underbrace{(\gamma_{\text{ICU},i} + \theta_{\text{ICU},i})\text{ICU}_i}_{\text{recovery or death in ICU}} \tag{30}$$

$$\frac{d\text{ICU}_i^v}{dt} = \underbrace{\delta_i(1-\kappa)I_i^v}_{\text{vaccinated ICU}} \quad - \underbrace{(\gamma_{\text{ICU},i} + \theta_{\text{ICU},i})\text{ICU}_i^v}_{\text{recovery or death in ICU}} \tag{31}$$

$$\frac{dD_i}{dt} = \underbrace{\theta_i \left(I_i + (1-\kappa)\left(I_i^n + I_i^v\right)\right)}_{\text{death without ICU}} + \underbrace{\theta_{\text{ICU},i}\left(\text{ICU}_i + \text{ICU}_i^v\right)}_{\text{death in ICU}} \tag{32}$$

$$\frac{dR_i}{dt} = \underbrace{\gamma_i(I_i + I_i^n)}_{\text{direct recovery}} + \underbrace{\gamma_{\text{ICU},i}\,\text{ICU}_i}_{\text{recovery}} - \underbrace{\Omega R_i}_{\substack{\text{waning} \\ \text{post-infection immunity}}} \tag{33}$$

$$\frac{dR_i^v}{dt} = \underbrace{\gamma_i I_i^v}_{\text{direct recovery}} + \underbrace{\gamma_{\text{ICU},i}\,\text{ICU}_i^v}_{\text{recovery from ICU}} - \underbrace{\Omega R_i^v}_{\substack{\text{waning} \\ \text{post-infection immunity}}} \tag{34}$$

$$\frac{du_i^{\text{current}}}{dt} = \underbrace{\phi_i(H_u)}_{\text{current first vaccinations}} \tag{35}$$

$$\frac{dw_i^{\text{current}}}{dt} = \underbrace{\varphi_i(H_w)}_{\text{current booster vaccinations}} \tag{36}$$

$$\tag{37}$$

Table S3. Model parameters (in order of first appearance) related to infection dynamics. * :**Levin et al. (2020)Salje et al. (2020)Bauer et al. (2021)Linden et al. (2020)** The parameters referring to Table S2 are age-dependent.

Pa	Meaning	Value (default)	Unit	Source
γ	Recovery rate	Tab. S2	day^{-1}	He et al. (2020); Pan et al. (2020)
δ	Avg. hospitalisation rate ($I \to$ ICU)	Tab. S2	day^{-1}	$*$
κ	Reduction of hospitalisation rate (given infection) for individuals with waned immunity	0.8	–	Eq. 9
θ	Avg. death rate	Tab. S2	day^{-1}	$*$
γ_{ICU}	Recovery rate from ICU	Tab. S2	day^{-1}	$*$
θ_{ICU}	Avg. ICU death rate	Tab. S2	day^{-1}	$*$
C_{ij}	Contact matrix	–	–	Mistry et al. (2021)
β	Spreading rate	0.5	day^{-1}	Eq. 6
Ψ	Influx of infections	1	people/day	Assumed
R_0	Basic reproduction number (Delta variant)	5.0	–	Liu and Rocklöv (2021)
ρ	Rate of leaving exposed state	0.25	day^{-1}	Bar-On et al. (2020); Li et al. (2020)
μ	Sensitivity to seasonality	0.267	–	Gavenčiak et al. (2021)
d_0	Day when the time series starts	240	day	Chosen
d_μ	Day with the strongest effect on seasonality	0	day	Gavenčiak et al. (2021)
Ω	Waning immunity rate (base)	$\frac{1}{225}$	day^{-1}	Tartof et al. (2021), Eq. 8
η	Vaccine eff. against transmission 5 months after vaccination	0.5	–	Tartof et al. (2021)
κ_{obs}	Observed vaccine eff. against severe disease 5 months after vaccination	0.9	–	Tartof et al. (2021)

S3.1 Initial conditions

A primary task for defining the initial conditions is distributing the population size of $M = 10^6$ individuals onto our model compartments (Fig. S1). In reality, however, there are no well-defined compartments. For example, a person vaccinated a few months ago cannot be classified into either a V or W^n compartment, but is instead in a vaccinated state with reduced vaccine effectiveness. Furthermore, available data on vaccinated or infected individuals is often age-stratified by different age groups or not age-stratified at all. To approach these data challenges, we obtain the initial conditions through the following procedure (Fig. S5):

We postulate that we want to look at a population that is 60% vaccinated and 20% recovered (including the non reported cases). Let the resulting numbers of people be called $V^{\mathrm{tot}} = 0.6M$ and $R^{\mathrm{tot}} = 0.2M$, respectively. These values are inspired by the situation in Germany as of September 1st 2021. Next, we take German data on daily new infections N and ICU occupancy ICU$^{\mathrm{tot}}$ at this point in time Ritchie et al. (2021); am RKI (2020). These four values will be used to build all the

Table S4. Model parameters (in order of first appearance) related to the behavioural feedback loops. The range column describes the range of values used in the various scenarios.

Parameter	Meaning	Value (default)	Unit	Source
p_R, b_R	Shape and rate parameters of the memory kernel for the risk perception relevant to immediate health-protective behaviour, respectively	0.7, 4.0	–	Assumed
τ_u, τ_w	Memory time of the ICU capacity and delay to immunisation	2, 6	weeks	Assumed
$p_{\mathrm{vac}}, b_{\mathrm{vac}}$	Shape and rate parameters of the memory kernel for the risk perception relevant to vaccination, respectively	0.4. 6.0	–	Assumed
k^ν	Weighting factors for the contextual contact matrices	Tab. 1, main text	–	Assumed
$u^{\mathrm{base}}, w^{\mathrm{base}}$	Base fractions of vaccine acceptance (first and booster, respectively)	Tab. S1	–	Wouters et al. (2021)
χ_u, χ_w	Fraction of the population refusing vaccine (first and booster, respectively)	Tab. S1	–	Betsch et al. (2020)
α_u, α_w	Sensitivity of the population to ICU occupancy	0.02	people^{-1}	Eq. 15
ϵ	Curvature parameter for the softplus function describing the vaccination rate	1	–	Chosen
t_u, t_w	Organization time for vaccine (first and booster resp.)	7	days	Assumed
H_{max}	Risk perception above which no further adoption of voluntary health-protective behaviour occurs	37	–	Fitted to Betsch et a
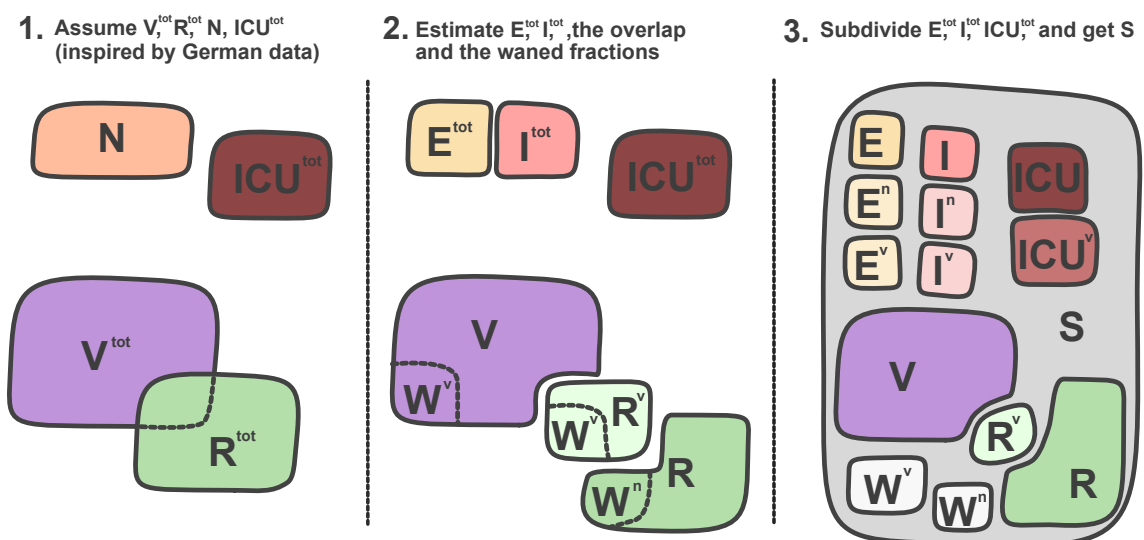
Supplementary Figure S5: **The procedure of obtaining initial conditions for the model compartments.** Starting with parts of the population attributed to different states N, ICU, V^{tot}, and R^{tot}, we calculate reasonable values for the initial conditions of all compartments step by step. Compartment sizes in the figure are chosen arbitrarily and do not represent actual size in terms of people.

other compartments. First, however, we have to uniformly age-stratify these values. ICU occupancy and the number of new COVID-19 cases can be obtained in an age-stratified way for the case of Germany. For the number of vaccinated and recovered, we assess countries that report age-stratified data, such as Denmark, and distribute the total numbers V^{tot} and R^{tot} onto the various age groups as can be seen in Tab. S6. Given the initial values for V_i^{tot}, R_i^{tot}, N_i and $\text{ICU}_i^{\text{tot}}$ for every age group i, we calculate the values for all other compartments:

Immune compartments separated by vaccination status and previous infection

First, we consider the possibility that individuals were both previously vaccinated and infected. Thus, to avoid overestimating the number of immunised individuals, we estimate the overlap between V_i^{tot} and R_i^{tot}: As a first order estimate, we assume that the probability of being vaccinated and having recovered are independent of each other. That way, the probability of being both vaccinated and recovered is given as the product of the two probabilities:

$$\text{Prob}(x \in V_i^{\text{tot}} \wedge x \in R_i^{\text{tot}}) = \text{Prob}(x \in V_i^{\text{tot}}) \cdot \text{Prob}(x \in R_i^{\text{tot}}) \tag{38}$$

Accordingly, the fraction of vaccinated in the total population for age group i, $\frac{V_i^{\text{tot}}}{M_i}$, is the same as the fraction of vaccinated in the recovered part of the population, $\frac{R_i^v}{R_i^{\text{tot}}}$. Hence, the initial numbers of recovered vaccinated, R_i^v, and unvaccinated individuals, R_i, are estimated via

$$R_i^v = \frac{V_i^{\text{tot}}}{M_i} R_i^{\text{tot}} \text{ and } R_i = R_i^{\text{tot}} - R_i^v. \tag{39}$$

Consequently, we receive the number of vaccinated individuals without previous infection by subtracting the overlap:

$$V_i = V_i^{\text{tot}} - R_i^v. \tag{40}$$

This process is illustrated in Fig. S5.

Waned compartments separated by immunity status

Next, we consider the fraction of vaccinated and recovered individuals whose immunity has waned (see Tab. S6): For the recovered, we assume that the time point at which infections took place in the past was age-independent and thus attribute the same fraction of waned natural immunity to all age groups. However, this assumption does not hold for vaccine-induced immunity because older age groups were typically vaccinated at an earlier point in time. We subtract the waned fractions from the compartments V_i, R_i and R_i^v, obtaining W_i^n and W_i^v.

Susceptible compartment

The susceptible compartment S_i comprises of all individuals not belonging to any of the other compartments. It can be calculated via

$$S_i = M_i - V_i - R_i - R_i^v - W_i^n - W_i^v - N_i - \text{ICU}_i^{\text{tot}}. \tag{41}$$

Exposed and infectious compartments separated by immunity status

We estimate the initial conditions for the exposed and infected compartments by first estimating $E_i^{\text{tot}} = E_i + E_i^n + E_i^v$ and $I_i^{\text{tot}} = I_i + I_i^n + I_i^v$ by

$$E_i^{\text{tot}} = \frac{1}{\rho} N_i \quad \text{and} \quad I_i^{\text{tot}} = \frac{1}{\gamma_i + \delta_i + \theta_i} N_i. \tag{42}$$

The fractions $\frac{1}{\rho}$ and $\frac{1}{\gamma + \delta + \theta}$ are the average times spent in the exposed and infected compartments, respectively (approximately).

To find out how E_i^{tot} and I_i^{tot} distribute onto their sub-compartments, i.e., for the different immune status and age groups, we look at their origin: Because all the infections in E_i originate from S_i, the ones in E_i^n from W_i^n and the ones in E_i^v from W_i^v, we can distribute E_i^{tot} onto the sub-compartments via

$$E_i = \frac{S_i}{S_i + W_i^n + W_i^v} E_i^{\text{tot}}, \quad E_i^n = \frac{W_i^n}{S_i + W_i^n + W_i^v} E_i^{\text{tot}}, \quad E_i^v = \frac{W_i^v}{S_i + W_i^n + W_i^v} E_i^{\text{tot}} \tag{43}$$

and analogously for I_i^{tot}.

ICU compartments separated by vaccination status

To determine the distribution of $\text{ICU}_i^{\text{tot}}$ onto the compartments ICU_i and ICU_i^v, we consider that the probability to require ICU care for individuals in the compartments I_i^n and I_i^v is reduced by a factor of $(1 - \kappa)$. Hence,

$$\text{ICU}_i^v = \frac{I_i^v (1 - \kappa)}{I_i + (I_i^n + I_i^v)(1 - \kappa)} \text{ICU}_i^{\text{tot}} \quad \text{and} \quad \text{ICU}_i = \text{ICU}_i^{\text{tot}} - \text{ICU}_i^v. \tag{44}$$

The initial condition for the dead is set to $D_i = 0$, for the currently vaccinated to $u_i^{\text{current}} = V_i^{\text{tot}}$ and for the currently boostered to $w_i^{\text{current}} = 0$. For the initial condition of H_*, values of past ICU occupancy development are needed. Here, we assume a constant past value of the ICU occupancy at $t \leq d_0$ for both ICU compartments.

S4   SENSITIVITY ANALYSIS

The results of this model depend on the choices of all parameters involved. While some epidemiological parameters are well understood and quantified at this point in the pandemic, some other parameters of our model remain uncertain, but might have a large impact on the results. In this section we analyse the sensitivity of our results to changes in parameters. We vary each parameter independently across its assumed range (see Sec. S4.2) and look at how this affects the maximal ICU occupancy observed in the first (winter) and second (spring) waves. We choose a moderate scenario (Scenario 3) for the analysis and look at how the two peaks of ICU occupancy (one in winter, one after lifting restrictions) change in magnitude.

S4.1 Sensitivity to additional parameters

For a more precise analysis we introduce new parameters to our model (Tab S7). Firstly, we consider the possibility of previously immunised individuals having a reduced viral load and thus being less infectious. This has been reported for vaccinated individuals e.g. in Harris et al. (2021) for the Alpha variant of SARS-CoV-2, but is unclear for current and future variants. In the model, it can be represented by a change in I^{eff}, introducing a parameter σ for reduced viral load in the infectious compartments I^n and I^v:

$$I_i^{\text{eff}} = (I_i + \sigma(I_i^n + I_i^v) + \Psi M_i) \tag{45}$$

Next, we include the possibility that post-infection and vaccine-induced immunity wane at different rates Ω_n and Ω_v, respectively. Lastly, we introduce a parameter that affects the shape of $k_{\text{seasonality}}$. The transmission of SARS-CoV-2 is strongly reduced in outdoor encounters in comparison to indoor encounters. Thus, winter typically offers more opportunities for viral spread than summer because more activities are performed inside. However, the transition between summer and winter might look different than the standard sinusoidal suggested in Eq. 7. In particular, it could be the case that above a certain temperature most activities move outside all at once, resulting in a steeper transition between summer and winter as soon as temperatures allow for it. To model this, we introduce an exponent $\xi \in [0, 1]$ that modifies the sinusoidal:

$$k_{\text{seasonality}} = 1 + \mu \cdot \text{sgn}\left(\cos\left(t^\star\right)\right) \cdot \left|\cos\left(t^\star\right)\right|^\xi \quad \text{with} \quad t^\star = 2\pi \frac{t + d_0 - d_\mu}{360}. \tag{46}$$

That way, for $\xi \to 0$ the cosine in $k_{\text{seasonality}}$ becomes a step function.

S4.2 Parameter ranges

The way we vary parameters differs between age-dependent and non-age-dependent parameters as well as between parameters bound to the $[0, 1]$ interval (e.g., κ) and those belonging to arbitrary intervals. For the age-independent parameters $\kappa, \sigma, \xi \in [0, 1]$ we vary them in the range $[0.5, 1]$ (for κ and σ) and $[0, 1]$ (for ξ). For the age-dependent rates with arbitrary range, δ_i, $\gamma_{\text{ICU},i}$, θ_i, and $\theta_{\text{ICU},i}$, we consider a range around their default value by a factor of two. For example, for δ_i we vary across the ranges $[\frac{\delta_i^{\text{default}}}{2}, 2\delta_i^{\text{default}}] \forall i$ at the same time for all age-groups. Figure S7 summarises these results.

Parameters related to the memory kernel p_R, b_R, p_{vac}, and b_{vac} as well as the sensitivities to vaccine uptake α_u and α_w are also varied around their default value by a factor of two.

For age-dependent parameters related to vaccine uptake $u_i^{\text{base}}, w_i^{\text{base}}, \chi_{u_i}$, and χ_{w_i} which are bound to the interval $[0, 1]$, we look at their base value multiplied by a factor in the range $[0.8, 1.2]$ and vary one parameter for all age groups at the same time. Figure S8 summarises these results. Parameters $\tau_u, \tau_w, t_u, t_w, H_{\text{max}}$, and the influx Ψ are varied in a range chosen broad enough such that an effect is observable.

The average immunity waning times $(\Omega^n)^{-1}$ and $(\Omega^v)^{-1}$ are varied in the range between 4 months and 1 year and the waning rates thus is the range of the inverse values.

S4.3 High impact parameters

In this section we discuss parameters that have a large impact on the quantitative results when being varied.

As expected, the waning rate of vaccine-induced immunity Ω^v, leads to much higher waves when increased. The peak of the wave after lifting restrictions is more than doubled for an average waning time of 4.5 months instead of the 7.5 months used as default.

The vaccine efficacy κ also plays an important role in the second wave, as by that time, most infections will originate from the waned compartments.

Naturally, the transition rates to ICU δ_i have a large impact on the magnitude of the waves. Interestingly, the impact is a lot stronger for the second wave than for the first wave. The reason is that the first wave mainly affects the unvaccinated younger age groups that are less likely to transition to ICU, whereas the second wave affects all age groups similarly.

One of the main uncertainties in our model is the choice of the sensitivity parameters α_u and α_w that modulate vaccine uptake in dependence of risk perception H_u and H_w. Lower values imply a population less reactive to threat, which results in higher waves as can be seen in Fig. S8. On the other hand, for large values of α_u and α_w, ICU occupancy seems to plateau, not decreasing any further. This suggests a limitation on what voluntary vaccination alone can do to prevent bringing ICUs to capacity limits (given our model assumptions).
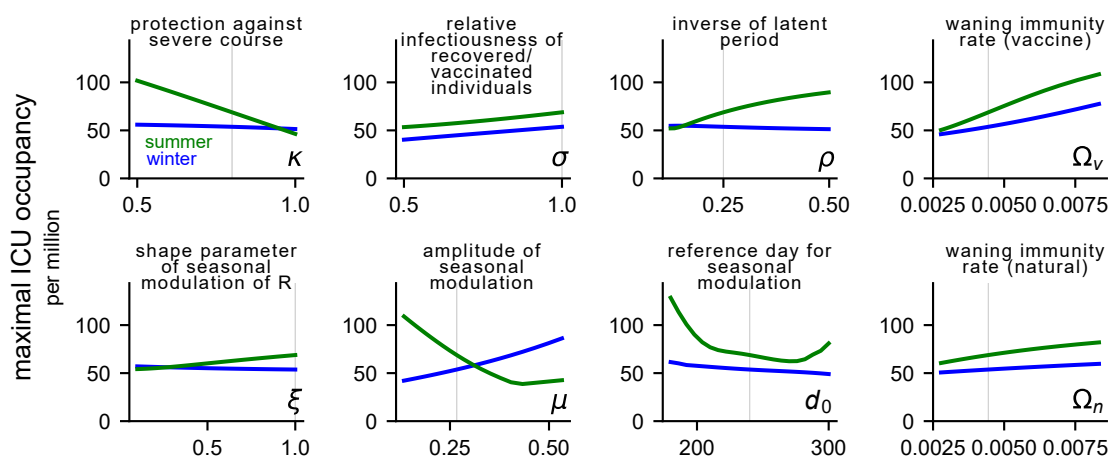
Supplementary Figure S6: **Propagation of parameter uncertainties.** Parameters are varied independently across their assumed range. The measured quantity is the maximum ICU occupancy observed in the first wave (blue) and the second wave (green). A vertical line indicates the default value of the parameter. Thus, the points where the green and blue curve intersect the vertical line have the same y-coordinate in all plots.

S5 AGE-STRATIFIED RESULTS

Figures S10-S14 show the age-stratified results for all scenarios of the main text.
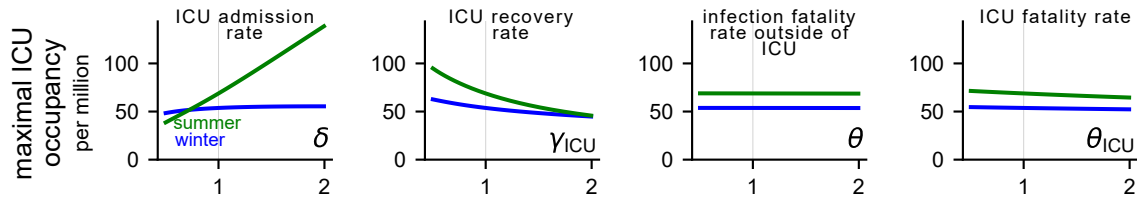
Supplementary Figure S7: **Propagation of parameter uncertainties related to age-dependent transition rates.** Parameters are varied independently across their assumed range. Note that the parameters are age-dependent (vector like) and the x-axis indicates a multiplicative factor applied to all values of the vector at the same time, instead of a single averaged parameter value. Therefore, the default parameter value indicated by the grey vertical line is always at 1.
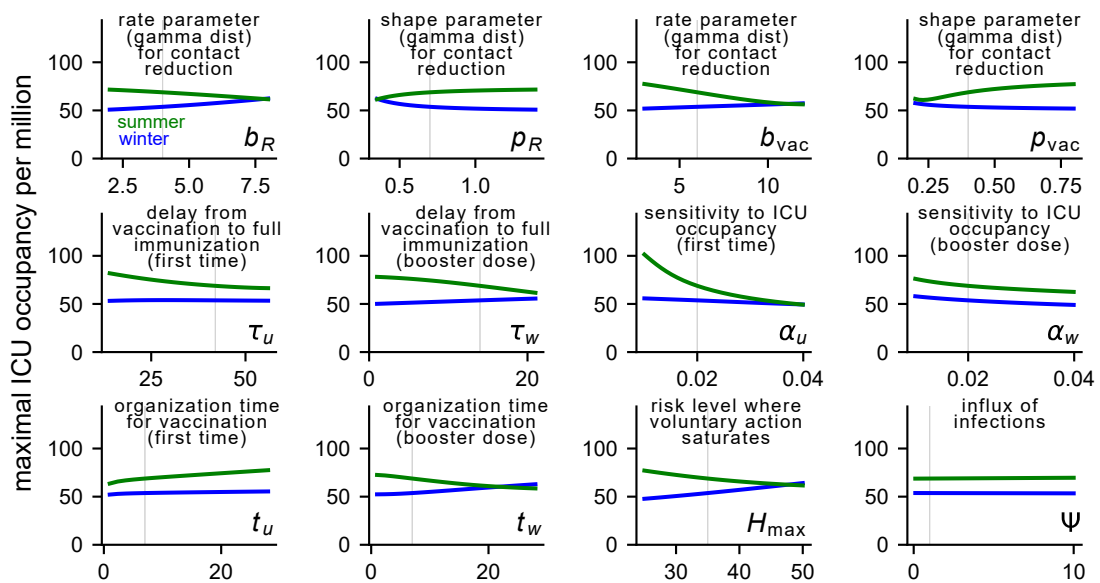
Supplementary Figure S8: **Propagation of vaccine uptake- related parameter uncertainties.** Parameters are varied independently across their assumed range. The measured quantity is the maximum ICU occupancy observed in the first wave (blue) and the second wave (green). A vertical line indicates the default value of the parameter. Thus, the points where the green and blue curve intersect the vertical line have the same y-coordinate in all plots.
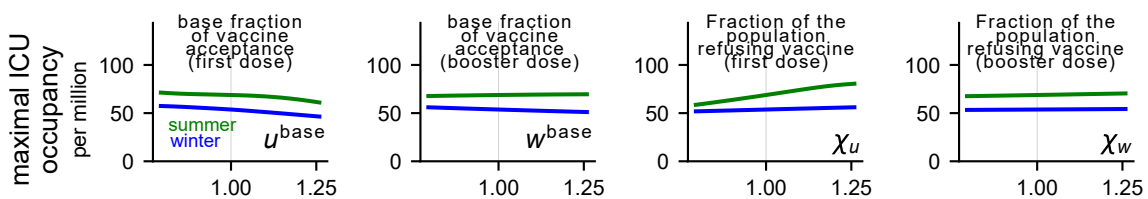
Supplementary Figure S9: **Uncertainty propagation of age-dependent parameters related to vaccine uptake.** Parameters are varied independently across their assumed range. Note that the parameters are age-dependent (vector like) and the x-axis indicates a multiplicative factor applied to all values of the vector at the same time, instead of a single averaged parameter value. Therefore, the default parameter value indicated by the grey vertical line is always at 1.

Table S5. Model variables.

Variable	Meaning	Unit	Explanation
M	Population size	people	Default value: 1,000,000
S	Susceptible compartment	people	Non-infected people, who may acquire the virus.
V	Vaccinated compartment	people	Non-infected, vaccinated people. Less likely to be infected or develop severe symptoms
W^n	Waned post-infection immunity compartment	people	Non-infected people whose post-infection immunity has already waned, thus may acquire the virus.
W^v	Waned vaccine immunity compartment	people	Non-infected people whose vaccine-induced immunity has already waned, thus may acquire the virus.
E	Nonvaccinated exposed compartment	people	Nonvaccinated, non-previously-infected people exposed to the virus.
E^n	Nonvaccinated, waned exposed compartment	people	Nonvaccinated, previously-infected people exposed to the virus whose post-infection immunity has waned.
E^v	Vaccinated exposed compartment	people	Exposed people with waned vaccine immunity.
I	Infectious compartment	people	Infectious people from the susceptible compartment S.
I^n	Nonvaccinated, waned infectious compartment	people	Infectious people from E^n.
I^v	Vaccinated infectious compartment	people	Infectious people with waned vaccine-induced immunity.
ICU	Nonvaccinated hospitalised	people	Nonvaccinated hospitalised people (from I and I^n).
ICU^v	Vaccinated hospitalised	people	Previously-vaccinated, hospitalised people (from I^v).
R	Unvaccinated Recovered	people	Unvaccinated recovered people (with or without requiring intensive care).
R^v	Vaccinated Recovered	people	Vaccinated recovered people (with or without requiring intensive care).
H_*	Avg. ICU occupancy	people	Auxiliary variable measuring the memory on past ICU occupancy.
$u^{\text{current}}, w^{\text{current}}$	Vaccinated individuals, independent of the compartment	–	Integral over the vaccination rates ϕ, φ.
$k_{\text{seasonality}}$	Seasonal variation of SARS-CoV-2 transmission	–	Eq. 7.
$k_{\text{NPI,self}}$	Reduction of infections due to mandatory NPIs and voluntary behaviour	–	Sec. S1.3
$\phi(t), \varphi(t)$	Administration rate of first-time and booster vaccine doses (resp.)	doses/day	Eq. 11, 13

Table S6. Initial conditions by age group. The total population size in the model is $M = 10^6$. The column $\frac{V_i^{\text{tot}}+R_i^{\text{tot}}-R_i^v}{M_i}$ shows the effective fraction of the population that is immune, which for the entire population is 68% (with $\sum_i R_i^{\text{tot}}/M = 0.2$ and $\sum_i V_i^{\text{tot}}/M = 0.6$). Sources: 1: Bauer et al. (2021), 2: Ritchie et al. (2021), 3:am RKI (2020)

ID	age group	M_i/M	$\frac{V_i^{\text{tot}}}{M_i}$	$\frac{R_i^{\text{tot}}}{M_i}$	N_i	$\text{ICU}_i^{\text{tot}}$	$\frac{W_i^v}{V_i+R_i^v}$	$\frac{W_i^n}{R_i}$	$\frac{V_i^{\text{tot}}+R_i^{\text{tot}}-R_i^v}{M_i}$
1	0-19	0.18	0.15	0.2	18.5	0.14	5%	50%	0.32
2	20-39	0.25	0.56	0.2	16.8	1.24	5%	50%	0.65
3	40-59	0.28	0.67	0.2	15.9	4.90	10%	50%	0.74
4	60-69	0.13	0.77	0.2	6.4	3.10	20%	50%	0.82
5	70-79	0.09	0.88	0.2	3.5	2.46	30%	50%	0.90
6	80+	0.07	0.95	0.2	2.3	1.62	40%	50%	0.96
Source	-	1	assumed	assumed	2	3	assumed	assumed	calculated

Table S7. Additional model parameters introduced in the sensitivity analysis.

Parameter	Meaning	Value (default)	Unit	Source
σ	Relative viral load of recovered/vaccinated individuals	1	—	Levine-Tiefenbrun et al. (2021)
Ω_n	Waning rate of post-infection immunity	$\frac{1}{125}$	day^{-1}	Tartof et al. (2021)
Ω_v	Waning rate of vaccine immunity	$\frac{1}{125}$	day^{-1}	Tartof et al. (2021)
ξ	Shape of the seasonality function $k_{\text{seasonality}}$	1	—	Gavenčiak et al. (2021)
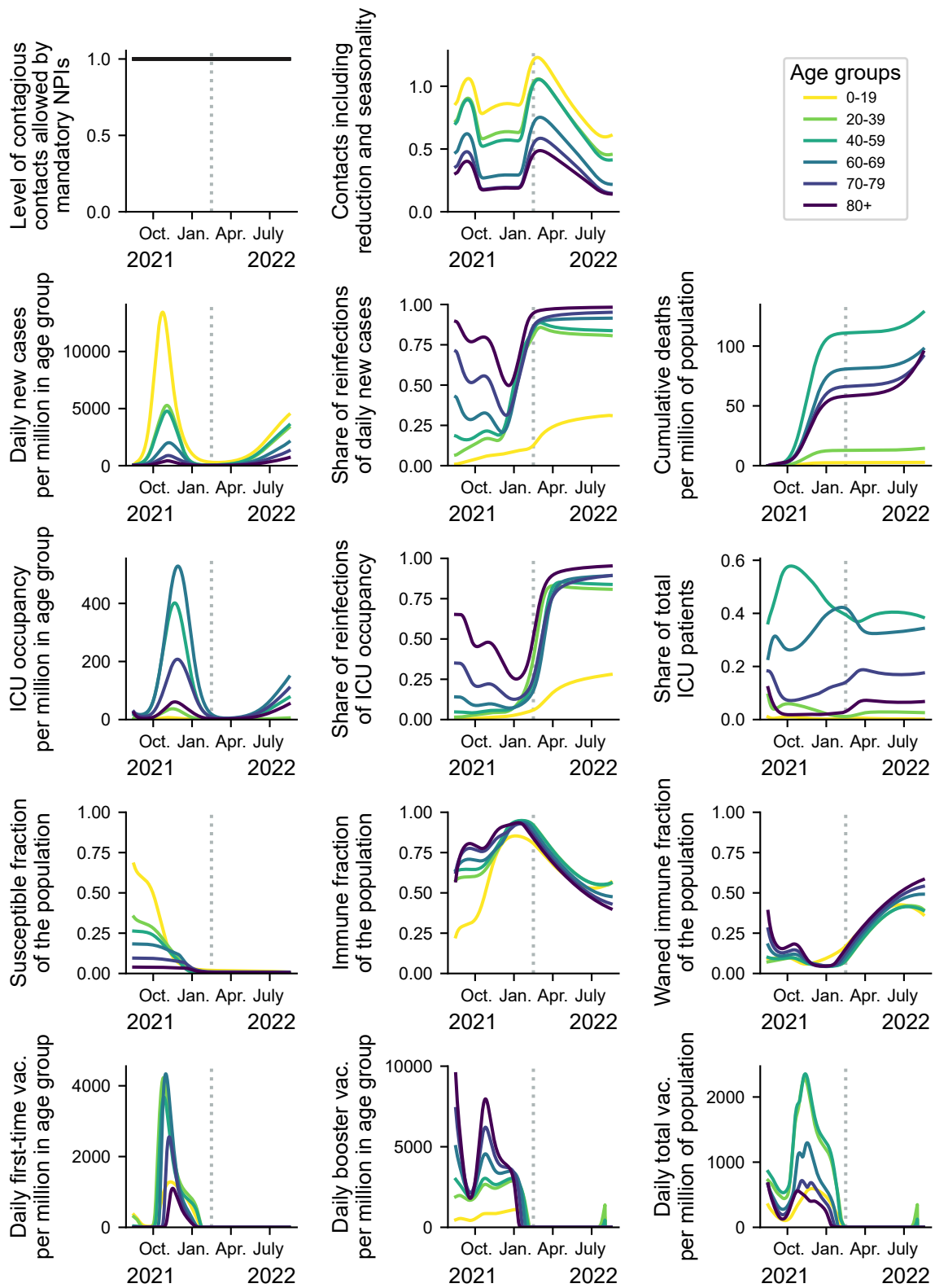
Supplementary Figure S10: **Age-stratified results for scenario 1.**
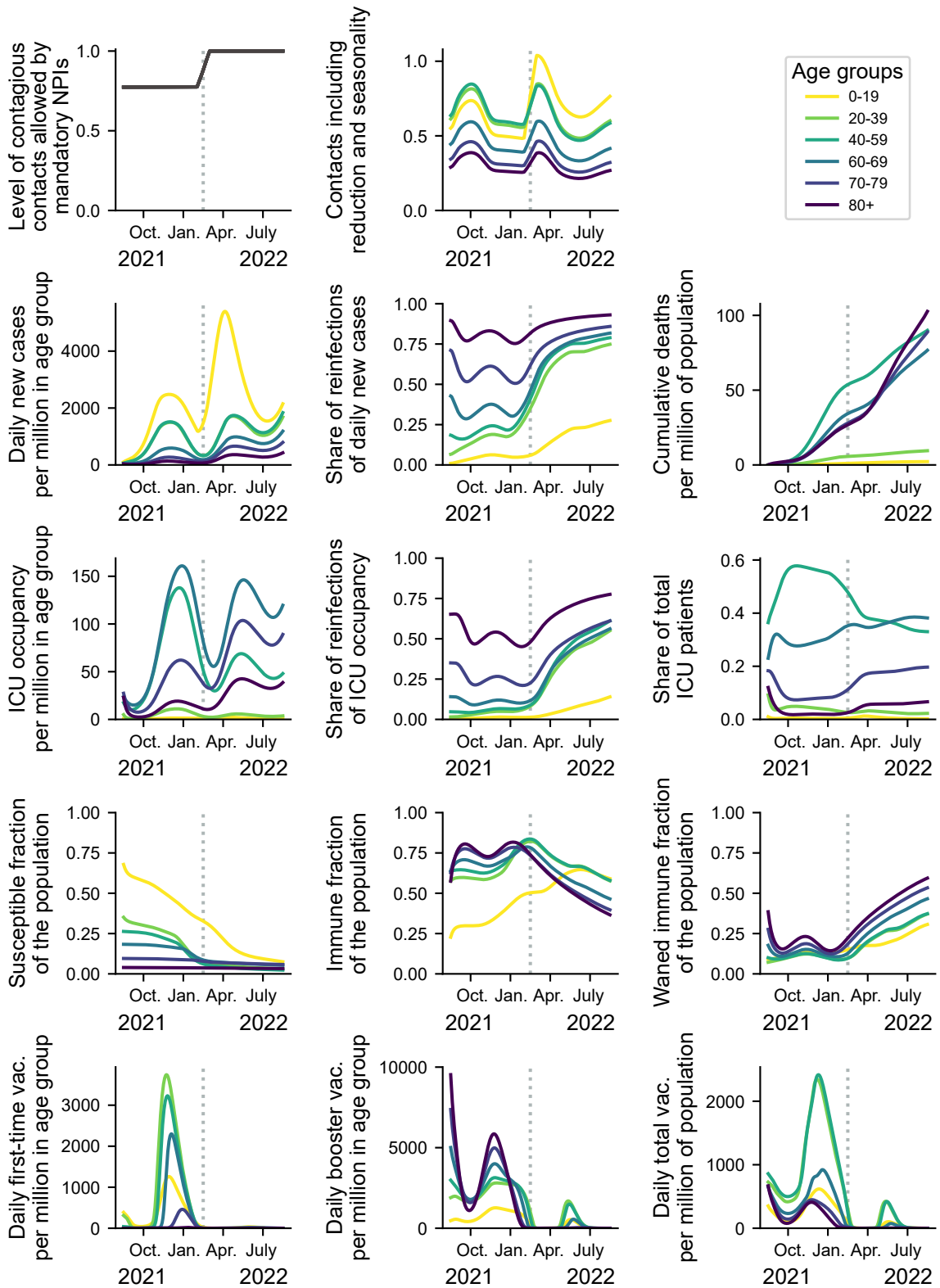
Supplementary Figure S11: **Age-stratified results for scenario 2.**
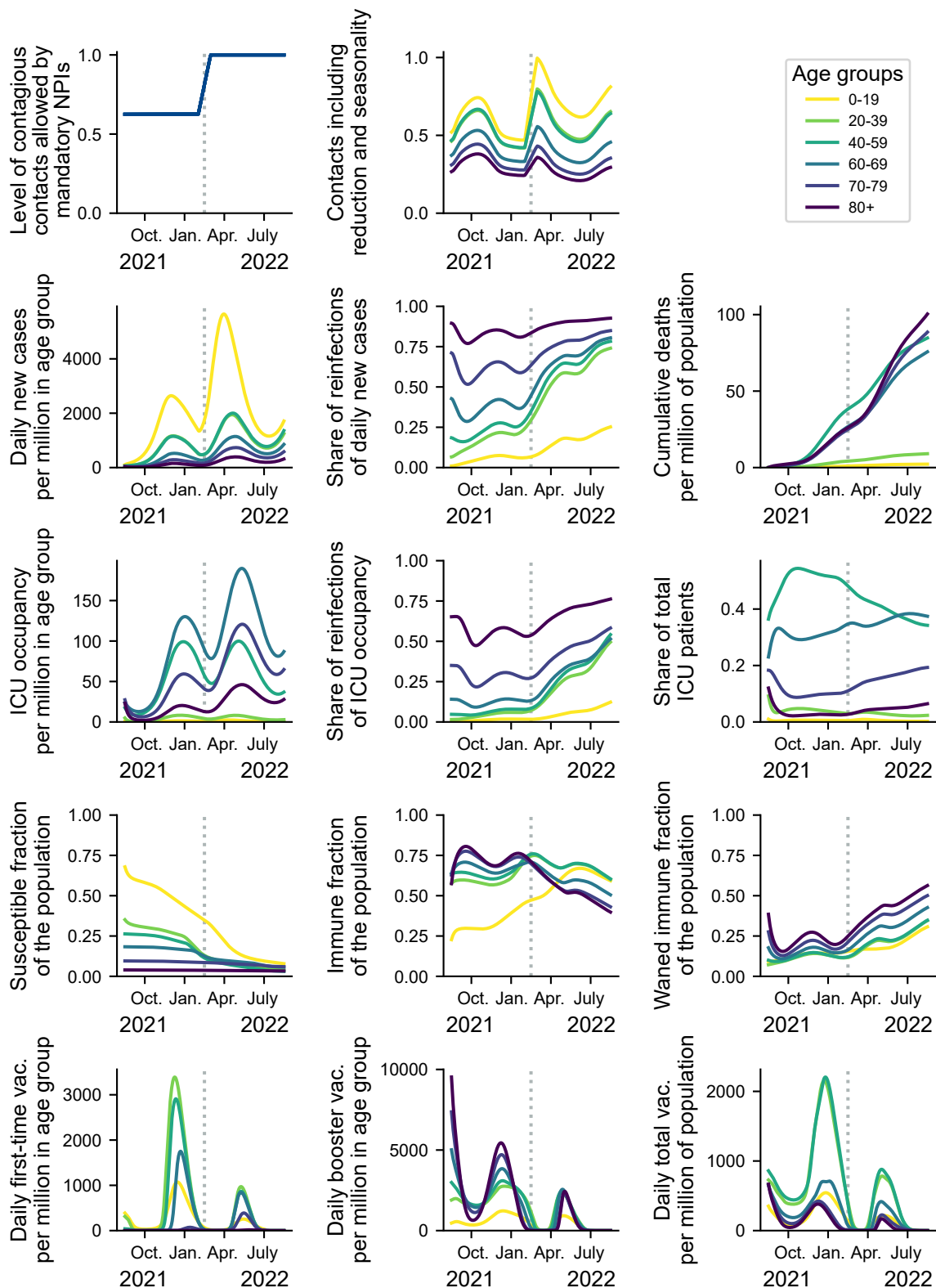
Supplementary Figure S12: **Age-stratified results for scenario 3.**
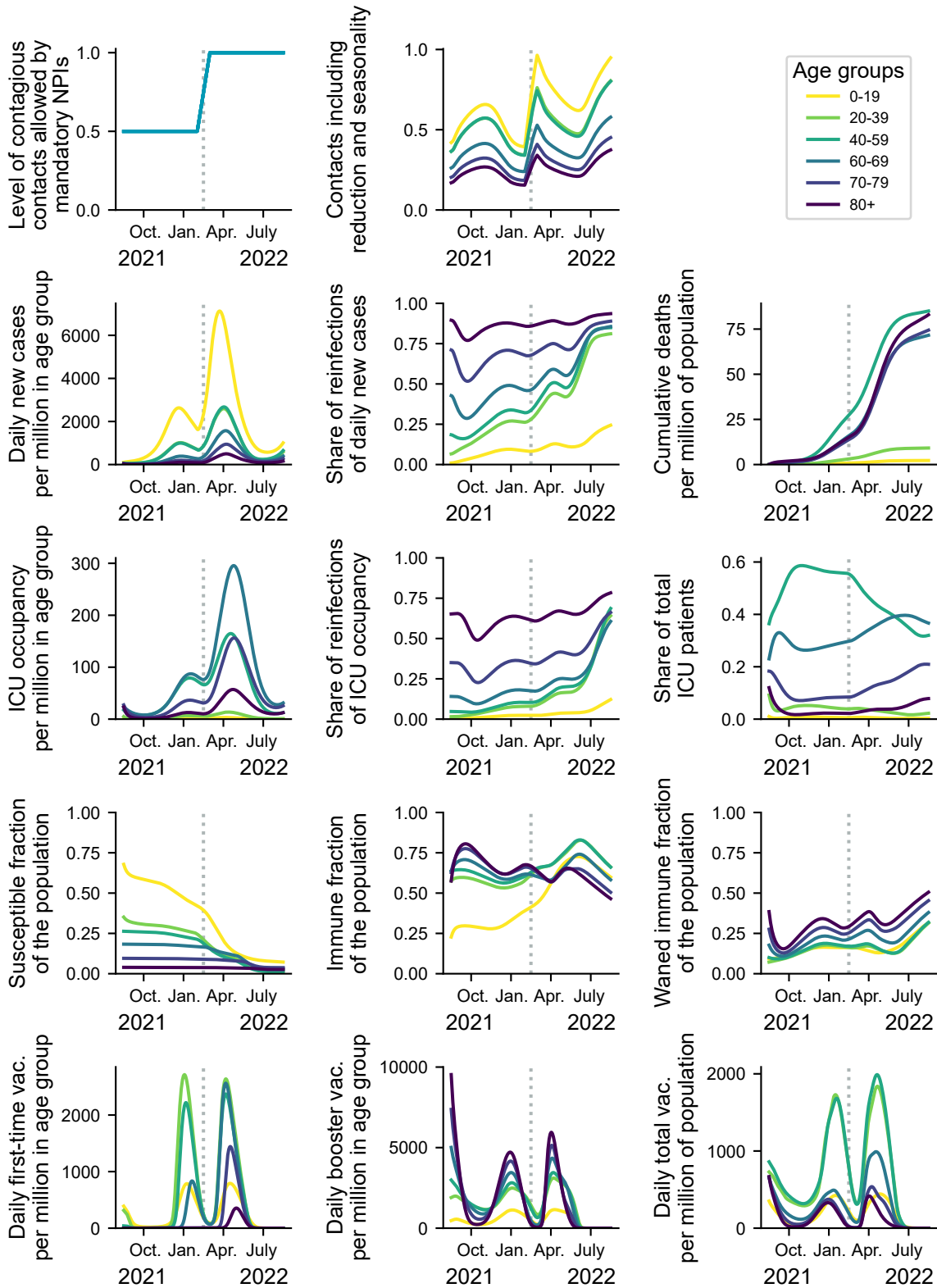
Supplementary Figure S13: **Age-stratified results for scenario 4.**
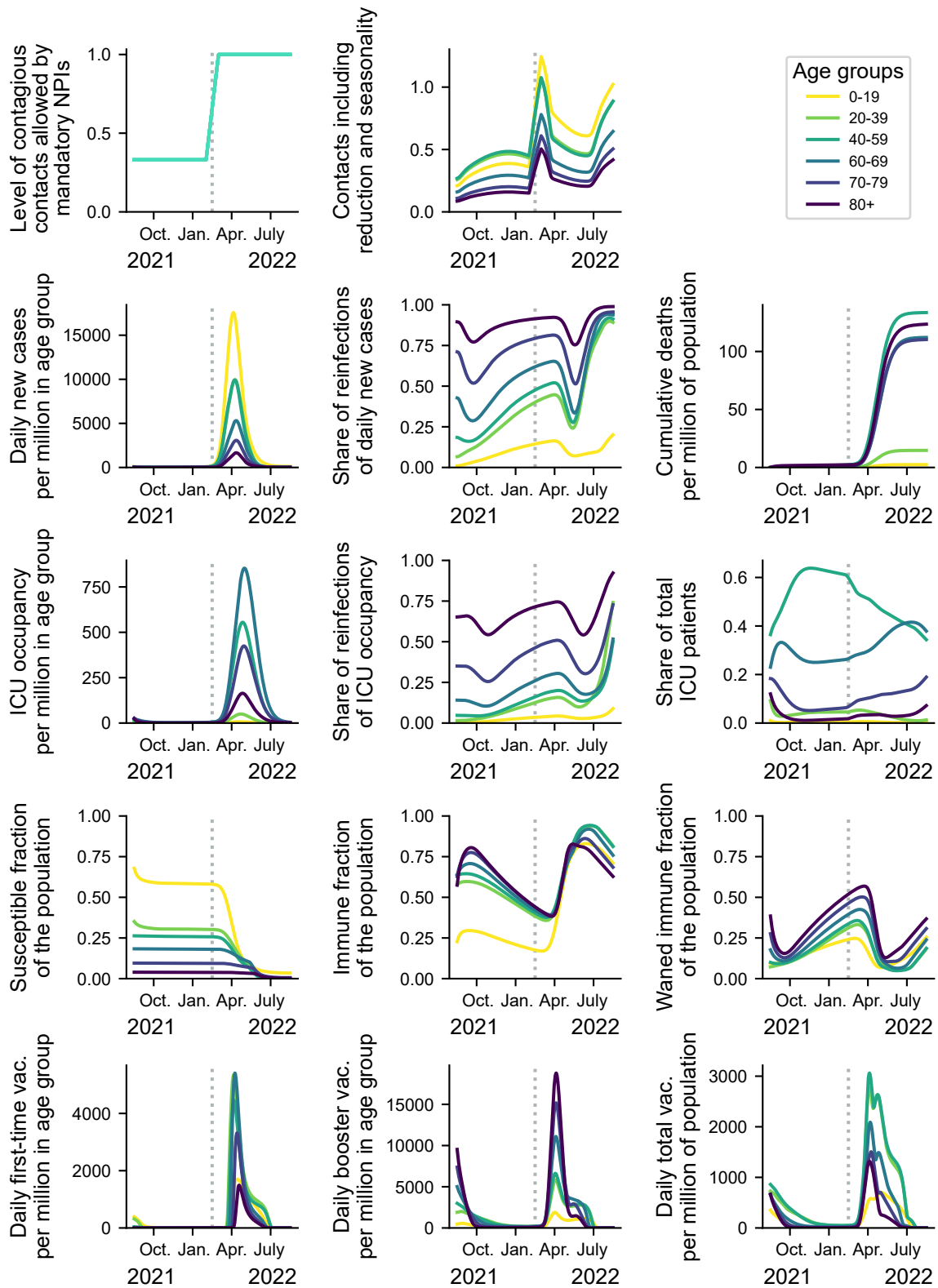
Supplementary Figure S14: **Age-stratified results for scenario 5.**

REFERENCES

Zauberman G, Kim BK, Malkoc SA, Bettman JR. Discounting time and time discounting: Subjective time perception and intertemporal preferences. *Journal of Marketing Research* **46** (2009) 543–556.

Mistry D, Litvinova M, y Piontti AP, Chinazzi M, Fumanelli L, Gomes MF, et al. Inferring high-resolution human mixing patterns for disease modeling. *Nature communications* **12** (2021) 1–12.

Diekmann O, Heesterbeek J, Roberts MG. The construction of next-generation matrices for compartmental epidemic models. *Journal of the Royal Society Interface* **7** (2010) 873–885.

Gavenčiak T, Monrad JT, Leech G, Sharma M, Mindermann S, Brauner JM, et al. Seasonal variation in sars-cov-2 transmission in temperate climates. *medRxiv* (2021). doi:10.1101/2021.06.10.21258647.

Thomas SJ, Moreira Jr ED, Kitchin N, Absalon J, Gurtman A, Lockhart S, et al. Safety and efficacy of the bnt162b2 mrna covid-19 vaccine through 6 months. *New England Journal of Medicine* (2021).

Puranik A, Lenehan PJ, O'Horo JC, Niesen MJ, Virk A, Swift MD, et al. Durability analysis of the highly effective bnt162b2 vaccine against covid-19. *medRxiv* (2021).

Turner JS, Kim W, Kalaidina E, Goss CW, Rauseo AM, Schmitz AJ, et al. Sars-cov-2 infection induces long-lived bone marrow plasma cells in humans. *Nature* (2021) 1–5.

Tartof SY, Slezak JM, Fischer H, Hong V, Ackerson BK, Ranasinghe ON, et al. Effectiveness of mrna bnt162b2 covid-19 vaccine up to 6 months in a large integrated health system in the usa: a retrospective cohort study. *The Lancet* **398** (2021) 1407–1416.

Chemaitelly H, Tang P, Hasan MR, AlMukdad S, Yassine HM, Benslimane FM, et al. Waning of bnt162b2 vaccine protection against sars-cov-2 infection in qatar. *New England Journal of Medicine* (2021).

Pegu A, O'Connell SE, Schmidt SD, O'Dell S, Talana CA, Lai L, et al. Durability of mrna-1273 vaccine–induced antibodies against sars-cov-2 variants. *Science* **373** (2021) 1372–1377.

Naaber P, Tserel L, Kangro K, Sepp E, Jürjenson V, Adamson A, et al. Dynamics of antibody response to bnt162b2 vaccine after six months: a longitudinal prospective study. *The Lancet Regional Health-Europe* **10** (2021) 100208.

Ritchie H, Mathieu E, Rodés-Guirao L, Appel C, Giattino C, Ortiz-Ospina E, et al. Coronavirus pandemic (covid-19). *Our World in Data* (2021). Https://ourworldindata.org/coronavirus.

Bauer S, Contreras S, Dehning J, Linden M, Iftekhar E, Mohr SB, et al. Relaxing restrictions at the pace of vaccination increases freedom and guards against further covid-19 waves. *PLoS computational biology* **17** (2021) e1009288.

Levin AT, Hanage WP, Owusu-Boaitey N, Cochran KB, Walsh SP, Meyerowitz-Katz G. Assessing the age specificity of infection fatality rates for COVID-19: systematic review, meta-analysis, and public policy implications. *European Journal of Epidemiology* (2020). doi:10.1007/s10654-020-00698-1.

Salje H, Kiem CT, Lefrancq N, Courtejoie N, Bosetti P, Paireau J, et al. Estimating the burden of SARS-CoV-2 in France. *Science* **369** (2020) 208–211.

Linden M, Mohr SB, Dehning J, Mohring J, Meyer-Hermann M, Pigeot I, et al. Case numbers beyond contact tracing capacity are endangering the containment of COVID-19 . *Dtsch Arztebl International* **117** (2020) 790–791. doi:10.3238/arztebl.2020.0790.

He X, Lau EHY, Wu P, Deng X, Wang J, Hao X, et al. Temporal dynamics in viral shedding and transmissibility of COVID-19 . *Nature Medicine* (2020) 1–4.

Pan F, Ye T, Sun P, Gui S, Liang B, Li L, et al. Time course of lung changes on chest CT during recovery from 2019 novel coronavirus (COVID-19) pneumonia. *Radiology* (2020) 200370.

Liu Y, Rocklöv J. The reproductive number of the delta variant of sars-cov-2 is far higher compared to the ancestral sars-cov-2 virus. *Journal of travel medicine* (2021).

Bar-On YM, Flamholz A, Phillips R, Milo R. Science forum: SARS-CoV-2 (COVID-19) by the numbers. *Elife* **9** (2020) e57309.

Li R, Pei S, Chen B, Song Y, Zhang T, Yang W, et al. Substantial undocumented infection facilitates the rapid dissemination of novel coronavirus (SARS-CoV-2). *Science* **368** (2020) 489–493.

Wouters OJ, Shadlen KC, Salcher-Konrad M, Pollard AJ, Larson HJ, Teerawattananon Y, et al. Challenges in ensuring global access to COVID-19 vaccines: production, affordability, allocation, and deployment. *The Lancet* (2021).

Betsch C, Wieler LH, Habersaat K. Monitoring behavioural insights related to covid-19. *The Lancet* **395** (2020) 1255–1256.

[Dataset] am RKI IT. Tagesreport aus dem DIVI-Intensivregister. `https://doi.org/10.25646/7625` (2020). doi:10.25646/7625.

Levine-Tiefenbrun M, Yelin I, Alapi H, Katz R, Herzel E, Kuint J, et al. Viral loads of delta-variant sars-cov-2 breakthrough infections after vaccination and booster with bnt162b2. *Nature Medicine* (2021) 1–3.

Harris RJ, Hall JA, Zaidi A, Andrews NJ, Dunbar JK, Dabrera G. Impact of vaccination on household transmission of sars-cov-2 in england. *medRxiv* (2021).

APPENDIX D: SUPPLEMENTARY INFORMATION TO CHAPTER 6:
"IMPACT OF THE EURO 2020 CHAMPIONSHIP ON THE SPREAD
OF COVID-19"

Jonas Dehning[1],[¶], Sebastian B. Mohr[1],[¶], Sebastian Contreras[1], Philipp Dönges[1], Emil Iftekhar[1], Oliver Schulz[2], Philip Bechtle[3],[*], and Viola Priesemann[1],[4],[5] [†]

[1]Max Planck Institute for Dynamics and Self-Organization, Am Faßberg 17, 37077 Göttingen, Germany.
[2]Max Planck Institute for Physics, Föhringer Ring 6, 80805 München, Germany
[3]Physikalisches Institut, Universität Bonn, Nußallee 12, 53115 Bonn, Germany
[4]Institute for the Dynamics of Complex Systems, University of Göttingen, Friedrich-Hund-Platz 1, 37077 Göttingen, Germany.
[5]Institute of Computer Science and Campus Institute Data Science, University of Göttingen, Goldschmidtstraße 7, 24118 Göttingen, Germany
[¶] These authors contributed equally

Contents

[*]bechtle@physik.uni-bonn.de
[†]viola.priesemann@ds.mpg.de

S1   Data sources

We used the daily COVID-19 case numbers, resolved by age and country, as reported publicly by the state health institute or equivalent of each country covered in this work. The data was retrieved either directly or taken from COVerAGE-DB [1]:

- Germany: Robert Koch Institut
  `https://www.arcgis.com/home/item.html?id=f10774f1c63e40168479a1feb6c7ca74`

- France: Santé publique France
  `https://www.data.gouv.fr/fr/datasets/taux-dincidence-de-lepidemie-de-covid-19`

- England: National Health Service
  `https://coronavirus.data.gov.uk/details/download`

- Scotland: Public Health Scotland
  `https://www.opendata.nhs.scot/dataset/covid-19-in-scotland`

- Austria: Österreichische Agentur für Gesundheit und Ernährungssicherheit GmbH
  `https://covid19-dashboard.ages.at/`

- Belgium: Sciensano
  `https://epistat.wiv-isp.be/covid/`

- The Czech Republic: Ministerstvo zdravotnictví
  `https://onemocneni-aktualne.mzcr.cz/covid-19`

- Italy: Istituto Superiore di Sanità
  Aggregated by COVerAGE-DB from
  `https://www.epicentro.iss.it/coronavirus/sars-cov-2-sorveglianza-dati`

- The Netherlands: National Institute for Public Health and the Environment
  `https://data.rivm.nl/covid-19/`

- Slovakia: The Institute for Healthcare Analyses (IZA) of the Ministry of Health
  Aggregated by COVerAGE-DB from
  `https://github.com/Institut-Zdravotnych-Analyz/covid19-data`

- Spain: Ministry of Public Health
  Aggregated by COVerAGE-DB from
  `https://cnecovid.isciii.es/covid19/`

To estimate the deaths associated with the Euro 2020 cases we calculate the case fatality risk by using the number of deaths and number of cases as reported by Our World in Data (OWD) [2].

For showcasing the stringency of governmental measures (panel C in Fig. S24-S36), we used data from the Oxford COVID-19 Government Response Tracker [3] and the public health and social measures (PHSM) severity index [4] from the World Health Organization (WHO). For our correlational analysis of cases and human mobility (Fig. 3B and S4), we used data from the COVID-19 Community Mobility Reports [5] provided by Google. For correlation with pre-Euro 2020 incidences (Fig.S6B) we use case numbers as reported by the Johns Hopkins University (JHU) [6]. Lastly, we used data from Google Trends [7] to investigate people's interest in the Euro 2020 (Fig. S20).

S2 Supplementary analysis: our results in context
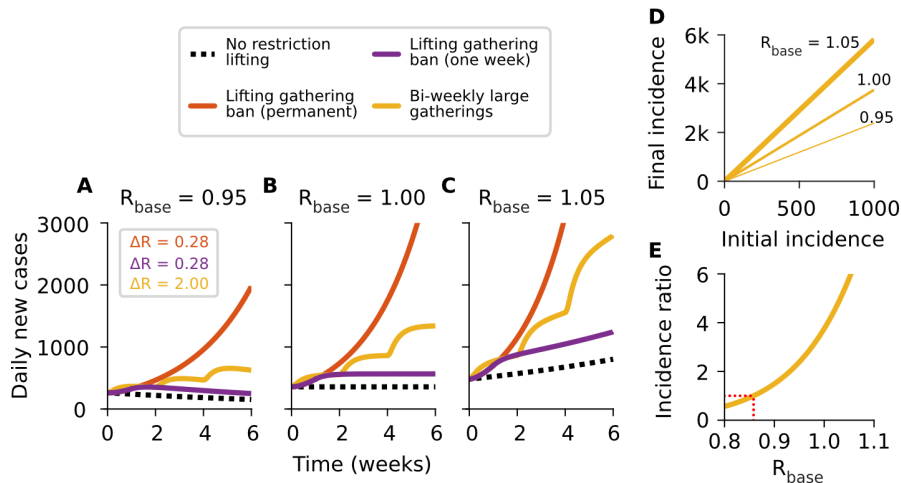
Supplementary Figure S1: **Our results in context: How much of an effect do short but strong increases of transmission have?** **A–C:** Understanding Euro 2020 matches as point interventions where the reproduction number is allowed to increase drastically from its base level R_{base} for one day ($\Delta R = 2.0$, yellow curve), we compare its cumulative effect with different scenarios of lifting restrictions. These effects are in the order of magnitude of those reported in the literature [8]. The purple lines represent the same effect as a single increase but distributed over one week ($\Delta R = 0.28 \approx 2/7$), while the red curve represents a permanent lifting of those restrictions. The effect of the yellow and purple interventions is similar for $t \leq 2$ weeks because the product between ΔR and the duration of the intervention is the same. **D:** We observe long-term effects of consecutive interventions even when R_{base} is lower than one (red dotted line). The impact of these effects increases exponentially with R_{base}. **E:** Similarly, the final incidence (after six weeks) increases with R_{base}. The red dotted line indicates that an incidence ratio larger than one can already result from values of R_{base} smaller than one. Altogether, the cumulative effect of short but strong interventions (such as Euro 2020 matches) can be compared to lifting all bans on gatherings for a certain period of time. Curves were generated using a linear SEIS model without immunity for illustrative purposes.

To put our results in context, we compare the impact that different hypothetical scenarios of lifting of restrictions would have on case numbers (Fig. S1). Using a linear SEIS model for illustrative purposes, we evaluate three scenarios: i) Recurrent, bi-weekly (period $T = 2$ weeks) large events that strongly increase the reproduction number over its base level R_{base} for one day by $\Delta R_s = 2.0$ (yellow curves). This effect size is comparable to what we inferred for some heated matches (e.g., Scotland - England for Scotland: $\Delta R_{\text{match}} = 3.5\,[2.9, 4.2]$, England - Italy for England: $\Delta R_{\text{match}} = 2.0\,[1.6, 3.5]$, England - Italy for Italy: $\Delta R_{\text{match}} = 0.9\,[-0.7, 4.4]$, and the Czech Republic - Denmark for the Czech Republic: $\Delta R_{\text{match}} = 2.7\,[0.8, 4.4]$). ii) A temporary one-week lifting of restrictions, with an effect equal to a single-day large event by distributing the increase in R_{base} over a week: $\Delta R_w = 0.28 \approx 2/7$ (purple curves). iii) A permanent lifting of restrictions to the level of the second scenario: $\Delta R_p = 0.28$ for the considered time span (red curves). The value for ΔR_s in the first scenario is comparable to the largest effects found for the England-Scotland matches, while those in the second and third scenarios are similar to the effect of banning all private gatherings of 2 people or more as reported in [8].

The effect of interventions is comparable whenever the products between ΔR and the duration of the interventions are the same (e.g., yellow and purple curves for $t \leq 2$ weeks in Fig. S1A, B). In other words, the cumulative effect of short but strong interventions (such as Euro 2020 matches), can be compared to

lifting all bans on gatherings for a certain period of time. However, for regularly recurring interventions of size ΔR_s, we observe permanent long-term effects when $R_{\text{base}} + \Delta R_s/T \geq 1$; the impact of recurring interventions increases disproportionately over time (Fig. S1A–C). Controlling the long-term effect of recurrent increases of the reproduction number is possible if the underlying reproduction number R_{base} is small enough. Small changes of R_{base} substantially impact the outcome, even below the $R_{\text{base}} = 1$ threshold, and in an exponential manner (Fig. S1D, E). This underlines the importance of control strategies if large-scale events are expected to temporally increase the spread of COVID-19.

On the other hand, quantitatively, the expected size z of an infection chain depends on the effective reproduction number R_{eff}. As long as R_{eff} is larger than one, the infection chains can become arbitrarily large. But even if $R_{\text{eff}} < 1$, one single infection is expected to cause $z = (1 - R_{\text{eff}})^{-1}$ infections before the chain dies out. For example, if $R_{\text{eff}} = 0.9$, a single infection caused by the Euro 2020 implies $z = 10$ infections in the total chain. Thus, in comparison, the primary cases have only a small contribution; the majority of the impact of an event like the Euro 2020 is the spread of subsequent infections into the general population (e.g., Fig. 2A).

S3   Supplementary Tables

Country	Median percentage of primary cases	Median percentage of subsequent cases	Median percentage of primary and subsequent cases	Probability that football increased cases
Avg.	3.2% [1.3%, 5.2%]	-	-	> 99.9%
England	12.4% [5.6%, 22.5%]	36.0% [27.9%, 44.7%]	47.8% [36.0%, 62.9%]	> 99.9%
Czech Republic	9.7% [3.3%, 16.2%]	47.8% [24.2%, 58.7%]	57.7% [28.7%, 72.6%]	> 99.9%
Scotland	3.3% [1.3%, 8.1%]	36.6% [28.6%, 43.9%]	40.8% [30.9%, 50.3%]	> 99.9%
Spain	2.8% [-1.1%, 9.2%]	24.1% [-16.3%, 60.6%]	26.9% [-16.9%, 69.2%]	91.8%
Italy	2.1% [-5.8%, 10.9%]	16.1% [-230.2%, 69.5%]	18.7% [-235.6%, 78.4%]	74.1%
Slovakia	1.6% [-7.7%, 10.2%]	15.5% [-88.2%, 50.6%]	17.3% [-95.7%, 60.0%]	70.8%
Germany	1.4% [-1.8%, 4.2%]	22.1% [-36.3%, 44.8%]	23.6% [-38.0%, 48.6%]	86.7%
Austria	1.2% [-2.2%, 4.8%]	24.0% [-62.9%, 60.8%]	25.2% [-65.0%, 65.2%]	79.4%
Belgium	0.6% [-2.3%, 4.2%]	9.2% [-60.0%, 47.9%]	9.8% [-62.2%, 51.8%]	67.6%
France	0.5% [-0.2%, 1.4%]	23.1% [-8.4%, 45.8%]	23.6% [-8.6%, 47.0%]	94.1%
Portugal	0.3% [-2.6%, 2.7%]	-4.4% [-55.1%, 24.5%]	-4.1% [-57.4%, 26.9%]	60.6%
The Netherlands	-1.5% [-3.3%, -0.2%]	-49.1% [-111.7%, -1.4%]	-50.6% [-114.6%, -1.7%]	1.5%

Supplementary Table S1: **Credible intervals from the posterior distribution** of the number of football related cases divided by the total number of cases during the championship. CI denotes 95% credible interval.

Country	Primary cases per mil. people (male)	Primary cases per mil. people (female)	Primary and subsequent cases per mil. people
Avg.	-	-	2228 [986, 3308]
England	3595 [2661, 5729]	1686 [1143, 3453]	10600 [8185, 13875]
Czech Republic	94 [40, 142]	65 [22, 108]	459 [229, 577]
Scotland	1352 [940, 1758]	351 [222, 517]	7897 [6136, 9529]
Spain	594 [-217, 1722]	387 [-160, 1346]	4518 [-2840, 11595]
Italy	55 [-121, 227]	27 [-77, 131]	319 [-4001, 1335]
Slovakia	8 [-30, 38]	4 [-19, 25]	57 [-313, 196]
Germany	15 [-16, 36]	7 [-11, 24]	174 [-280, 359]
Austria	42 [-70, 141]	23 [-45, 100]	642 [-1646, 1661]
Belgium	34 [-112, 198]	18 [-81, 155]	411 [-2611, 2174]
France	43 [-12, 95]	27 [-8, 76]	1515 [-552, 3008]
Portugal	41 [-331, 340]	25 [-247, 251]	-449 [-6294, 2960]
Netherlands	-186 [-328, -31]	-98 [-222, -13]	-4805 [-10851, -166]

Supplementary Table S2: **Cases attributed to the Euro 2020 per million inhabitants** and related 95 % credible intervals in the male and female population. Primary and primary plus secondary cases are shown separately. Subsequent cases are almost gender-symmetric in all countries (see also Fig. S2). This indicates that also possible unobserved characteristics of the primary football-related infections in terms of other factors – such as age – are most likely distributed over the whole population in the course of subsequent infections.

Country	Primary cases (male)	Primary cases (female)	Primary and subsequent cases	Estimated deaths associated with primary and subsequent cases
England	93619 [69591, 145127]	43872 [29946, 87030]	567280 [436870, 747399]	1227 [945, 1616]
Czech Republic	494 [215, 753]	346 [116, 558]	4920 [2455, 6182]	60 [30, 75]
Scotland	3478 [2444, 4481]	908 [574, 1320]	41720 [31766, 50146]	90 [69, 108]
Spain	13570 [-4463, 40212]	8870 [-3339, 31389]	211952 [-122694, 546650]	503 [-291, 1298]
Italy	1535 [-3399, 6718]	750 [-2219, 3824]	17810 [-243916, 79338]	170 [-2327, 757]
Slovakia	21 [-87, 100]	11 [-47, 67]	320 [-1809, 1087]	4 [-24, 14]
Germany	618 [-629, 1460]	306 [-440, 944]	14626 [-23538, 29644]	304 [-489, 616]
Austria	178 [-308, 626]	97 [-179, 436]	6078 [-15534, 15387]	34 [-86, 85]
Belgium	191 [-600, 1091]	101 [-441, 834]	5352 [-31477, 24778]	14 [-84, 66]
France	1357 [-331, 2920]	857 [-219, 2325]	95929 [-40644, 190114]	423 [-179, 838]
Portugal	202 [-1683, 1667]	122 [-1229, 1255]	-5205 [-72249, 29231]	-22 [-300, 121]
Netherlands	-1573 [-2756, -277]	-838 [-1859, -106]	-82805 [-181983, -3149]	-75 [-164, -3]
Total	114769 [81915, 167796]	56781 [36247, 100400]	844609 [396860, 1253494]	1689 [794, 2507]

Supplementary Table S3: **Total cases attributed to the Euro 2020** and related 95 % credible intervals. The associated deaths are calculated under the assumption that the cases were equally distributed among age-groups and using the case fatality risk for the respective country in the time window of the Euro 2020.

Country	$\Delta R_{\mathrm{match}}^{\mathrm{mean}}$	Delay D
Avg.	0.46 [0.18, 0.75]	
England	0.75 [0.01, 1.66]	4.55 [4.36, 4.94]
Czech Republic	1.26 [-0.50, 3.19]	5.53 [4.75, 6.32]
Scotland	1.09 [-2.77, 4.69]	3.52 [3.35, 3.74]
Spain	0.37 [-0.72, 1.83]	6.91 [5.43, 7.82]
Italy	0.28 [-1.11, 1.79]	5.51 [3.96, 7.11]
Slovakia	0.32 [-2.27, 2.56]	5.00 [3.67, 7.28]
Germany	0.33 [-0.62, 1.12]	6.82 [5.69, 8.43]
Austria	0.28 [-0.90, 1.45]	4.58 [3.46, 6.37]
Belgium	0.11 [-0.61, 0.92]	5.09 [3.71, 6.69]
France	0.30 [-0.46, 0.97]	3.68 [3.13, 4.46]
Portugal	-0.02 [-1.33, 1.34]	5.49 [4.30, 6.55]
Netherlands	-0.74 [-3.30, 1.36]	5.70 [4.28, 6.00]

Supplementary Table S4: **Average effect of Euro 2020 matches on the spread of COVID-19, per country.**

Country	Matches played	Matches hosted	Union	Time between first and last match of the country (days)
England	7	8	9	28
Czech Republic	5	0	5	19
Scotland	3	4	5	8
Spain	6	4	7	22
Italy	7	4	8	30
Slovakia	3	0	3	9
Germany	4	4	5	14
Austria	4	0	4	13
Belgium	5	0	5	20
France	4	0	4	13
Portugal	4	0	4	12
Netherlands	4	4	5	14

Supplementary Table S5: **Number of matches** played by the national team in the Euro 2020, matches played in the country and the union of the two categories. The union denotes the sum of the first two numbers without the overlapping matches.

S4   Supplementary Figures
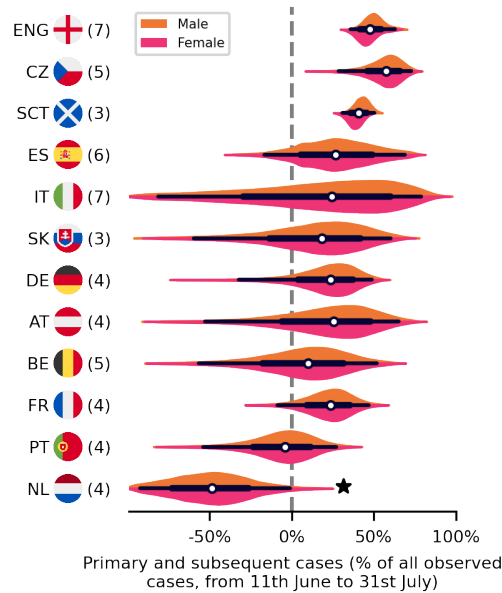
Supplementary Figure S2: **Overview of the sum of primary and subsequent cases accountable to the Euro 2020**. Calculations account for cases until July 31st, i.e., about three weeks after the championship finished. In the Netherlands (⋆) the "freedom day" occurred on the same time as the Euro 2020. This effect also had a gender imbalance, thus, making it hard for our model to extract the Euro 2020 effect (see. Fig. S31). White dots represent median values, black bars and whiskers correspond to the 68% and 95% credible intervals (CI), respectively, and the distributions in color (truncated at 99% CI) represent the differences by gender ($n = 12$ countries).
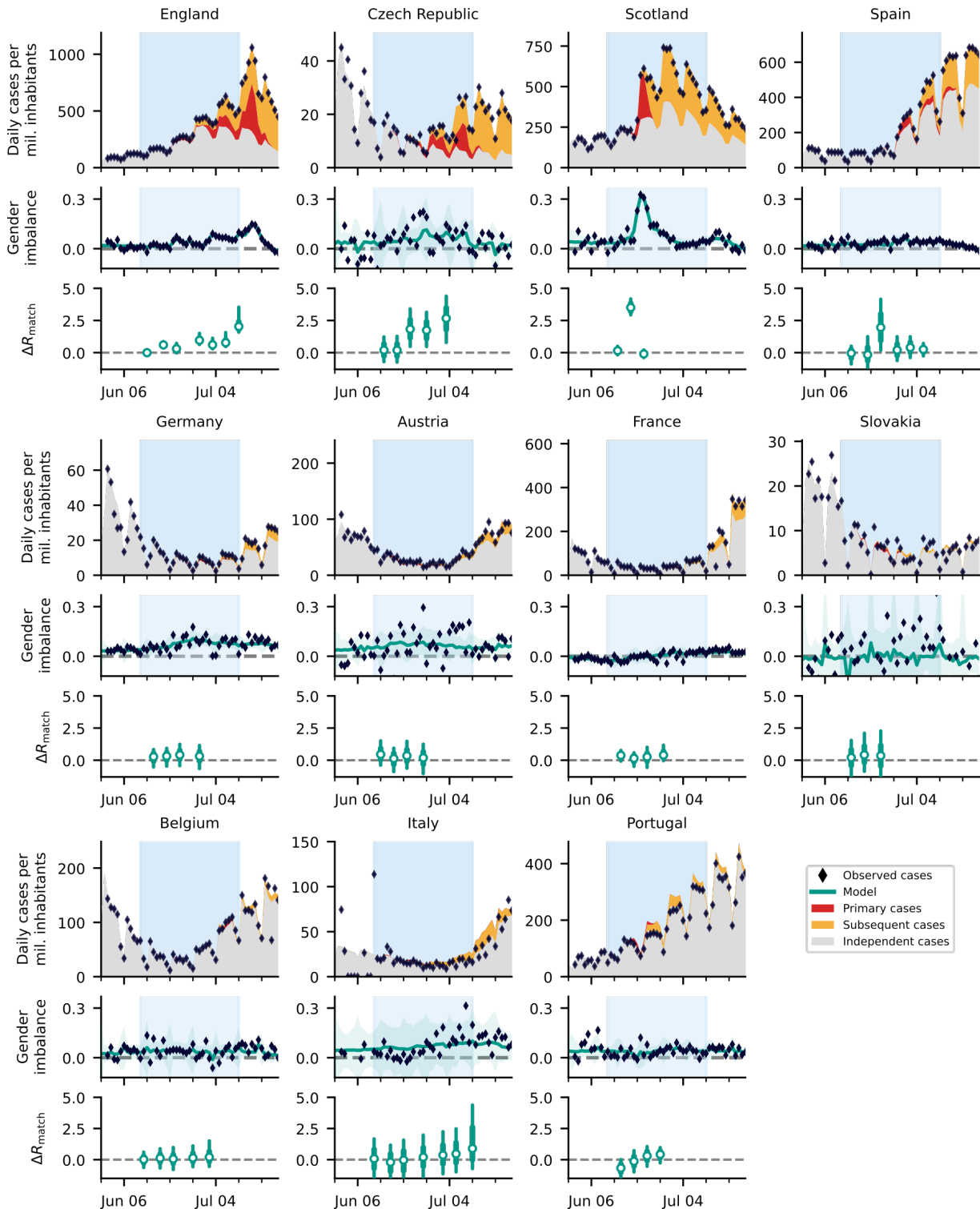
Supplementary Figure S3: **Overview of cases in all considered countries apart from the Netherlands** We split the observed incidence (black diamonds) of the three countries with the largest effect size into i) cases independent of Euro 2020 matches (gray area), ii) primary cases (directly associated with Euro 2020 matches, red area), and ii) subsequent cases (additional infection chains started by primary cases, orange area). See Figure 2 for more details. The turquoise shaded areas correspond to 95% CI. In the box plots, white dots represent median values, turquoise bars and whiskers correspond to the 68% and 95% credible intervals (CI), respectively.
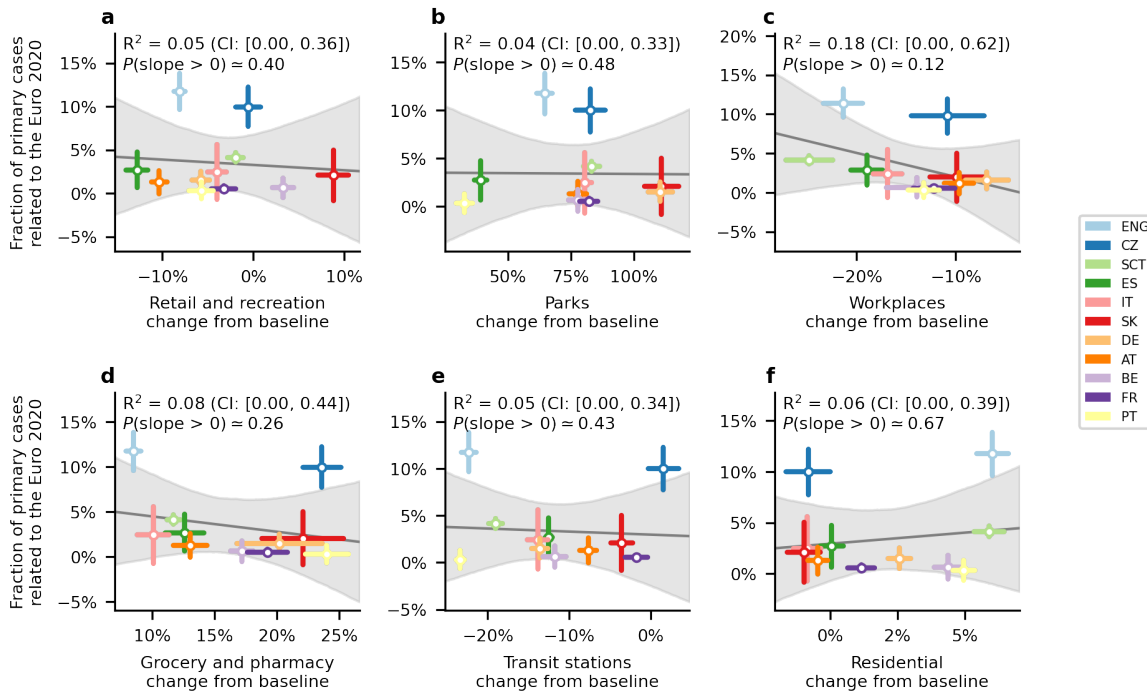
Supplementary Figure S4: **We found no significant correlation between cases arising from the Euro 2020 and human mobility.** Using mobility data from the "Google COVID-19 Community Mobility Reports" [5], we tested for correlation against the fraction of Euro 2020 related cases. Using the different categories (**A-F**) from the Mobility Report we found no significant correlation in either. The gray line and area are the median and 95% credible interval of the linear regression ($n = 11$ countries; The Netherlands was excluded for this analysis). Whiskers denote one standard deviation.
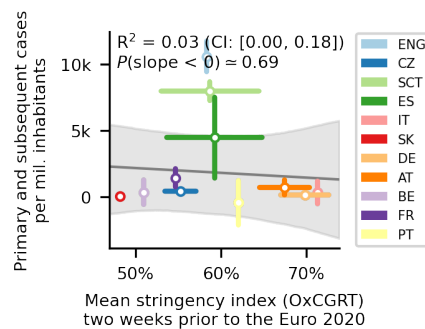
Supplementary Figure S5: **We found no significant correlation between cases arising from the Euro 2020 and the stringency of governmental interventions.** We correlated the average Oxford governmental response tracker [3] in the two weeks before the championship with the total number of cases per million inhabitants related to football gatherings. The gray line and area are the median and 95% credible interval of the linear regression ($n = 11$ countries; The Netherlands was excluded for this analysis). Whiskers denote one standard deviation.
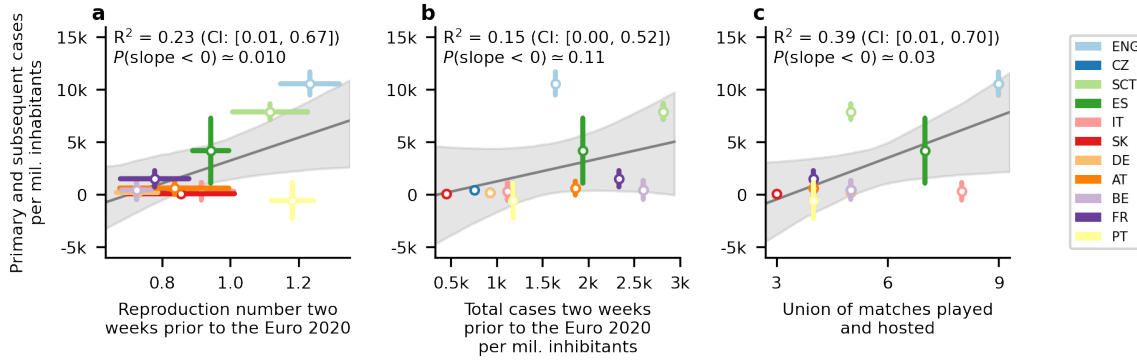
Supplementary Figure S6: **We found slight trends in the correlations between the impact of Euro 2020 and the base reproduction number and country popularity.** While these correlations are below the classical significance threshold of 0.05, they are less explanatory than the potential for spread (defined in Fig. 3). There was no significant correlation between the initial COVID-19 incidence and the impact of the Euro 2020. The gray line and area are the median and 95% credible intervals of the linear regression ($n = 11$ countries; The Netherlands was excluded for this analysis). Whiskers denote one standard deviation.
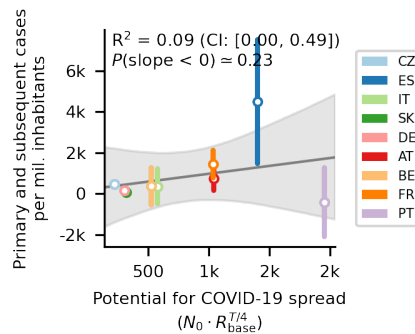
Supplementary Figure S7: **Prediction of the impact of Euro 2020 matches without the two most significant countries in the main model (England and Scotland).** The potential for spread, i.e., the number of COVID-19 cases that would be expected during the time T a country is playing in the Euro 2020 ($N_0 \cdot R_{pre}^{T/4}$) is still correlated with the number of Euro 2020-related cases after removing the two most significant entries from the analysis but not significantly. The observed slope without the most significant countries (median: 0.76, 95% CI: [-1.46, 3.04]) is consistent within its uncertainties with the slope including all countries (median: 1.62, 95% CI: [1.0, 2.26])). Due to the post-hoc nature of the removal of the most significant entries, this result is only shown for information. The gray line and area are the median and 95% credible interval of the linear regression ($n = 9$ countries; The Netherlands, England and Scotland were excluded for this analysis). Whiskers denote one standard deviation.
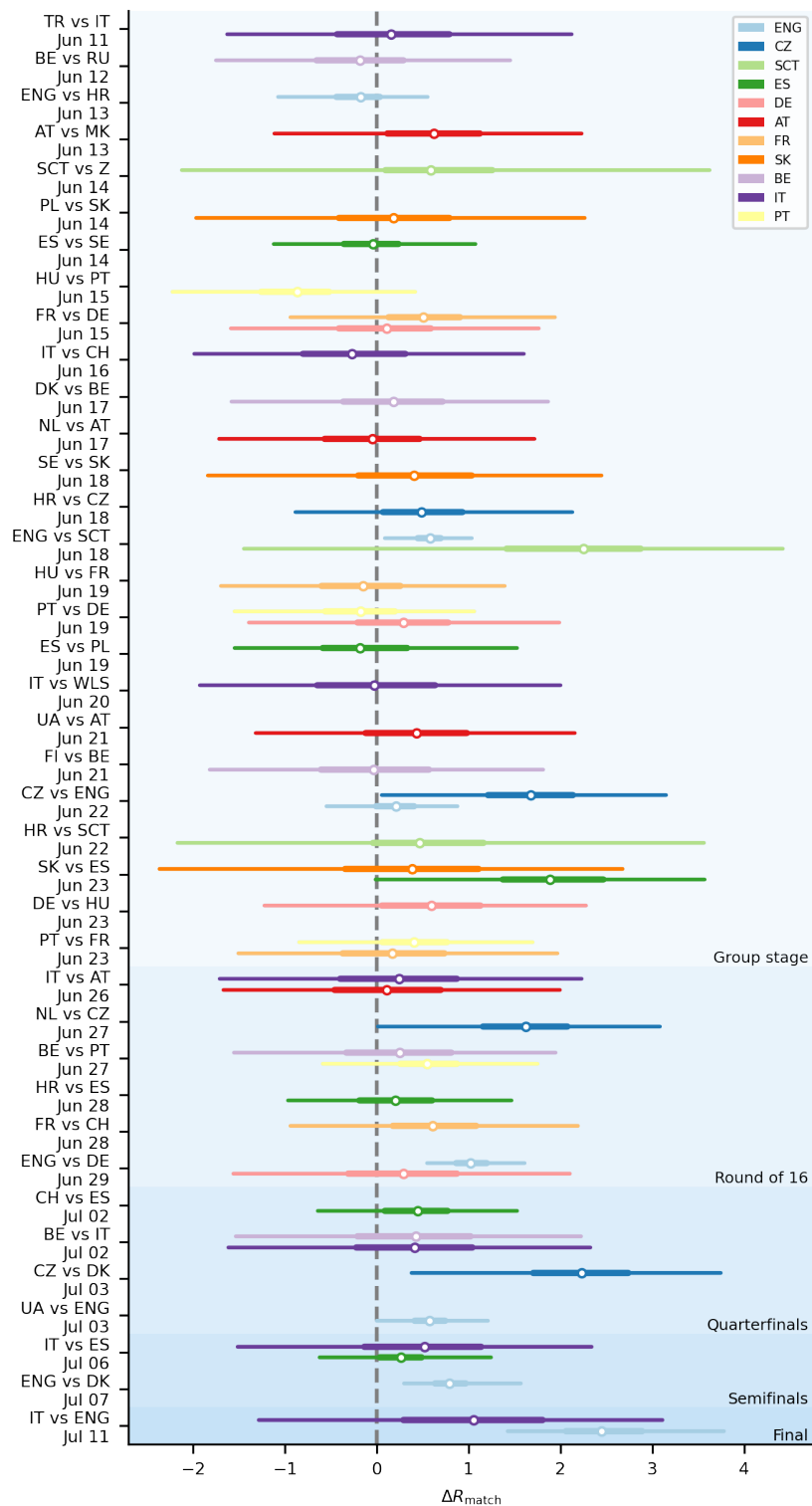
Supplementary Figure S8: **Effect of single Euro 2020 matches on the spread of COVID-19 across competing countries.** White dots represent median values, colored bars and whiskers correspond to the 68% and 95% credible intervals (CI).

S4.1 Model including the effect of stadiums
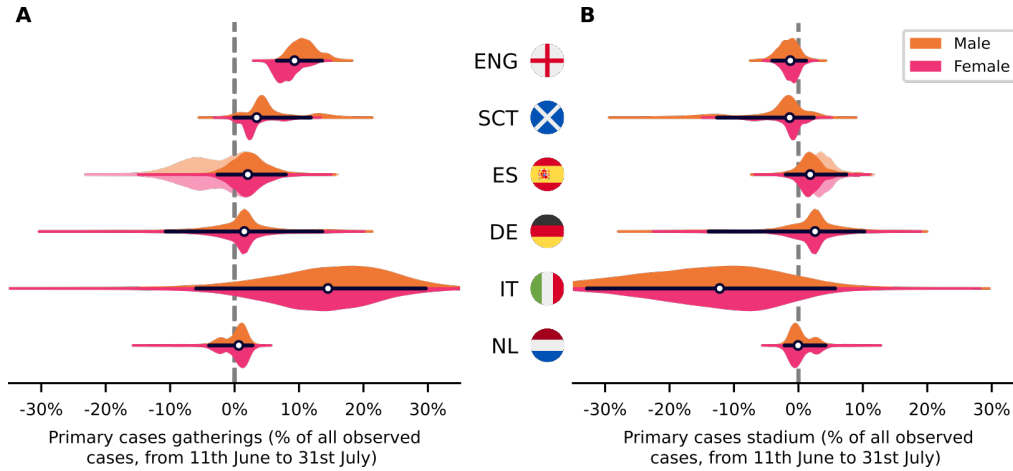
Supplementary Figure S9: **Including in our model the potential local transmission around the stadium where the matches occur does not significantly increase the overall effect.** In addition to the effect of football-related gatherings (**A**), we extended our model to include an additive effect on the reproduction number when a country hosted a match (**B**) (for those countries that hosted matches, i.e. $n = 6$ countries). We assume that local transmissions in and around the stadium would be detected mainly in the venue's country. However, football-related cases in a country where matches have a significant contribution to COVID-19 spread are tied to the dates of matches played by the country's team (A) and not to the country of the stadium venue (B), which is especially visible for England and Scotland. This also explains why previous attempts at measuring Euro 2020-related cases focusing on stadium venues were inconclusive. For Spain, an increase in the base reproduction number close to the date of a match makes the model inconclusive. In transparent is the region of the posterior of which we suppose that the model identifies the increase incorrectly; that is, where the posterior delay is smaller than 5.5 days. White dots represent median values, black bars and whiskers correspond to the 68% and 95% credible intervals (CI), respectively, and the distributions in color (truncated at 99% CI) represent the differences by gender.

S4.2 Testing the detection of a null-effect
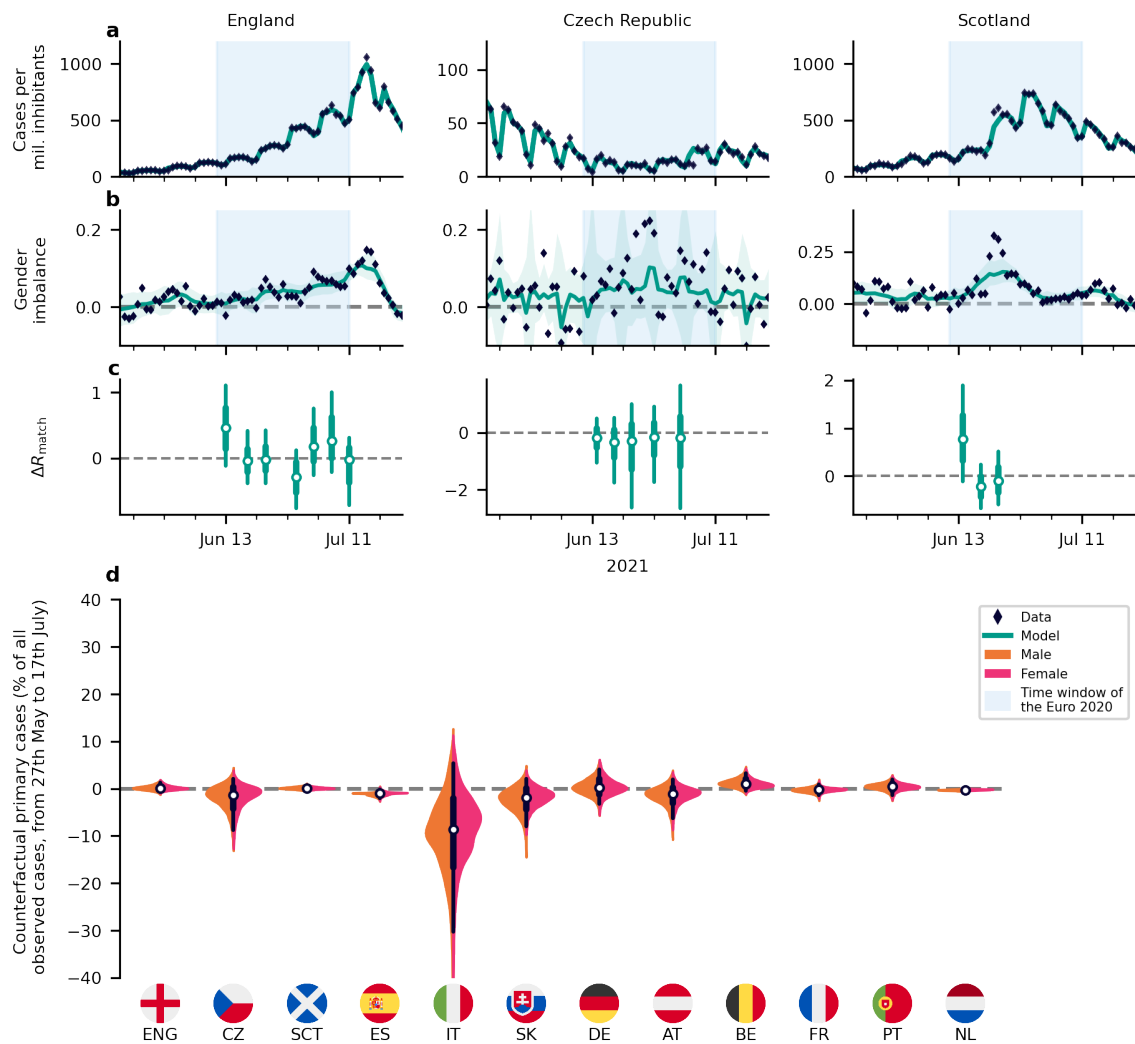
Supplementary Figure S10: **A temporal offset of 14 days leads to no inferred effect.** An artificial offset of the match data of 14 days decouples the gender ratio changes and the matches. This leads to no inferred effect of the championship – even in the three countries with the largest effect sizes in the main model (**A-C**). White dots represent median values, black bars and whiskers correspond to the 68% and 95% credible intervals (CI) ($n = 12$ countries). Shaded turquoise area denotes 95% CI.
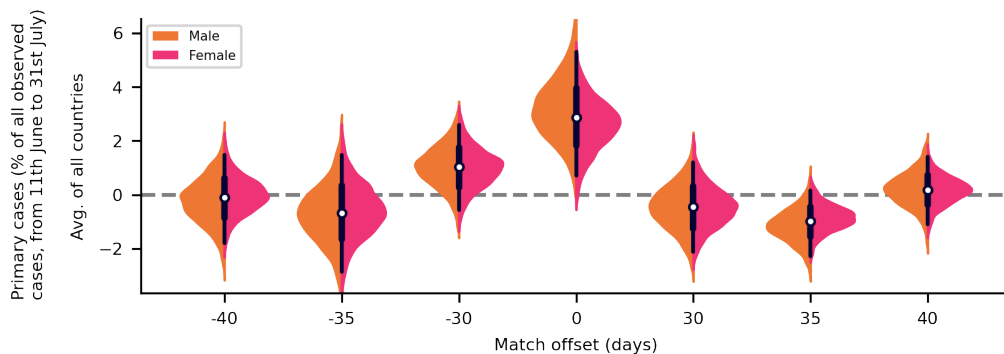
Supplementary Figure S11: **Changing the days of the match by a large offset results in a non-significant effect.** To test the reliability of our results, we ran counterfactual scenarios where the date of the matches was moved to lie outside the championship period. As expected, such offsets lead non-significant results of the average effect size across countries. White dots represent median values, black bars and whiskers correspond to the 68% and 95% credible intervals (CI) ($n = 11$ countries, The Netherlands was excluded for this analysis).

S4.3   Robustness of parameters
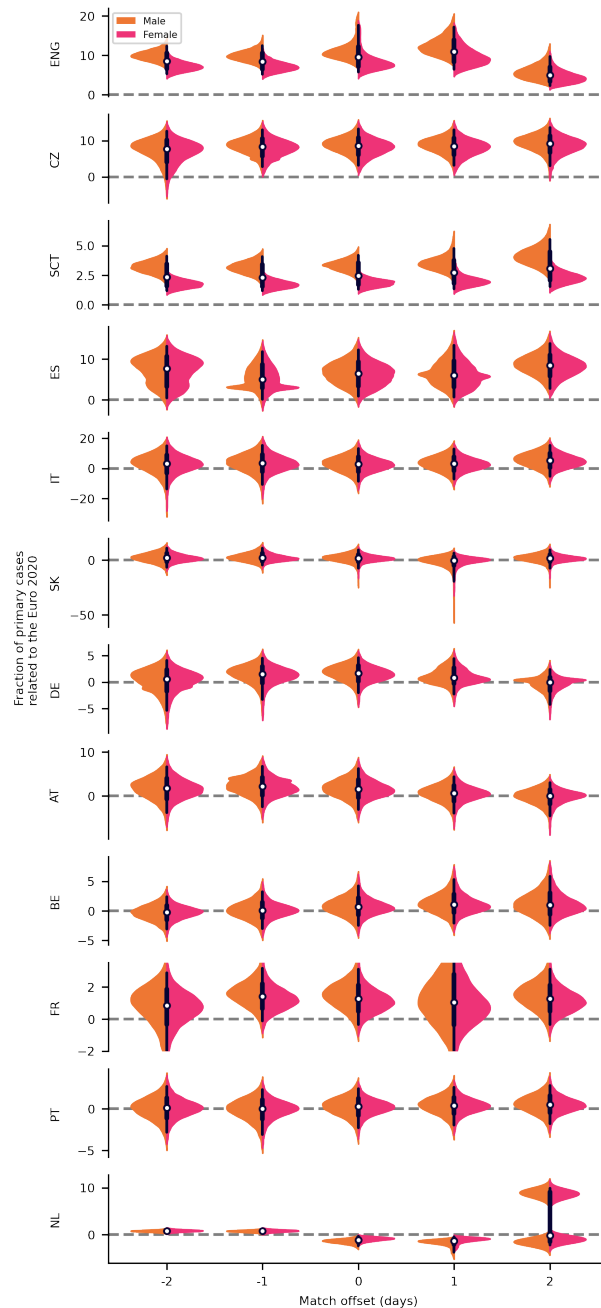
Supplementary Figure S12: **Robustness test for the effect of the temporal association between matches and cases by varying the effective delay.** We applied an artificial variation of all match days in a positive or negative direction. Under these relatively small variations of the delay, the gender imbalance is strong enough to lead to a stable effect size as the prior of the delay still allows for a sufficient shift of the posterior delay. The model run for France with a 1-day offset is missing because of an unknown, sampling-based error. White dots represent median values, black bars and whiskers correspond to the 68% and 95% credible intervals (CI), respectively, and the distributions in color (truncated at 99% CI) represent the differences by gender ($n = 11$ countries, The Netherlands was excluded for this analysis).
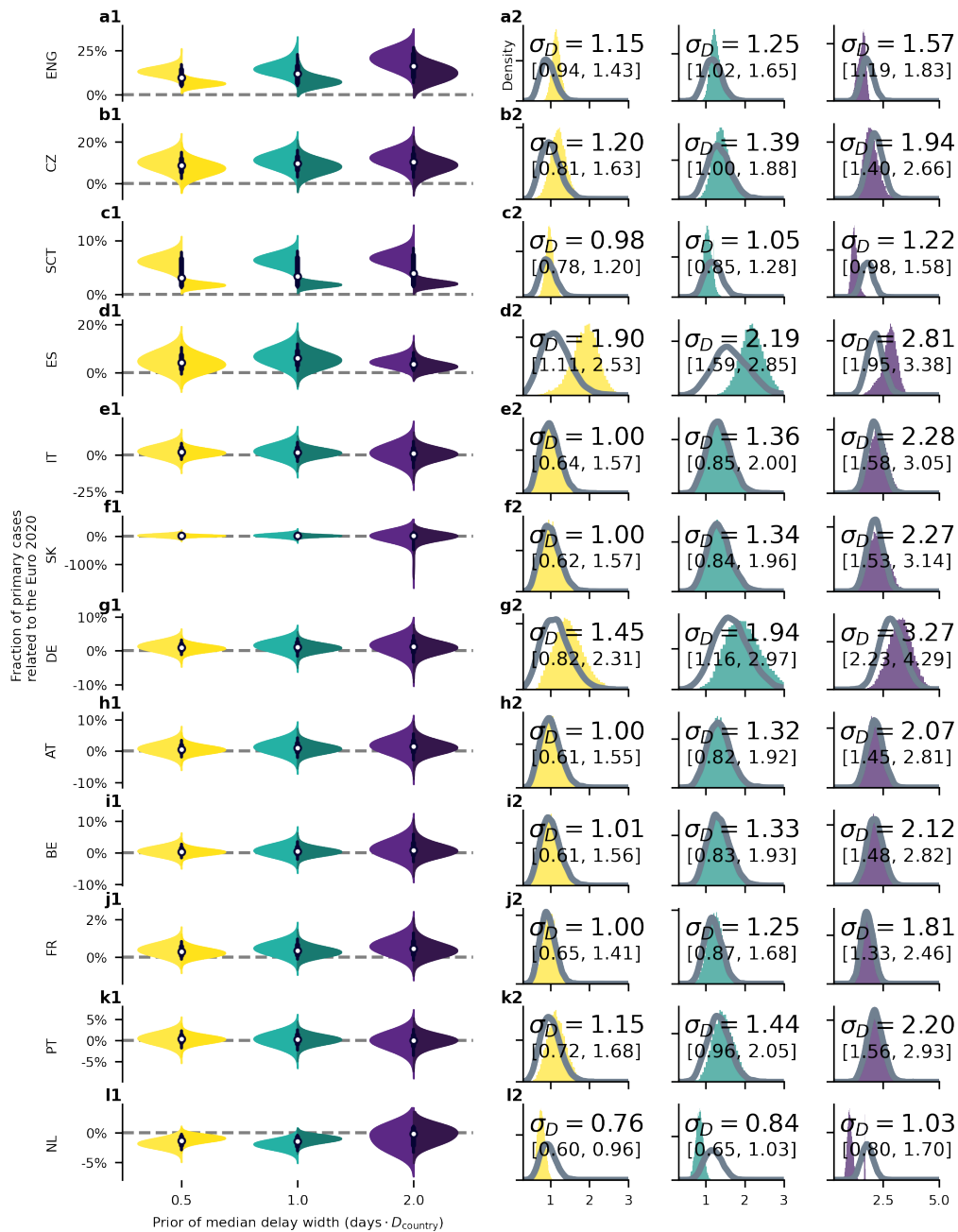
Supplementary Figure S13: **Robustness test for the effect of the width of the delay kernel.** In this robustness test, we varied the prior for the width of the delay kernel from the country-specific default (green) towards smaller (yellow) and larger (purple) widths (left column). In the violin plots, the left side is the prior for men; the right side for women. The right column shows the priors and resulting posterior of the standard deviation of the delay kernel σ_D. Except for England and Scotland (**A2, D2**), the data does not constrain this parameter. The results are not significantly modified in any country by changing the prior assumptions on this parameter (left column). On average, allowing for larger widths increases the effect size over the reported results. White dots represent median values, black bars and whiskers correspond to the 68% and 95% credible intervals (CI), respectively, and the distributions in color (truncated at 99% CI) represent the differences by gender.
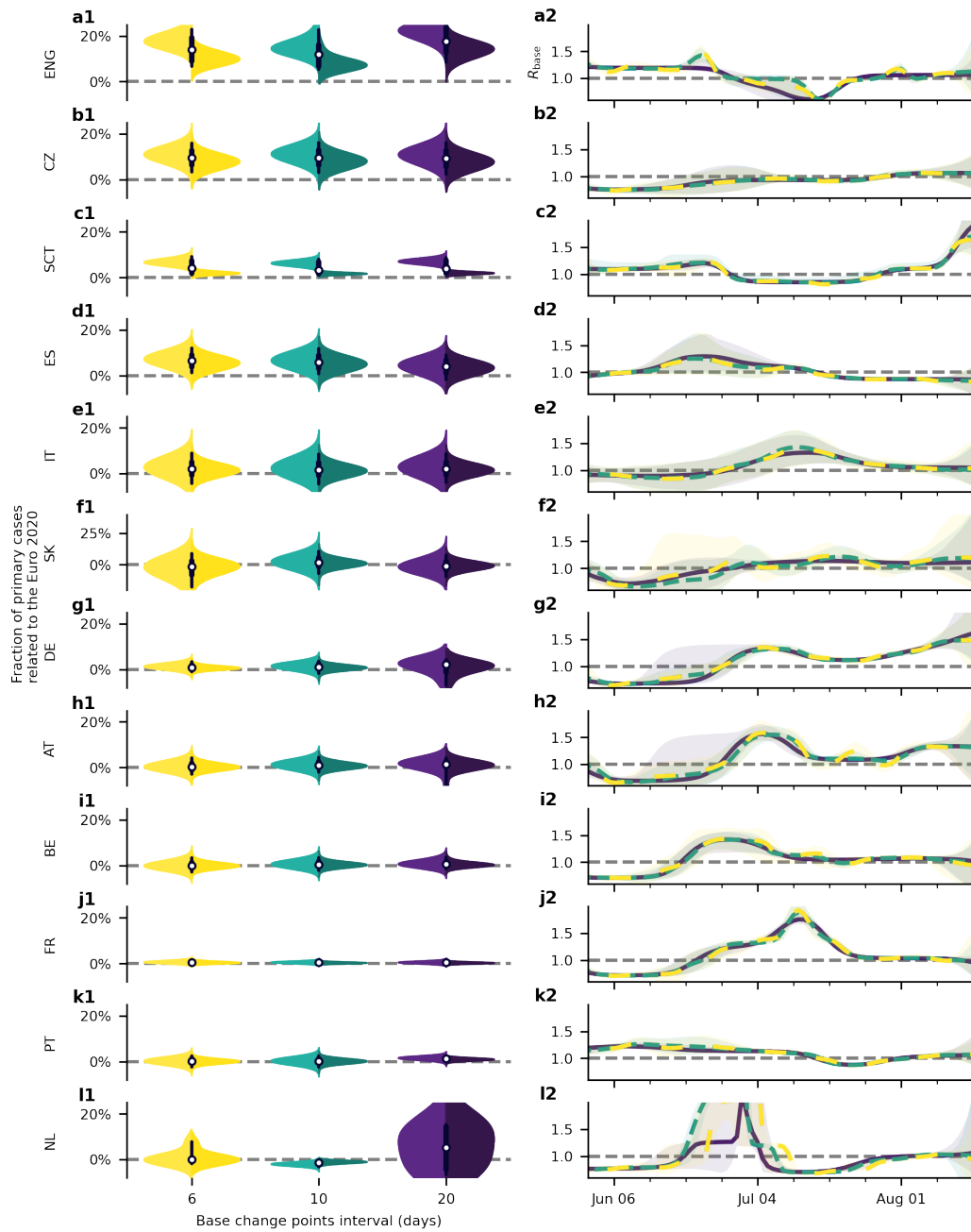
Supplementary Figure S14: **Robustness test for the effect of the allowed base reproduction number variability.** We propose models with three different base change point intervals: 6 days (yellow), 10 days (green), and 20 days (purple). In the violin plots, the left side is the distribution for men; the right side for women. We do not find significant differences in the fraction of football-related cases (left column) nor in the base reproduction numbers R_{base} (right column). On average, allowing less variation in R_{base} – i.e., removing the freedom of the model to absorb potential gender-symmetric and non-time-resolved cases related to football matches into short-timescale variations of R_{base} – increases the effect size over the reported baseline results. Shaded areas in panels ***2** correspond to 95% CI. White dots represent median values, black bars and whiskers correspond to the 68% and 95% credible intervals (CI), respectively, and the distributions in color (truncated at 99% CI) represent the differences by gender.
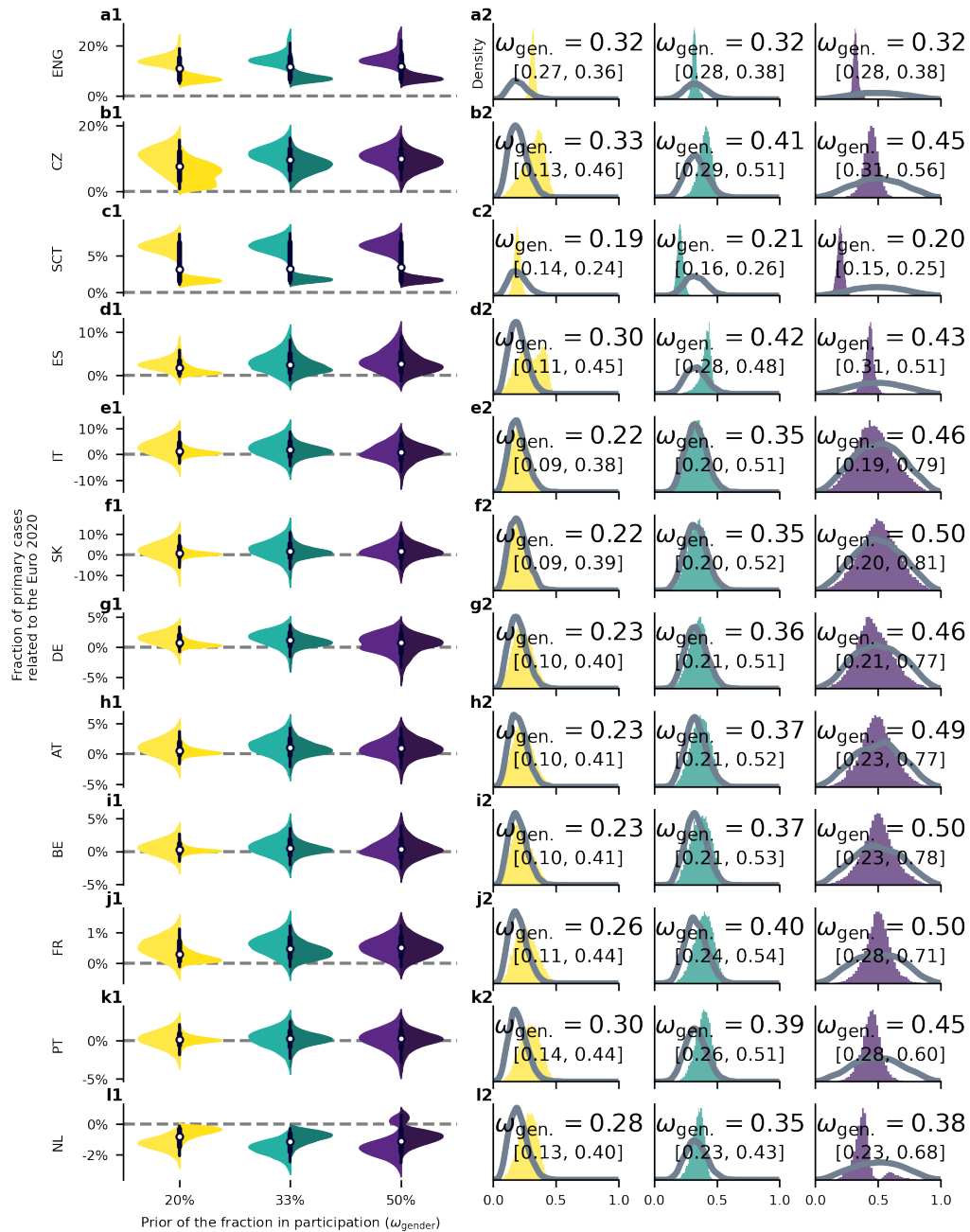
Supplementary Figure S15: **Robustness test for the effect of the fraction of female participation in football related gatherings** The default model employs a relatively constraining prior for the fraction of female participation in football-related gatherings (green) motivated by [9]. To check for the influence of this assumption, in an alternative model, we assume a more uninformative prior with mean female participation of 50% participation (purple) instead of 20% (green) (**A2-G2**). We do not find large differences in the results. On average, the total fraction of cases attributed to football matches grows when allowing the assumption of larger female participation in the fan gatherings. Hence, more cases are attributed to the Euro 2020 overall than in the baseline model. At the same time, a constraint used by the model for associating cases and matches is relieved. Thus, on average, the uncertainty of the posterior slightly grows (**A1-G1**). White dots represent median values, black bars and whiskers correspond to the 68% and 95% credible intervals (CI), respectively, and the distributions in color (truncated at 99% CI) represent the differences by gender.
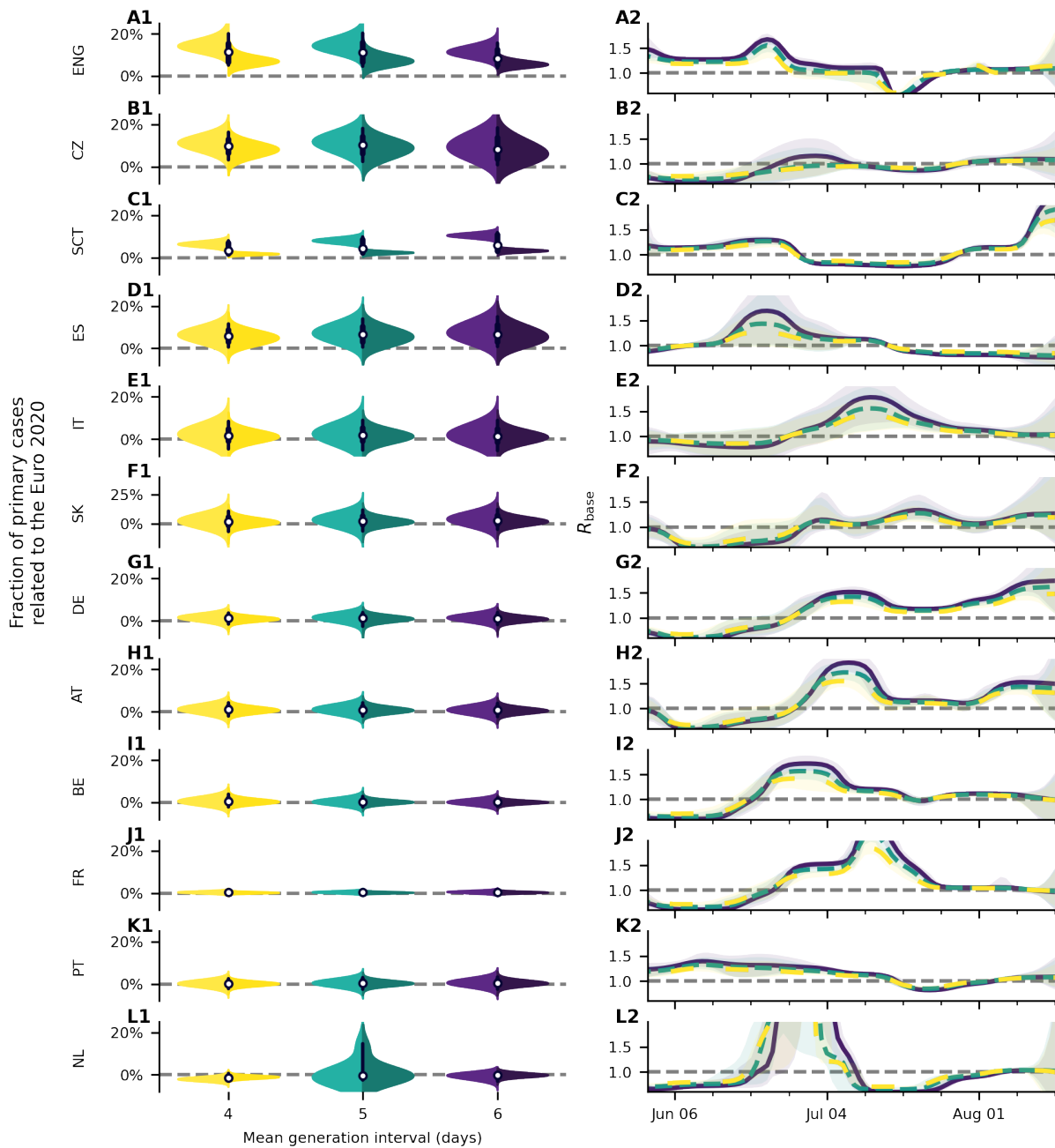
Supplementary Figure S16: **Robustness test for the effect the generation interval.** We propose models with three different generation intervals: with a mean of 4 days (yellow), 5 days (green), and 6 days (purple). The lack of significant difference in the fraction of football-related cases (left column) shows that if we assume a longer generation intervals than our base assumption of 4 days our conclusions do not change. One remarks that the the base reproduction numbers R_{base} (right column) increases with a longer assumed generation interval, which is expected because a the increase of cases that needs to be modeled stays fixed. In the violin plots, the left side is the distribution for men; the right side for women. Shaded areas in the right column correspond to 95% CI. White dots represent median values, black bars and whiskers correspond to the 68% and 95% credible intervals (CI), respectively, and the distributions in color (truncated at 99% CI) represent the differences by gender.
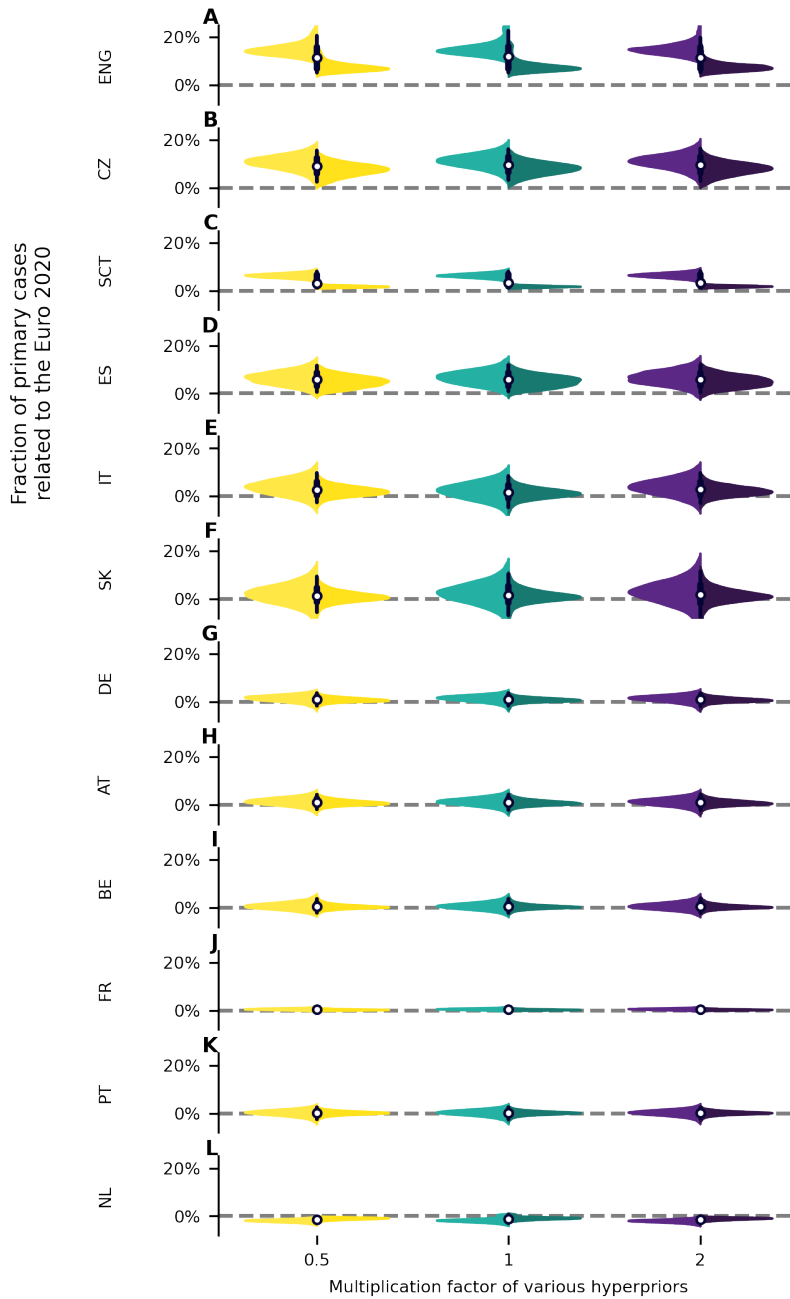
Supplementary Figure S17: **Robustness test for the remaining priors not studied in the previous figures.** Many of the priors in the model are relatively uninformative for the model. In these runs, we increased and decreased the prior value of the equations (16), (26), (35), (51), (52) and (54) by a factor of 2. In the violin plots, the left side is the distribution for men; the right side for women. White dots represent median values, black bars and whiskers correspond to the 68% and 95% credible intervals (CI), respectively, and the distributions in color (truncated at 99% CI) represent the differences by gender.
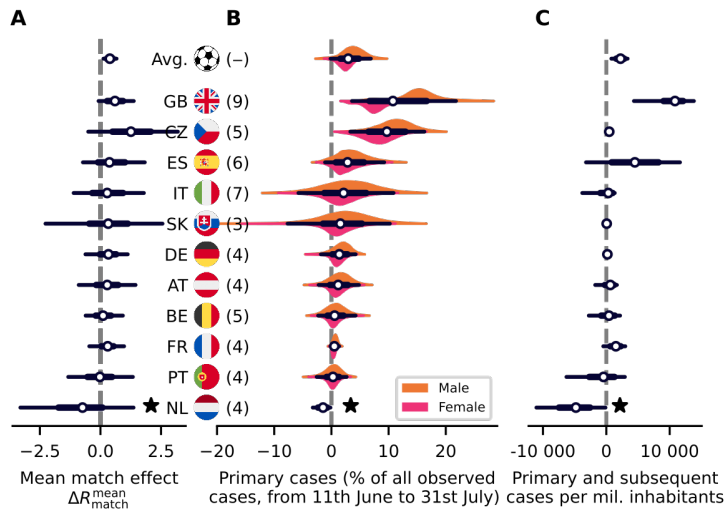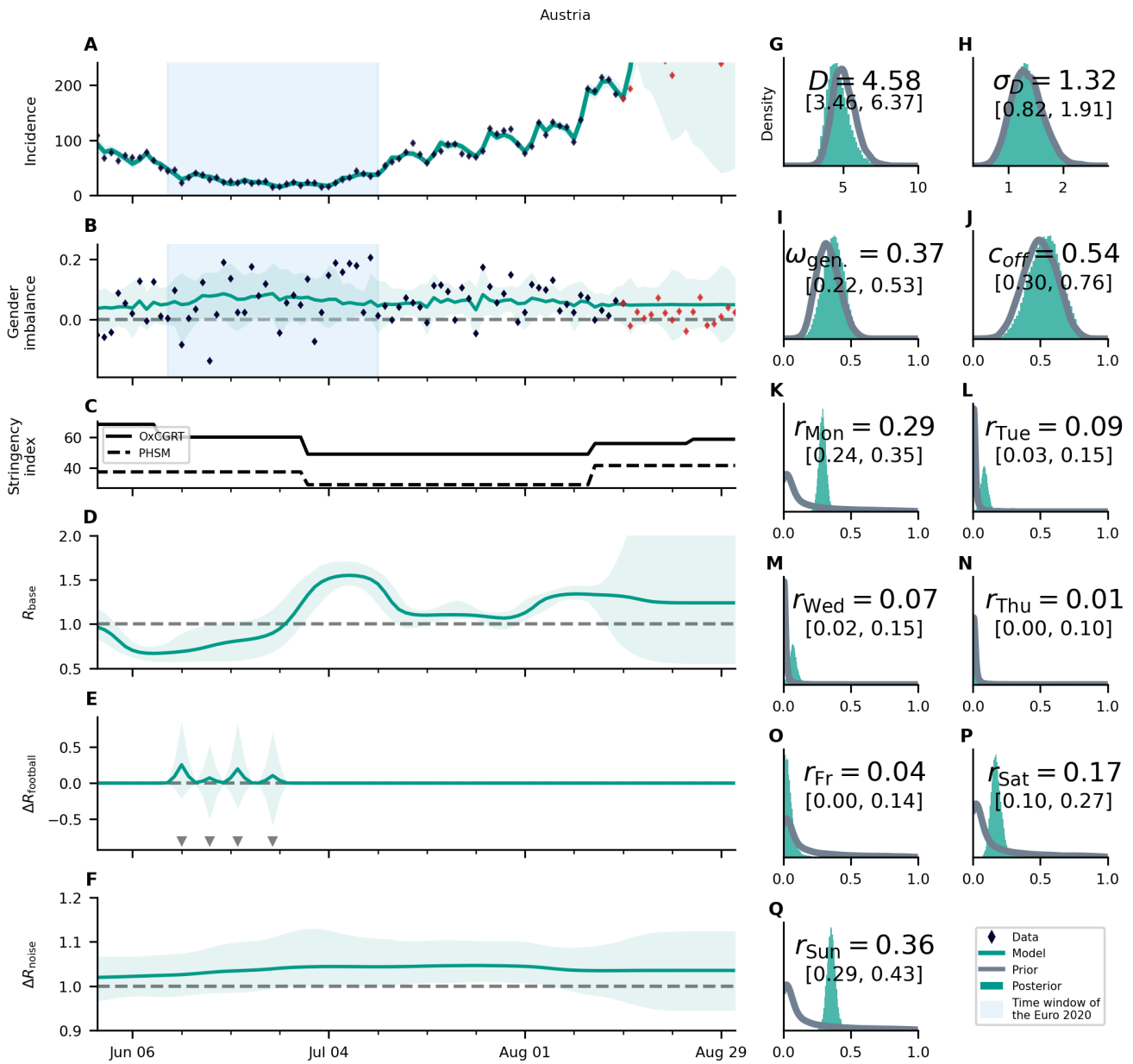
Supplementary Figure S18: **The combination of the case numbers of England and Scotland leads to similar results.** Because England and Scotland had each a team participating in the Euro 2020 we analyzed them separately, even if both are part of the United Kingdom. Here we added the case numbers of both (denoted as GB) and combined their matches for a new model run. The overall results do not change much in this alternative parametrization. White dots represent median values, black bars and whiskers correspond to the 68% and 95% credible intervals (CI), respectively, and the distributions in color (truncated at 99% CI) represent the differences by gender ($n = 11$ countries).

S4.4 Further analyses
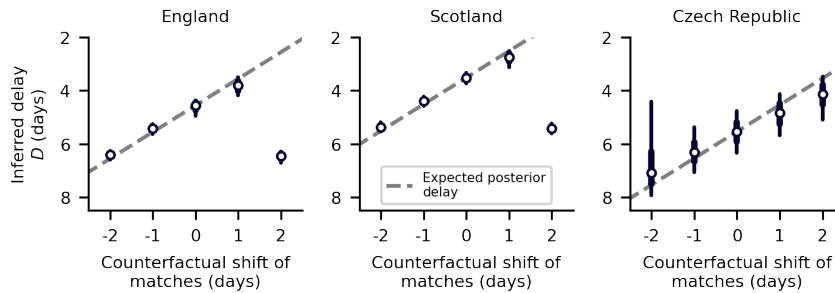
Supplementary Figure S19: **Our model is able to identify the delay between infection and reporting of it.** We tested counterfactual scenarios for England, Scotland and the Czech Republic where the dates of the matches were changed. Despite the same prior delay, the model managed to adapt the inferred delay to match the expected delay from the original model. White dots represent median values, black bars and whiskers correspond to the 68% and 95% credible intervals (CI).
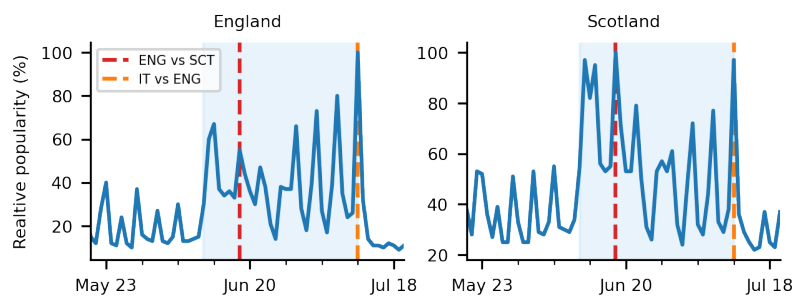
Supplementary Figure S20: **Relative popularity of the search term "football" in England and Scotland** measured using "Google Trends" [7] in the category "sport news". Vertical red lines represent the final and match of Scotland vs England, respectively.
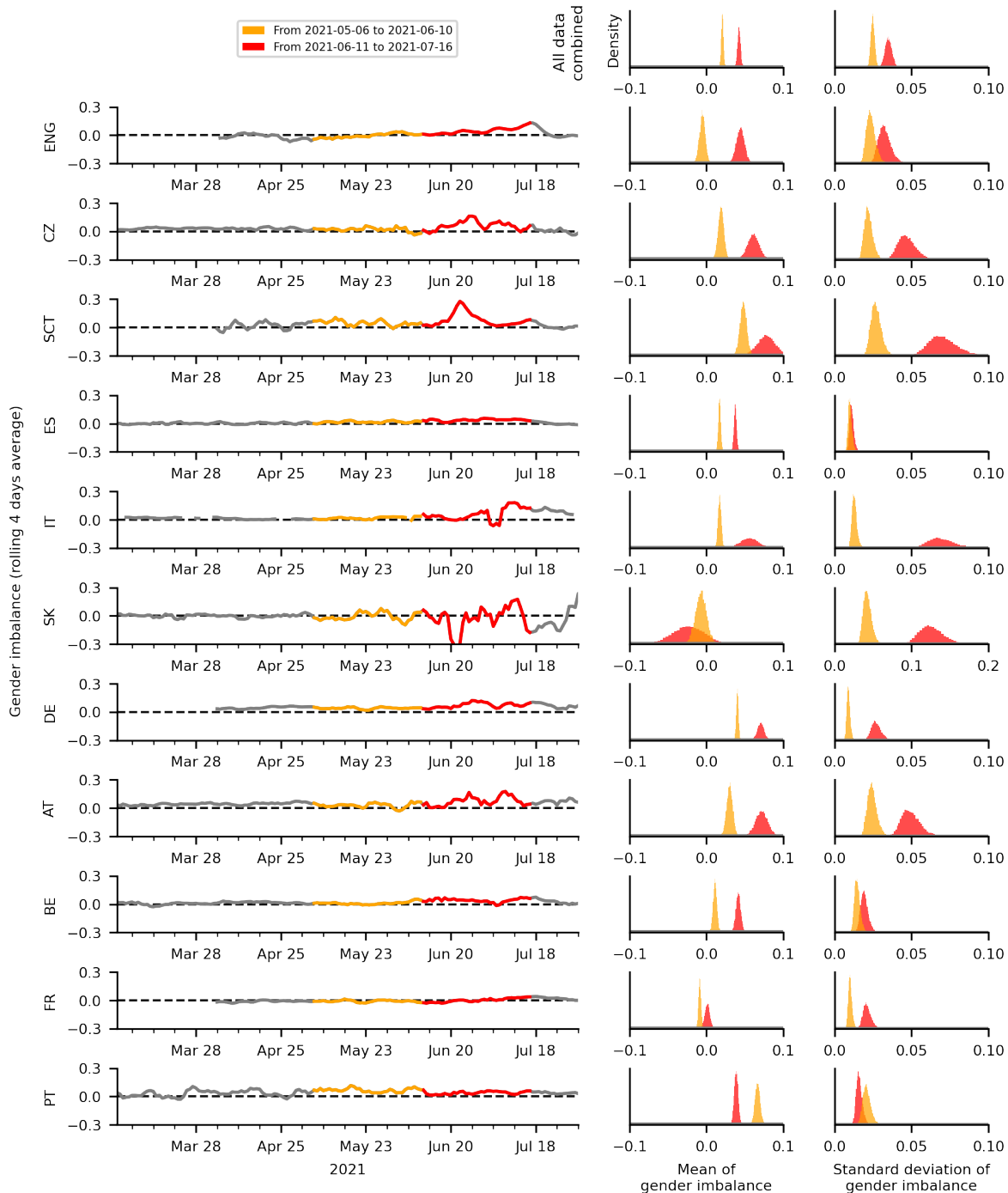
Supplementary Figure S21: **Male-female imbalance over time shows the largest deviations during championship.** We plotted the gender imbalance directly from our data (left column). All countries which showed significant effects had their largest imbalance change during or slightly after the championship (red), and also a number of non-significant countries display this behavior. In addition, the standard deviation of the imbalance during the championship (red) was on average larger than before the championship (orange, right column). This indicates that the large changes in imbalance during the championship were highly unusual and can't be attributed to chance alone. The red time period are the 30 days of the tournament plus the 5 days after and the orange time period the ones up to 35 days before the tournament.
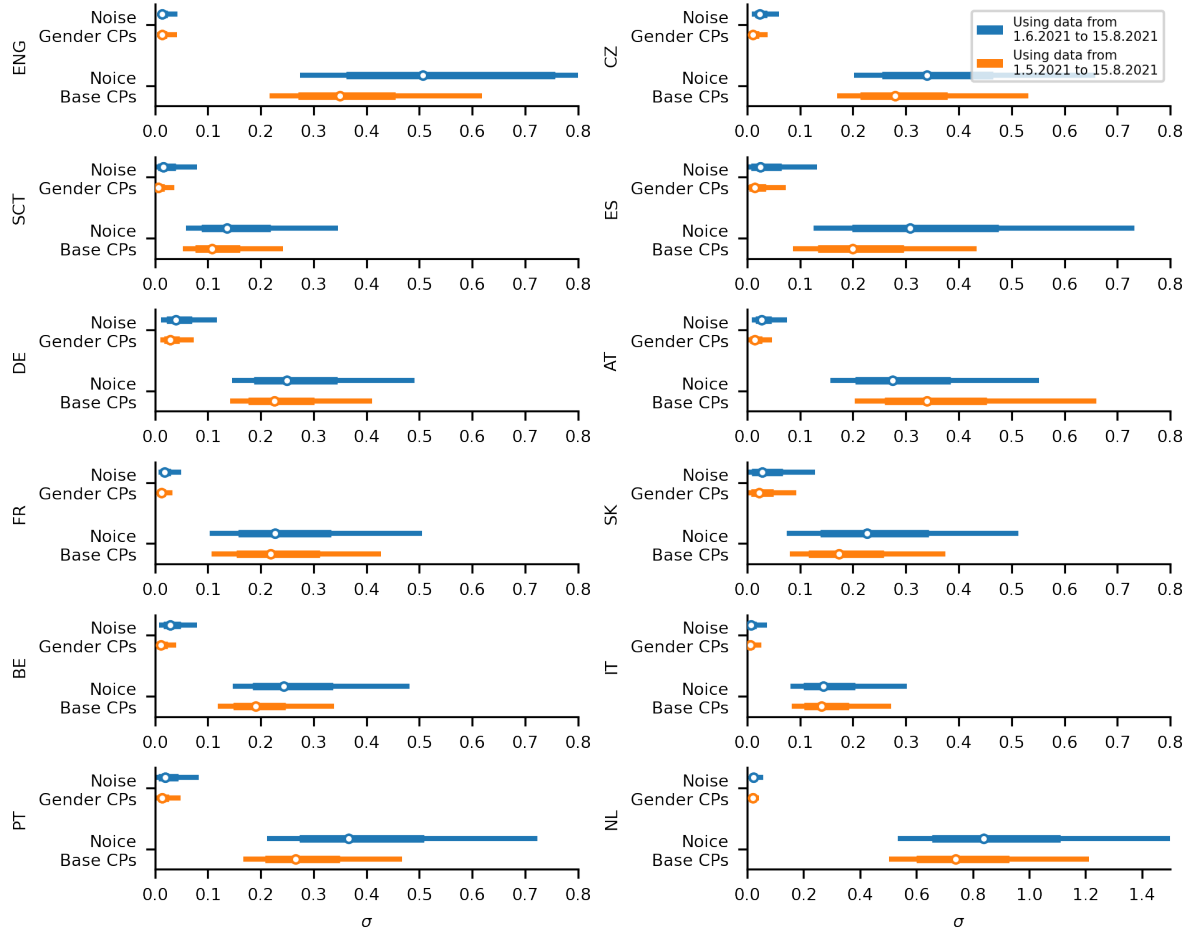
Supplementary Figure S22: **The inferred noise terms do not depend strongly on the length of the analyzed time-period.** We plotted the size of our gender noise term $\sigma_{\Delta\tilde{\gamma}}$ and the size of the change-points of the base reproduction number $\sigma_{\Delta\gamma}$. When beginning the run of our model a month earlier (blue), the noise terms do not change significantly compared to our base model (orange). White dots represent median values, colored bars and whiskers correspond to the 68% and 95% credible intervals (CI).
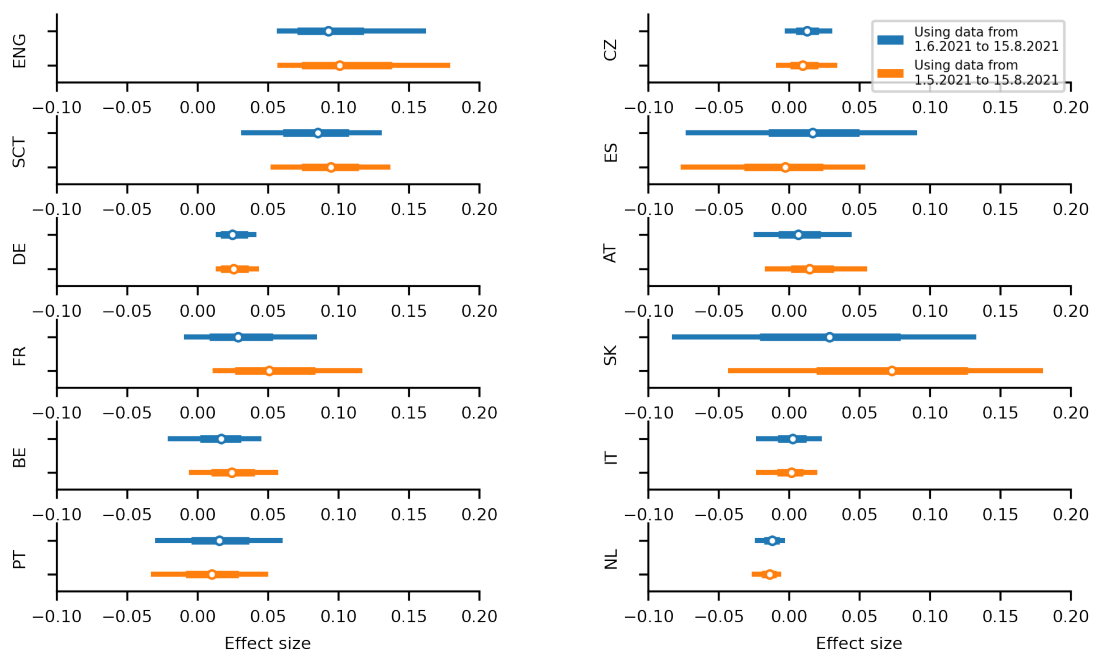
Supplementary Figure S23: **The inferred effect size (percentage of football-related primary infections) do not depend strongly on the length of the analyzed time-period.** To showcase that the total length of the analyzed period doesn't change significantly our results, we compare the percentage of football-related primary infections one-month-longer runs (blue) compared to our base model (orange). White dots represent median values, colored bars and whiskers correspond to the 68% and 95% credible intervals (CI).

S4.5   Posterior of parameters
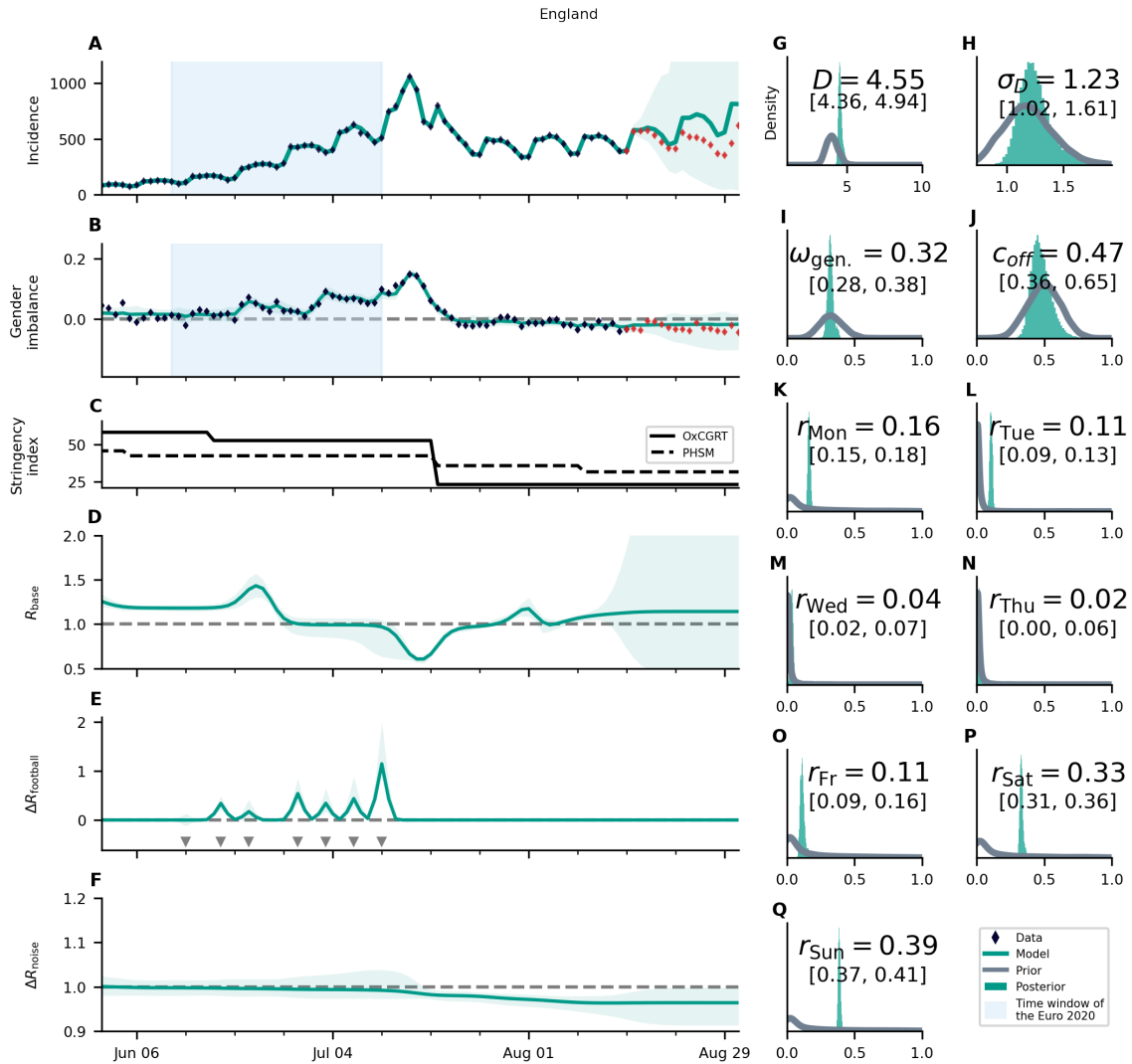
Supplementary Figure S24: **Overview of the posterior for England.** We compare (**A**) the time-dependence of the incidence before, during (blue shaded area) and after the championship; (**B**) the gender imbalance of observed cases; (**C**) Oxford governmental response tracker (OxCGRT) [3] and public health and social measures severity index (PHSM) [4] (not part of the model); (**D**) the gender-symmetric base reproduction number R_{base}; (**E**) the gender-asymmetric football reproduction number R_{football}; (**F**) gender-asymmetric noise related reproduction number R_{noise}; and (**G**) to (**Q**) the prior and posterior of various parameters. In mid July the incidence starts dropping. In contrast, the number of deaths continues to increase. Together, this indicates that the testing policy was changed around that time. England is one of the two countries where the delay D and the female participation in fan activities dominating the additional transmission can be measured and significantly constrained with the data compared to the prior distribution (**G** and **I**). Red diamonds show data not used for the analysis. This comes with an increase in the uncertainty in the model prediction. One notes two slight bumps of the base reproduction number: one during and one after the end of the championship. The first bump may indicate that our model is not able to fully attribute a part of the effective reproduction number to $\Delta R_{\text{football}}$ and is attributing the effect of England's matches in the group phase to the base reproduction number instead. The second bump might be explained hereby: During the championship there may be generally more social contacts, which are not in temporal synchronization with the matches, and therefore not explained by $\Delta R_{\text{football}}$ but by R_{base} instead. Hence, after the championship the base reproduction number decreases and increases again when measures are lifted (**C**). The turquoise shaded areas correspond to 95% credible intervals.
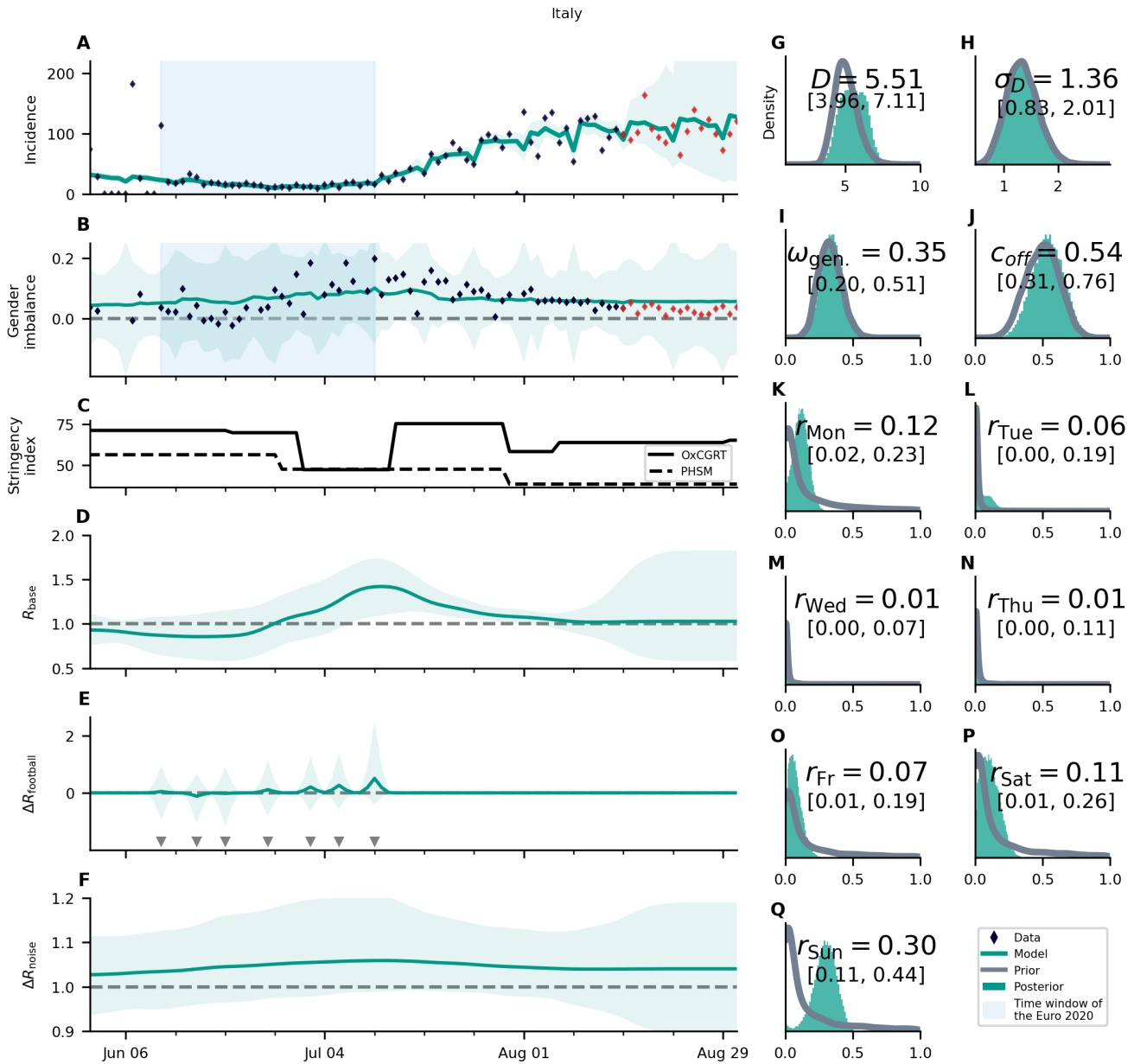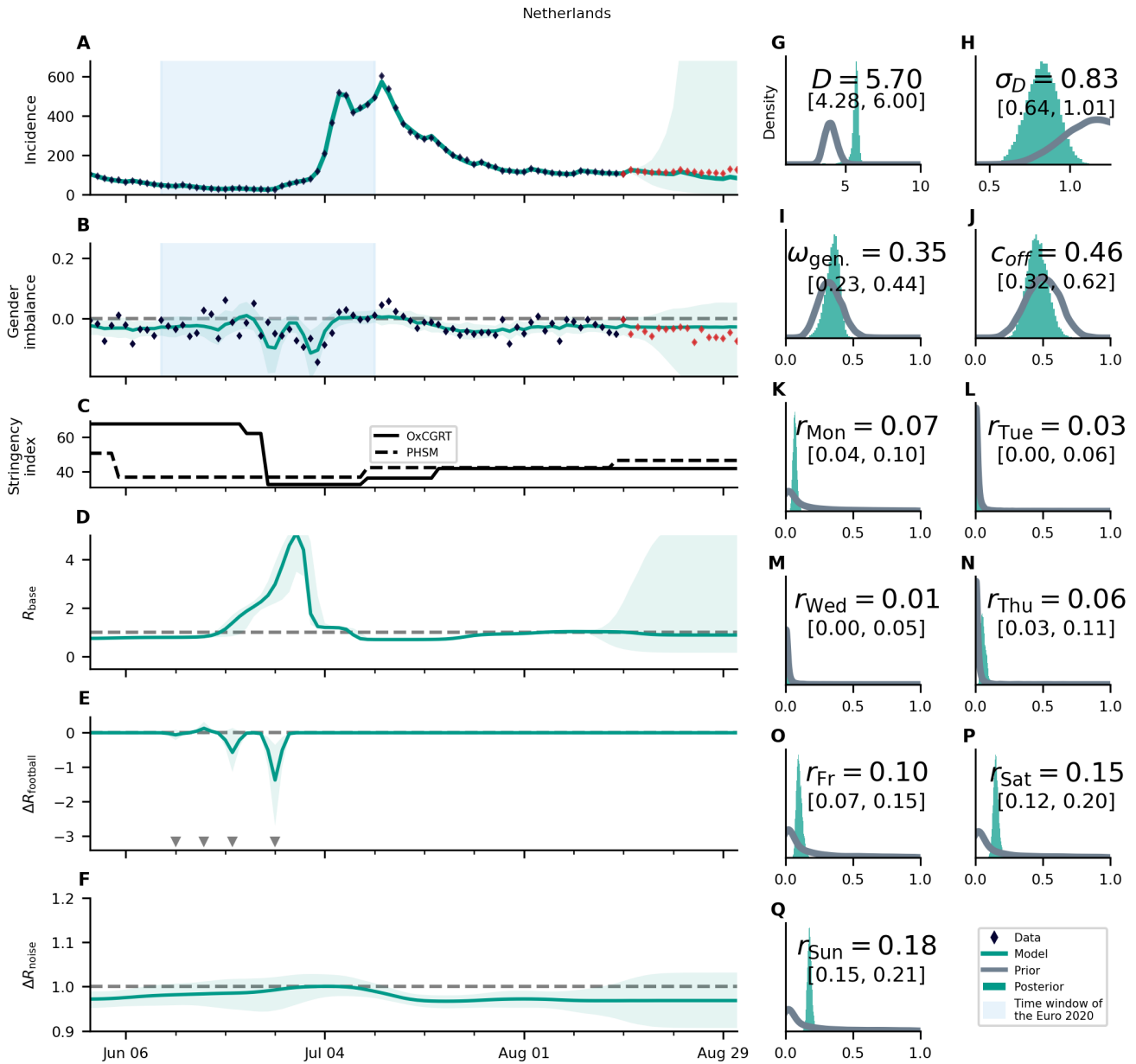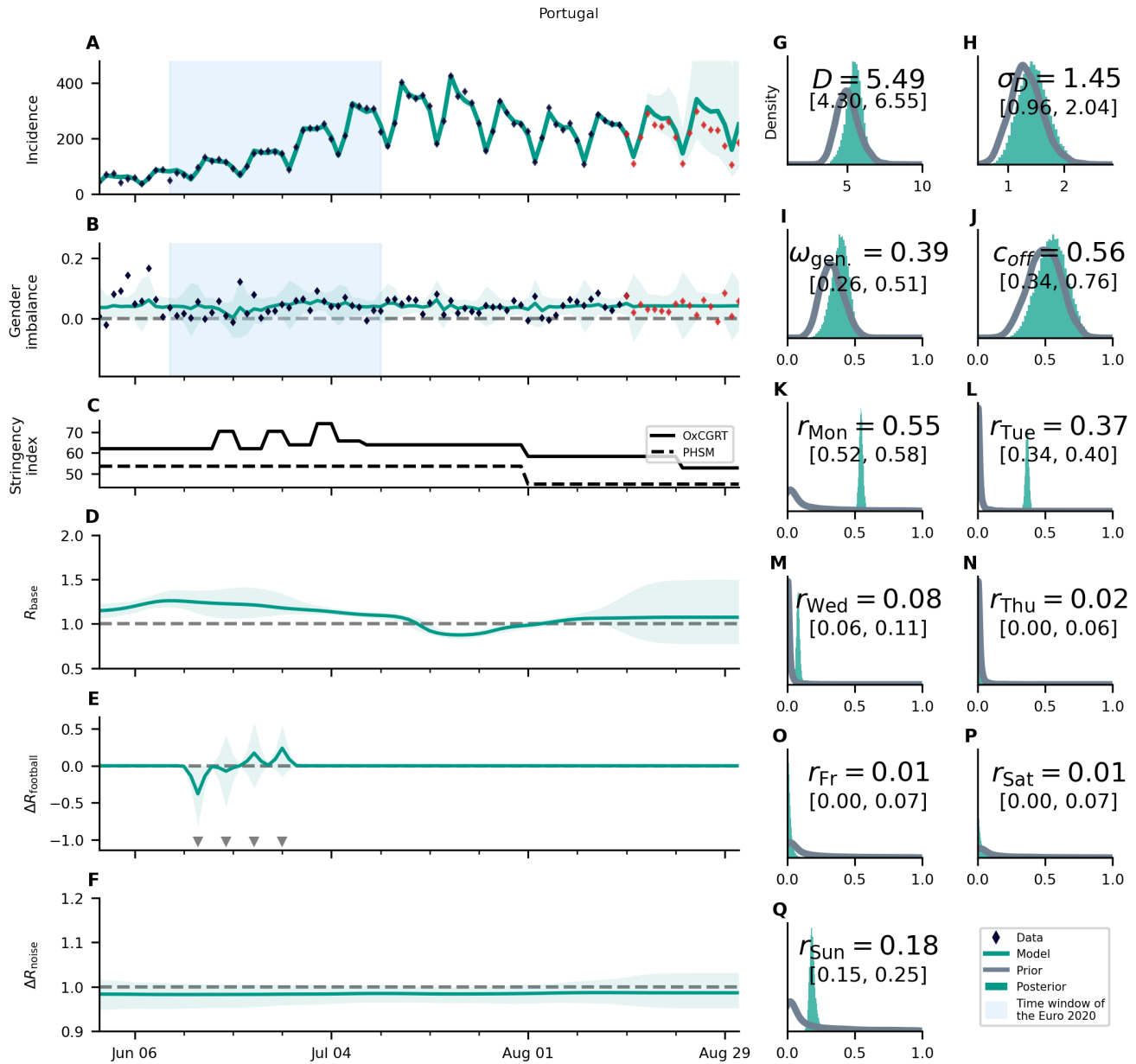
Supplementary Figure S25: **Overview of the posterior for Austria.** For an explanation of the panel structure, see supplementary Fig. S24. Austria shows a low significance for assigning cases to matches. The increase of R_{base} coincides with the relaxation of restrictions **C**, but the subsequent decrease is not explained. The turquoise shaded areas correspond to 95% credible intervals.
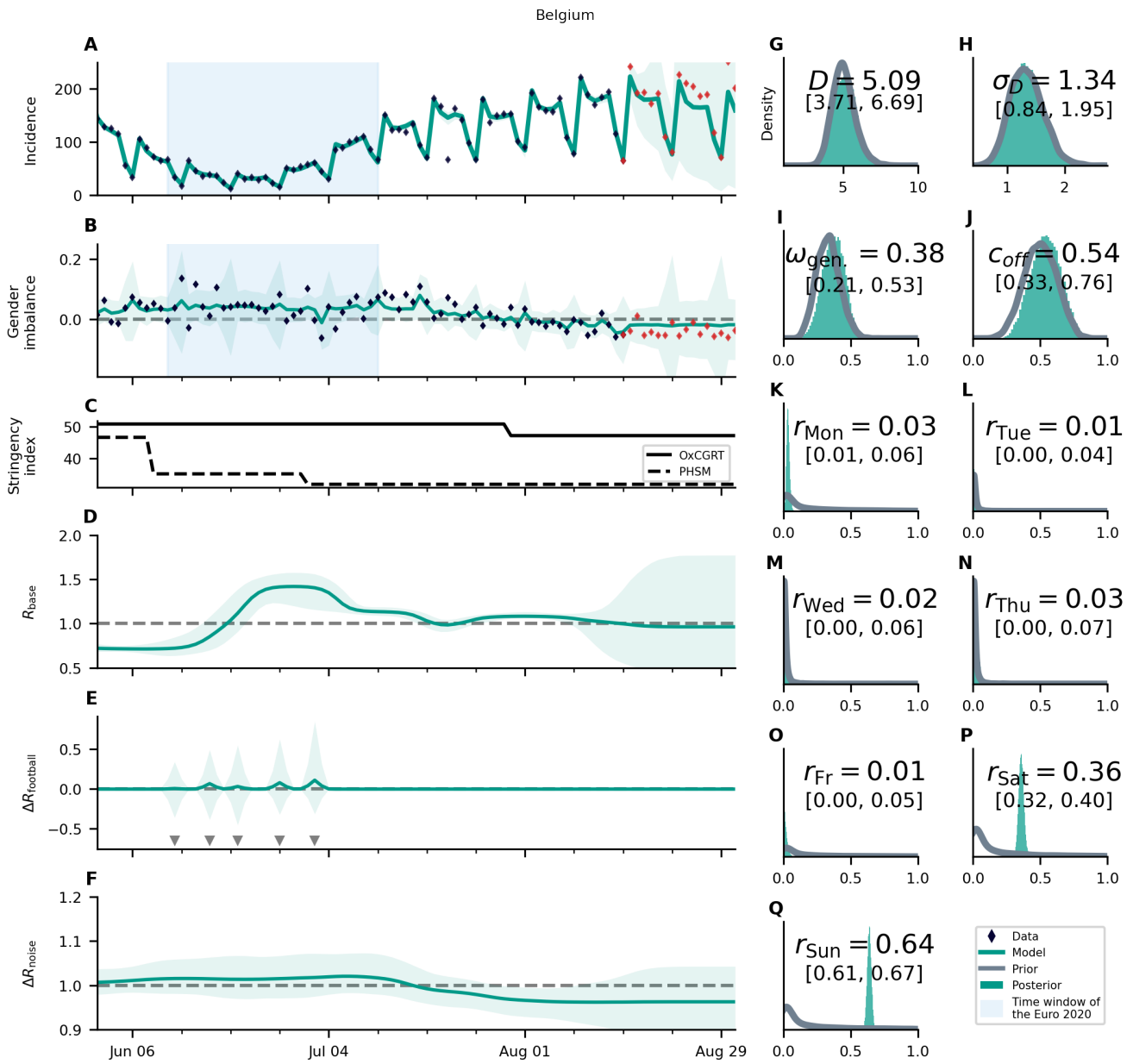
Supplementary Figure S26: **Overview of the posterior for Belgium.** For an explanation of the panel structure, see supplementary Fig. S24. Belgium shows a low significance for assigning cases to matches, but an intermittent increase of R_{base} during the championship. The turquoise shaded areas correspond to 95% credible intervals.
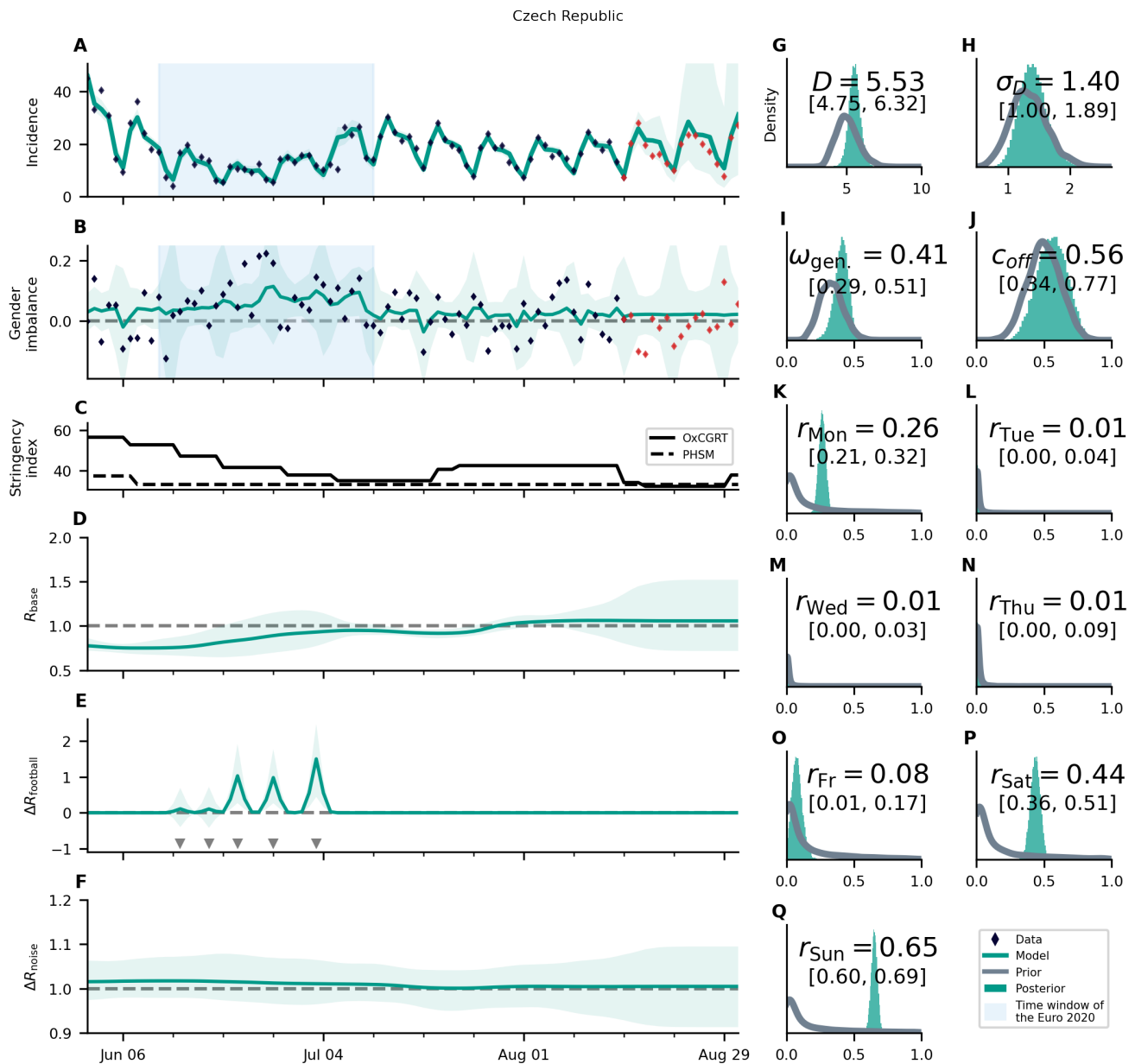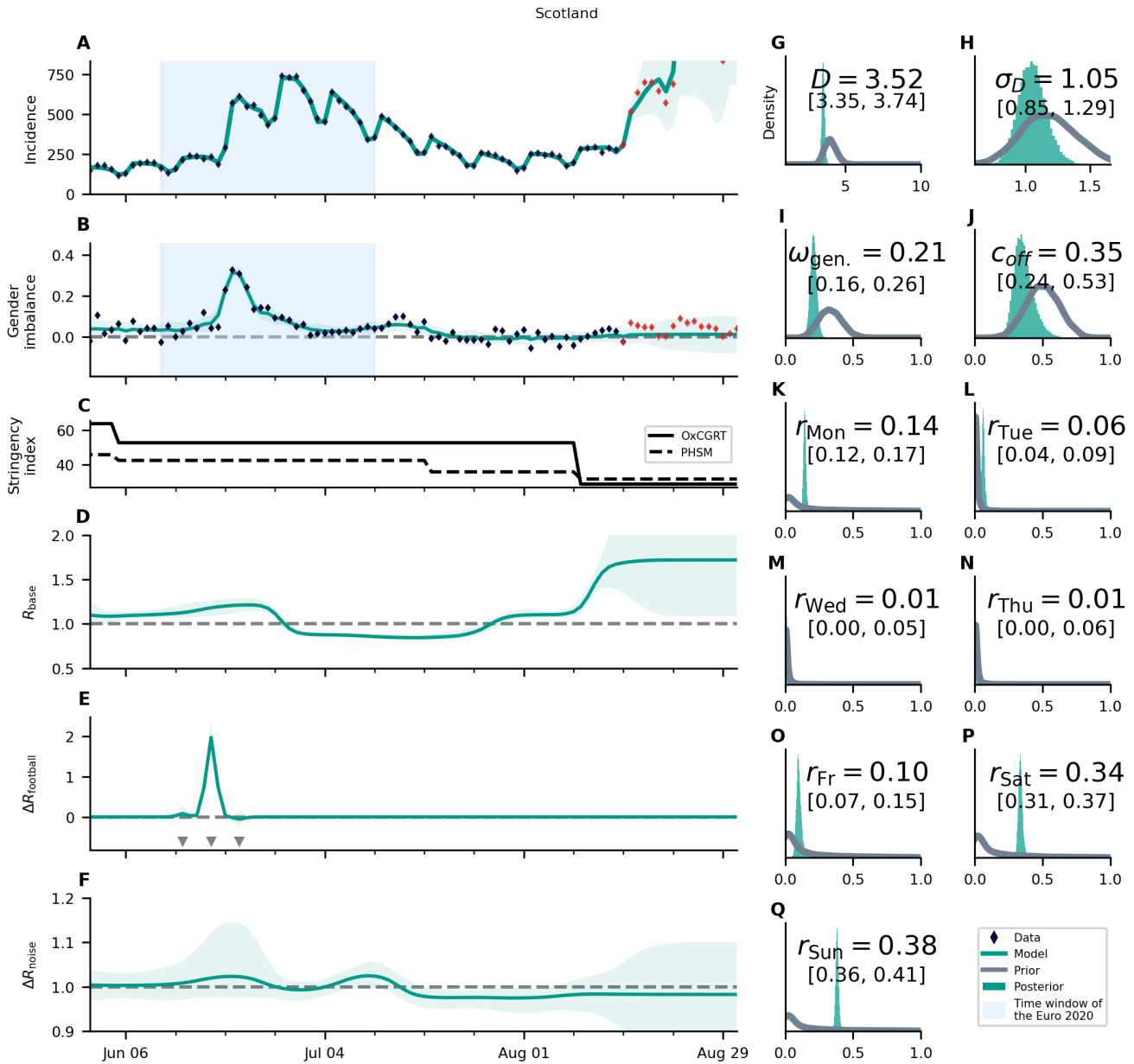
Supplementary Figure S27: **Overview of the posterior for the Czech Republic.** For an explanation of the panel structure, see supplementary Fig. S24. The overall incidence is relatively low, which increases the noisiness of the data. This is especially apparent in the gender imbalance (**B**). The base reproduction number is slowly increasing during the analyzed time-period, which can be partially explained by a decrease of the stringency index (**C**). The match effects are greater for later matches, beginning from the last group match until the quarterfinals (**E**), which is the expected variation. The turquoise shaded areas correspond to 95% credible intervals.
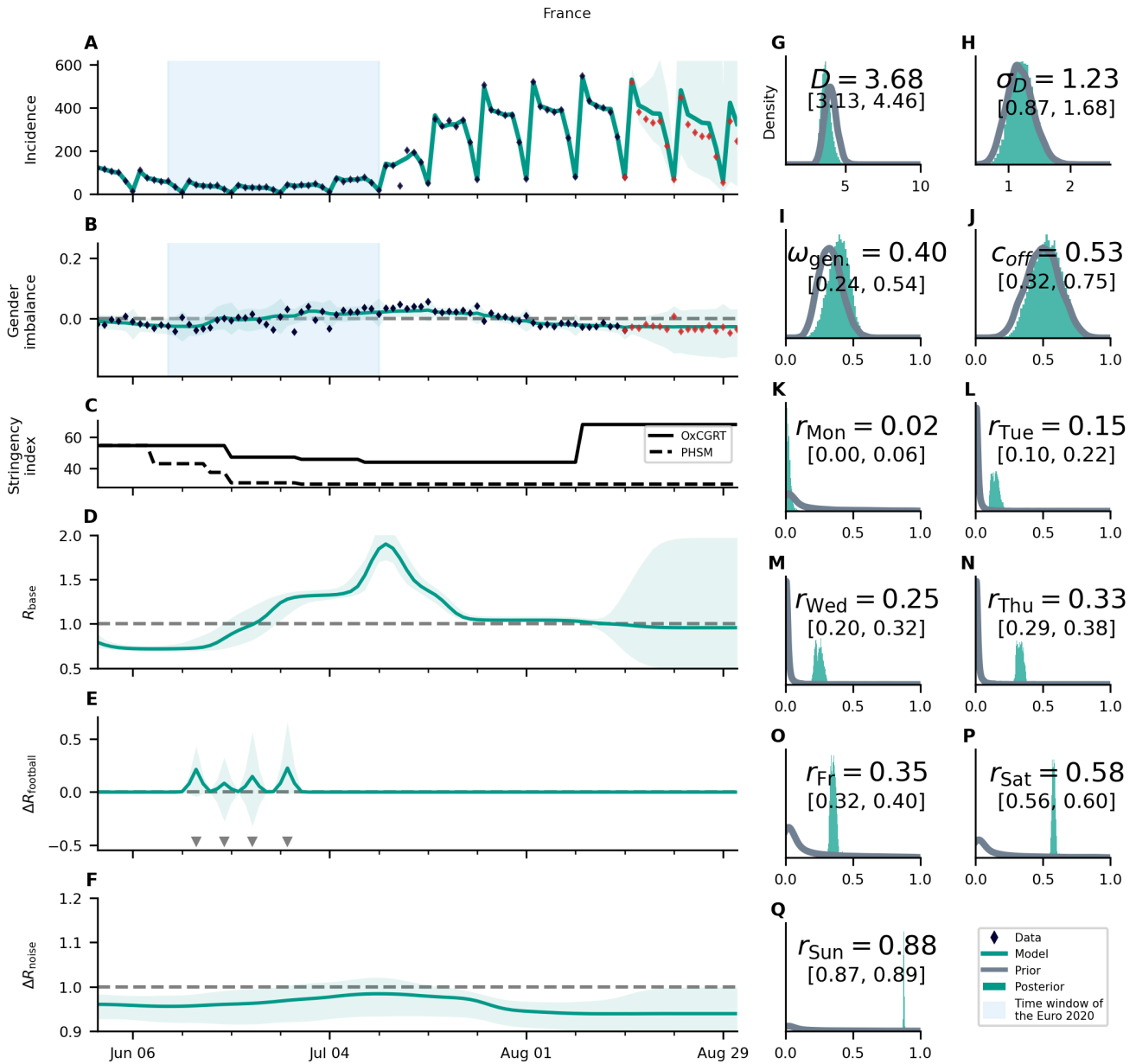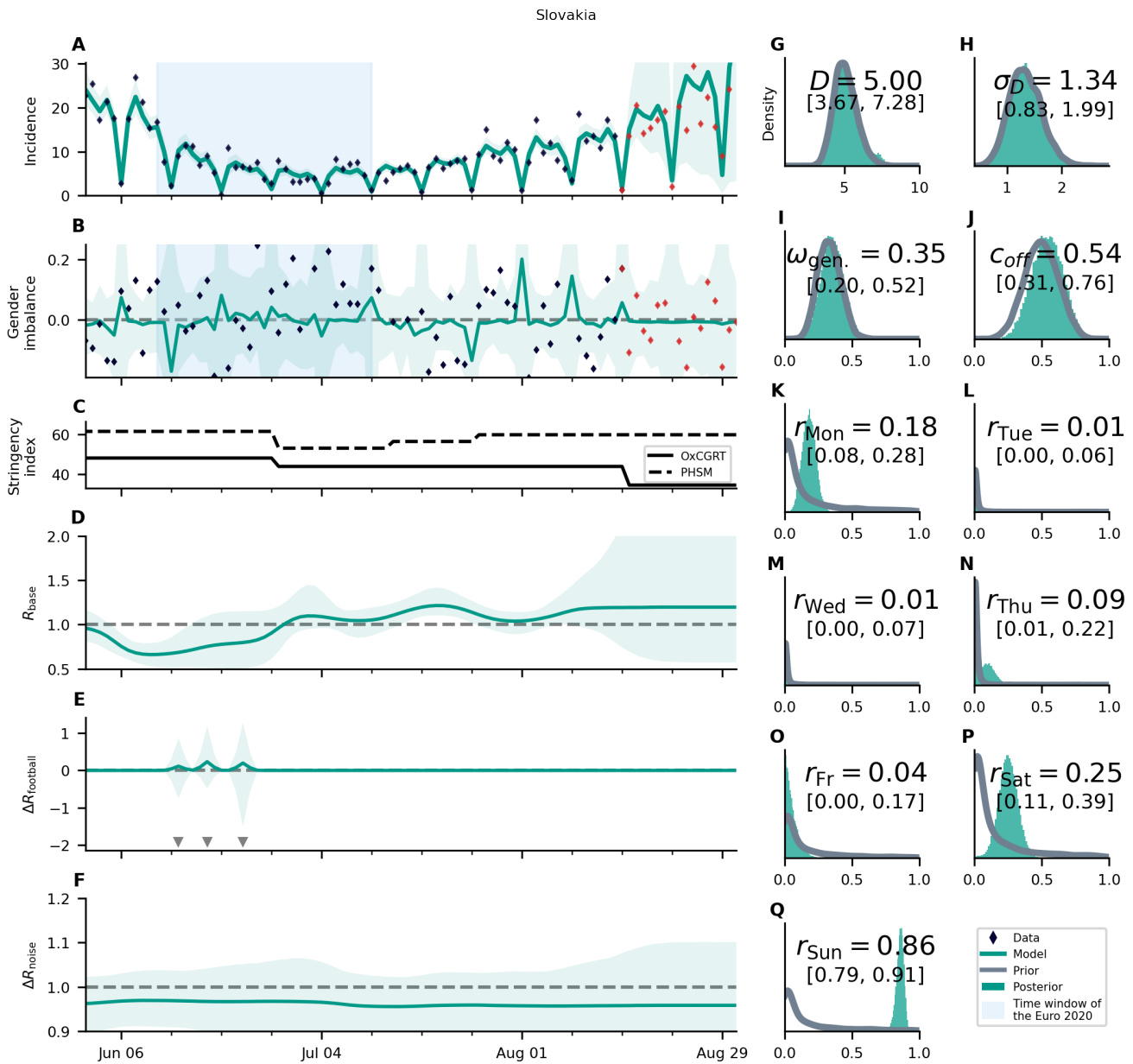
Supplementary Figure S28: **Overview of the posterior for France.** For an explanation of the panel structure, see supplementary Fig. S24. France shows a very pronounced increase of R_{base} over the course of the championship and a very small fraction of cases assigned to matches of the French team. This hints at a rather gender-neutral effect of match-induced infections in France, in agreement with the results shown in Fig. S15. The peak of R_{base} occurs on July 11th when clubs etc re-opened. It is unclear why the base reproduction number decreases this much again afterwards. The turquoise shaded areas correspond to 95% credible intervals.
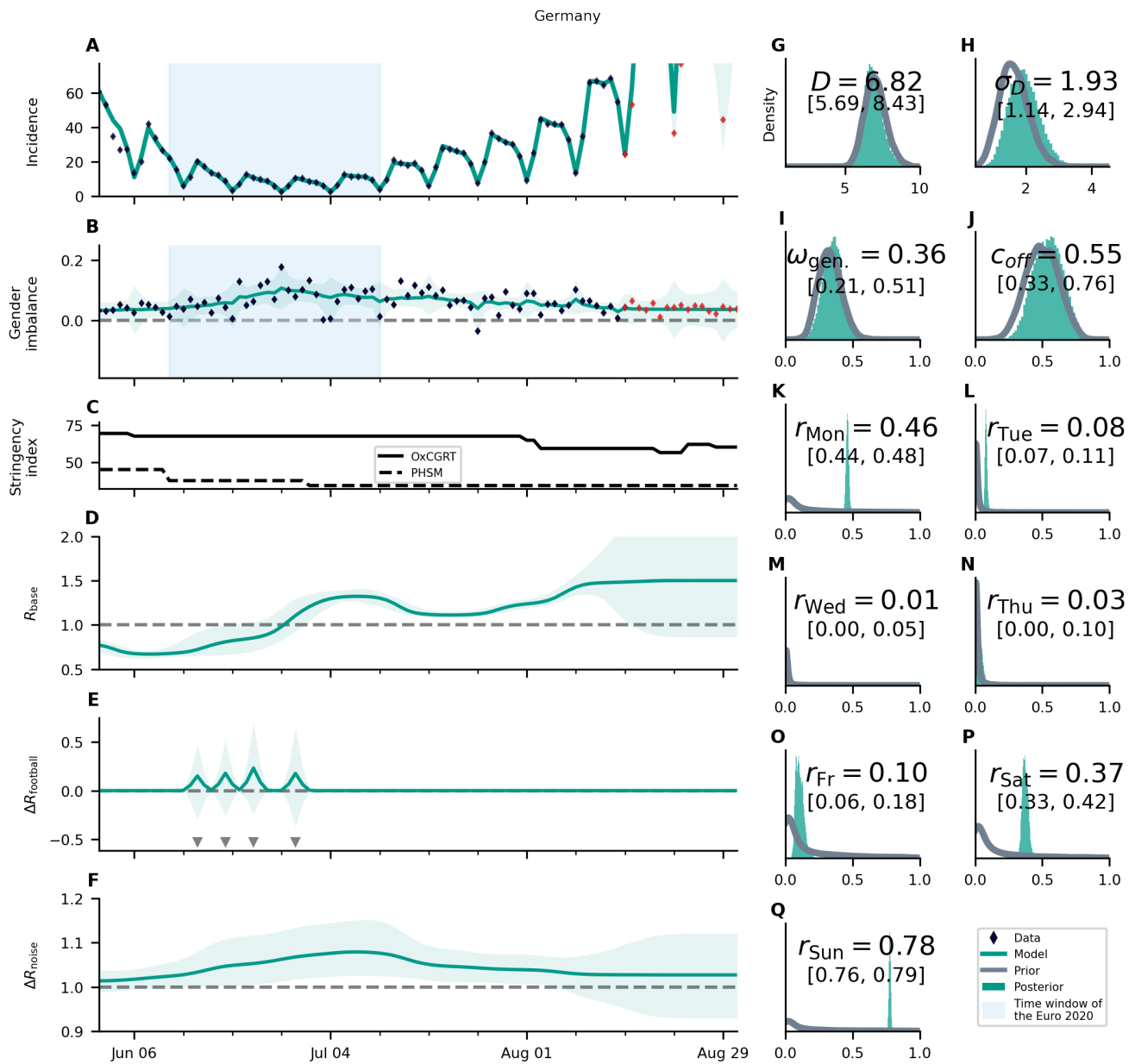
Supplementary Figure S29: **Overview of the posterior for Germany.** For an explanation of the panel structure, see supplementary Fig. S24. Germany shows an increase of R_{base} and of the gender imbalance over the course of the championship (**B**). It might be the case that the Euro 2020 contribution is not tightly tied to matches of the German team, prohibiting the model to explain the observed gender imbalance via the individual matches (**E**), leading to an increase of ΔR_{noise} instead (**F**). The turquoise shaded areas correspond to 95% credible intervals.

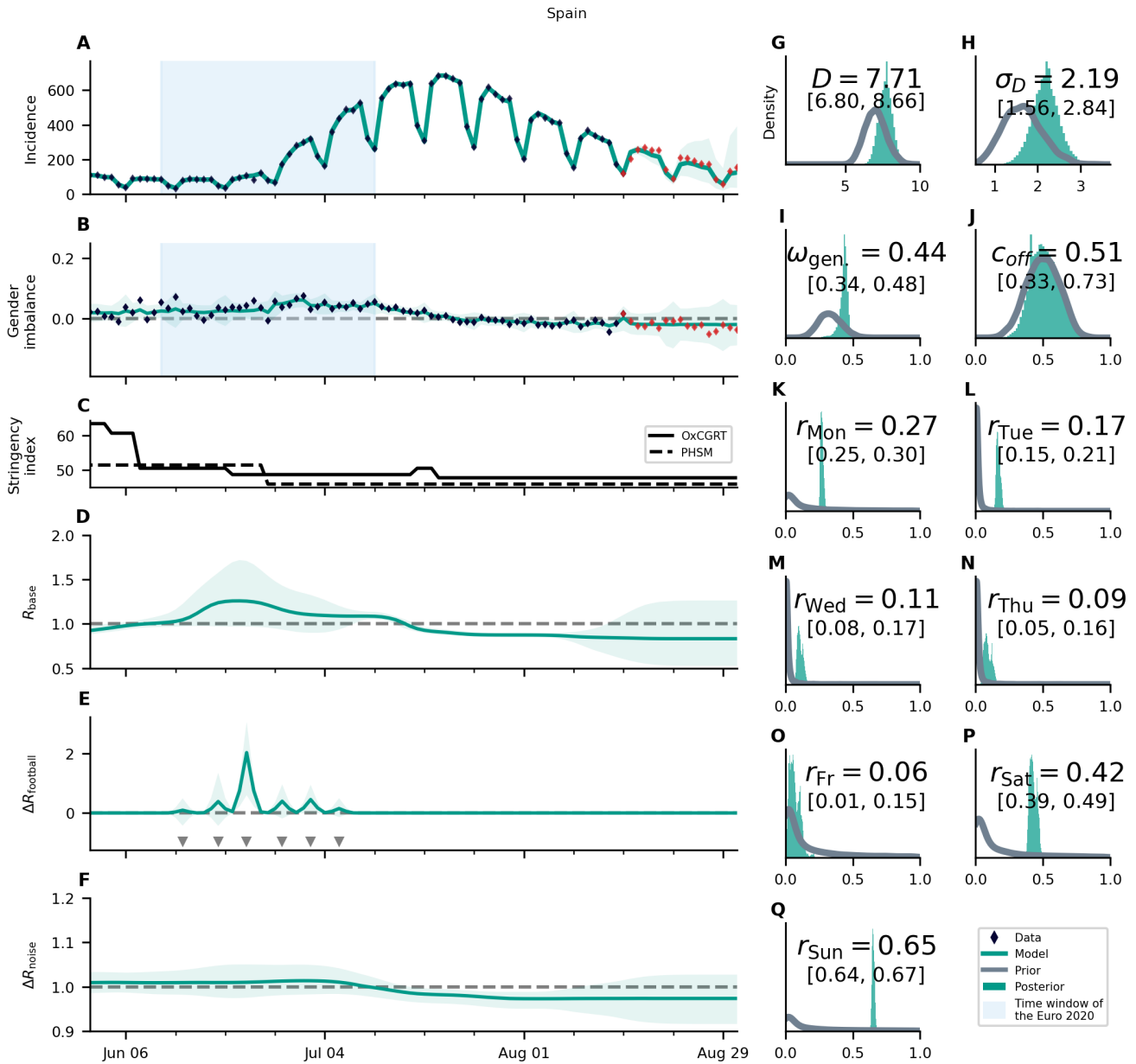Supplementary Figure S30: **Overview of the posterior for Italy.** For an explanation of the panel structure, see supplementary Fig. S24. Italy is one of the countries where an intermittent increase in R_{base} is observed (**D**). The development of the base reproduction number also coincides well with the relaxations and reinstatement of restrictions (**C**). Match-related football effects are not clearly visible (**E**). The turquoise shaded areas correspond to 95% credible intervals.
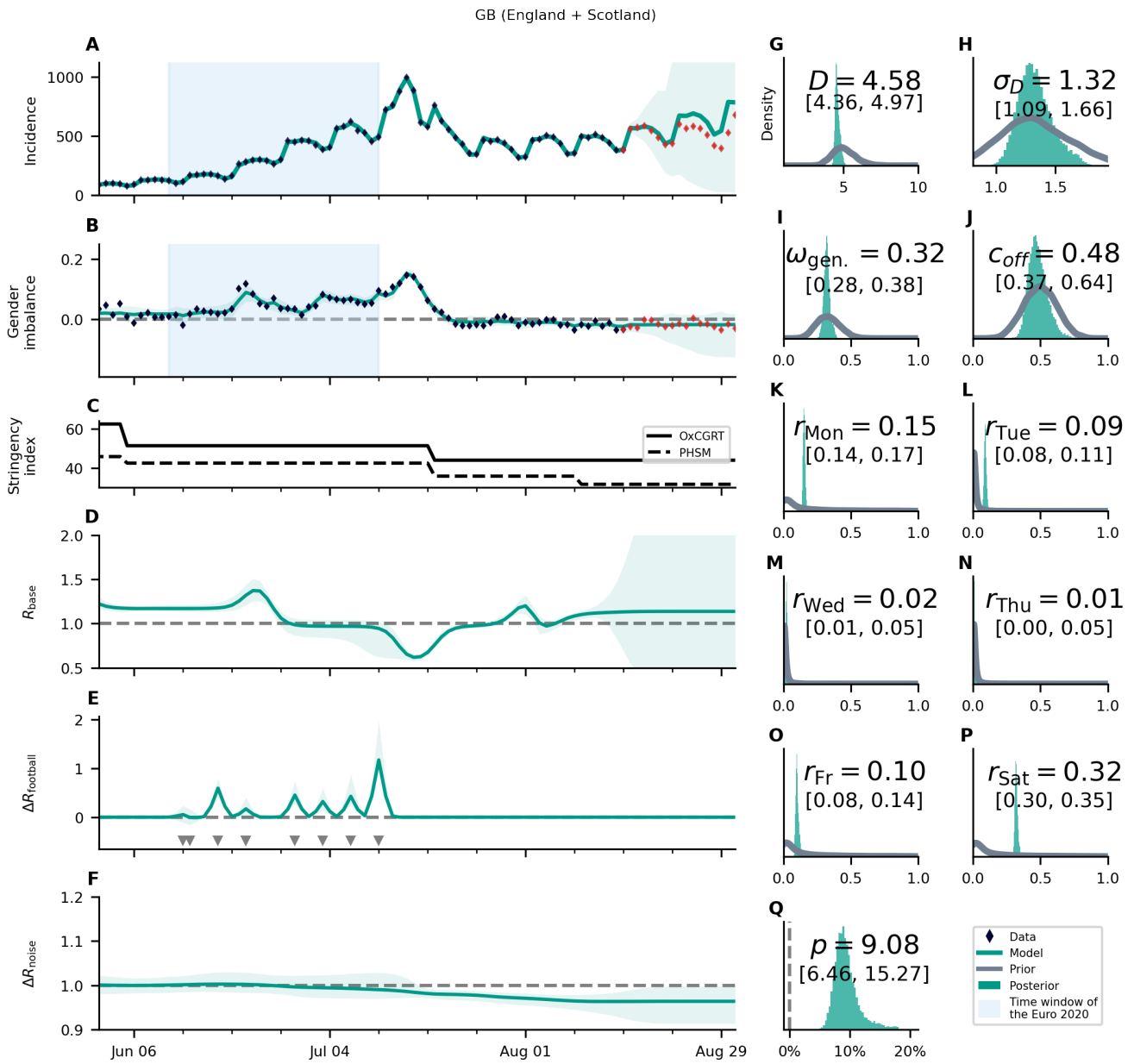
Supplementary Figure S31: **Overview of the posterior for the Netherlands.** For an explanation of the panel structure, see supplementary Fig. S24. The country wide "freedom day" on June 26th [10] is clearly visible in the incidence numbers **A** as well as the posterior base reproduction number **B**. Its effects overshadow possible effects from the Euro 2020 and we removed this country from subsequent analyses. The turquoise shaded areas correspond to 95% credible intervals.

Supplementary Figure S32: **Overview of the posterior for Portugal.** For an explanation of the panel structure, see supplementary Fig. S24. Together with England, Portugal has the highest R_{base} before the championship. It is the only country in which a decrease of R_{base} over the course of the championship is observed. The fact that R_{base} remains low after the championship could be a hint that the possible increase of cases due to the Euro 2020 in Portugal is small compared to the reduction stemming from unrelated changes. The turquoise shaded areas correspond to 95% credible intervals.

Supplementary Figure S33: **Overview of the posterior for Scotland.** For an explanation of the panel structure, see supplementary Fig. S24. Scotland is the country with the most significant effect of a single match, in this case against England. While this is in full agreement press reports (see also Fig. S20), the prior assumption of an exceptional large effect of this game is not built into the model. This clear association, thus, is a successful validation of the model functionality. The relaxation of governmental restrictions on August 9th is also well reflected in the development of the base reproduction number. The turquoise shaded areas correspond to 95% credible intervals.

Supplementary Figure S34: **Overview of the posterior for Slovakia.** For an explanation of the panel structure, see supplementary Fig. S24. Hardly any significant effects, apart from a small but long-lasting increase in R_{base}, are observed. The turquoise shaded areas correspond to 95% credible intervals.

Supplementary Figure S35: **Overview of the posterior for Spain.** For an explanation of the panel structure, see supplementary Fig. S24. The national state of emergency ended in Spain on June 21st, in the middle of the championship. The model has therefore some difficulty to separate the effect of the relaxation of restrictions and the one of the matches, which translates into wide credible intervals in R_{base} (**C**) and $\Delta R_{\text{football}}$ (**D**). The turquoise shaded areas correspond to 95% credible intervals.

Supplementary Figure S36: **Overview of the posterior for the combined data of England and Scotland** For an explanation of the panel structure, see supplementary Fig. S24. The turquoise shaded areas correspond to 95% credible intervals.

S4.6 Chain mixing of selected parameters
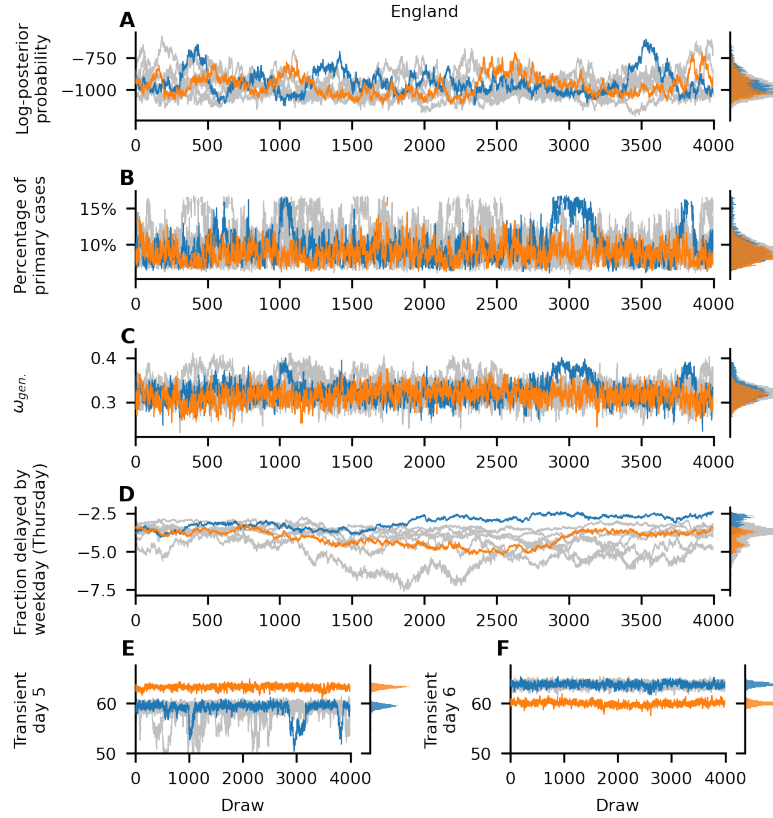
Supplementary Figure S37: **Chain mixing of selected parameters for England** Here we plot the unnormalized log-posterior probability (**A**) and selected parameters (**B** – **F**) as function for each draw and MCMC chain. Orange and blue depict two chains with the highest between-chain variance, the two least converging chains. The gray lines and histogram represent the ensemble of all chains. For our parameters of interest (**B**, **C**) the posterior distribution mixes well, even if the individual chains do not mix well in some other parameters (**D** – **F**), indicating that despite the degeneracy of some parameters, the inference of our parameters of interest is not affected. Panel **D** is a plot of the parameter with the worst mixing (the highest $\mathcal{R}$-hat value). Panels **E** and **F** show that the non-converging behavior can be explained as the exchange between two nearly degenerate solutions in two of the auxiliary parameters.
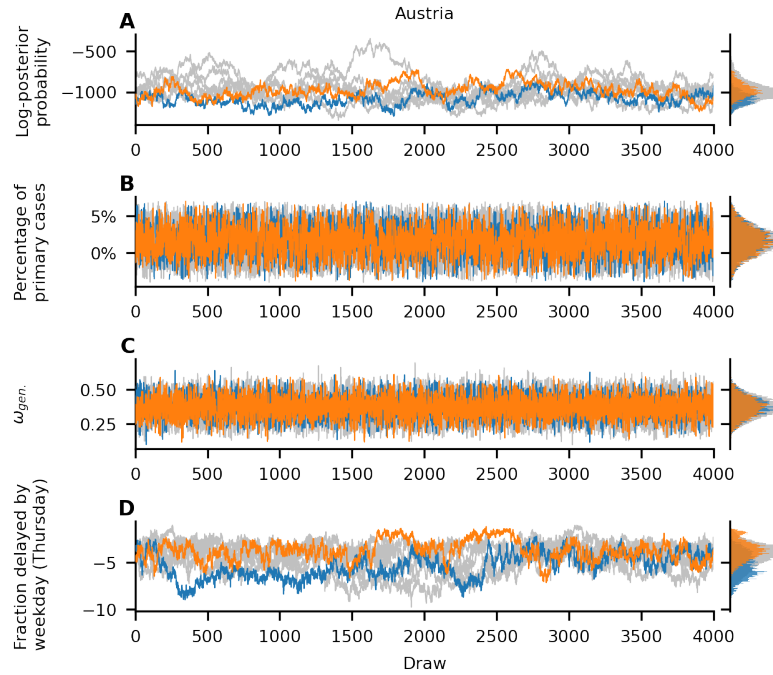
Supplementary Figure S38: **Chain mixing of selected parameters for Austria** Here the fraction of cases delayed by weekday on Thursdays is the parameter with the highest $\mathcal{R}$-hat values as seen in panel **D**. For a further detailed description of the panels see supplementary Fig. S37.
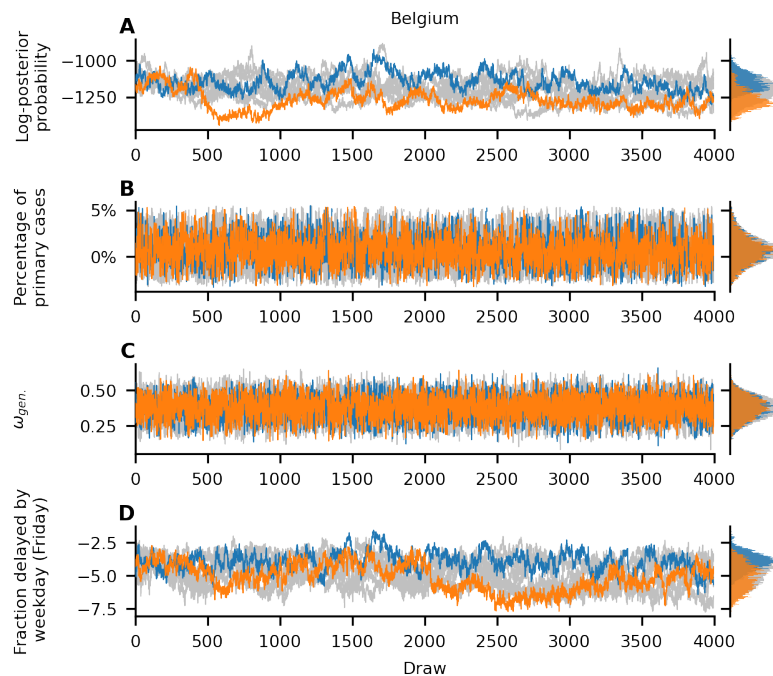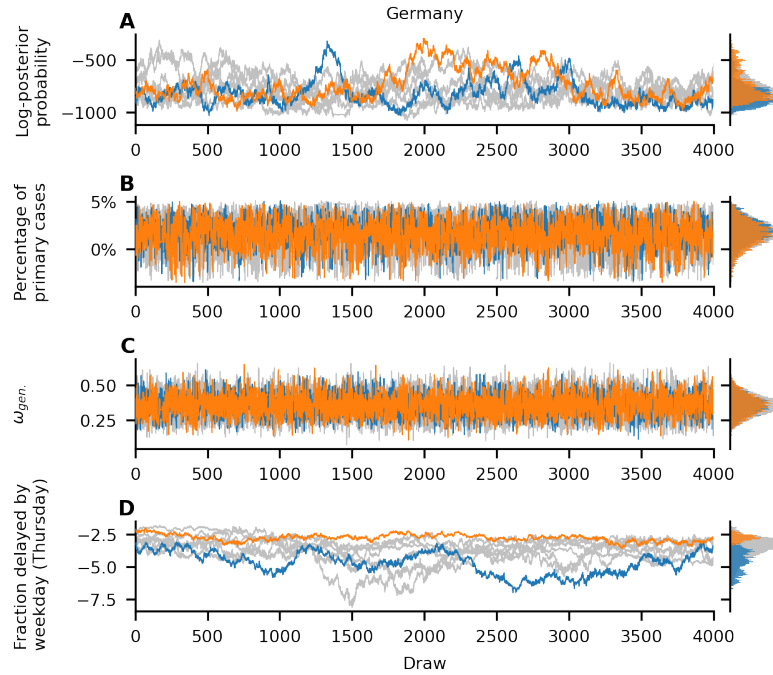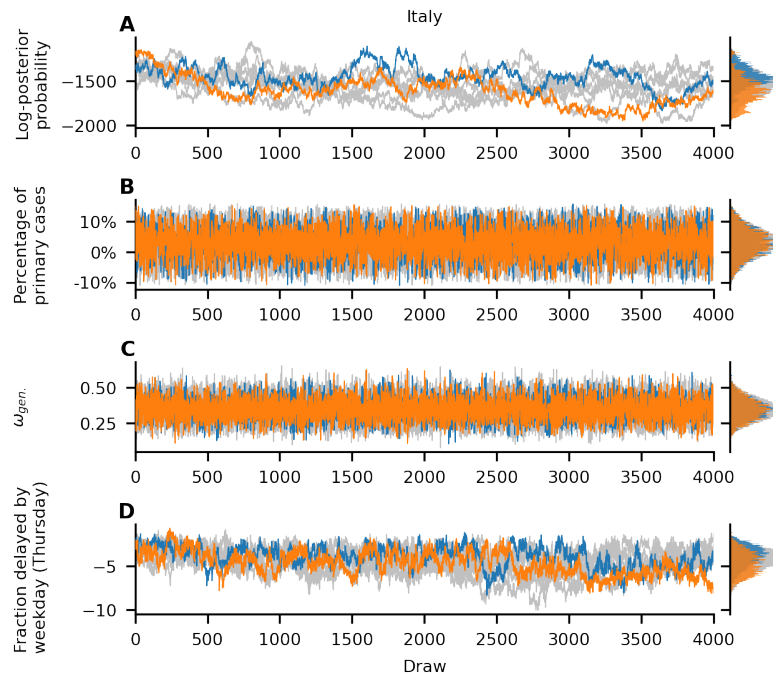

Supplementary Figure S39: **Chain mixing of selected parameters for Belgium** Here the fraction of cases delayed by weekday on Fridays is the parameter with the highest $\mathcal{R}$-hat values as seen in panel **D**. For a further detailed description of the panels see supplementary Fig. S37.
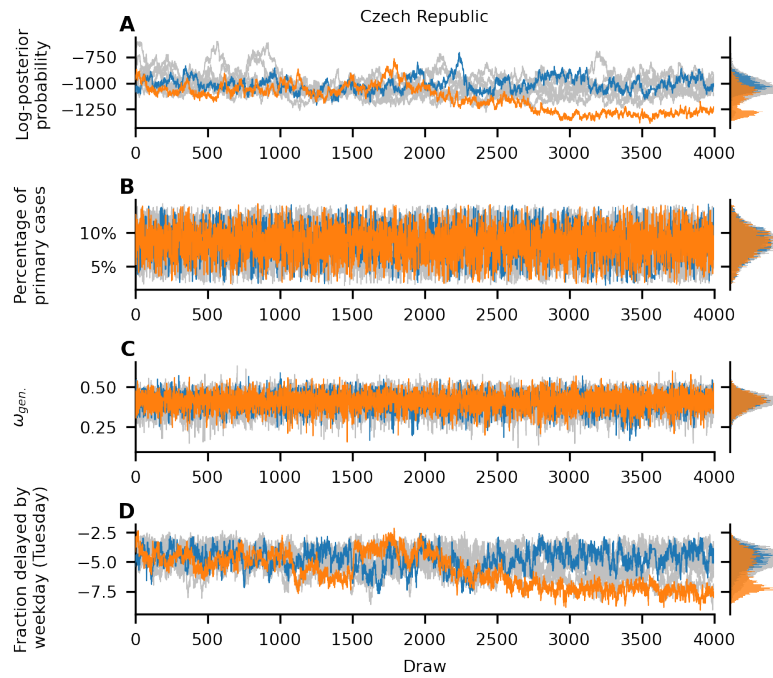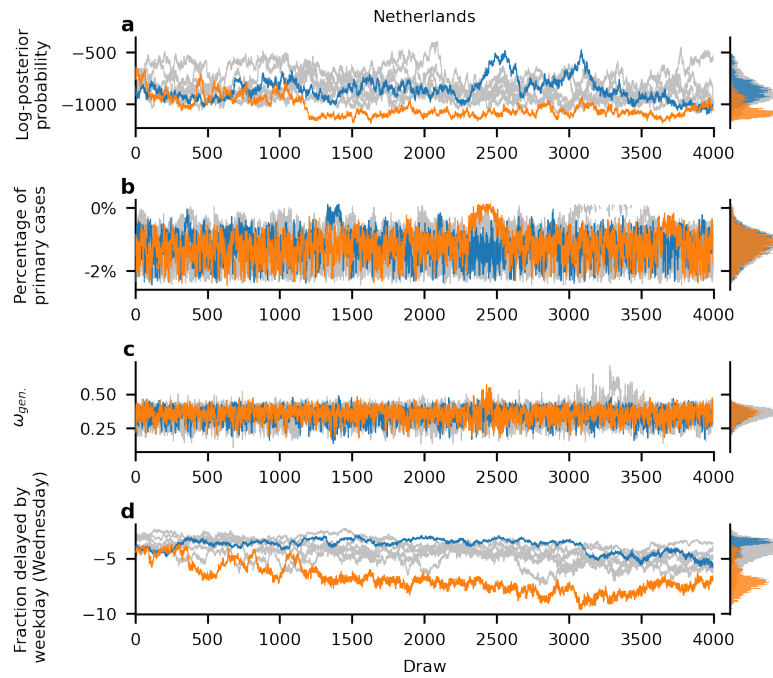
Supplementary Figure S40: **Chain mixing of selected parameters for Czech Republic** Here the fraction of cases delayed by weekday on Thursdays is the parameter with the highest $\mathcal{R}$-hat values as seen in panel **D**. For a further detailed description of the panels see supplementary Fig. S37.
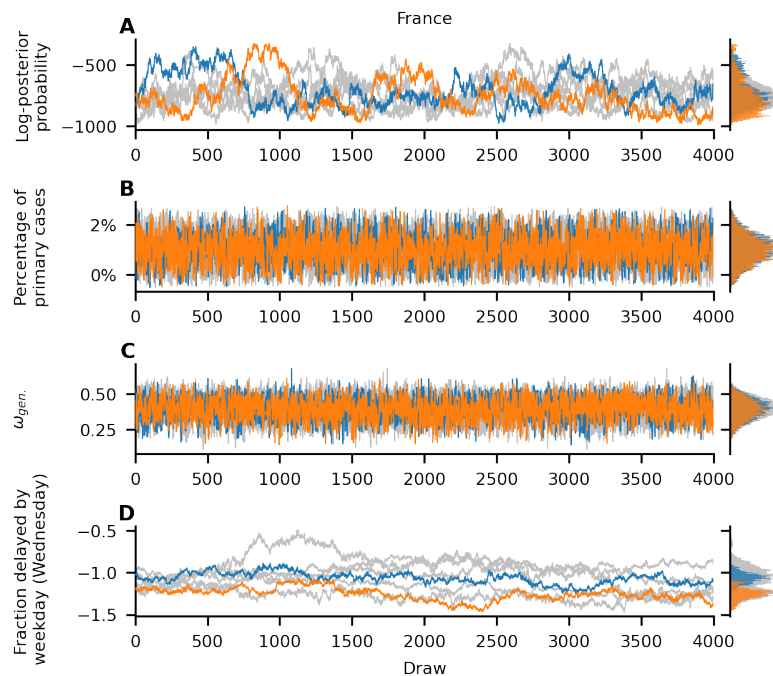
Supplementary Figure S41: **Chain mixing of selected parameters for France** Here the fraction of cases delayed by weekday on Wednesdays is the parameter with the highest $\mathcal{R}$-hat values as seen in panel **D**. For a further detailed description of the panels see supplementary Fig. S37.
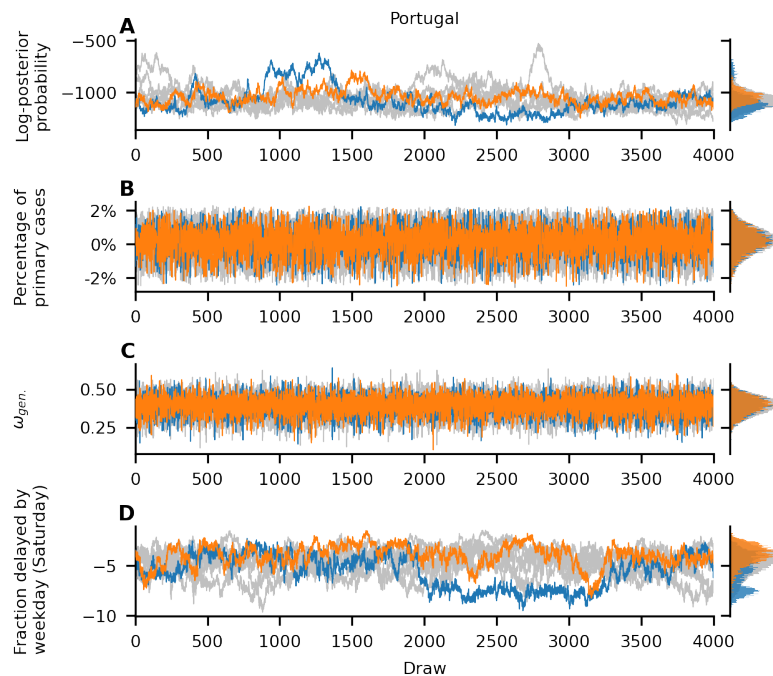
Supplementary Figure S42: **Chain mixing of selected parameters for Germany** Here the fraction of cases delayed by weekday on Thursdays is the parameter with the highest $\mathcal{R}$-hat values as seen in panel **D**. For a further detailed description of the panels see supplementary Fig. S37.

Supplementary Figure S43: **Chain mixing of selected parameters for Italy** Here the fraction of cases delayed by weekday on Thursdays is the parameter with the highest $\mathcal{R}$-hat values as seen in panel **D**. For a further detailed description of the panels see supplementary Fig. S37.
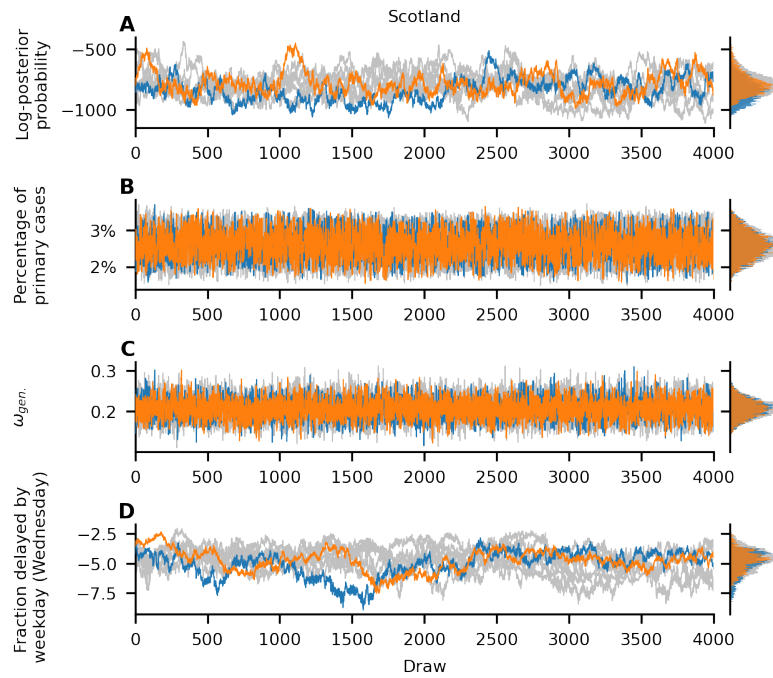
Supplementary Figure S44: **Chain mixing of selected parameters for Portugal** Here the fraction of cases delayed by weekday on Wednesdays is the parameter with the highest $\mathcal{R}$-hat values as seen in panel **D**. For a further detailed description of the panels see supplementary Fig.   S37.
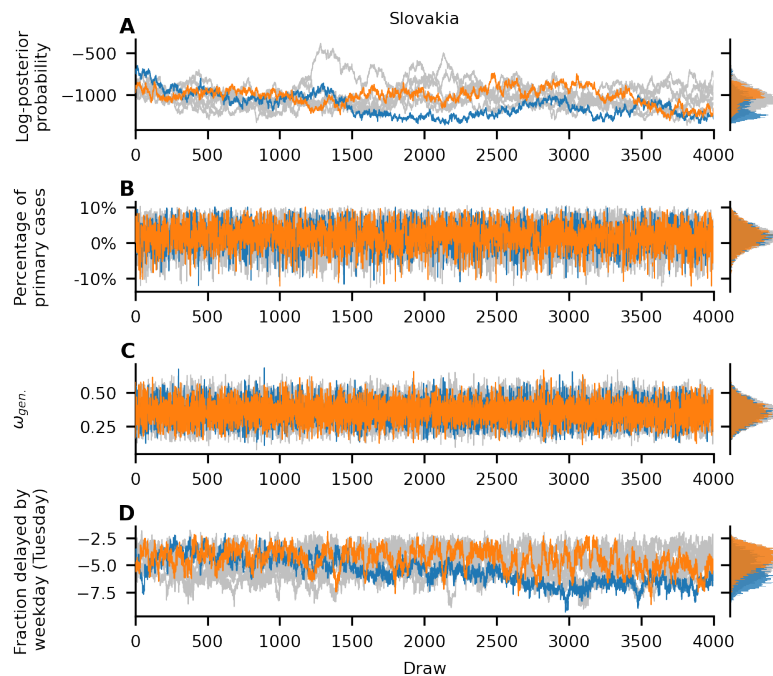

Supplementary Figure S45: **Chain mixing of selected parameters for Portugal** Here the fraction of cases delayed by weekday on Saturdays is the parameter with the highest $\mathcal{R}$-hat values as seen in panel **D**. For a further detailed description of the panels see supplementary Fig.   S37.
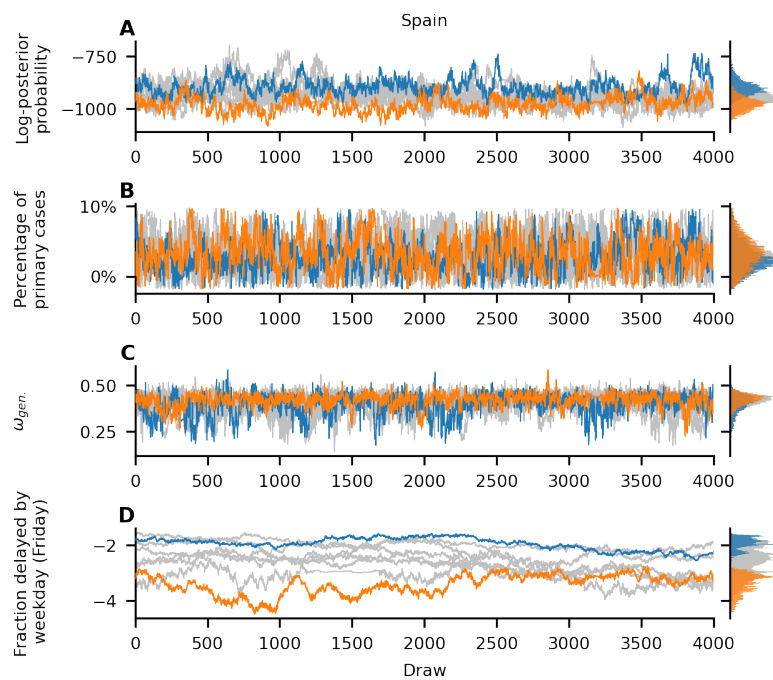
Supplementary Figure S46: **Chain mixing of selected parameters for Scotland** Here the fraction of cases delayed by weekday on Wednesdays is the parameter with the highest $\mathcal{R}$-hat values as seen in panel **D**. For a further detailed description of the panels see supplementary Fig. S37.

Supplementary Figure S47: **Chain mixing of selected parameters for Slovakia** Here the fraction of cases delayed by weekday on Thursdays is the parameter with the highest $\mathcal{R}$-hat values as seen in panel **D**. For a further detailed description of the panels see supplementary Fig. S37.

Supplementary Figure S48: **Chain mixing of selected parameters for Spain** Here the fraction of cases delayed by weekday on Fridays is the parameter with the highest $\mathcal{R}$-hat values as seen in panel **D**. For a further detailed description of the panels see supplementary Fig. S37.

Supplementary References

[1] T. Riffe, E. Acosta, Data Resource Profile: COVerAGE-DB: a global demographic database of COVID-19 cases and deaths, *International Journal of Epidemiology* **50**, 390–390f (2021).

[2] E. O.-O. Max Roser, Hannah Ritchie, J. Hasell, Coronavirus Pandemic (COVID-19), *Our World in Data* (2020). `https://ourworldindata.org/coronavirus`, (Europe, America, and Oceania and Asia).

[3] T. Hale, *et al.*, A global panel database of pandemic policies (Oxford COVID-19 Government Response Tracker), *Nature Human Behaviour* **5**, 529–538 (2021).

[4] A systematic approach to monitoring and analysing public health and social measures (PHSM) in the context of the COVID-19 pandemic: underlying methodology and application of the PHSM database and PHSM Severity Index (2020).

[5] COVID-19 Community Mobility Reports, `https://www.google.com/covid19/mobility/`.

[6] E. Dong, H. Du, L. Gardner, An interactive web-based dashboard to track COVID-19 in real time, *The Lancet Infectious Diseases* **20**, 533 - 534 (2020).

[7] Google Trends, `https://trends.google.de/trends`.

[8] M. Sharma, *et al.*, Understanding the effectiveness of government interventions against the resurgence of COVID-19 in Europe, *Nature communications* **12**, 1–13 (2021).

[9] S. Lagaert, H. Roose, The gender gap in sport event attendance in Europe: The impact of macro-level gender equality, *International Review for the Sociology of Sport* **53**, 533-549 (2018).

[10] Oxford COVID-19 Government Response Tracker, Blavatnik School of Government and University of Oxford, `https://covidtracker.bsg.ox.ac.uk/`.